

DOCTORAL SCHOOL
MATERIALS, RADIATION AND ENVIRONMENTAL SCIENCES
DEPARTMENT OF EARTH SCIENCES
LGCgE - CIVIL ENGINEERING AND GEO-ENVIRONMENT LABORATORY

DISSERTATION

To obtain the grade of
DOCTOR OF THE UNIVERSITY LILLE 1
SCIENCES AND TECHNOLOGIES

Discipline: Geosciences
Speciality: Petroleum geology
presented and publicly supported by

Abdalratha SAHAAB

13 December 2017

**PALEOENVIRONMENTAL CONDITIONS AND DIAGENETIC EVOLUTION OF
THE MISHRIF FORMATION (NASIRIYAH OIL FIELD, IRAQ)**

JURY

Mr Gilles BERGER	Research Manager	CNRS / University Paul Sabatier, Toulouse	Rapporteurs for the thesis defence
Mr Olivier DUGUE	Professor	Universtiy of Caen- Normandie	
Mr Renaud TOULLEC	Lecturer	UniLaSalle, Beauvais	External examiner
Mr Arnaud GAUTHIER	Professor	University Lille 1	Supervisor
Mr Michel DUBOIS	Professor	University Lille 1	Supervisor

Abstract

The aim of the present study is related to understand the paleofluid-rock interactions in carbonate rocks and its relation to oil potential. Paleogeography studies, geological descriptions and geochemistry analyses of the carbonate reservoir rocks were conducted on the Mishrif Formation of the Nasiriyah oil field (south-east of Iraq) will help us to understand and realize these relationships.

Cretaceous represents the most productive period in Iraq and Arab Gulf States. It contains about 80% of Iraqi oil reserves. Rocks of the Mishrif represent the high quality in chemical aspect because these rocks include the bioclastic, microbial and detrital limestones.

The data of drill cores from 5 drill holes (NS-1 to NS-5), exploration reports and production data of the Nasiriyah oil field have been used. The microfacies analyses show that Mishrif includes foraminifera, coral, rudist, algae, microbialite, *favreina* microcoprolite, pellets, peloids, aggregate grains and rounded clastic grains. Therefore, shallow-water environments represent Mishrif paleoenvironments, from the evaporitic zone to the back-reef zone of the interior carbonate platform shelf.

The microfacies analyses indicate the final mass extinction of organisms in the upper Cretaceous. Two stages of the extinction are observed. The first stage of demise represents the solitary existence of the rudists, large Foraminifera (*alveolina*) and Echinodermata. The second stage consists of the presence of planktonic foraminifera (*Globigerina* ooze, *Oligostegina* and *Globotruncana* assemblages), associated with the absence of all types of the previous fossils except the Charophytes (green algae).

The transport system in the Mishrif contains stylolite networks, fractures, and porosity systems. The scanning electron microscope (SEM) shows the balanced distribution of the transport systems regardless of the microfacies type. The porosity systems reflect dissolution process. Indeed, primary porosity is represented by the interparticle and fenestral porosity and the secondary porosity is classified as the dissolution pores, vuggy, moldic, outgassing, intercrystalline, post-stylolite and fracture porosity.

Cementation process exhibits four phases of the cementation events. The first phase took place before the hydrocarbon migration. The second occurred during the hydrocarbon migration. The third phase happened after the process of the hydrocarbon migration and the last phase represented the thermochemical sulfate reduction by the distribution of bitumen.

The petroleum migration pathways can be represented by two events. The petroleum fluid inclusions in the blocky calcite cement represent the first stage of the petroleum migration. The second stage of the migration process is represented by the high density of the primary petroleum fluid inclusions in the cemented fracture, lately occurred in the NS-5 well.

The aqueous fluid inclusions are mainly composed of H₂O-MgCl₂ system. Homogeneous temperatures of the aqueous fluid inclusions range from 150 to 175°C. Homogeneous temperatures of the petroleum fluid inclusions in the latter fractures represent high degrees from 225 up to 250°C.

Keywords: Petroleum geology, Mishrif Formation, Nasiriyah oil field, Petroleum fluid inclusions, Microfacies, Diagenesis process, Porosity, Carbonate mud,

Résumé

Le but de cette étude est de comprendre les relations entre les roches carbonatées et les paléofluides qui les traversent. Les études paléogéographiques et les descriptions géologiques ainsi que les analyses géochimiques des roches réservoirs ont été réalisées sur la Formation de Mishrif dans le champ pétrolier de Nasiriyah (sud-est de l'Iraq) afin de comprendre et mettre en évidence ces relations. Le Crétacé représente la période la plus productive en Irak et dans les Pays du Golfe. Il représente environ 80% des réserves irakiens en pétrole.

Les données de 5 forages carotés (NS-1 à NS-5), les rapports de prospections et les données de production du champ de Nassiriya, ont été utilisés. Les analyses des microfaciès montrent que la Formation de Mishrif contient une grande variété d'organismes tels que des foraminifères, des coraux, des rudites ainsi que des algues, *microbialites*, des pellets, des peloides, des grains aggrégé et des grains arrondis. Par conséquent, la formation de Mishrif serait représentative d'un environnement d'eau de subsurface de la zone évaporitique jusqu'à la zone de récif arrière.

Les analyses de microfaciès indiquent l'extinction finale des organismes au cours du Crétacé supérieur. La forte disparition des corps des fossiles s'est produite en deux phases. La première phase de disparition représente l'existence unique de rudistes, et la présence de foraminifères (*alveovina*) ainsi que d'échinodermes. La seconde phase est représentée par la présence de foraminifères planctoniques (*Globigerina ooze*, *Oligostegina* et *Globotruncana*), accompagnés avec tous les types des fossiles précédents à l'exception de la Charophytes (algues verte).

Le système de transport des fluides dans la Formation de Mishrif se fait au travers des réseaux de stylolite, des fractures ainsi que du réseau poral. Les observations par microscopie électronique à balayage (MEB) montrent une distribution équilibrée des systèmes de transport indépendamment du type de microfaciès. Les types de porosité reflètent un processus de dissolution. En effet, la porosité primaire est représentée par les pores interconnectés et la porosité secondaire est représentée par la dissolution et les fractures.

Les processus de cimentation indiquent quatre phases d'évènements. La première phase a eu lieu avant la migration d'hydrocarbure. La seconde phase s'est produite pendant la migration de ces hydrocarbures. La troisième phase arrive après le processus de migration. Enfin, la quatrième phase est représentée par la distribution du bitume.

Les inclusions des fluides aqueuses sont composées du système $H_2O-MgCl_2$. Les températures homogènes des inclusions des fluides aqueuses varient entre 150 et 175 °C. Les températures homogènes des inclusions des fluides pétrolières représentent les degrés élevés de 225 à 250 °C.

Mots clefs : Géologie pétrolière, Formation de Mishrif, Le champ pétrolifère de Nassiriya, Inclusions de fluides de pétrole, Microfaciès, Diagenèse carbonatée, Porosité, Carbonate de boue

Acknowledgments

After an intensive period of four years, my thesis has carried out in the laboratory of civil engineering and geo-environment (LGCgE), at Lille1 University for sciences and technologies at Province of highest France. I think the final addition to my thesis must be the notes of thanks for people, whose gave me their confidence during this period.

Foremost, I would like to express my sincere gratitude to my supervisors Prof. DUBOIS Michel and Prof. GAUTHIER Arnaud; whose gave me the acceptance letter, which gave me permission to do my dissertation here in this laboratory. I would like also to thank them for their patience on me during the period of my Ph.D. because; I had lack of knowledge compare with their immense knowledge. They gave me self-confidence through depending on my abilities to build up my dissertation by myself.

Besides my supervisors, I would like to thank my committee members: chair Prof., Prof. DUGUE Olivier, and DR. BERGER Gilles, for their acceptance of assessment my dissertation, for their insightful comments and for their encouragement while defending on my thesis.

I express my warm thanks to Dr. TOULLEC Renaud from Polytechnic Institute of LaSalle Beauvais without his guidance and persistent help this dissertation would not have been finished. My sincere thanks also go to Prof. SHAHROUR Isam, who provided me an opportunity to join his team as the Ph.D. student.

It has been a period of intense learning for me, not only in the scientific field but also on a personal level. Writing this dissertation has had a big impact on me. I would like to reflect on the people who have supported and helped me so much throughout this period.

I thank my labmates for their wonderful collaboration, their discussions were motivating and they were always willing to help me. In particular, I am grateful to Dr. Frank Bourdelle, Dr. LLORET Emily, Dr. DURAND Cyril, Dr. NOFAL Salah, and Dr. MASALEHDANI Naze-Nancy.

I would like to thank all those who contributed in this work especially during the tests microscopy, preparation of thin sections and thick sections (VENTALON Sandra, RECOUNT Philippe, and REGNIER Sylvie). I am using this opportunity to express my gratitude to everyone who supported me throughout my Ph.D. at SN5 house.

This thesis would have never been possible without the financial support of Diyala University, which represented by the collaboration between Ministry of Higher Education of Iraq republic with Campus France Organization. I have a grateful gratitude to each of these public institutions.

I would also like to thank Mr. CHALANCON Adrien, who responsible for the Excellence Programs Department at Campus France and Mrs. HAZIM Marah, who responsible for the follow-up of Iraqi students at Campus France for their persistent help to prepare my documents.

Last but not the least; I would like to thank my family. You are always here near me, in my heart... in my thoughts...in my eyes. Finally, there are my friends...We were able to support each other during our period of study. Thank you very much, everyone!

List of contents

Abstract	3
Résumé	4
Acknowledgments	5
List of contents	7
List of figures	11
List of tables	19
General introduction.....	21
Objectives of the study	21
First chapter.....	25
1.1 Introduction	27
1.2 The Cenomanian-Early Turonian Sequence in the Mesopotamian Zone	30
1.3 Description of the Mishrif Formation	30
1.4 Regional geology of the area.....	31
1.5 Geological and structural setting of Iraq	36
1.6 Fault systems in Iraq	38
1.7 The Mesopotamian Zone.....	40
1.8 Stratigraphy and equivalents of the Mishrif Formation	42
1.9 Evolution of paleogeography during upper Cretaceous	45
1.10 The Kifl Formation.....	48
1.11 The Rumaila Formation	49
1.12 The Late Turonian-Early Campanian Sequence	51
1.13 The Khasib Formation.....	52
1.14 Previous Studies	54
1.15 Major Questions	56
1.16 Major Problematics	57
1.17 Objectives of the study	57
Second chapter.....	61
2.1 Introduction	63
2.2 Sampling.....	63
2.3 Petrographic Description.....	70
2.4 Characteristics of grains	70
2.5 Skeletal grains and microbial grains	70
2.5.1 Foraminifera	71
2.5.1.1 Benthic foraminifera	71
2.5.1.2 Planktonic foraminifera.....	76
2.5.2 Corals	79
2.5.3 Rudists.....	83
2.5.4 Mixed algae zone (Phylloid, Dasyclad and Charophytes)	87
2.5.5 Microproblematica	91
2.5.5.1 Microbialites.....	91

2.6 Non-Skeletal grains (microbial genetic and abiogenic grains)	95
2.6.1 Pellets and Peloidal grains.....	95
2.6.2 Aggregate grains	108
2.6.3 Rounded clastic grains	108
2.7 Matrix or groundmass	111
2.7.1 Micrite	111
2.7.2 Sparry calcite.....	112
2.8 Major criteria are used to differentiate among carbonate microfacies.....	113
2.9 Depositional microfacies.....	114
2.9.1 Lime mudstone microfacies (MF1).....	114
2.9.2 Lime wackestone microfacies (MF2).....	115
2.9.2.1 Lime wackestone submicrofacies bearing large benthic Foraminifera.....	115
2.9.2.2 Lime wackestone submicrofacies bearing Foraminifera.....	115
2.9.2.3 Lime wackestone submicrofacies bearing algae	116
2.9.2.4 Lime wackestone submicrofacies bearing bioclastic	116
2.9.2.5 Lime wackestone submicrofacies bearing rudist	116
2.9.2.6 Lime wackestone submicrofacies bearing lithoclastic	116
2.9.3 Lime packstone microfacies (MF3)	117
2.9.3.1 Lime packstone submicrofacies bearing Microbial carbonate grains	117
2.9.3.2 Lime packstone submicrofacies bearing Miliolid Foraminifera	117
2.9.3.3 Lime packstone submicrofacies bearing Favreina (microcoprolite grains)	118
2.9.4 Lime grainstone microfacies (MF4).....	118
2.9.4.1 Lime grainstone submicrofacies bearing patches of colonial corals.....	118
2.9.4.2 Lime grainstone submicrofacies bearing peloidal grains	119
2.9.4.3 Lime grainstone submicrofacies bearing aggregate-grains.....	119
2.9.5 Lime bindstone microfacies (MF5).....	119
2.10 Carbonate platform types and facies models.....	122
2.11 Depositional environments.....	125
2.11.1 Open marine interior platform environment	130
2.11.2 Restricted interior platform environment	131
2.11.3 Evaporitic or brackish interior platform environment.....	131
2.12 The maturity and evolution stages of the grains demise	133
Third chapter	137
3.1 Diagenetic processes	139
3.2 Factors affecting the efficiency of diagenesis processes.....	139
3.2.1 Pressure	139
3.2.2 Temperature	140
3.2.3 Diagenetic fluids	141
3.2.4 Location of the reservoir	141
3.3 Understanding the diagenetic environment by studying the final forms of pores	142
3.3.1 Introduction to the evolution stages of porosity.....	142
3.3.2 Primary porosity.....	143
3.3.3 Secondary porosity.....	143
3.3.4 Porosity evolution is related to the paleofluids and natural sediments	144

3.4 The important methods are used for understanding the diagenesis processes	149
3.4.1 Petrographic studies	149
3.4.1.1 Morphology of the calcite crystals	149
3.4.1.2 Patterns of the distributed cement in the Mishrif	155
3.4.1.2.1 Calcite cement	157
3.4.1.2.2 Dolomite cement	158
3.4.1.2.3 Exotic minerals in the calcite cement.....	164
3.4.1.3 The relationships between grains and cement have related to the compaction process.....	169
3.4.2 Geochemistry analyses	172
3.4.2.1 Elemental analysis of the cement composition by EDS technique	172
3.4.2.1.1 Calcium and magnesium elements.....	174
3.4.2.1.2 Iron and manganese elements	177
3.4.2.1.3 Silica, aluminum and titanium elements	178
3.4.2.1.4 Sodium, potassium and phosphorus elements.....	182
3.4.2.1.5 Conclusion.....	182
3.4.2.2 Fluid inclusions	188
3.4.2.2.1 Methods.....	188
3.4.2.2.1.1 Petrography	188
3.4.2.2.1.2 Fluorescence.....	189
3.4.2.2.1.3 Microthermometry	189
3.4.2.2.1.4 Microspectrometry Raman.....	189
3.4.2.2.2 Sample preparation.....	190
3.4.2.2.3 Results	190
3.4.2.2.3.1 Microthermometry	195
3.4.2.2.3.2 Raman microspectrometry	198
3.4.2.2.4 Conclusions	202
3.4.2.3 Postdated cementation steps in the stylolite systems	202
3.4.2.3.1 Conclusions	207
Discussion and general conclusion	211
Perspective	221
References	223

List of figures

Figure 1 : Iraqi oil reserves (Shafiq, 2009)	28
Figure 2: Map of Iraq showing a part of the Arabian Peninsula with the location of the main basins and oil fields, including the Nasiriyah oil field after (Al-Ameri et al., 2011). Top left: schematic map of the Nasiriyah oil field with location of the five drill holes (NS-1 to -5).....	29
Figure 3: Correlation of the Mishrif units between drill holes (source: South Oil Company, SOC)	31
Figure 4: Geological setting and structural features of the Arabian Peninsula (Alsharhan and Nairn, 1986, modified from (Powers et al., 1966)	32
Figure 5: Distribution of the main depositional facies of the Mishrif Formation across the Middle East region. Modified after (Dhahny 1998 cited by Aqrabi et al., 2010)	33
Figure 6: Fenced diagram showing the lithological variations and depositional environments in the Mid-Cretaceous across Arabian Peninsula (Alsharhan and Nairn, 1988).....	34
Figure 7: Stratigraphic and tectonic framework (facies and thickness of Upper Thamama and Lower Wasia Formations) of the Arabian Gulf area in the Middle East across the lower and middle Cretaceous (Barremian to Albian) (Wilson, 1975)	35
Figure 8: Fenced diagram showing the lithological variations and depositional environments in the mid-Cretaceous across Arabian Peninsula and Iran (James and Wynd, 1965).....	36
Figure 9: The Stable Shelf Zone, Unstable Shelf Zone and Zagros Suture (Jassim and Goff, 2006)	37
Figure 10: Distribution of faults and fault zones (A) and transversal blocks (B) (Jassim and Goff, 2006).....	39
Figure 11: Mesopotamian zone subdivided into the Euphrates subzone, the Tigris subzone and Zubair subzone (Jassim and Goff, 2006). The grey polygons represent residual gravity anomalies and the red polygons represent undrilled structures of the Mesopotamian Zone ...	41
Figure 12: Profile between Risha (located on NE Jordan) to Naft Khana (Iranian border) (Jassim and Goff, 2006)	42
Figure 13: Depositional system of Mishrif Formation in Iraq, across Cenomanian-early Turonian modified from (Cambridge Carbonates, 2008 cited in Aqrabi et al., 2010).....	43
Figure 14: Contour map of Mishrif Formation that occupies Central and Southern Iraq after (Aqrabi et al., 1998)	44
Figure 15: Stratigraphic section of the Nasiriyah oil field in well NS-1 (source: OEC)	45
Figure 16: Regional isopach map shows facies distribution across Cenomanian Early Turonian (Homci, 1975 cited in BUDAY, 1980)	47
Figure 17: Paleogeography map of Iraq during Cenomanian (Jassim and Goff, 2006).....	48
Figure 18: Isopach map shows the thickness of Rumaila Formation (Jassim and Goff, 2006)	51
Figure 19 : Isopach map of Iraq showing the thickness of Late Turonian- Early Campanian sequence (Jassim and Goff, 2006).....	52
Figure 20: Map of Iraq showing facies distribution across Late Turonian-Early Campanian (Jassim and Goff, 2006)	54
Figure 21: Stratigraphic correlation between sea level and evolution of carbonate platform during Cenomanian-Early Turonian (Jassim and Goff, 2006)	58

Figure 22: Stratigraphic correlation shows the many Formations, which belong to Late Turonian-Danian Megasequence (Jassim and Goff, 2006).....	59
Figure 23 : Location map is the Nasiriyah oil field (Al-Khafaji, 2015).....	64
Figure 24 : Example of cores drilled in the Nasiriyah oil field during the collection process of samples	65
Figure 25 : Samples are collected based on the stratigraphic units of the Mishrif Formation in the NS-1 well (source: South Oil Company, SOC).....	67
Figure 26 : Samples are collected based on the stratigraphic units of the Mishrif Formation in the NS-2 well (source: South Oil Company, SOC).....	67
Figure 27 : Samples are collected based on the stratigraphic units of the Mishrif Formation in the NS-3 well.....	68
Figure 28 : Samples are collected based on the stratigraphic units of the Mishrif Formation in the NS-5 well.....	68
Figure 29 : (A) The abundance of Miliolids (B) Typical chambers of Miliolid (NS-2 well at depth 2014.66 m, Mishrif Formation, SE Iraq).....	72
Figure 30 : The diversity is of benthic Foraminifera in well NS-1 at depth from 2033.80 m to 2064.50 m (Mishrif Formation, SE Iraq)	74
Figure 31 : Longitudinal section is of Chrysalidina, benthic Foraminifer. Chambers are arranged on the form of triserial with decrease of the number of chambers towards the end of the shell. Chambers are strongly overlapping. The final three chambers are occupying one-third to one-half of the shell length. Cenomanian-Turonian age in the NS-3 well at depth of 2024.25 m (Mishrif Formation, SE Iraq)	75
Figure 32 : Cross section of microplanktonic Foraminifera composed of many chambers in carbonate mud with a low proportion of cement. Coiling is fusiform. Chambers are arranged like grape clusters. Well NS-2 at depth 2014.66 m (Mishrif Formation, S Iraq).....	75
Figure 33 : The correlation of Upper Cretaceous is inferred from the analysis of the Mishrif Formation and of the lower part of the Khasib Formation in NS-5 well at depth from 1897.48 m to 1999.60 m, southeast Iraq	78
Figure 34: Polymorphous bodies of colonial corals (A) Colonial corals exist as a polygonal shape (cubic to rectangular), with framework pores (NS-5 well, depth 2031.65 m). (B) Microtabulate coral is a coral honeycomb (NS-5 well, depth 2051.77 m) (Mishrif Formation, Nasiriyah oil field, S Iraq).....	80
Figure 35 : Evolution of preservation stages of framestones (coral skeletons) in the Mishrif Formation in NS-5 well at depth 2014.10 m to 2078.32 m, SE Iraq.....	82
Figure 36 : Similarities and differences between the evolution of preservation stages of corals and diagenetic sketch over time (Flügel and Flügel-Kahler, 1997 cited in Flügel, 2010).....	83
Figure 37 : The growth of superstratal fabric (A) versus the growth of constratal fabric (B) (Gili et al., 1995).....	84
Figure 38 : Enlarged view of different rudist morphotypes. (A) Remnant of arcuate shape. (B) Framestones of vertical morphotypes of rudist were supported by sediments, which have accumulated during growth of their shells. Photos (C & D) show radial lid, which is recumbent as a fine rectangular structure. Photos (E & F) show encrusted rudist with calcite structure and dolomite crystals, which are surrounded them	85

Figure 39 : The compositional maturity of grains reflected matrix type, conditions of environment and diagenetic process. (A) Rudist is encrusted and slightly ribbed, Miliolida joins with rudist and there are many wispy stylolites (well NS-3 2024.25 m). (B) Rudist is encrusted and distinct ribbed (well NS-3 2024.25 m). Normal bivalves have represented geopetal structures in the images (C) NS-2 2002.52 m, (D) NS-1 2033.80 m and (E) NS-3 2024.25 m respectively 86

Figure 40 : The Distribution of Phylloid, Dasyclad and Charophytes alge during upper Cretaceous carbonate platform in the Nasiriyah oil field. 87

Figure 41 : Algae grains are significant grains in the Mishrif Formation. (A) Upright phylloid algae seems leaf-like in the NS-5 well at depth 2049.47 m. (B) Branched phylloid algae in NS-1 well at depth 2027.42 m. (C) Charophyte was a major sediment and producer was near back-reef setting in NS-3 well at depth 2014.67 m. (D) Dasycladaceans green algae are shown as a spiral shape of filamentous structures in NS-3 well at depth 2011.66 m. (E) Gyrogonite is well developed in NS-3 well at depth 2024.25 m. (F) Gyrogonite coincides with planktonic foraminifera that reflect the transgressions of sea in NS-2 well at depth 2014.66 m 89

Figure 42 : Lime bindstone microfacies (MF5). (A) Some phylloid algae are difficult to distinguish their origin, because they have poorly preserved and the calcareous grains are covering all remains of phylloid algae in NS-3 well at depth 2024.25 m. (B) Crown form of dasycladacean green algae is related to fluctuation of sea level in NS-3 well at depth 2011.66 m 90

Figure 43 : Microbial carbonate grains distribution in Upper Cretaceous at Nasiriyah oil fields ... 93

Figure 44 : Microbialites structures are in NS-1 well at depth 2052.90 m as a first cycle of the Microbialites deposition and the second cycle of the Microbialites deposition is at depth 2024.60 m in the same well..... 94

Figure 45 : Faecal pellets contain high content of organic matter and iron sulfides for that reason, they give grayish colour under transmitted light and they have indistinct photos under Cathodoluminescence microscope 98

Figure 46 : Peloids display different sizes and irregular shapes of grains 99

Figure 47 : Upper part of the stratigraphic column reflects the evolution stages of microfacies in the Mishrif Formation in NS-1 well..... 100

Figure 48 : Lower part of the stratigraphic column reflects the evolution stages of microfacies in the Mishrif Formation in NS-1 well..... 101

Figure 49 : Upper part of the stratigraphic column reflects the evolution stages of microfacies in the Mishrif Formation in NS-2 well..... 102

Figure 50 : Lower part of the stratigraphic column reflects the evolution stages of microfacies in the Mishrif Formation in NS-2 well..... 103

Figure 51 : Upper part of the Stratigraphic column reflects the evolution stages of microfacies in the Mishrif Formation in NS-3 well..... 104

Figure 52: Lower part of the stratigraphic column reflects the evolution stages of microfacies in the Mishrif Formation in NS-3 well..... 105

Figure 53 : Upper part of the stratigraphic column reflects the evolution stages of microfacies in the Mishrif Formation in NS-5 well..... 106

Figure 54 : Lower part of the stratigraphic column reflects the evolution stages of microfacies in the Mishrif Formation in NS-5 well..... 107

Figure 55 : The Mishrif Formation shows the different stages during forming of aggregate grains, which are used as differentiated standards to explain the distribution of paleoenvironment. Each of stage has different type from the shape, size, effect of microbial film, ratio of cement comparison of absence of carbonate mud and absence of terrigenous sediments.....	110
Figure 56: (A and B) Rounded clastic grains are existed in NS-1 well at depth 2033.80 m. Calcite evidently exhibits several twinning, with pieces of euhedral Dolomite. (C) Large rounded clastic grain from NS-3 well at depth of 1992.70 m. (D) Accumulated dolomite in the rounded clastic grain from NS-3 well at depth of 2071.21 m	111
Figure 57 : Microporosity of micrite reflects a typical microporous of carbonate reservoir in the Mishrif in NS-2 well at depth of 2014.66 m	112
Figure 58 : Sparry calcite is dominated crystals in the paleopore surrounded by micrite during micritization. Sample from well of NS-1 at depth 2033.80 m	113
Figure 59 : Synopsis of the standard facies belts in the rimmed shelf (Wilson, 1975).....	123
Figure 60 : Sedimentological and biological criteria determined the strict border between the Mishrif and Lower part of the Khasib formations in the NS-5 well at depth 1897.48 and 1899.32 m.....	125
Figure 61 : Vertical frequency of the grains distribution is in Mishrif according to data of (.....	127
Figure 62 : The potential environments of the Mishrif Formation, after.(Hallock and Glenn, 1986)	129
Figure 63 : Some types of the echinoderms exist in the different paleoenvironments in the Mishrif	130
Figure 64 : The potential sedimentary model shows the horizontal distribution of the microfacies in Mishrif Formation in the Nasiriyah oil field, southeast Iraq.....	132
Figure 65 : Depositional model reflects the types of microfacies of the Mishrif reservoir in Nasiriyah oil field.....	133
Figure 66 : Composition maturity of the grains is in NS-5 well at depth 2014.10 m	135
Figure 67 : Microbial bioherm likes semi-ductile calcite cement in the Mishrif. The quantity of carbonate mud increases by increasing the effect of pressure. Fractures occur by the effect of differential compaction in the calcite belt. The black arrows indicate to these fractures. Sample is taken from the NS-3 well at depth of 2007.32 m	139
Figure 68 : Pressure affects the shapes of moldic pores. (A) Biomoldic pores are rounded shape in the NS-3 well at depth 2024.25 m. (B) Biomoldic pores are elongated shape in the NS-5 well at depth of 2014.10 m.....	140
Figure 69 : Solid pyrobitumen is in the NS-3 well at depth 2003.53 m.....	141
Figure 70 : The patterns of secondary porosity are used as a critical tool to determine the diagenetic environments. The dissolution pores (A, B, C & D) are dominant pores in the NS-1, NS-2 and NS-3 wells. Cathodoluminescence shows the degassing pores (E & F) in the NS-2 well at depth 2062.60 m.....	146
Figure 71 : Primary porosity includes two types as the fenestral porosity and interparticle porosity in (C &D). Moldic porosity is evolved through diagenetic environment in the NS-5 well at depth of 2014.10 to 2031.65 m in (A, B, E & F)	147
Figure 72 : The main diagenetic environments and the common diagenetic processes are drawn based on the concept of porosity modification and evolution (Moore, 1989)	148

Figure 73 : Paragenetic sequence of the porosity evolution is shown the evolution of diagenetic fluids, found in the Mishrif in the Nasiriyah oil field	148
Figure 74 : scheme shows the growing calcite crystals under the theory of sideway poisoning by Mg cation (Folk, 1974).....	150
Figure 75 : SEM shows the transformation of the bladed calcite crystals to the dolomite grains. The red arrows indicate to the endings of the calcite crystals before the transformation process and the yellow arrows indicate to the endings of the calcite crystals during transformation process	152
Figure 76 : (A) Bladed calcite crystals (arrows red) are like dogtooth spar, evolved to equant cement calcite crystals (arrow black) in the NS-5 well at depth of 2014.10 m. (B) SEM image shows the form of cement as the dogtooth spar, which is dominated as prismatic grains in the most of the Mishrif Formation in the NS-5 well at depth of 2031.65 m.....	153
Figure 77 : PL Microscope shows the crystal shapes of the calcite cement and the final fabric of the calcite crystals	154
Figure 78 : SEM shows the coral spots, which have had different types of distribution patterns of the cements in Mishrif Formation at the well of NS-5 at depth of 2014.10 m	156
Figure 79 : Cathodoluminescence microscope shows syntaxial overgrowth fabrics cement at the older pore spaces in Mishrif Formation that may be reflects the nucleation patterns. (A) Phylloid algae grew as calcite cement in the well of NS-1 at depth of 2027.42 m. (B) Residue of the rudist calcite cement in the well of NS-5 at depth of 2051.77 m. (C) Luminescent dolomite zone is existed in the well of NS-2 at depth of 2005.55 m	161
Figure 80 : Cathodoluminescence microscope shows dolomite sediments, which have increased with the depth of the Mishrif Formation at the wells of NS-2, NS-3 and NS-5 at depths of 2062.60 m, 2070.21 m and 2075.19 m respectively	162
Figure 81 : Cathodoluminescence microscope shows the Medium size of crystals dolomite cement, which have synchronized with forming stylolite systems in the wells of NS-1 & NS-2 at depths of 2027.42 m and 2014.66 m respectively of the Mishrif Formation at Nasiriyah oil field.....	163
Figure 82 : Concurrent clay minerals have been evolved during the final products of the diagenesis processes. Clay minerals are engulfed in calcite cement that have formed wispy fabrics in the ghost texture (O.M means residue of the organic material, C.M means clay minerals). This photo is taken under SEM and sample belongs to the well of NS-3 at depth of 1992.70 m..	164
Figure 83 : Silicification process took place in the late stages of the diagenesis process at the well of NS-2 2014.66 m.....	166
Figure 84 : First stage of pyrite mineral has covered the foraminifer's structure in the advanced stages of diagenesis process at the well of NS-1 at depth of 2048.95 m.....	166
Figure 85 : Cubic pyrite has final distribution around secondary pore space in the well of NS-3 at depth of 2014.67 m.....	168
Figure 86 : Raman spectroscopy shows the integrated spectrum zone of pyrite and carbon minerals, which reflected the solid bitumen according to transmitted microscope analysis of the same point in Mishrif Formation at Nasiriyah oil field at well of NS-3 of depth 2003.53 m.....	168
Figure 87 : Raman spectroscopy shows the integrated spectrum zone of the minor pyrite mineral and the large band of carbon mineral, which reflected the bitumen in advanced stages of	

diagenesis process in Mishrif Formation at Nasiriyah oil field at well of NS-1 of depth 2033.80 m.....	169
Figure 88 : Cathodoluminescence microscope shows some of the differences between the early cement and the late cement that are related to redistribution process of elemental compositions in the Mishrif Formation at the wells of NS-3, NS-1 and NS-3 at depths of 2003.53 m, 2027.42 m and 1992.70 m respectively.....	171
Figure 89 : Distribution of main carbonate elements in calcite cement and dolomite cement. The interpretations are according to chemical composition of carbonate minerals	177
Figure 90 : The behavior of the silica and aluminium elements in carbonate rocks with respect to Eh-PH conditions	179
Figure 91 : Negative relationship is between silica and main carbonate elements	179
Figure 92 : Negative relationship is between aluminium and main carbonate elements	180
Figure 93 : Integrated zone of silica element in intracrystalline carbonate minerals under Eh-PH conditions, maybe lead us to identify the zone of stoichiometric interaction of calcium silicate mineral.....	180
Figure 94 : Integrated zone of aluminium and carbonate elements under conditions of high temperature, it maybe leads to identify the zone of stoichiometric interaction of calcium aluminates groups.....	181
Figure 95 : The behavior of Al and Ti elements in the carbonate rocks with respect to Eh-PH conditions	181
Figure 96 : SEM with EDS technique show various types of cement in the different distribution patterns at Mishrif Formation of Nasiriyah oil field in the wells of (A) NS-3 2011.66 m, (B) NS-3 1992.70 m, (C) NS-2 2014.66 m, (D) NS-3 2011.66 m, (E) NS-1 2024.60 m, (F) NS-2 2023.05 m, (G) NS-2 1993.10 m, and (H) NS-3 2014.67m.....	183
Figure 97 : EDS Cartography shows the elements distribution for hydrothermal calcium-silicate cement in the (Figure 96) at the well of NS-2 at depth of 2023.05 m.....	185
Figure 98 : EDS Cartography shows the elements distribution for later secondary dolomite cement in the (Figure 96.A) at the well of NS-3 at depth of 2011.66 m	187
Figure 99 : EDS technique shows spectrum of elemental composition in the well of NS-3 at depth of 2011.66 m	187
Figure 100 : Distribution patterns of many fluid inclusions in the Mishrif Formation in the Nasiriyah oil field. (A) Petroleum fluid inclusions have filled some etches pits as a primary fluid inclusion in well NS-2 at depth 2005.55 m. (B) Petroleum fluid inclusions have filled micro-fracture as a secondary fluid inclusion in well NS-5 at depth 2014.10 m.....	191
Figure 101 : Pseudosecondary petroleum fluid inclusions distributed as trails. (A). The red arrows have indicated to remains of bitumen, black arrows indicate trails of petroleum fluid inclusion and yellow arrows indicate locations of pores in well NS-1 at depth 2033.80 m. (B) Clear trails of the petroleum fluid inclusions in calcite in well NS-2 at depth 2048.26 m.....	192
Figure 102 : The comparison between transmitted light colour on the left side and fluorescent light colour on the right side can be used as a critical tool to distinguish between aqueous fluid inclusions and petroleum fluid inclusions as well, to discriminate among the components of petroleum fluid inclusions too.....	193
Figure 103 : Some of classical textures of the petroleum fluid inclusions are existed in carbonate rocks at Mishrif Formation. The proportion between liquid and vapour at room temperature	

can be used for identification the petrographic and chemical properties of petroleum fluid inclusions.....	194
Figure 104 : Histogram of the homogenisation temperatures (Th °C) shows the multi-generations of Th (°C) aqueous and petroleum fluid inclusions based on their frequencies under microthermometer microscope.....	196
Figure 105 : Ice melting temperature (Tm ice) versus homogenisation temperature (Th)	196
Figure 106 : Primary aqueous inclusions in calcite.....	197
Figure 107 : Raman spectrum shows multiphase inclusion, which is in the calcite cement around moldic porosity in the NS-3 well at depth of 2014.67 m	198
Figure 108 : Raman spectrum of the fluid inclusion shows the pyrite and silicate peaks in the NS-3 well at depth 2014.67 m	199
Figure 109 : Raman spectrum shows the peak of N ₂ gas in the NS-1 well at depth 2033.80 m....	199
Figure 110 : Raman spectrum of a fluid inclusion indicative of the presence of H ₂ S gases in well NS-3 at depth 2024.25 m.....	200
Figure 111 : Raman spectrum shows the range of H ₂ S peaks in the NS-1 well at depth 2033.80 m	200
Figure 112 : Fluid inclusions show multi-peaks of methane in the NS-3 well at depth 2024.25 m	201
Figure 113 : Raman spectrum shows the peak of dissolved carbon in water.....	201
Figure 114 : The images are gained by BSE and EDS elemental map of the stylolite in muddy carbonate rocks.....	206
Figure 115 : Spectrum of elemental analysis is acquired by EDS technique, which is accompanied to SEM.....	206
Figure 116 : Scheme of stylolite shows the data are generated by using EDS technique, near the vicinity of stylolite with absence of the sulfate element in the center of stylolite	207
Figure 117: Scheme of stylolite shows the data are generated by using EDS technique, which look alike as a cross section of the stylolite in presence of the sulfate element.....	207
Figure 118 : Fenestral porosity is a pore space, developed by degassing process within the bioturbated wackestone microfacies in the NS-1 well at depth of 2033.80 m. Solution seams are associated by fenestral porosity.....	209

List of tables

Table 1: Distribution of samples is related to reservoir units	66
Table 2 : Thin sections of samples prepared for microfacies analysis.....	69
Table 3 : Synopsis of the microfacies data has built from various samples took from the Mishrif Formation. These samples reflected a microfacies type (MFT), represented the equivalent textures of the Dunham and they determine type of the depositional environments	120
Table 4 : The values of vertical distribution of the fossils include high frequencies in the wells	126
Table 5 : First group of the grains includes high frequency of the best indicators of the paleoenvironments	127
Table 6 : Second group of the grains includes frequency less than 10 m in the depth	128
Table 7 : First analysis of the elemental composition shows the atomic percentage for the elements concentration, which are generated by EDS technique from various samples of the calcite cements and the dolomite cements. Synopsis data are before normalization process.....	176
Table 8 : Second analysis of the elemental composition shows the atomic percentage of the elements in the poststylolite at the well of NS-3 at depth of 1992.70 m. Synopsis data are before normalization process	176
Table 9 : Thick sections samples prepared for fluid inclusion analysis.....	190
Table 10 : The stylolite data are generated by using EDS technique.....	204
Table 11 : Petrography of the fluid inclusions and microthermometry data.....	243

General introduction

The exploration and management hydrocarbon fields are the main reasons to study carbonate reservoirs that allow learning more about how to find hydrocarbon reservoirs, extract resources and manage the oil, gas, or other resources. Middle East carbonate reservoirs contain around 50% of the world oil reserves (Nurmi and Standen, 1997). Carbonates hold about half of the world oil, gas and extensive deposits of the metallic ores (Ahr, 2011).

Cretaceous succession has been extensively studied because it contains the abundance of hydrocarbon reservoirs. It represents the most productive period in Iraq and Arab Gulf States. Cretaceous succession contains about 80% of the Iraqi oil reserves. Cretaceous succession is divided into two intervals: i) Upper Cretaceous. ii) Lower Cretaceous. This study will highlight the Mishrif Formation, which belongs to the Upper Cretaceous during Cenomanian-Early Turonian age. Mishrif is an important carbonate reservoir throughout the Middle East that has explored in the different countries such as Iraq, Kuwait, Saudi Arabia, Qatar, United Arab Emirates, Oman, Iran, the eastern south border of Turkey and the eastern north border of Syria.

Mishrif reserves are accommodating more than one-third of the proven Iraqi oil reserves. Rocks of the Mishrif represent the high chemically quality because these rocks include the bioclastic, microbic and detrital limestones. Microfacies analyses show the fossils types, including coral, algal, foraminifera, rudist, microbial limestone and abiogenic limestone with reservoir porosity is exceeded 22% (Handel, 2006) and the permeability ranges from 23-775 mD (Jreou, 2013a). A shallow-water environment to back reef environment of the carbonate shelf dominates the Mishrif Formation.

The 19 wells of Nasiriyah oil field contain Mishrif Formation as a major reservoir. Mishrif extends throughout the Mesopotamian Basin and his thickness reaches to 200 m in the wells of the Nasiriyah oil field at the subsurface depths around 1,900–2,100 m. However, most of the used data to study this reservoir are cuttings of the drill cores, exploration reports, and production data of the Nasiriyah oil field.

Study of the paleofluid includes the distribution of multi-generational fluid inclusions. The major elements and trace elements affect the stability of the metastable minerals. Aggressive pore fluids are an important factor that formed during hydrocarbon maturation or hydrocarbon thermal degradation after petroleum migration process. Aggressive pore fluids are produced by mixing process or interaction process between the diagenetic fluids.

Objectives of the study

This study has been focused on the properties of the Mishrif Formation, belonged to Cenomanian-Early Turonian age. Mishrif is the most promising productive Formation in the Nasiriyah oil field. The detailed study deals with the relationships between paleogeographic proxies and the evolution of tectonic activity in the northern part of the Arabian Peninsula during upper Cretaceous. Summary of the major problems are related to microfacies analysis, depositional environments and some observations of the Mass extinction in upper Cretaceous.

The final objective is focusing on the diagenetic environment, which is related to the porosity evolution during the evolution of Paleofluid.

In order to achieve these objectives, this thesis is presented in three main chapters, which are subdivided into several parts:

- **First chapter** is an important chapter because it gives information about the area of study and this information has subdivided into: - First part is a classic part, which deals with general context of the study area that contains the introduction, objectives of the study, method of study and previous studies. The second part explains the formations in two sequences at the upper Cretaceous. The first sequence is a Cenomanian-Early Turonian, which contains the Mishrif, Kifl and Rumaila formations. The second sequence is a Late Turonian-Early Campanian, which contains the Khasib Formation. The third part deals with geological and paleogeographical characteristics as a local scale. The geological features of the north parts of Arabian Peninsula represent the regional scale of this study. Fourth part represents the discussion and the conclusion points; the first point summarizes the major problems in the Mishrif Formation. The second point highlights the Paleogeography evolution during the Cenomanian-Early Turonian across the Arabian platform. On one hand, the major factor in this chapter is a site of the Mishrif reservoir in the large carbonate basin at the Middle East that has undergone to effect of the Tethys Ocean by microfacies distribution and the paleodepositional environments. On the other hand, the impacts of the fault systems and the differentiation compaction of the buried rocks column.
- **Second chapter** is called microfacies analysis and paleodepositional environments. Petrography study is an important tool that is used to highlight on fifth goals in this chapter. First objective deals with sampling and characteristics of the grains in detail. Mishrif includes many of the various grains, which classify depend on the genetic origin of these carbonate grains. There are three types of the genetic origin, included the biological, microbial and abiogenic grains. Previous types of the genetic origin divide into two groups of the grains in this study. The first group is skeletal and microbial grains that consist of the benthic and planktonic Foraminifera, Corals, Rudist, Mixed algae zone contains Phylloid, Desyclad and Charophytes algae. Finally, Microproblematica contains Microbialite and *Favreina* microcoprolite as a microbial origin. The second group is the Non-Skeletal grains include the microbial and abiogenic origins. Non-Skeletal grains contain the Pellets, Peloids, aggregate grains and rounded clastic grains. The study of textures, fabrics grains and the condition of deposition process reveal the influences of biological, microbial and non-biological origin. In this chapter, the sequence of described grains confirms that carbonate grains are interrelated with each other.

Second objective deals with the matrix or groundmass, which is represented by the micrite and sparry calcite. The third objective is a Microfacies analysis, which consists of lime mudstones microfacies, lime wackestone microfacies, lime packstone microfacies, lime grainstone microfacies and lime bindstones microfacies that is divided into various sub-microfacies. The fourth objective shows the types of Paleodepositional environments of the interior platform that includes the reef patches of open marine, restricted and evaporitic environments. Finally, the fifth objective deals with the maturity and evolution stages of the grains demise as conclusion points.

Third chapter deals with the diagenetic study, which has been used to detect the passages of the paleofluid in the Mishrif by study the evolution and expansion of the pores, stylolite and fractures systems. The first step deals with the general context of diagenesis process and the factors, which are affected the efficiency of diagenesis processes such as pressure, temperature, diagenetic fluids and the basin site factor. The second step is related to study the diagenetic environment by study the final forms of the pores systems. The second step is concurrent with study the chemical evolution stages of the paleofluid. Other important methods are used to understand the diagenetic stages in the Mishrif. Diagenetic studies consist of several procedures, which are mainly concerned with the cement types, shapes, and patterns of calcite cement. The conclusions of diagenetic studies suggest the huge distribution of blocky calcite cement as a major type of cement in the Mishrif. The volume of medium size of the dolomite crystals reflects the intermediate stage of the evolution stages of the diagenetic environment. Exotic cement includes siliciclastic cement, evaporitic cement, pyrite and bitumen with huge amounts of the mud carbonate. The third step is the geochemical analyses, including the elemental composition analyzed by the EDS technique and fluid inclusions analysis to detect the chemical composition of paleofluid and the source of paleofluid.

First chapter
THE STUDY AREA AND EVOLUTION OF PALEOGEOGRAPHY
DURING LATE CRETACEOUS

1.1 Introduction

The Nasiriyah oil field was mapped by 2D seismic in 1975 and oil was discovered in the Mishrif, Yamama and Nahr Umr reservoirs, respectively based on their depths. In 1978, well NS-1 was drilled. The Mishrif Formation is Cenomanian-Early Turonian in age, according to Chatton and Hart, (1962c). It represents a heterogeneous formation originally described as organic detrital limestones with algal, rudist, and coral-reef layers, capped by limonitic fresh water limestones. The Mishrif Formation has a thickness of 170, 171.5, 171.5, 177 and 180.2 meters respectively in five drill holes (NS-1, NS-2, NS-3, NS-4, and NS-5) in the Nasiriyah field (Handel, 2006). From 2008 to 2011, a 3D seismic survey was acquired. Total reserves of oil are estimated to be 16 billion barrels. However, 19 wells have been drilled to the depth of the Mishrif reservoir and as estimation for 2013-14; they are producing a little more than 40,000 barrels oil per day (bopd).

The Mishrif formation is located in an anticline of a relatively narrow belt extending NW-SE across the central Mesopotamian Basin (SE of Iraq). This formation contains more than one-third of the proven Iraqi oil reserves. In this study, the Mishrif Formation has been investigated in several wells in Nasiriyah oil field, located about 38 km at the NW of Nasiriyah City in Thi-Qar Province. This study focuses on facies analysis, depositional environments, diagenetic processes, and their effects on properties of the Mishrif Formation, which is the most promising productive formation in the study area. The lower contact of the Mishrif Formation is conformable with the underlying unit, the Rumaila Formation. The upper contact of the Mishrif Formation is unconformable with the Khasib Formation.

Although geological investigations of the Arabian Peninsula have initially lagged behind those of Western Europe, the very great economic importance of the hydrocarbon potential legitimates the study of Cretaceous and Jurassic rocks forming the shelf. This shelf has acted as a powerful motive for a detailed study.

We have modified our vision in light of the intensive investigation by many companies. The information became a base for facies stratigraphic terminology, but many terms are not consistent with facies definition or position of stratigraphic boundaries (Alsharhan and Kendall, 1986), leading to conflicting terminologies. The Cretaceous succession has been extensively studied because it contains abundant reservoir intervals. It is the most productive interval in Iraq and it contains about 80% of the country oil reserves (Figure 1).

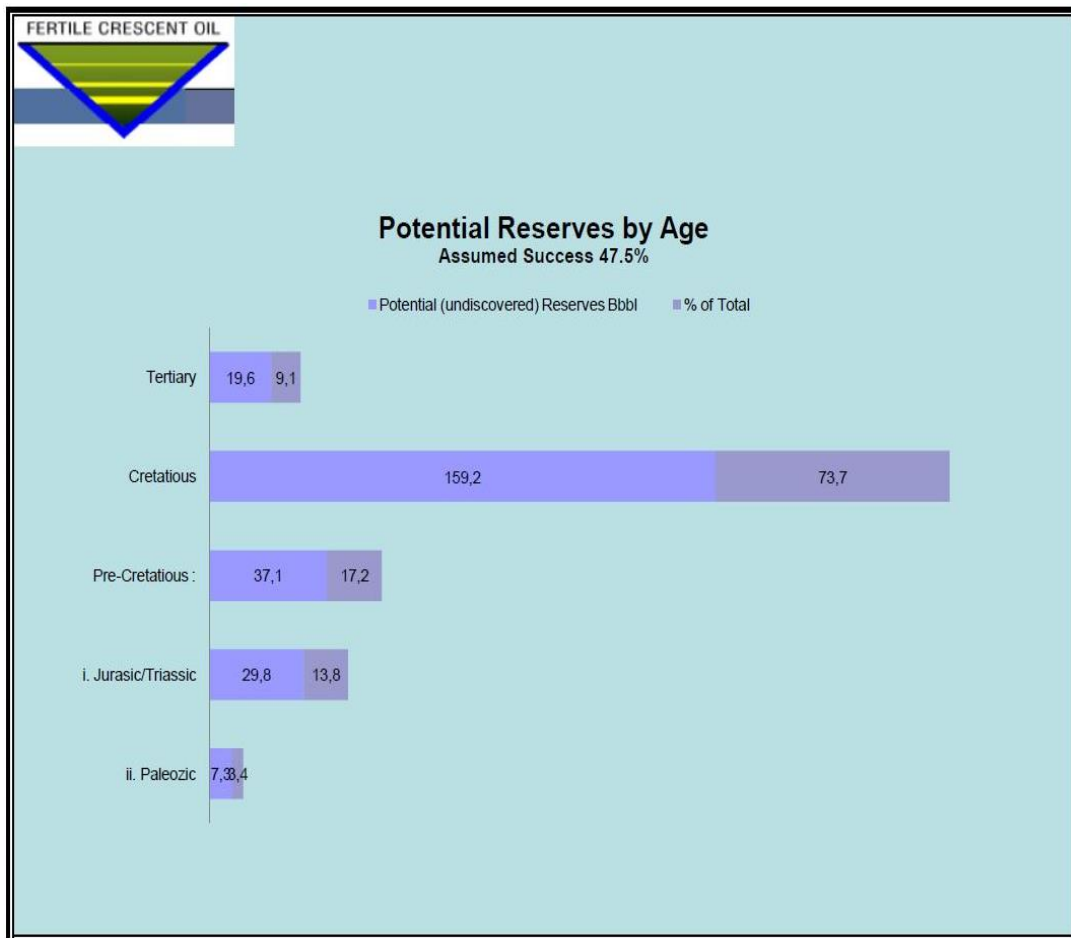


Figure 1 : Iraqi oil reserves (Shafiq, 2009)

Mishrif Formation extends throughout the Arabian Peninsula. In the Mesopotamian Basin, the thickness can reach 200 m in the Nasiriyah District at depths of around 1,900–2,100 m (Figure 2).

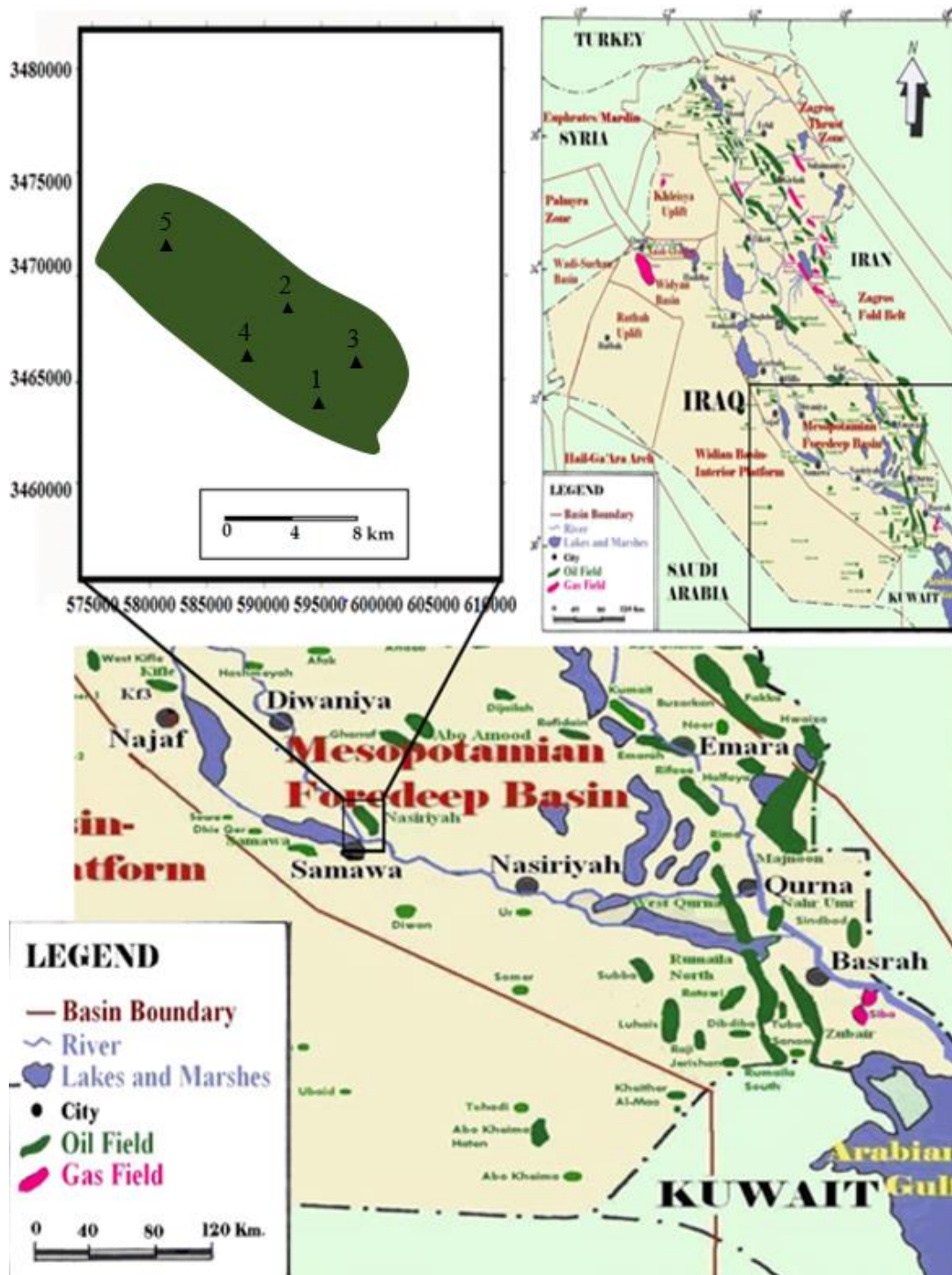


Figure 2: Map of Iraq showing a part of the Arabian Peninsula with the location of the main basins and oil fields, including the Nasiriyah oil field after (Al-Ameri et al., 2011). Top left: schematic map of the Nasiriyah oil field with location of the five drill holes (NS-1 to -5)

1.2 The Cenomanian-Early Turonian Sequence in the Mesopotamian Zone

The Cenomanian-Early Turonian Sequence is regionally represented in numerous formations such as Mishrif, Rumaila and Kifl (Chatton et al., 1961) that will explain in detail in the following sections, as well as Rutba, M'sad, Ahmadi, Dokan, and Upper Balambo, all inside the Iraqi territory. Outside Iraq, some contemporaneous formations are represented by the shaly-calcareous part of the Kazdhumi Formation and perhaps the *Oligostegina* in Sarwak of the eastern parts of Zagros-Iran (Furst, 1970). However, our study will focus on the most productive formations in the Mesopotamian Zone of Southern Iraq: Mishrif, Rumaila and Kifl.

Chatton and Hart (1962b) proposed to regroup the previous Mahliban, Fahad and Maotsi formations of the NW Mesopotamian Zone into the Rumaila Formation. Moreover, Chatton and Hart (1962c) recommended to include the neritic and partly reef forming limestones of the M'sad, Gir Bir and Mergi formations, into the Mishrif Formation. Finally, as emphasized by Buday (1980a), they introduced Kifl as a new formation.

The Cenomanian-Early Turonian sequence includes many events such as the deformation of the NE margin of the Arabian plate adjacent to the Tethys Ocean and an extended effect of the Najd Fault system, as well as the transgression of the sea onto the regions of NW Mesopotamian Zone and Rutba high.

1.3 Description of the Mishrif Formation

The Nasiryah oil field lies in the Mesopotamian Basin, representing the easternmost unit of the stable shelf (Jassim and Goff, 2006). The Mesopotamian Basin occupies most of SE and Central Iraq and is bounded in the NE by the folded ranges of Pesh-i-Kuh to the east and Hemrin and Makhul Mountains to the north. The W and SW boundary is controlled by faults (Aqrabi et al., 1998). The study area is an anticline structure generally orienting NW-SE (Aqrabi et al., 2010) and has an extension of 30 km long by 10 km width. The main oil accumulation zones are successively the Mishrif, the Yamama and the Nahr Umr formations according to their depth. The Mishrif Formation is very heterogeneous with permeability ranging from 23 to 775 mD, which reflects a wide diversity of rock characteristics. The API gravity of oil is typically 23-36.6, averaging around 25.

According to the correlation between units obtained from South Oil Company (SOC) based on the well logging data (Figure 3), the Mishrif Formation can be divided into six units (Handel, 2006) that includes:

- Cap rock
- Upper Mishrif
- Shale
- First reservoir unit #1
- Barrier rocks
- Reservoir unit #2 is divided into 2 sub-units:
 - Zone of high-saturated oil
 - Zone of high-saturated water

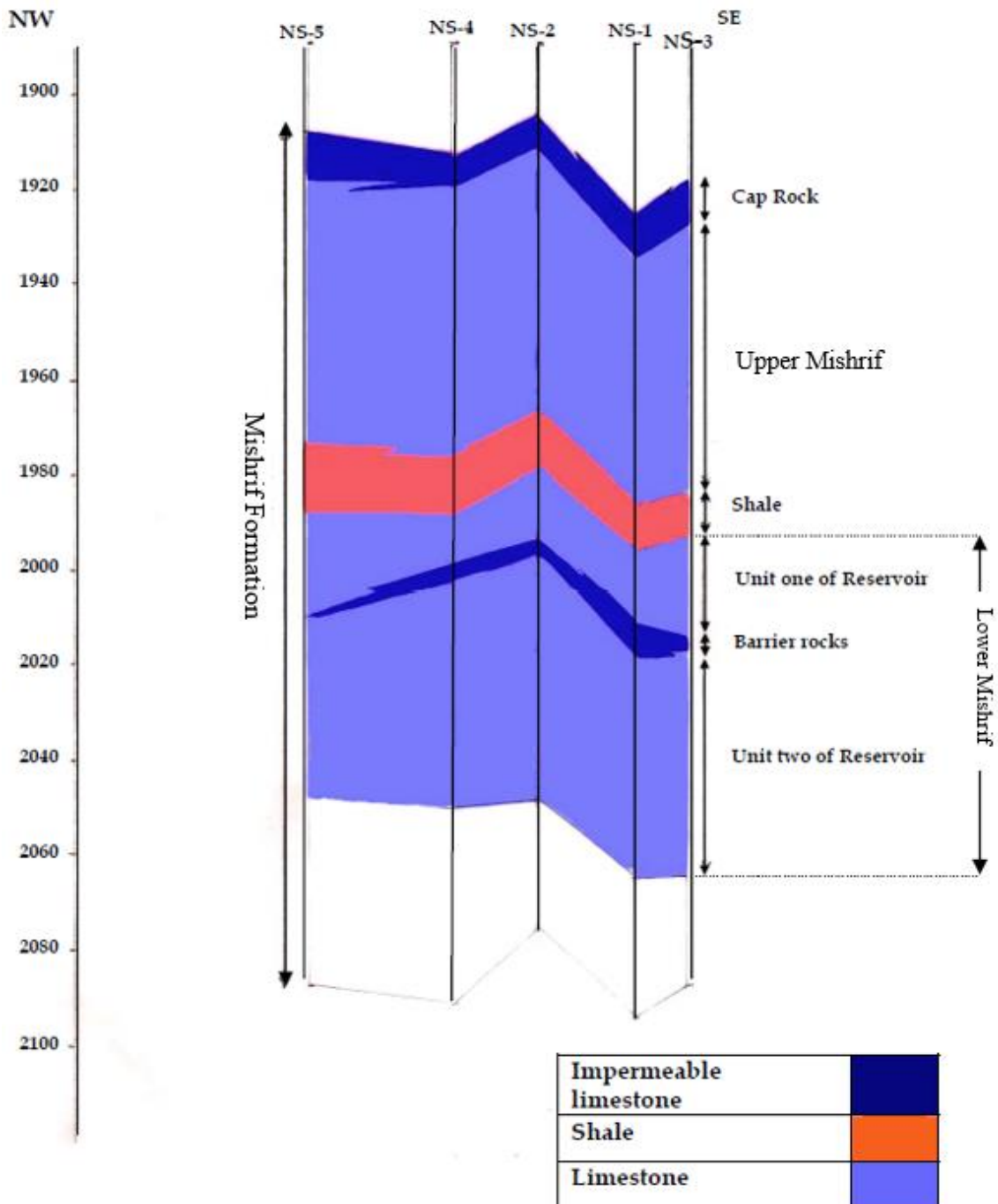


Figure 3: Correlation of the Mishrif units between drill holes (source: South Oil Company, SOC)

1.4 Regional geology of the area

Iraq is considered as a part of the Arabian Peninsula, which has three natural boundaries: it is separated from Africa by the Red Sea; from Iran by the Arabian Gulf and the Gulf of Oman; and in the south by the Arabian Sea (Figure 4). The Peninsula is broadly flexured, with two obvious elements orienting NE-SW: the Rub Al-Khali depression, and the broad anticlinal structure (Central Arabian Arch) (Alsharhan and Nairn, 1986).

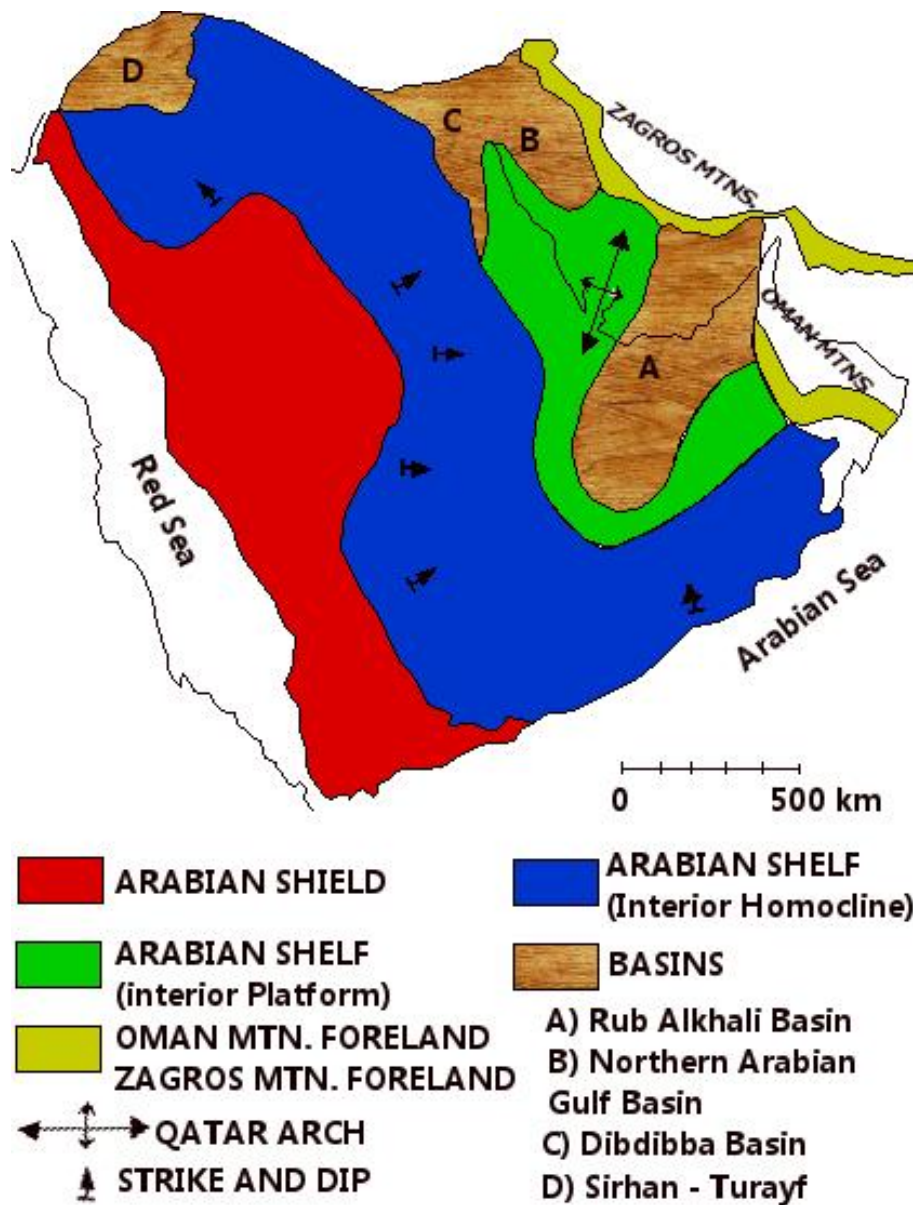


Figure 4: Geological setting and structural features of the Arabian Peninsula modified after (Alsharhan and Nairn, 1986 & Powers et al., 1966)

The Arabian Peninsula is affected by three main geotectonic units (Figure 4) described by Henson (1951) and Powers et al. (1966):

- The Arabian shield: a vast and complex area of Precambrian igneous and metamorphic rocks occupying the western and central part of the Arabian Peninsula.
- The Arabian shelf: the continuation northward and eastward of the Arabian shield below a cover of continental and shallow marine Phanerozoic sediments.
- The mobile belt of Zagros and Oman mountains lying north and NE of the Arabian shelf.

The lithofacies distribution map of the Mishrif Formation shows the complex distribution of the facies types. The shelf margin is represented by rudist biostrome facies, including the Nasiriyah oil field (Figure 5).

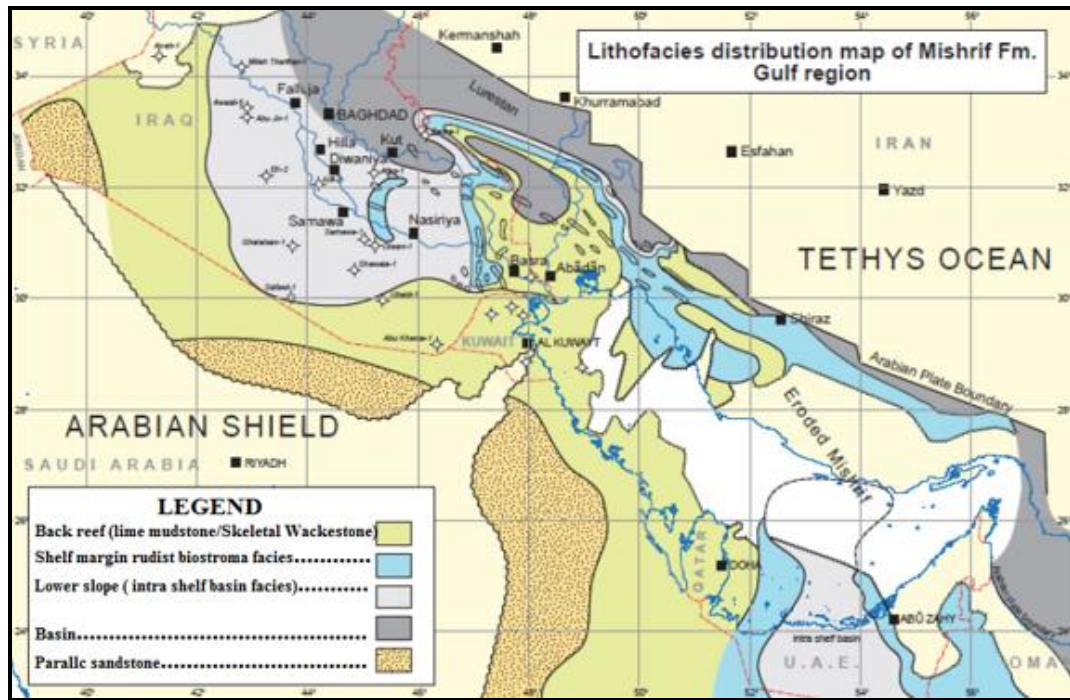


Figure 5: Distribution of the main depositional facies of the Mishrif Formation across the Middle East region. Modified after (Dihny 1998 cited by Aqrabi et al., 2010)

The Mesopotamian Basin is located in central and SE of Iraq in the corner between Arabian Shield and the folded ranges of the Zagros. In addition, it represents the continuation of the Arabian shelf especially for the Mishrif, Mauddoud and Nahr Umr formations, which extend across countries of the Arabian Peninsula (Iraq, Kuwait, Saudi Arabia, Qatar, U.A.E., and N.W.Oman) as well as in the W of Iran. Two clastic-carbonate cycles are visible in the NE part of the Arabian Gulf: The lower Nahr Umr-Mauddud cycle and an upper Wara-Mishrif cycle (Figure 6) (Alsharhan and Nairn, 1988).

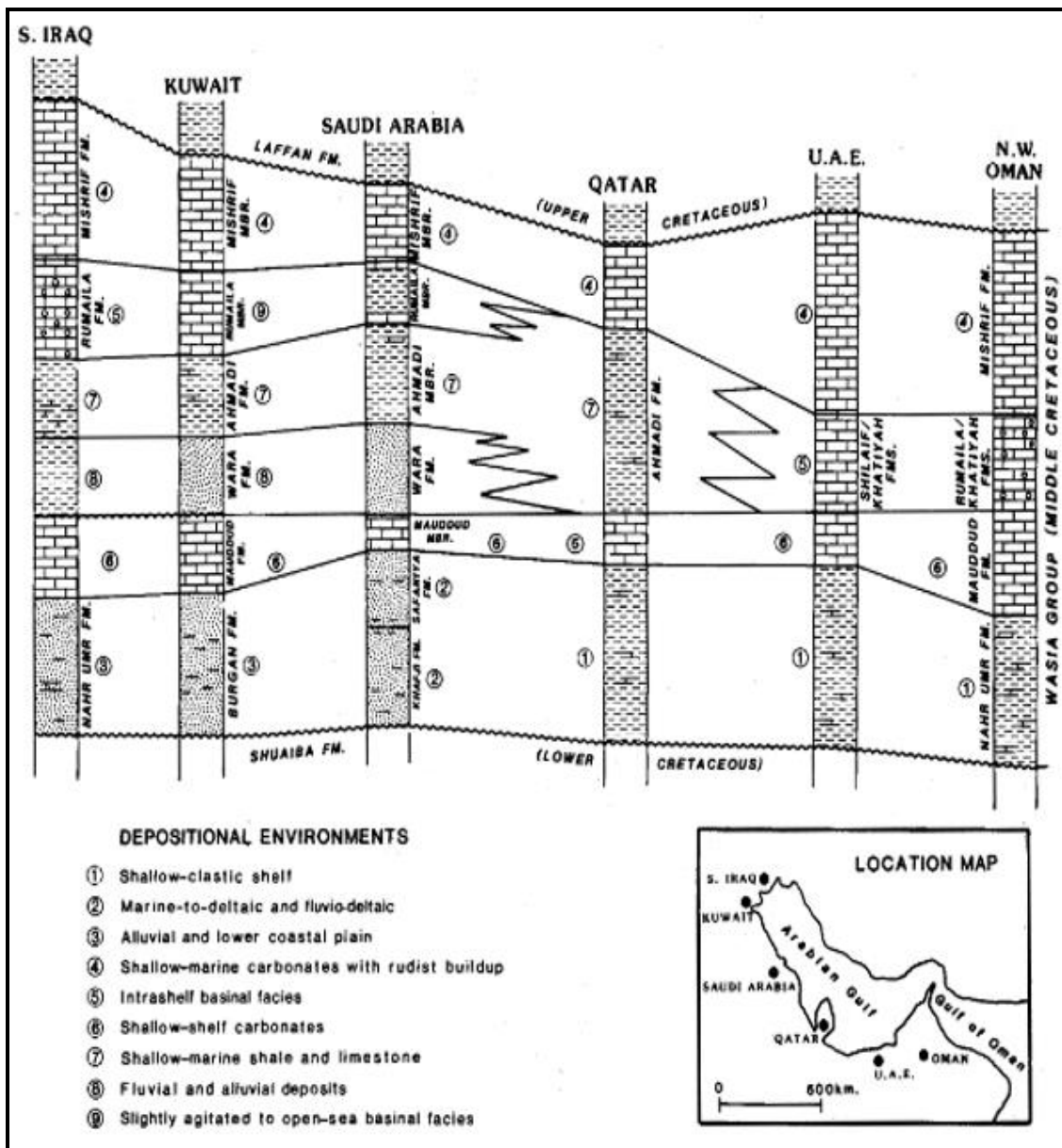


Figure 6: Fenced diagram showing the lithological variations and depositional environments in the Mid-Cretaceous across Arabian Peninsula (Alsharhan and Nairn, 1988)

Note that the lithologic interpretation is taken mainly from reference sections. In the Figure 6, the boundary between the lower and upper cycles is horizontally placed to highlight variations in lithology (Alsharhan and Nairn, 1988). The important geological features of the Arabian Peninsula and Iran are the stratigraphic and the tectonic framework. Mesozoic limestones in the Zagros geosyncline has a high thickness of carbonate buildups. The shallow water of carbonate layer overlies the center of the Zagros geosyncline, characterized by very thin in thickness that probably reaches to a half or quarter of the basinal thickness.

The Mosul Uplift of Iraq, the Zagros front of Iran and Rub Al-Khali basin of Saudi Arabia have the same age and the same facies characteristics. In addition, early Cretaceous facies are extending through the center and south Iraq to the N of the Arabian Peninsula and NW of Iran. The tectonic effect of Zagros has played a major role in the redistribution the Mesozoic facies (Figure 7).

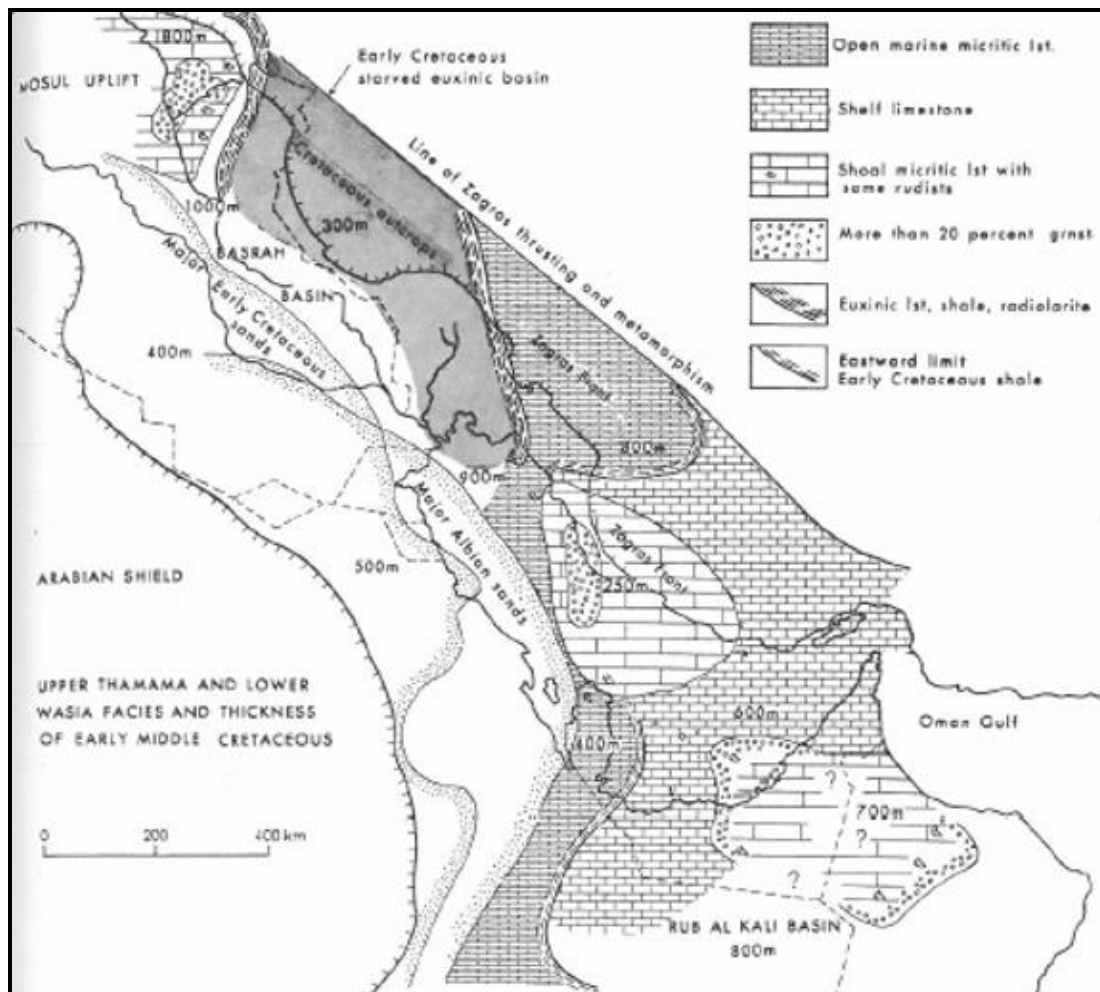


Figure 7: Stratigraphic and tectonic framework (facies and thickness of Upper Thamama and Lower Wasia Formations) of the Arabian Gulf area in the Middle East across the lower and middle Cretaceous (Barremian to Albian) (Wilson, 1975)

Off the coast of Iran, the second cycle is entirely represented by the Sarvak Formation. The limestone shows a trend from a lower, deeper-water sequence of thin-bedded, fine-grained argillaceous carbonates with *Pithonella*, passing up into massively bedded, neritic limestone with rudists and rich microfauna (Figure 8) (James and Wynd, 1965).

Economically, the Mishrif Formation is considered as essential in the study area, compared to the Mauddoud and Nahr Umr formations for three reasons: the Mishrif Formation represents a heterogeneous formation, containing large accumulations of organic material and affected by numerous structures containing oil and gas and it is relatively the most shallow formation relative to the Earth surface. In addition, to the S and SE of Iraq, the largest accumulation is in the Rumaila North, Rumaila South, West Qurna, Zubair, Majnoon, and Halfaiya fields. At least 15 other commercial oil accumulations in the Mishrif Formation have been discovered in southeast Iraq: Abu Ghirab, Ahdab, Amara, Buzurgan, Dujaila, Jabel Fauqi, Gharraf, Hawaiza, etc, (Aqrawi et al., 2010).

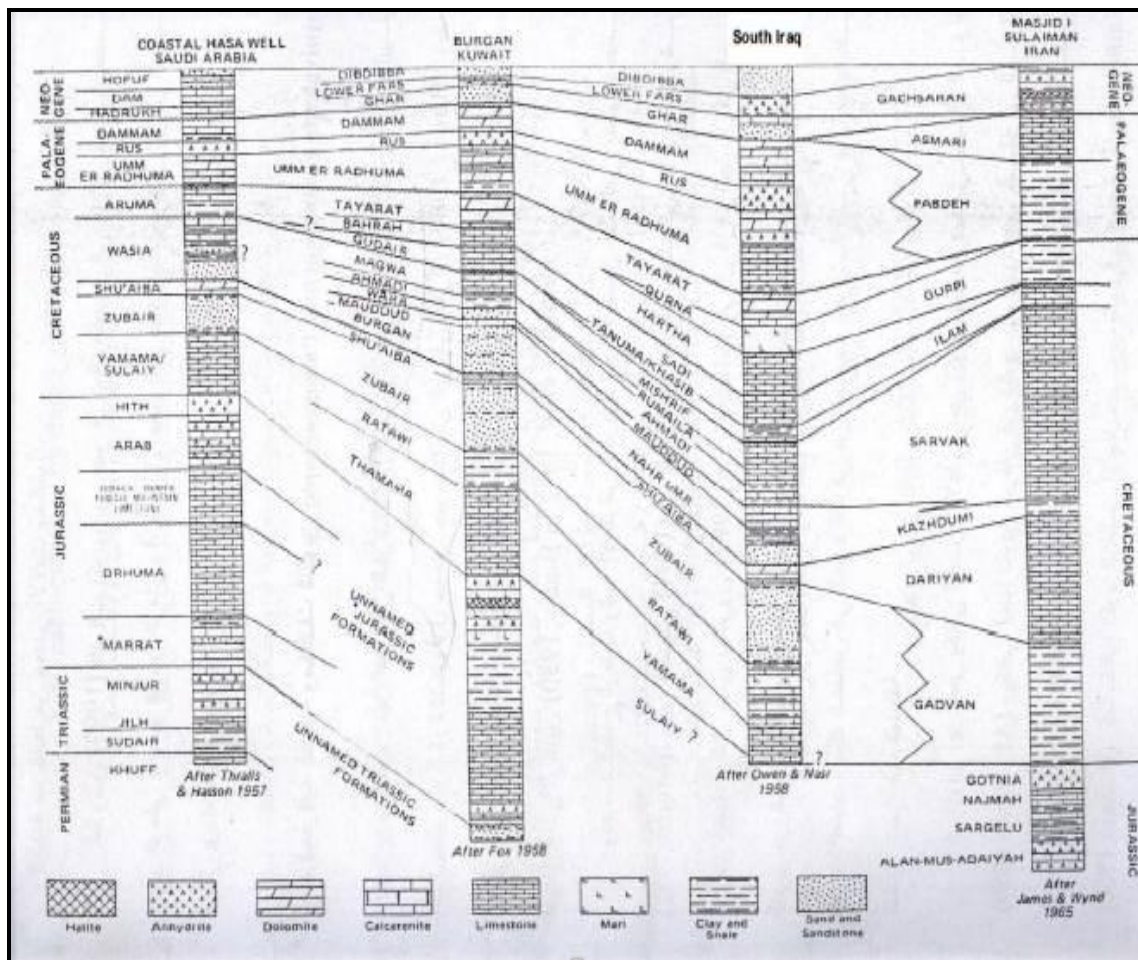


Figure 8: Fenced diagram showing the lithological variations and depositional environments in the mid-Cretaceous across Arabian Peninsula and Iran (James and Wynd, 1965)

1.5 Geological and structural setting of Iraq

Iraq can be divided into three tectonically different areas: the Unstable Shelf, the Stable Shelf and the Zagros Suture (Figure 9). These three areas contain tectonic subdivisions.

The Unstable Shelf mainly includes folded terranes. The Stable Shelf contains major buried arches and anti-forms and is composed at least of the Salman and the Rutba-Jezira zones. There is a major discrepancy concerning the place of the Mesopotamian Zone. Indeed, Buday and Jassim (1984, 1987) consider this zone as a part of the Unstable Shelf. In their opinion, the Unstable Shelf is limited to the W by the boundary of the Mesopotamian depression that is running along the Euphrates River near Nasiriyah City. However, according to Jassim and Goff (2006), the Mesopotamian Zone belongs to the Stable Shelf.

We adopted the boundary of the Stable Shelf Unit according to Jassim and Goff (2006) as the Mesopotamian Zone is now considered as a part of the Stable Shelf. The southeastern boundary of the Stable Shelf is now taken at the limit of the Late Tertiary long anticlines of Makhul-Hemrin-Pesht-i-Kuh. NW-SE tectonic features affect all zones (Figure 9).

The Mesopotamian Zone is the easternmost unit of the stable shelf. The folded Pesh-i-Kuh in the E, and the mountains of Hemrin and Makhul in the N bound Mesopotamian Zone. The SW boundary is controlled by faults (the Euphrates Boundary Fault Zone). The

Mesopotamian Zone was probably uplifted during the Hercynian deformation and it has remained stable till Late Permian.

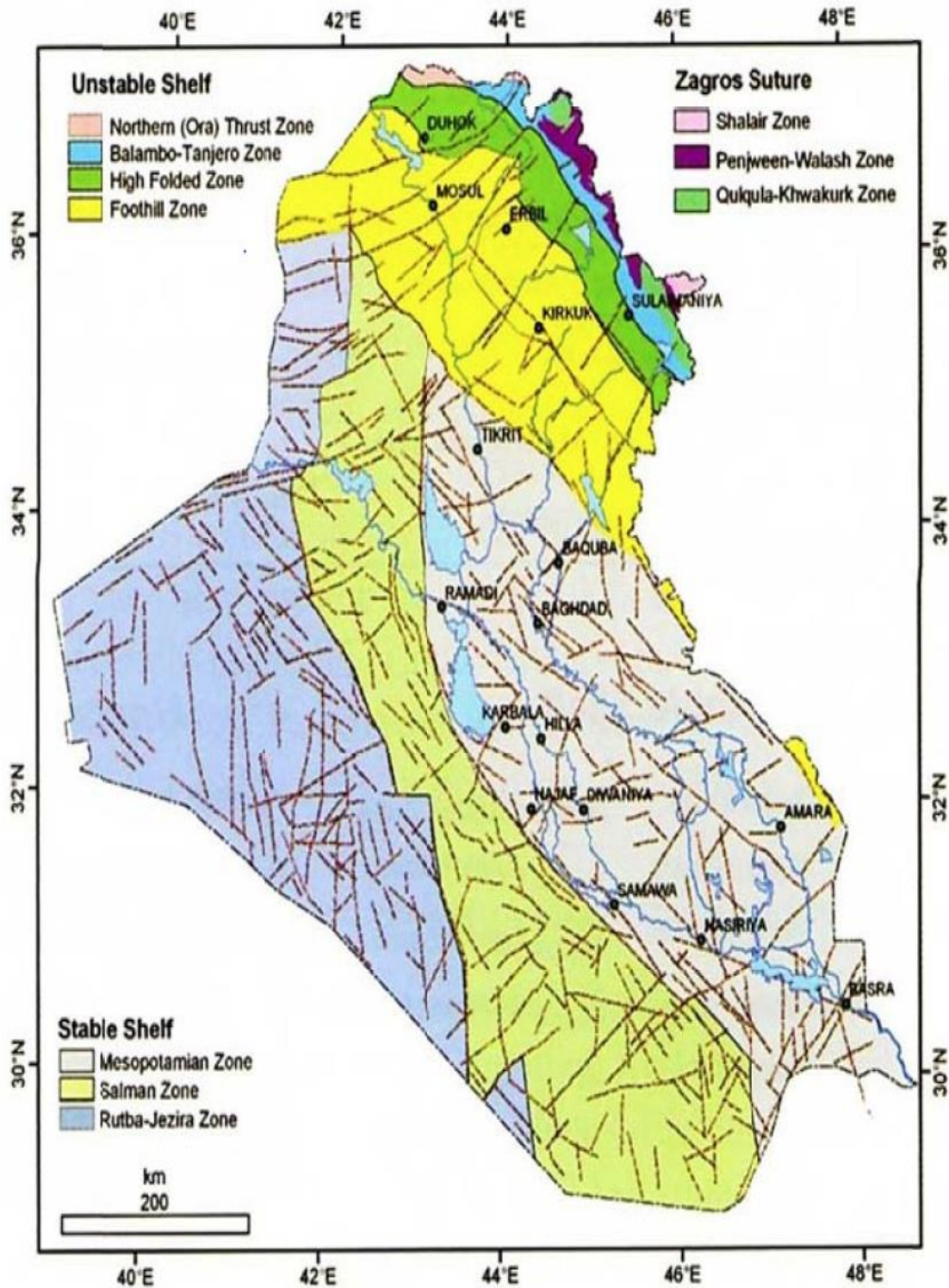


Figure 9: The Stable Shelf Zone, Unstable Shelf Zone and Zagros Suture (Jassim and Goff, 2006)

The Mesopotamian Zone contains buried faulted structures below the Quaternary cover, separated by broad synclines. The folded structures have a main NW-SE direction in the eastern part of the zone and N-S in the southern part, but some NE-SW oriented structures also occur. The structures in the Mesopotamian Zone usually have positive residual gravity

anomalies. Only a few structures have negative residual gravity anomalies in the southern zone of the Zubair Subzone (Jassim and Goff, 2006). For that reason, we can say that the study area has characteristics of a passive margin, i.e. extensional tectonics, growth faulting and a relatively slow, but steady subsidence (Moore, 2001).

1.6 Fault systems in Iraq

Two types of fault can be distinguished in Iraq. In the first type, the faults are related to the Najd Fault System extending from the Arabian Peninsula to Iraq. The second type is the Transversal Fault System that has a direction almost from the E to the W and has created the transversal blocks in Iraq (Figure 10). The Najd Fault is also very significant in Iraq. It forms the boundaries between the Stable Shelf and the Unstable Shelf. The Najd Fault contains numerous fault zones in Iraq. The major ones have SE-NW direction. The following important fault zones are, from NW to SE (Figure 10):

- The Tar Al Jil Fault Zone.
- The Euphrates Boundary Fault Zone.
- The Ramadi-Musaiyib Fault Zone.
- The Tikrit-Amara Fault Zone.
- The Makhul-Hemrin Fault Zone.
- The Kirkuk Fault Zone.

The Euphrates Boundary Fault Zone (EBFZ) is located in southern Iraq. It is running along the Euphrates River and it goes further to the Rutba area in western Iraq. EBFZ is one of the most prominent Najd fault zones. In the south, EBFZ comprises a series of step faults sometimes associated with grabens and forms the boundary between the Quaternary Mesopotamian Plain and the rocky desert of south-western Iraq. It is associated with a large number of sulphur springs. In western Iraq, EBFZ was reactivated during Late Jurassic and Cretaceous forming small fault bounded depressions filled in with fluvial sandstones (Jassim and Goff, 2006).

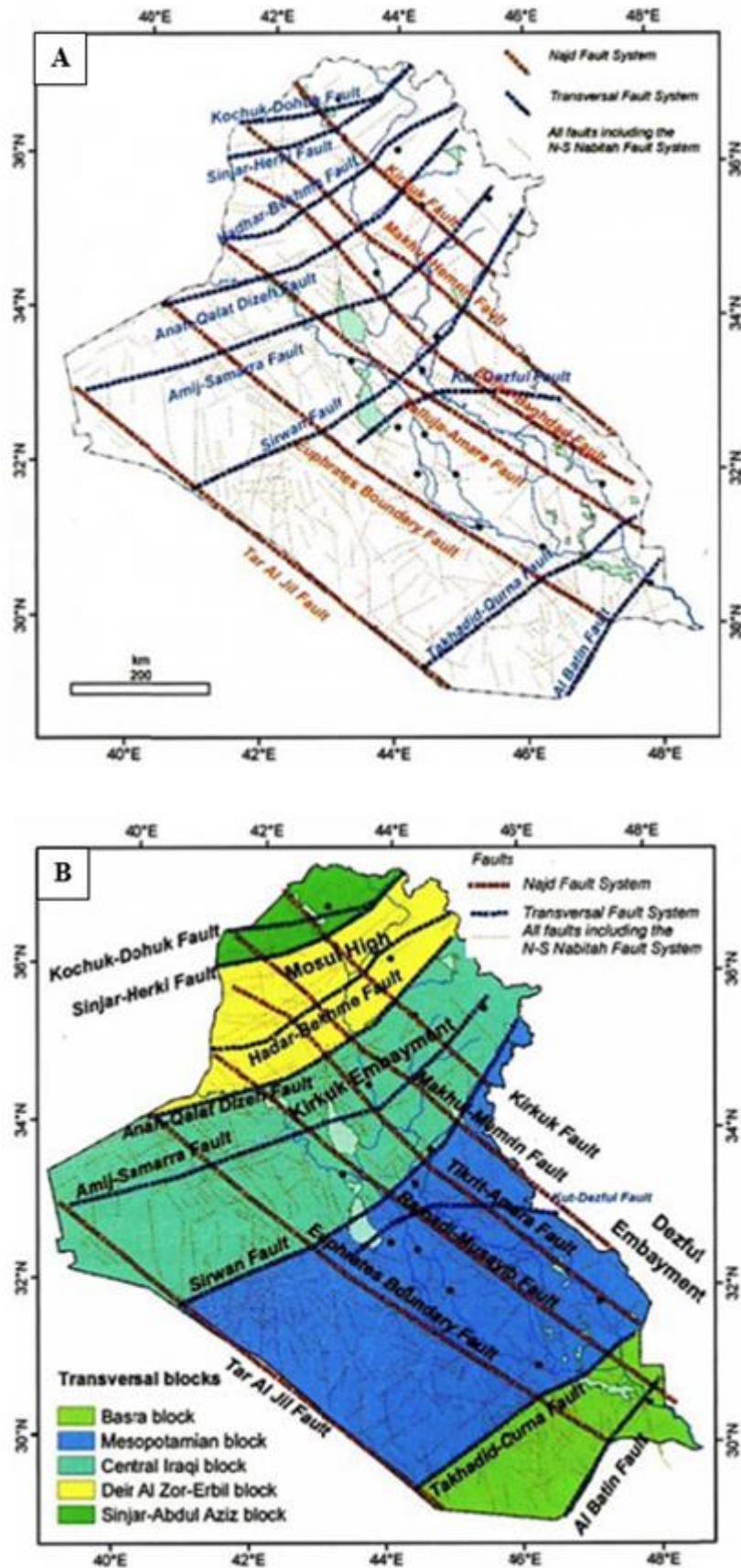


Figure 10: Distribution of faults and fault zones (A) and transversal blocks (B) (Jassim and Goff, 2006)

1.7 The Mesopotamian Zone

The Mesopotamian Zone is divided into three subzones depending on their structures (Figure 11):

- The Zubair Subzone towards the south of the Mesopotamian Zone with N-S extending structures
- The Euphrates Subzone towards the west
- The Tigris Subzone towards the northeast with structures have NW-SE direction.

The Mesopotamian Zone characterizes by thick sedimentary deposits. The Euphrates and Tigris rivers make an important contribution to the thickness of the sedimentary pile, particularly for Quaternary. The sedimentary thickness increases towards the east of the Mesopotamian Zone and for that reason, the Tigris subzone is thicker than the Euphrates Subzone.

The Euphrates Subzone is a monoclinal structure dipping to the NE with short anticlines of approximately 10 km length and structural noses. Some NW-SE oriented anticlines (20-30 km long) lie near to and parallel to the Euphrates Boundary Fault especially between Samawa and Nasiriyah (study area). The anticlines are related to horsts and grabens developed along the fault zone.

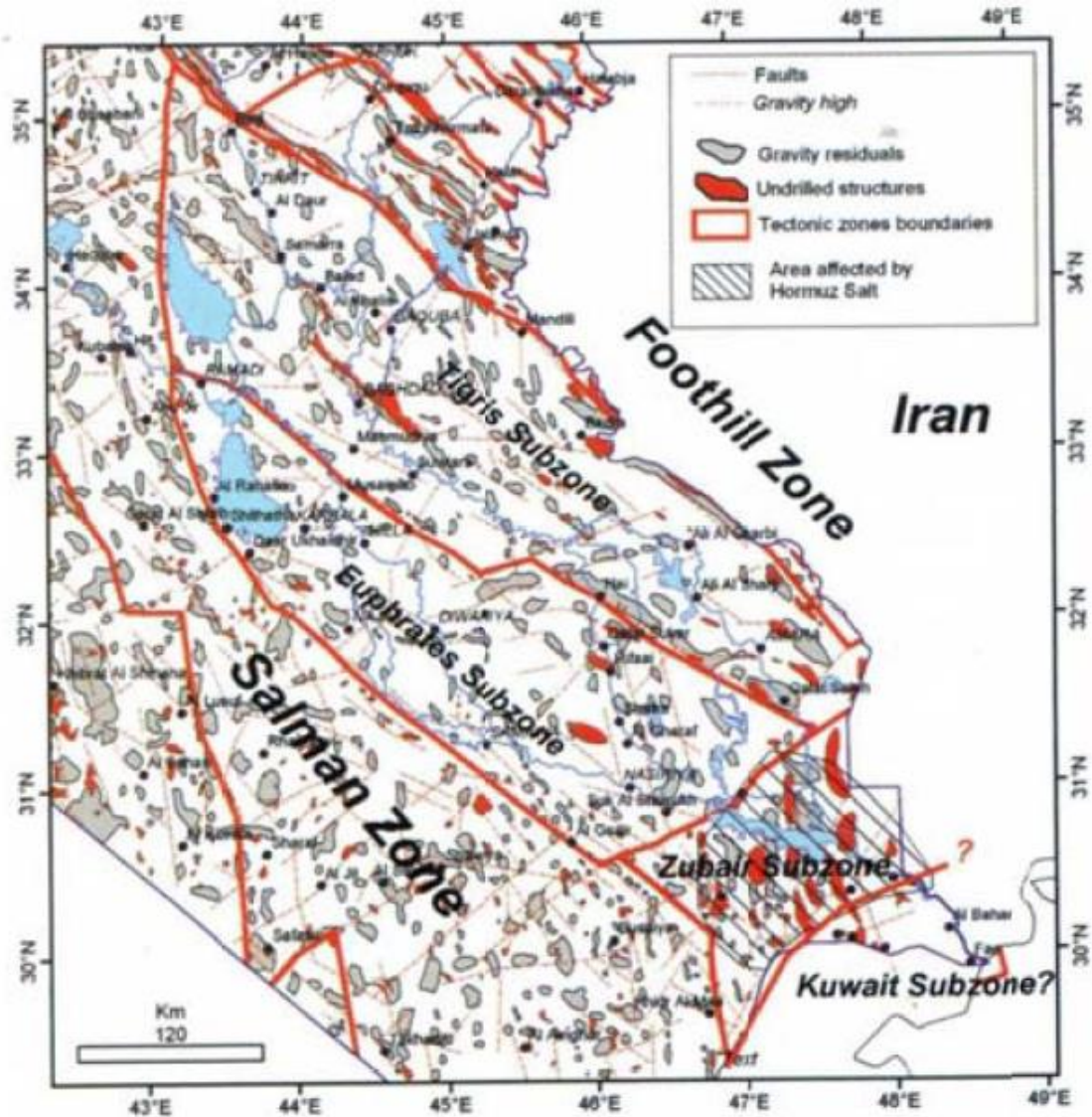


Figure 11: Mesopotamian zone subdivided into the Euphrates subzone, the Tigris subzone and Zubair subzone (Jassim and Goff, 2006). The grey polygons represent residual gravity anomalies and the red polygons represent undrilled structures of the Mesopotamian Zone

The basement of the Mesopotamian Zone is generally 7-9 km deep. A stratigraphic column comprises up to 1500 m of Infracambrian, 2500-5000 m of Paleozoic, 1500-2200 m of Triassic, 1100 m of Jurassic, 500-700 m of Lower Cretaceous, 700-1400 m of Upper Cretaceous, 200-900 m of Paleogene, and 150-1500 m of Neogene and Quaternary section (Figure 12). Quaternary sediments alone are up to 300 m thick (Jassim and Goff, 2006).

The basement of the Mesopotamian Zone is generally 7-9 km deep. A stratigraphic column comprises up to 1500 m of Infracambrian, 2500-5000 m of Paleozoic, 1500-2200 m of Triassic, 1100 m of Jurassic, 500-700 m of Lower Cretaceous, 700-1400 m of Upper Cretaceous, 200-900 m of Paleogene, and 150-1500 m of Neogene and Quaternary section (Figure 12). Quaternary sediments alone are up to 300 m thick (Jassim and Goff, 2006).

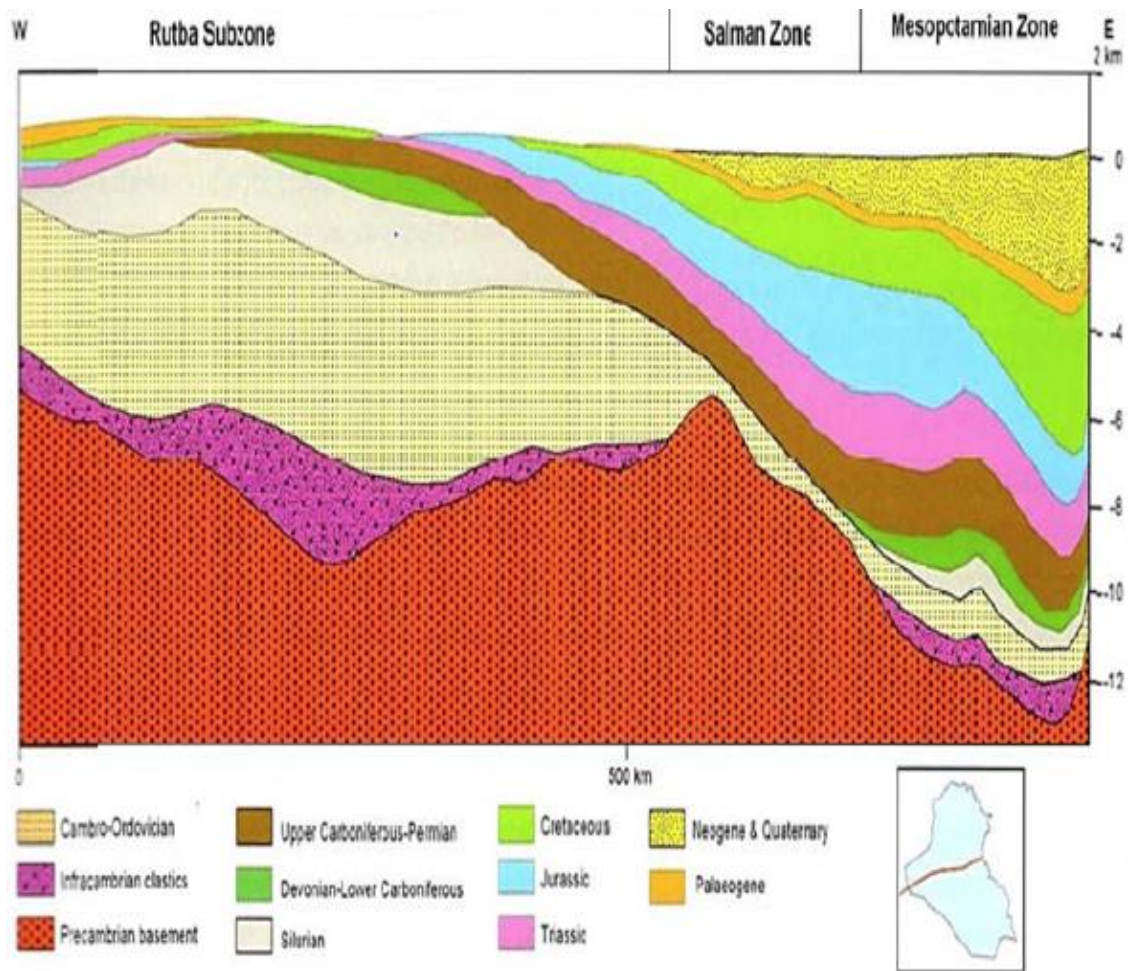


Figure 12: Profile between Risha (located on NE Jordan) to Naft Khana (Iranian border) (Jassim and Goff, 2006)

The Mesopotamian Basin of southern and central Iraq in the Mid-Cretaceous (early Albian nearly Turonian) sequence consists of two sedimentary cycles (Buday, 1980a). The Nahr Umr and Mauddud formations and their equivalents represent the older cycle of the early Albian-early Cenomanian age. The transgressive Ahmadi Shale Formation, covered by the chalk/marly limestones of the Rumaila Formation, set the first step of the Upper cycle (Cenomanian-early Turonian). The second step of the Upper cycle corresponds to the regressive Mishrif Formation (middle Cenomanian-early Turonian), which in turn grades up into the Kifil Formation evaporites in numerous oilfields in the west of the basin (Fuloria, 1976).

1.8 Stratigraphy and equivalents of the Mishrif Formation

Cretaceous reservoir rocks are abundant, especially in southern Iraq. However, four reservoir units contain most of the oil of the region; Yamama, Zubair, Nahr Umr and Mishrif. Other formations are locally important and include Sulaiy, Ratawi, Shu'aiba, Mauddud, Rumaila, Khasib-Tanuma-Sa'di, Hartha and Tayarat (Jassim and Goff, 2006) (Figure 15).

In the Middle East, the Cretaceous sequence has two unconformities, which are late Aptian (or early Albian) unconformity and early Turonian unconformity. These regional unconformities usually divide Cretaceous into three parts (Harris et al., 1984). The Ratawi, Zubair and Shu'aiba formations are existed in the Early Cretaceous.

In southern and southwestern Iraq, the Nahr Umr, Mauddud, Wara, Ahmadi, Rumaila and Mishrif formations exist in the Mid-Cretaceous. In western Iraq, the Mid-Cretaceous is composed of the Rutbah and M'sad formations. In southern Iraq, the Late Cretaceous contains the Khasib, Tanuma, Sa'di, Hartha, Qurna and Tayarat formations (Nairn and Alsharhan, 1997)(Chatton and Hart, 1962c) including all the organic detrital neritic limestone units of Cenomanian-Early Turonian age, such as the M'sad, Gir Bir, and Mergi formations into the Mishrif Formation. They placed the freshwater limestone into the newly introduced Kifl Formation. However, Ditmar and Iraqi-Soviet Team (1971) proposed to recognize the Gir Bir and M'sad as an independent unit because of its distinctive facies, unlike the Mishrif Formation. Indeed, the M'sad Formation was deposited in a coastal, locally supratidal environment (Figure 13).

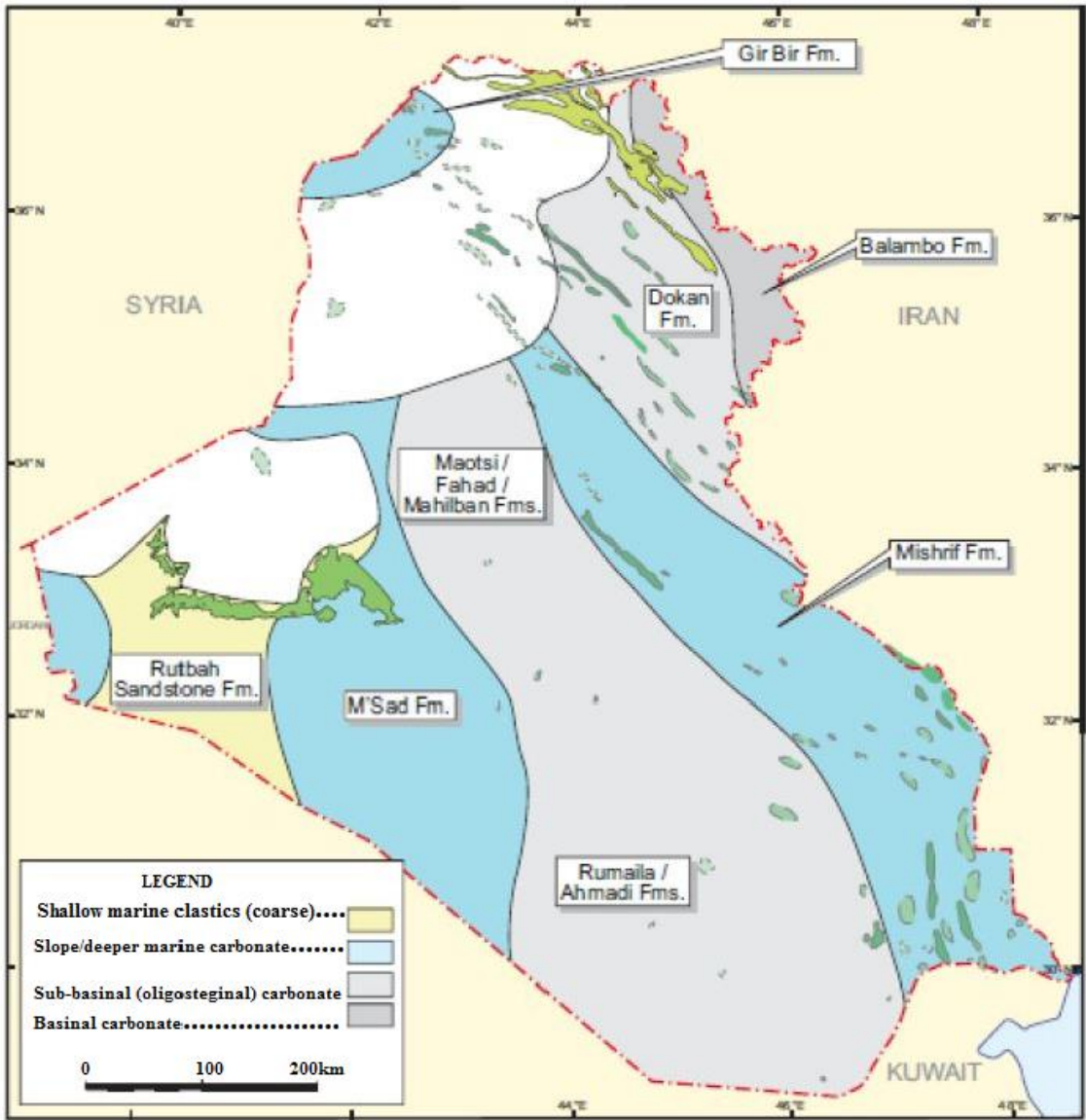


Figure 13: Depositional system of Mishrif Formation in Iraq, across Cenomanian-early Turonian modified from (Cambridge Carbonates, 2008 cited in Aqrawi et al., 2010)

The Mishrif Formation occupies a relatively narrow belt running NW-SE across central and southeastern Iraq (Figure 13). Reservoir quality decreases towards the Najaf

intrashelf basin to the southwest. The reservoir is huge in the center of the Mishrif Formation where the thickness is higher, in southeastern Iraq along the border with Iran (Mazeel, 2011) (Figure 14).

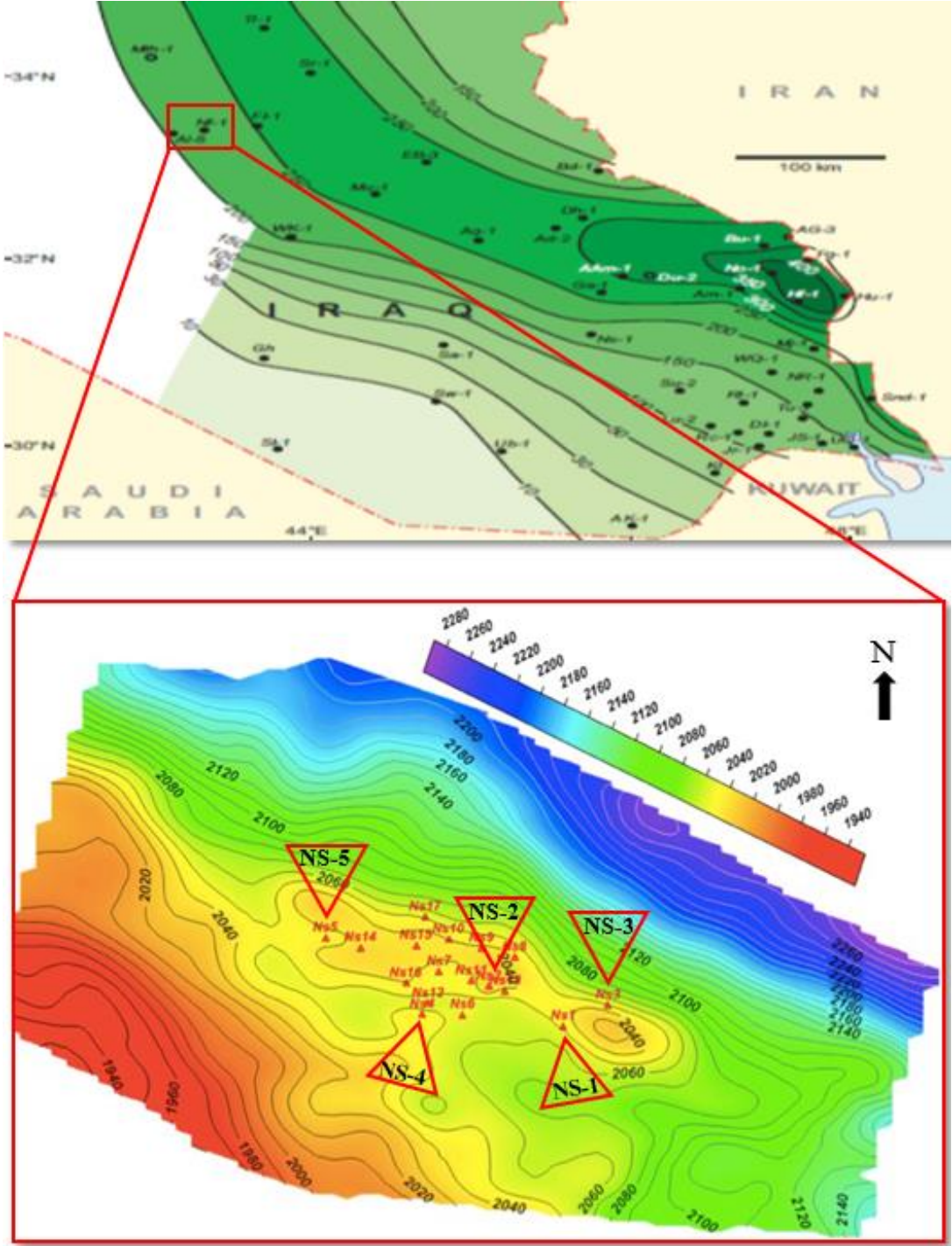


Figure 14: Contour map of Mishrif Formation that occupies Central and Southern Iraq after (Aqrabi et al., 1998)

The Mishrif Formation reservoir (Cenomanian-early Turonian) of the Mesopotamian Basin accommodates more than one-third of the proven Iraqi oil reserves within rudist-bearing stratigraphic units. Huge accumulations of rudist strata occurred along an exterior shelf margin of the basin through an axis that runs from Hamrin to Badra and southeast of that, with interior margins around an intrashelf basin (Aqrabi et al., 2010).

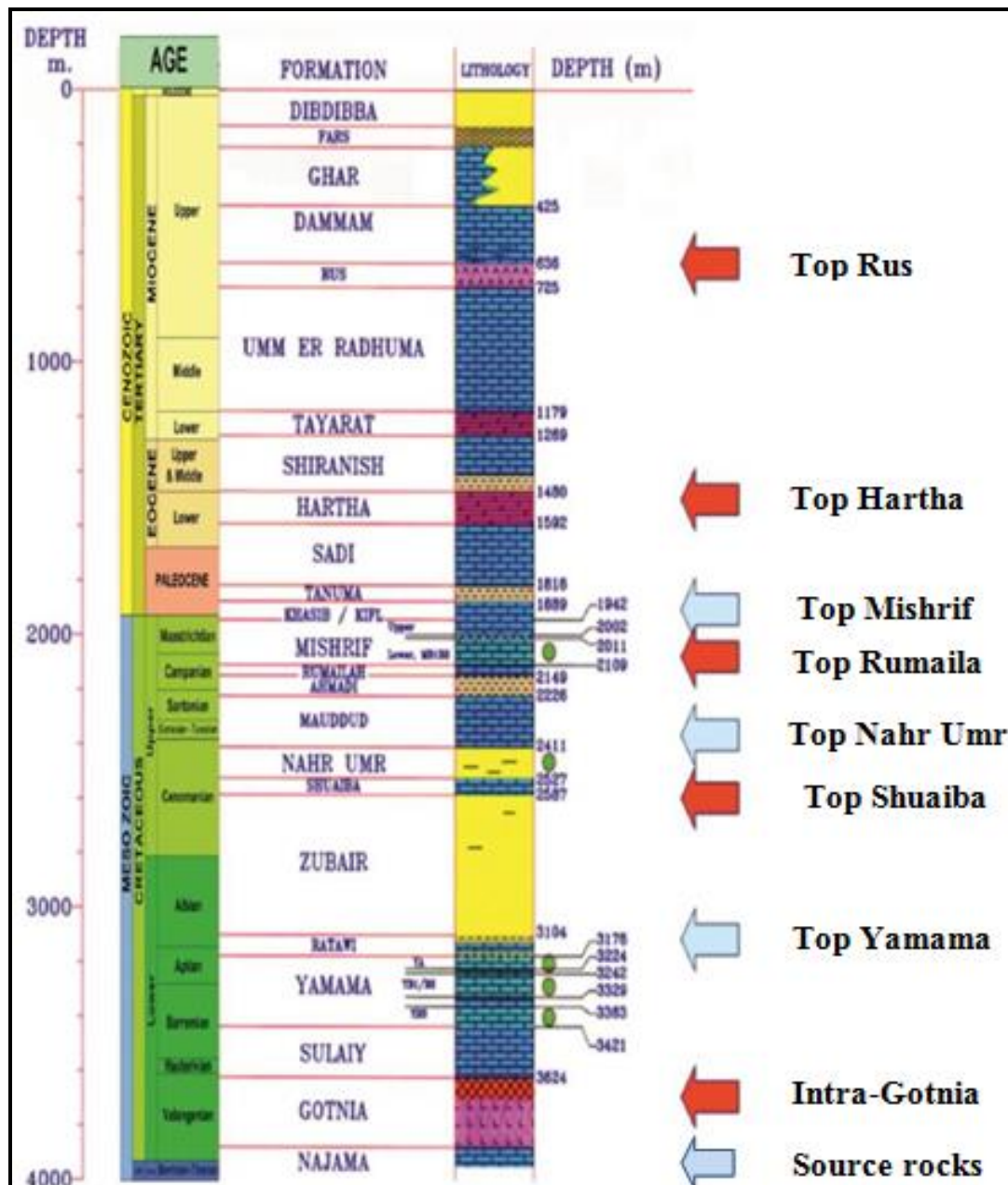


Figure 15: Stratigraphic section of the Nasiriyah oil field in well NS-1 (source: OEC)

1.9 Evolution of paleogeography during upper Cretaceous

The regional paleogeography of the study area includes several stages starting in Albian up to the upper limit of Cretaceous (Buday, 1980a). Cretaceous orogenesis had an impact on the palaeogeographic evolution in several places of Iraq. Moreover, the longitudinal ridges and transversal blocks of Iraq occurred during Cenomanian-Early Turonian sequence by reactivation impact of obduction in the northeastern margin of the Arabian Plate in the Tethys Ocean. In addition, the reactivation effect of the Najd Fault system, which has arisen from the center of the Arabian Plate, has affected the study area during Cenomanian-Early Turonian.

The Cenomanian–Early Turonian sequence deposited during the tectonic unrest. The extreme complex distribution of facies and sedimentary lacks in the Mesopotamian zone are

due to the presence of numerous reliefs such as the isolated Mosul and Rutba highs, and several other ridges extending NW-SE as well as the Kirkuk Embayment, which controls on the Foothills region in Iraq (Figure 16 and Figure 17).

In addition, the Late Turonian-Early Campanian sequence resembles the previous sequence of Cenomanian–Early Turonian. It also deposited during a significant tectonic activity because of the Austrian and Sub-Hercynian folding in the Alpine geosyncline during Middle Cretaceous. The best evidence on the tectonic disorders during both sequences are:

- The formation of the Toros-Zagros Mountains in the northeastern Iraqi boundaries with Iran and Turkey.
- The formation of the eugeosynclinal folding, which started in the geosyncline during Late Albian and Early Cenomanian and going on with increased activity during the Cenomanian-Early Turonian (Buday, 1980a).
- The deposition of sediments was not interrupted during this period. Subsidence was important therefore intense because of continuous folding and compression processes, responsible (for) the formation of the Rumaila Facies.
- In the southwestern part of the miogeosynclinal area, the Tikrit-Samarra-Amara palaeoridge became a very important ridge, including the reef shelf facies with supergiant oil fields in southern Iraq. It is worth mentioning that both the palaeoridge and the anticline structure of Nasiriyah oil field have the same NW-SE direction
- In SW of the Tikrit-Samarra-Amara ridge, embayment along the Euphrates formed relatively wide space, occupying the southwestern parts of the Mesopotamian Zone up to the slopes of the Rutba and Khleisia Uplifts almost up to the Haditha-Tikrit areas (Homci, 1975 cited in Buday, 1980).
- As an example of a tectonic unstable zone, the Kirkuk Embayment formed in the area of the Foothill Subzone, with the characteristics of an isolated deep basin (microfacies) between the Balambo basin in the NE and the Rumaila basin in the SW. The euxinic shale layers have appeared in the Gulneri Formation, which was considered as a locally Formation at the top of Cenomanian - Early Turonian sequence. The distribution of microfacies of Gulneri Formation is poorly understood in the subsurface (Jassim and Goff, 2006).
- At the end of the Cenomanian - Early Turonian Sequence, an intense tectonic activity generated numerous wide grabens along the Euphrates River south of the Mesopotamian zone. Subsequently, the Turonian-Lower Campanian Sequence started.
- In the southwestern parts of the Stable Shelf, the Khasib Formation formed at the base of the Late Turonian-Lower Campanian sequence and recorded an important sea transgression. In the southwestern areas of Iraq, this event occurred later than in geosynclinal areas of NE Iraq. Transgression led to disconformable boundary and hiatus.
- Late Turonian-Lower Campanian sediments were eroded during the uplift of numerous areas, i.e. the Balambo-Tanjero Zone and the adjacent parts of the Unstable Shelf (Mosul High) as well as over large areas of the Rutba-Jezira Zone in the Stable Shelf. Uplift of these zones resulted from the compression during Late Campanian and the ophiolite obduction initially in NE of Iraq (Dunnington, 1958).

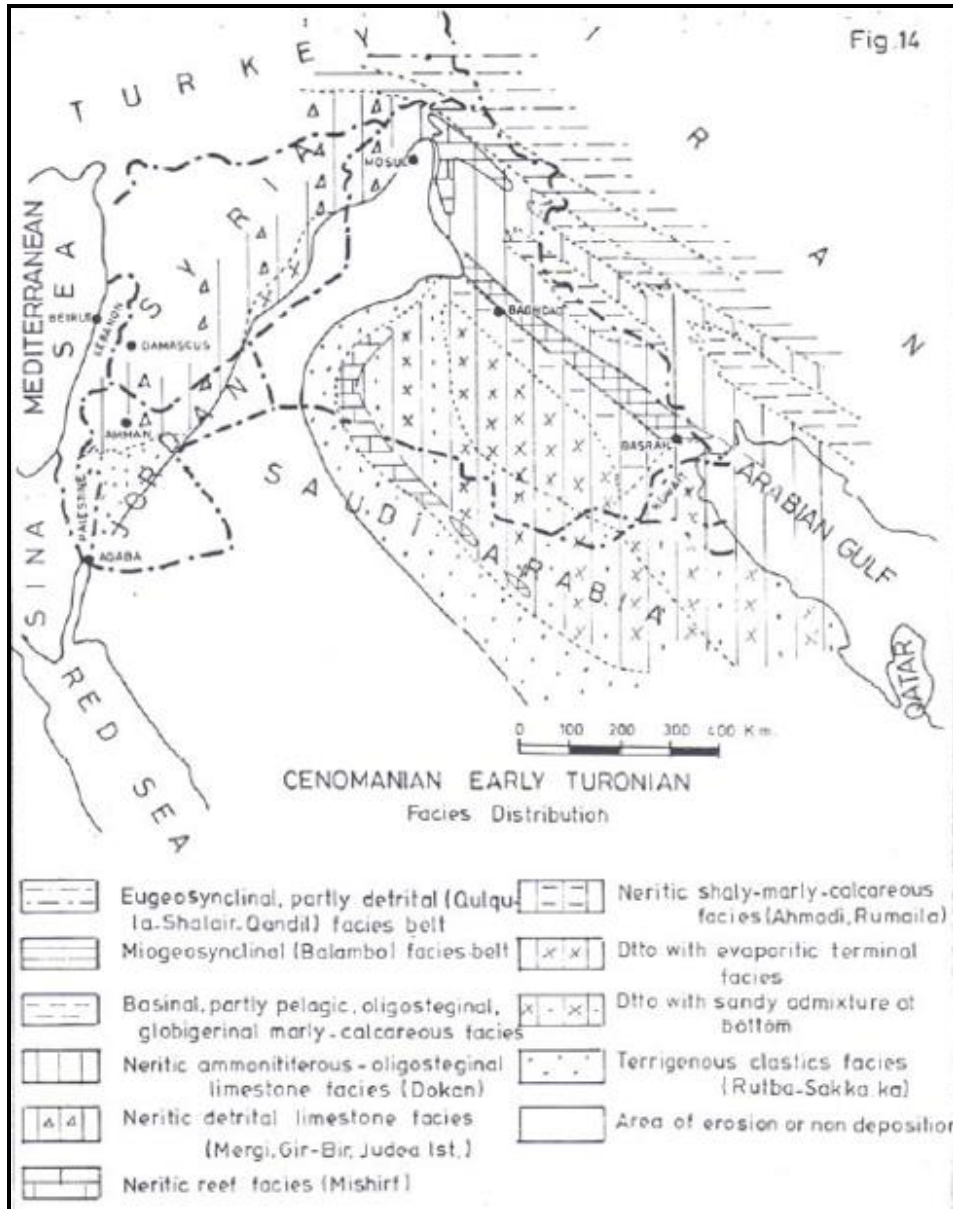


Figure 16: Regional isopach map shows facies distribution across Cenomanian Early Turonian (Homci, 1975 cited in BUDAY, 1980)

- In the southwestern basin, intra-Senonian uplift led to the widespread erosion of the Late Turonian deep-water carbonates deposited in grabens.

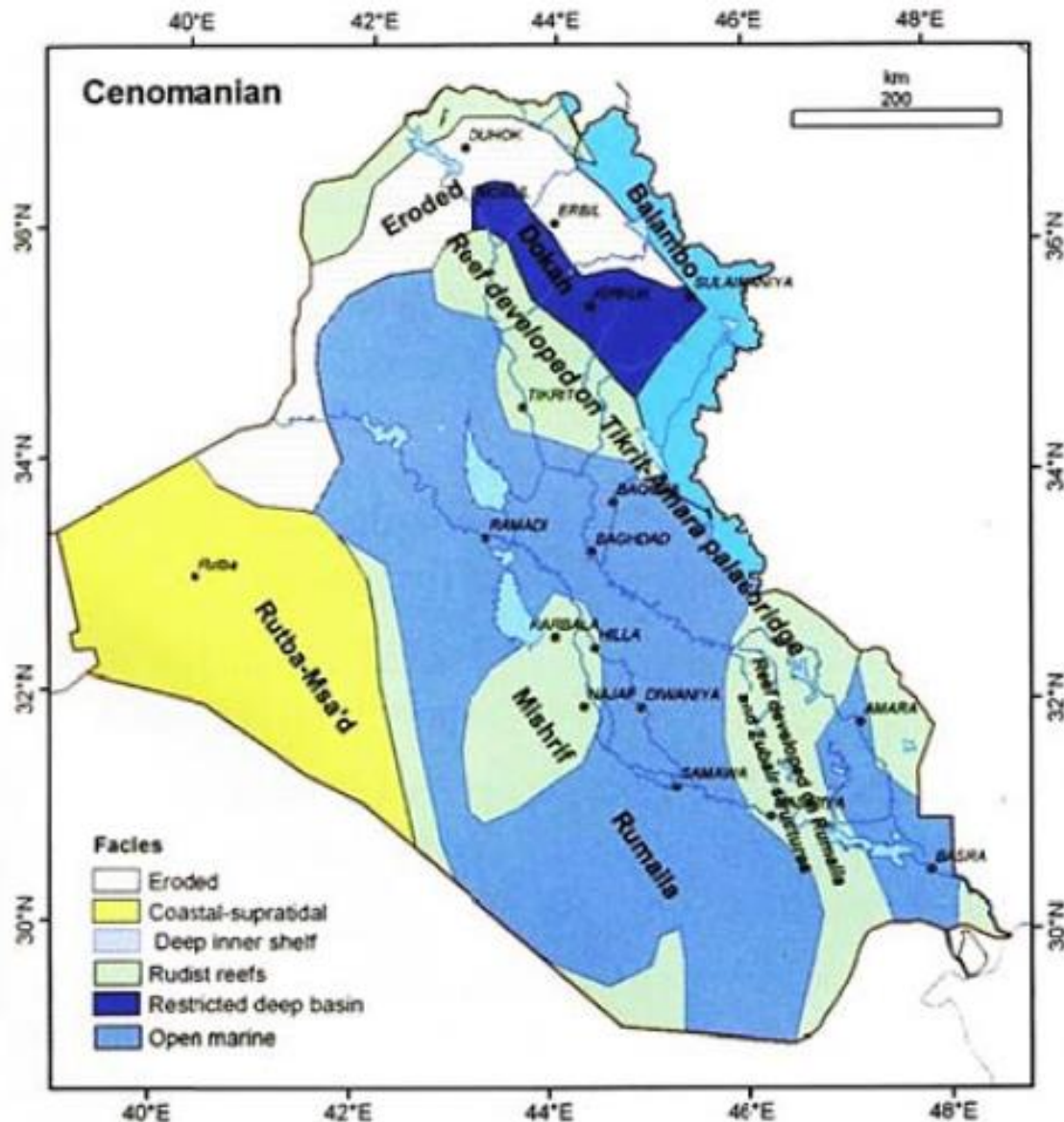


Figure 17: Paleogeography map of Iraq during Cenomanian (Jassim and Goff, 2006)

The diversity of paleogeography during Cenomanian-Early Turonian was emphasized by (Buday, 1980a). Indeed the tectonic reactivation processes along the NE Tethyan margin resulted in the re-emerging of longitudinal NW-SE ridges with reef shelf development such as the Tikrit/Samarra/Amara Paleoridge and another transversal blocks such as the Mosul, Rutba Highs and Kirkuk Embayment (Jassim and Goff, 2006) (Figure 17).

1.10 The Kifl Formation

In the Mesopotamian Zone, the youngest unit of the Cenomanian-Early Turonian Sequence is the Kifl Formation. Chatton and Hart (1961) defined this formation as an independent stratigraphic unit, in the type section of wells in the region of Kifl, NW of Nasiriyah oil field. Before 1961, layers of the forthcoming Kifl Formation were considered as parts of the Mishrif, Rumaila and Fahad formations.

The thickness is relatively weak (around 19 m), increasing to 45 m towards Baghdad. It extends as a braid in several wells in the south central Iraq, including Samawa-1, Ghalaisan-

1, Shawayah-1, Nasiriyah-1, Afaq-1, Merjan-1, Ubaid-1 and East Baghdad-1 as well as Kifl-2. For this reason, the depocenter of formation is considered as located in the south center of Iraq (Jassim and Goff, 2006).

The Kifl relic basin was extending towards the north but precise indications are scarce and unclear. The most northerly known evidence of the Kifl facies are found near Fallujah and Samarra (Buday, 1980a), the basin is limited to the W by the Abu Jir Subzone and to the E by the crestal parts of the Musaiyib-Nahr Umr paleouplift.

Based on its stratigraphic position, the Kifl Formation is assumed to be Early Turonian in age (Jassim and Goff, 2006). According to other opinions, Kifl belongs more widely to the Cenomanian-early Turonian sedimentary cycle (Al-Naqib, 1967). This conclusion is supported by the presence of uncommon miliolids and textularids. In fact, a Cenomanian age cannot be excluded because of the two reasons (Buday, 1980a). Firstly, the absence of fossils in the report of (Chatton and Hart, 1961) leads to assigning a very vague age for the Kifl Formation. Secondly, Kifl appears to develop in continuity after the underlying Cenomanian formations, particularly Mishrif in the Nasiriyah oil field.

The formation had no correlative facies in Iraq (Buday, 1980a), probably because terranes have been cut out by the intra-Turonian erosion or because the time of his deposition coincides with the uplift. Correlative terranes are probably present in areas where sedimentation was continuous during Upper Cretaceous, for instance in the miogeosynclinal imbricated Zone (Balambo Formation, N of Iraq).

The Kifl Formation is predominantly composed of white crystalline anhydrite with streaks of green marls and chalky pellet limestones locally cemented by an anhydritic matrix. Cream-colored porcelaneous anhydritic marly limestone occurs at the base (Al-Naqib, 1967). Buday (1980a) described similar features for Kifl in the type section, i.e. the predominance of anhydrite, oolitic and pseudoolitic limestones, and locally, some dolomitic or marly limestones and subordinate shales. Thus, the Kifl Formation is lithologically defined as an evaporitic lagoon with mostly marine hypersaline sedimentation but locally from freshwater in partly separated lagoons.

In the Kifl type section, the Kifl formation overlies the Rumaila formation (formerly called Maotsi Formation). The contact is gradual and is marked at the limit between continuous white-creamy chalky limestone with *Oligostegina* and anhydritic marly limestone. In our study area, the Nasiriyah oilfield, the lower contact of the Kifl formation is conformable with the underlying Mishrif formation. The Khasib formation overlies the Kifl formation. The contact is unconformable, with a sedimentary break, and it is placed at the limit from anhydrite to shale. Around Fallujah (center of Iraq), the overlying formation was designed formerly as the Pilsener Limestone, which in fact partly corresponds to the Khasib formation (Buday, 1980a).

1.11 The Rumaila Formation

Historically, the age of the Rumaila Formation was attributed to Rabatin (1952) who described first the Rumaila Formation in Zubir wells in the Mesopotamian Zone (Bellen et al., 1959). Rumaila is a great basin in the Cenomanian-Early Turonian. It includes the Cenomanian formations of the southern-southwestern Iraq as well as their equivalent in NW

of the Mesopotamian Zone such as Mahliban, Fahad and Maotsi formations. Owen and Nasr (1958) changed the age of Rumaila Formation to the Cenomanian-Early Turonian and emphasized that the Rumaila formation passes further southeast into the Magwa Formation in Kuwait. Bellen et al. (1959) emphasize the great diversity of Foraminifera represented by *Oligostegina*, *Globigerina*, *hedbergella*, and rare *Orbitolina concava* var. This confirms the Cenomanian-Early Turonian age (Chatton and Hart, 1961).

However, some authors now reject the idea to include the Mahilban, Fahad and Maotsi formations into the Rumaila Formation. Indeed the age of those formations is strictly Cenomanian-Early Turonian whereas the age of Rumaila sediments extends more widely from the uppermost Albian to the early Turonian. Rumaila appears to be as a collection of heterogeneous facies, which would include the Mishrif and possibly several other facies. Limestones are semipelagic (as evidenced by the *Hedbergella* and *Oligostegina*) and deeper basinal conditions are not recorded (Radoicic, 1987).

The Formation was mainly distributed on the Stable Shelf to the east of the Rutba-Jezira Zone and it almost covers the Mesopotamian Zone to the W of the Tikrit-Samarra-Amara Palaeoridge. Along E and NE of the Mesopotamian margins, the Rumaila Formation progressively replaces the Mishrif Formation. In the N and NE of Awisl-Samarra area, the Rumaila Formation is absent or it is replaced by other equivalent Cenomanian Formations such as the Mishrif Formation. The Rumaila Formation extends to the Makhul area (Homci, 1975 cited in Buday, 1980).

In the wells of the type area, Rumaila includes fine-grained, marly, limestones with *Oligostegina* including marly layers, passing downward to fine-grained, chalky limestones. Sometimes, dolomite, dolomitic limestones, and subordinate shales are found in and around the type area (Bellen et al., 1959). Buday (1980a) assumes a deep subsiding basin with locally restricted conditions.

The stratigraphic boundaries of Rumaila considerably vary depending on the location inside the Mesopotamian Zone (north *versus* south). This is mainly due to the variability of the basal facies (Mahliban, Fahad or Motsi) in addition to the relative vicinity to Rutba high.

Indeed, the lower boundary of Rumaila in southern Iraq is generally conformable and gradual with the Ahmadi Formation. Rumaila is conformably overlain in places by Mishrif and elsewhere by Kifl. Towards N and NW of the Mesopotamian Zone, the lower boundary is unconformable because of a transgression, particularly in the Mahliban facies. The upper boundary is similarly not uniform especially with Turonian (Kometan Formation) or Senonian (Sa'di Formation). For the same reasons, the thickness is highly variable. Thus, in the type area (Basra, southern Iraq), the thickness reaches 120 m. Towards N and NW of the Mesopotamian Zone (Awasil-Fallujah-Samarra area), the thickness reaches 240 m. The variation of thickness suggests a depocenter located in the Salman Zone and in the eastern parts of Mesopotamian Zone based on the isopach map (Figure 18).

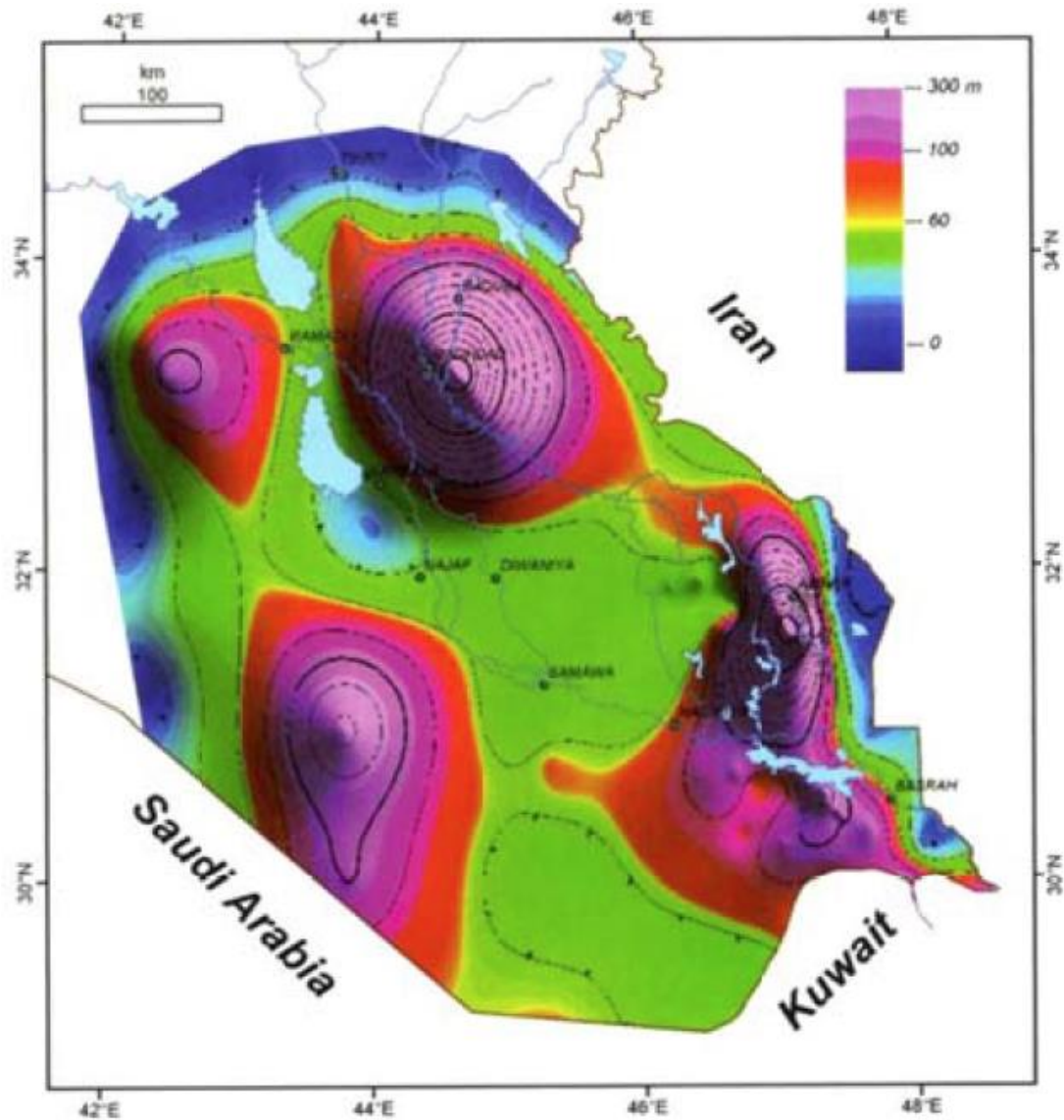


Figure 18: Isopach map shows the thickness of Rumaila Formation (Jassim and Goff, 2006)

1.12 The Late Turonian-Early Campanian Sequence

The Khasib, Tanuma, Sa'di, Kometan and Gulneri formations represent the Late Turonian-Early Campanian sequence. The sequence includes two main facies. Firstly, Khasib, Tanuma and Sa'di contain the deep inner shelf and lagoonal facies. Secondly, Kometan and Gulneri formations represent the outer shelf and basinal facies. In southwestern basins, intra-Senonian uplift led to the widespread erosion of the shelf sediments.

The Turonian-Lower Campanian sequence is characterized by two main breaks. The first break separates the Earliest Turonian from the remaining Turonian and comprises the almost complete Iraqi territory with the notable exception of the miogeosynclinal area. The second break corresponds to the end of the sequence cycle and it is marked by the widespread transgression of the Upper Campanian-Maastrichtian cycle. Moreover, the tectonic activity all along the considered period led to numerous local breaks, unconformities, facies changes and patchy distribution in the Iraqi territory.

The sediments of the Turonian-Lower Campanian sequence cannot be considered as contemporaneous. Firstly, the sediments deposited near the geosynclinal area, which comprised Kometan and Gulneri, were deposited earlier. Secondly, the sedimentation of Khasib, Tanuma and Sa'di covered lately the Stable Shelf and the adjacent parts of the Mobile Shelf (Buday, 1980a). The isopach map shows the thickness of Late Turonian-Early Campanian sequence (Figure 19) (Jassim and Goff, 2006).

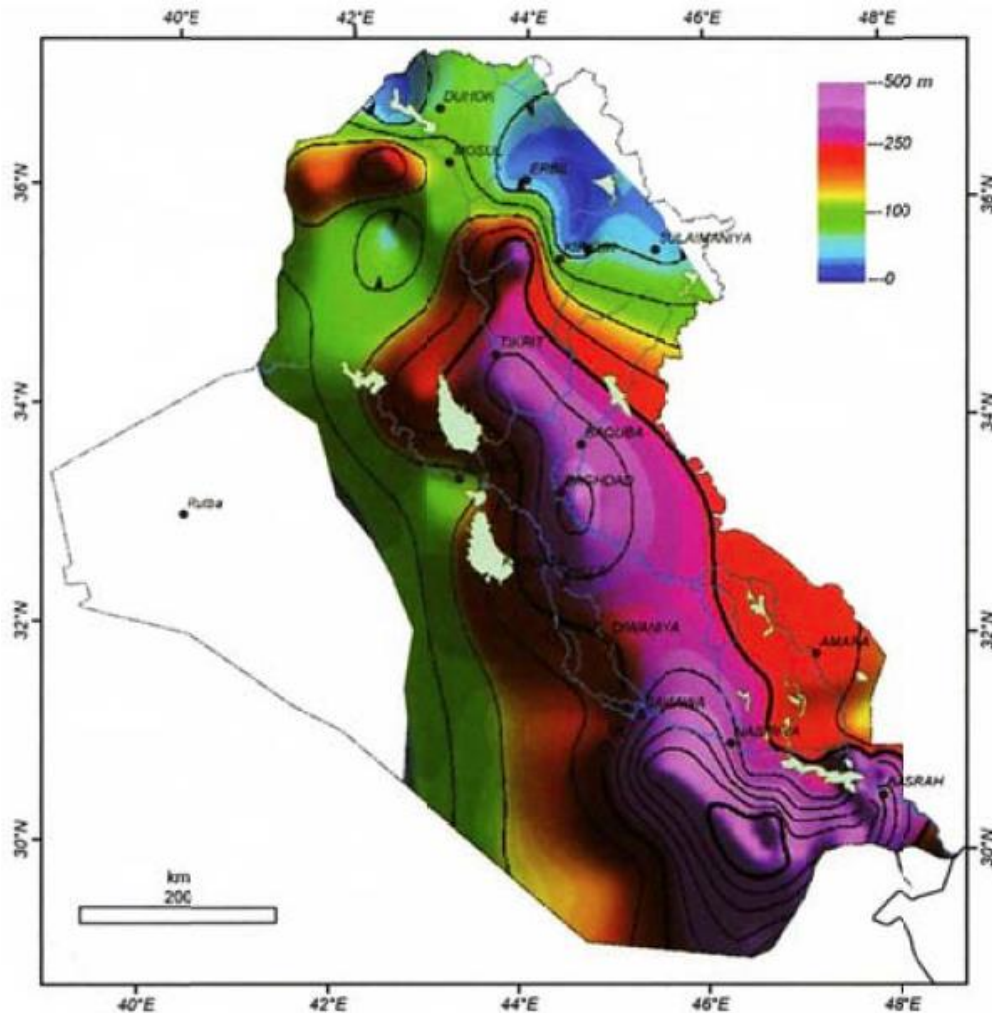


Figure 19 : Isopach map of Iraq showing the thickness of Late Turonian- Early Campanian sequence (Jassim and Goff, 2006)

1.13 The Khasib Formation

The Khasib Formation has the highest thickness in southern Iraq (225 m in the Zubair oil field) and its thickness increases towards to the eastern boundaries with Iran.

The age of Khasib Formation (Figure 20) still remains controversial because it contains different facies and lithologies. The Khasib Formation is classically sub-divided into two: Lower and Upper. Nevertheless, this subdivision is not systematically present in each well section. The lower part comprises dark grey to greenish-gray shales based on the microfacies analysis. Fossils are *Globigerina*, *Oligostegina* and *Globotruncana* assemblages. Grey fine-grained marly limestones, containing different lithologies and fossils, represent the upper part. For that reason, the paleoenvironment was highly diversified (Bellen et al., 1959).

Moreover, there is a difference of opinion among many workers listed in (Buday, 1980a) that are:

- Owen and Nasr (1958) for the first time, who defined Khasib and supposed a Lower Senonian age of the Formation.
- Bellen et al. (1959) gave an upper Campanian age.
- Chatton and Hart (1961) proposed that Khasib belonged to the Turonian-Lower Campanian.
- Darmonoian (1975) argued for a Late Turonian to Coniacian.

As the transgression of the Late Turonian-Lower Campanian Cycle lately occurred in the southwestern parts of Iraq, Ditmar et al. (1972) emphasized that Khasib represents the oldest Formation of this cycle.

The depositional environment of lower Khasib includes gray to greenish gray sediments alternating with black shale and seems to be a purely marine environment based on *Globotruncana* assemblages. These paleoenvironmental indications were only rarely found in well NS-5 at the depth from 1897.48 m until 1999.60 m. The shaly layers as well as the presence of pyrite confirm the marine origin in an euxinic.

In the Ahdeb (AD) oil field, located between Nomina and Kut (Wasit Province), 180 km southeast Baghdad, lower Khasib is represented by micritic wackestones with planktonic foraminifera, passing through green algae packstones and ends with bioclastic grainstones (upper Khasib). The very important differences of lithologies between upper and lower Khasib are real reasons for segregating both and placing a major unconformity surface. Upper Khasib records a shallow marine carbonate platform (Zhao et al., 2012).

It is very difficult to find suitable equivalents of Khasib in Iraq. The lower part of the Mutriba Formation in Kuwait seems to be such an equivalent (Douban and Medhadi, 1999).

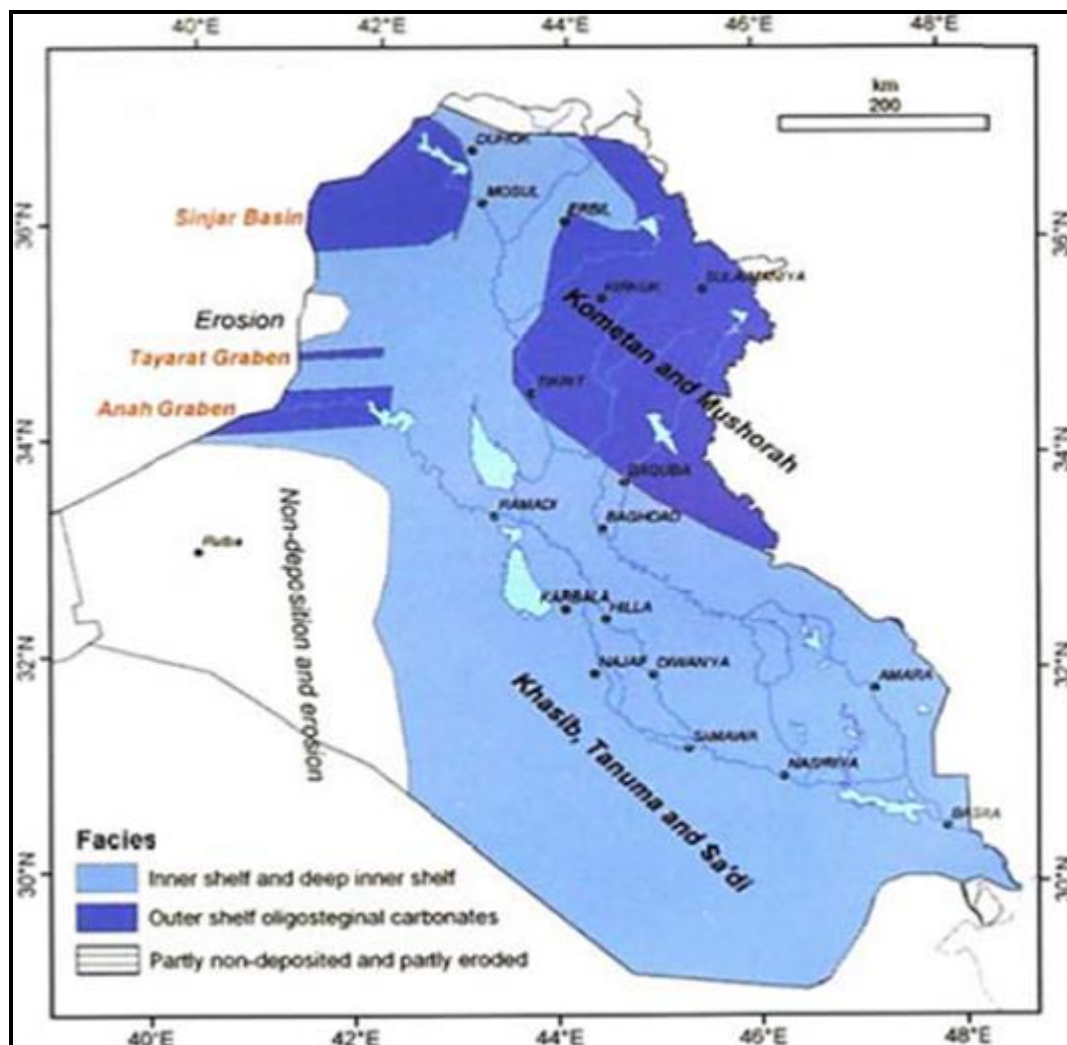


Figure 20: Map of Iraq showing facies distribution across Late Turonian-Early Campanian (Jassim and Goff, 2006)

1.14 Previous Studies

Many geological studies have been done on the Mishrif Formation, on various topics and at various times especially in relation to the oil exploration. These studies include stratigraphic, petroleum geochemistry, geophysics, mineralogy, depositional environment and facies studies.

Henson (1940 cited in Buday, 1980) described stratigraphy and environment of the marine Cenomanian represented by the M'sad Formation, considered as a facies of the Mishrif Formation in the stable shelf to the west of the Abu Jir subzone mainly on the slopes of the Rutbah Uplift. The Mishrif Formation was studied by many researchers, whose first was (Rabanit, 1952), who defined the formation in Zubair area southern Iraq. The Mishrif Formation represents a very complex sequence defined originally as complex of detrital limestones, containing sometimes algal, rudist and coral-reef limestones; capped by limonitic fresh water limestones that have previously called Khatiyah Formation (Buday, 1980a).

Other studies carried out on the Mishrif Formation by Smout (1956) determined Turonian as an age of formation. Fox (1957 cited in Al-Zaidi, 2013) also determined the Mishrif Formation. Owen and Nasr (1958), described the thickness and lithology of the

Mishrif Formation. According to the original description with the exception of its uppermost part, the Mishrif Formation of the type area is composed of grey-white, dense, algal limestones with gastropods and shell fragments above, brown, detrital, porous, partly very shelly and foraminiferal limestones, with banks of Rudists below (Bellen et al., 1959).

Chatton and Hart (1962) inserted all organic detrital neritic limestone formations of Cenomanian-Early Turonian age such as M'sad, Gir Bir and Mergi formations into the Mishrif Formation. Dunnington (1967b) has described the expansion of Mishrif Formation at northwestern parts of the Foothill Zone in northern Iraq. (Ditmar and Iraqi-Soviet Team, 1971) described the Gir Bir and M'sad as separate formations and excluded on the other hand the Mergi formation. They have accepted in principle the ideas of Chatton and Hart (1961-1962), who suggest to include into the Mishrif Formation all organic detrital neritic limestone units of Cenomanian-Early Turonian age, such as the M'sad, Gir Bir, and Mergi Formations.

(Gaddo, 1971) suggested that the Mishrif Formation contains rudist biostromes, forming under the effect of different paleoenvironments. (Al-Khersan, 1973) studied the Mishrif Formation environment and divided the environment into five different types represented by intertidal, subtidal, banks margins, banks and open sea environments. (Al-Siddiki, 1978) studied the microfacies of the Mishrif Formation in southeastern Iraq and proposed the thickness of Mishrif Formation in the north of Majnoon Field to be nearly 400 m.

(Buday, 1980a) proposed the structural features of the Samarra, Dujaila and Amara Ridge, which extend southwards to Burgan High, are influenced by the distribution of shallow water facies of the Mishrif Formation. (Belaribi, 1982) studied the sedimentary environment and the distribution of facies in the Mishrif Formation (southern Iraq) and determined six sedimentary facies: lagoonal, shallower, subbasinal, coral reef and fresh water facies. (Al Naquib, 1985) studied the geology of the Arabian Peninsula in southwestern Iraq. This study covers the whole Iraqi territory south of latitude 32°N., and west of the Euphrates River. He explained the systematic units of stratigraphy system and the oldest rocks (Lower Triassic?) in the outcrop located in the Ga'ara depression.

(Al-Nuaimy, 1990) studied the environment of the Mishrif Formation and proposed the Cenomanian- Early Turonian as age of the Mishrif Formation. (Al-Sharhan, 1995) studied the facies variation, diagenesis and exploration potential of the Cretaceous rudist bearing carbonates of the Arabian Gulf. (Nairn and Alsharhan, 1997) developed a study of Cretaceous rocks in southern Iraq, including sedimentology and petroleum geology. (Aqrabi et al., 1998) studied the facies and environment of the Mishrif Formation in the Mid Cretaceous and proposed that the Mishrif Formation rudist-bearing carbonates as an important reservoir sequence in the Mesopotamian basin of Iraq.

(Al-Khalidi, 2004) found the different types of porosity such as integranular, intercrystalline, fracture, melodic, intragranular and vuggy porosity in the Mishrif Formation in the Halfayia oil field. The first three types are within effective porosity and divided the formation into six reservoir units and six barrier units. He also identified fourteenth secondary microfacies in well HF-1 and recognized the rudist boundstone and packstone-wackstone as the most important facies in the reservoirs. (Jassim and Goff, 2006) published a book about the geology of Iraq and they have explained the structural, tectonic and geological setting of

Iraq. (Handel, 2006) studied the reservoir properties of the Mishrif Formation in the Nasiriyah field. She used self-potential and gamma-ray logs to describe the lithological units.

(Al-Dabbas et al., 2010) carried out an in-depth study of the characteristics of the depositional facies and their environments. They pointed out that allochems in the Mishrif Formation were dominated by bioclasts, whereas peloids, ooids, and intraclasts are less abundant. They determined that the sedimentary microfacies of the Mishrif Formation include mudstone, wackestone, packstone, grainstone, floatstone, and rudstone, which have been deposited in a basinal, outer shelf, slope followed by shoal reef and lagoonal environments in southern Iraq. (Aqrabi et al., 2010) carried out the stratigraphic sequence analysis, which led to three complete order sequences (3rd) being distinguished. Eustatic sea level changes controlled the development of the sequence stratigraphy. Firstly, tectonism defined the sites of platform development that are complicated by the architectural heterogeneity of the depositional sequences.

(Volery et al., 2011) studied microporous in the micrite grains and suggested sizeable hydrocarbon reservoirs in this microporous. They created Mg maps obtained with X-ray EDS combined with scanning transmission electron microscopy (STEM) of micrite crystals from the Mishrif reservoir Formation (The Middle East, Cenomanian to Early Turonian). They found three types of Mg distribution, which were observed through micrite crystals from five different samples: (1) homogenous Mg concentration, (2) small Mg-enriched areas close to the center of the crystal, and (3) geometric Mg impoverishments near crystal edges and parallel to present crystallographic faces. (Al-Itbi, 2013) studied the reservoir characteristics by determining the microfacies and their associated environments in the Gharraf oil field. In addition, she studied the petrophysical properties of the Mishrif Formation in this oil field.

(AL-Zaidi, 2013) studied the Mishrif Formation in Nasiriyah oil field and determined the origin of oil samples belonging to one family, non-biodegraded, marine, and non-waxy deposits and he suggested that oil of Nasiriyah oil field generated from carbonate rocks, which deposited in an anoxic marine environment. For that reason, many researchers emphasized the oceanographic crisis in the carbonate platform (Cenomanian-Early Turonian).

1.15 Major Questions

There are two types of the questions, concerning the carbonate rocks in the platform that built up during Cenomanian-Early Turonian that are:

1. Questions derived from the characteristics of the Mishrif and Kifl formations:
 - ❖ The Permeability ranges from 23 to 775 mD (Jreou, 2013). Depending on the redistribution of the transport systems, including porosity system, stylolite nets, and fractures systems.
 - ❖ Oil reserves are surprisingly very large as they can reach approximately **16** billion barrels. Read more: <http://www.pcldiraq.com/index.php?p=area> or the total of the reserves in the reservoir reach to the **4** billion barrels of oil, according to the Russia's Lukoil Company. Read more: <https://sputniknews.com/business/201504281021473559/>
 - ❖ Did the progress of the diagenesis processes influence the characteristics of the Mishrif and Kifl formations in the Nasiriyah field?

- ❖ Microfacies studies show the gregarious distribution of coral bodies and Miliolida. Additionally, they indicate a drastic decline in abundance of rudists at the Cenomanian-Turonian boundary, where rudist became extinct.
- ❖ Mishrif displays high degree in the diversity of fossils but the low intensity of the genus such as large Foraminifera, Rudist, Algae (Chlorophyta) and Echinodermata. What does this information reflect?
- ❖ Did the effect of microorganisms (bacteria and cyanobacteria) affect the depositional environment of Mishrif and Kifl formations?

2. Questions are involved in the paleogeography of Mishrif Formation.

- ❖ The correlation between paleo-sea level and the evolution of the carbonate platform during Cenomanian-Early Turonian may be responsible for the fluctuation of the recorded fossils.
- ❖ The growth of the carbonate platform occurred during Cenomanian. Thus, it underwent a drastically reduced growth at the beginning of Early Turonian, associated with the rise of sea level of about 300 m (Figure 21 and Figure 22). This crisis represents the first stage of mass extinction.

1.16 Major Problematics

The paleogeographical and geological characteristics of the study area detect many problems, concerning the evolution of carbonate platform shelf that built up during Cenomanian-Early Turonian and these problems are:

- ❖ The correlation between paleo-sea level and the evolution of the carbonate platform during Cenomanian-Early Turonian may be reflected by the fluctuation of the recorded fossils.
- ❖ The carbonate platform grew during Cenomanian and it underwent to a drastically reduced in the growth at the beginning of Early Turonian, associated with the rise of sea level of about 300 m (Figure 21 and Figure 22). Did this crisis represent the first stage of mass extinction?
- ❖ Did the progress of the diagenesis processes influence the Microfacies characteristics and in the same time, they reflect a new tectono-sedimentary-diagenetic model of the Mishrif and Kifl formations in the Nasiriyah oil field?
- ❖ The redistribution of the transport systems in the Mishrif Formation, including porosity system, stylolite networks and fractures systems reflects the heterogeneity values of permeability.

1.17 Objectives of the study

The current study follows a three-stage approach. The first stage consists of identifying the relationships between paleogeographic proxies and the evolution of tectonic activity in the northern part of the Arabian Peninsula during upper Cretaceous. Indeed, one of the points evoked in this study is the effects of boundaries of the Tethys Ocean. The second stage will define the characteristics of paleoenvironmental conditions. The third stage is focusing on the diagenetic environment related to the porosity evolution.

The aim of this study is to shed light on new data on the Mishrif Formation in the Nasiriyah oil field and particularly:

- To establish stratigraphic correlations of the Cenomanian-Early Turonian Sequence and Late Turonian-Early Campanian Sequence, this latter being represented by the Khasib and Gulneri formations.
- To determine the characteristics of the Mishrif reservoir in the Mesopotamian Basin.
- To determine the paleogeographic evolution using many previous studies carried out in the region as well as based on the relative diversity of facies belts.
- To determine the southwestern boundary of the Tethys Ocean that is located in the NE of the Arabian Peninsula.
- To determine the upper boundary of the Mishrif Formation to the Khasib/Kifl formations on one hand, and to the underlying Rumaila Formation on the other hand.
- To analyze microfacies, depositional environments, diagenesis and its effects on reservoir properties.
- To investigate relationships between fossils and primary minerals formation.
- To bring to light changes of carbonate mineralogy and relationships with temperature and fluid circulation history.
- To investigate mineral textures, fluid composition and the properties of fluids using fluid inclusions.

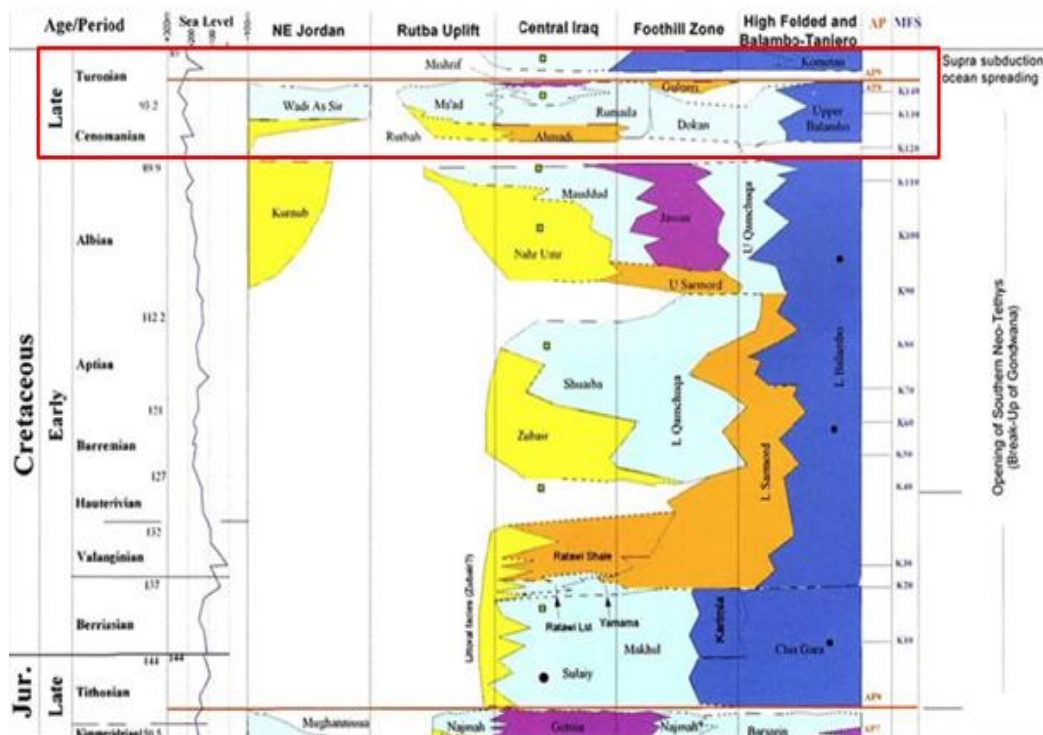


Figure 21: Stratigraphic correlation between sea level and evolution of carbonate platform during Cenomanian-Early Turonian (Jassim and Goff, 2006)

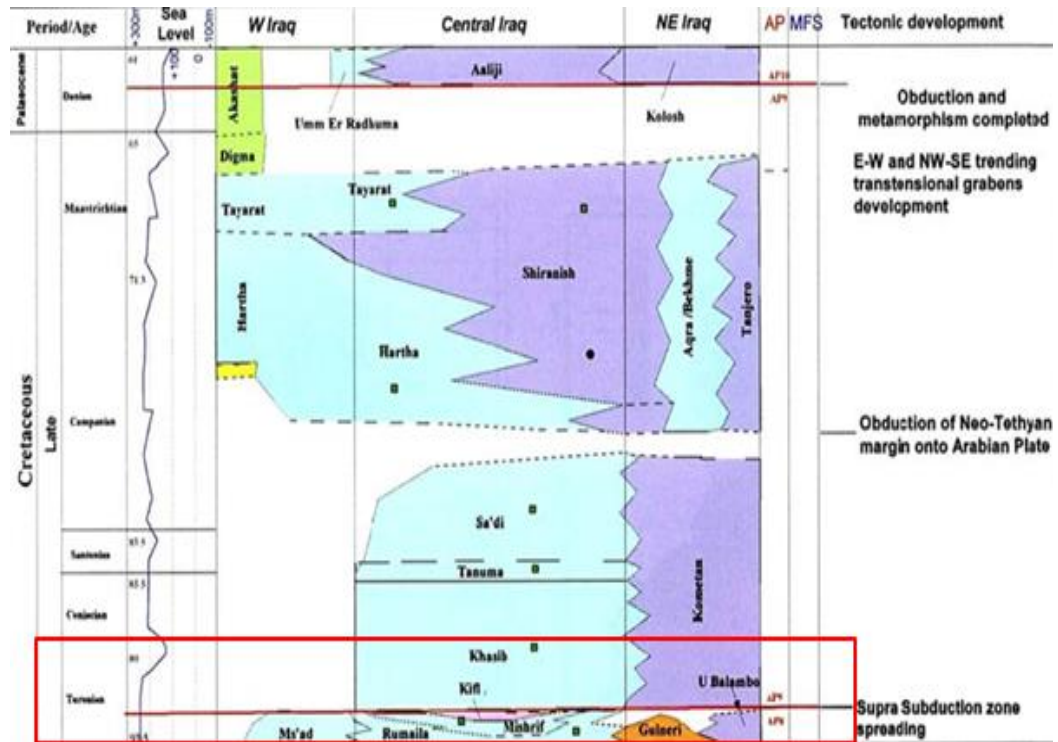


Figure 22: Stratigraphic correlation shows the many Formations, which belong to Late Turonian-Danian Megasequence (Jassim and Goff, 2006)

Second chapter
MICROFACIES ANALYSIS AND PALEODEPOSITIONAL
ENVIRONMENTS

2.1 Introduction

The second chapter focuses on microfossils, microproblematica (grains of uncertain origin), abiogenic grains, matrix or groundmass. The important criteria are used to distinguish amongst carbonate microfacies. The main topics are microfacies analysis, depositional environments and the factors that affect the distribution of organisms in the carbonate rocks of the Mishrif Formation. Finally, the maturity and evolution stages of the grains detected the mass extinction in the Upper Cretaceous.

The petrographic study reveals a range of microfacies, which often indicate to the shallow water marine paleoenvironment. On one hand, the size variation of the shells and the shells which are not fragmented indicate that marine currents were quiet. These paleoenvironments are included the abundance of microbial deposits. On the other hand, in the other zone of the same area study, there are more fragments of the shells and the significant amount of the mud carbonate that indicate to a strong compaction process occurred after the deposition process. The allochems include the foraminifera, corals, rudists, algae, microbialite, favreina microcoprolite, peloids, aggregate grains and rounded clastic grains.

Mishrif Formation includes the allochems sizes range between <0.10 mm and several millimeters. The large sizes of the grains include the large benthic foraminifera, phylloid algae, coral, rudist, oncoids, clastic rounded and aggregate grains, which are > 1mm. In the inside, the small sizes of the grains are the peloids, pellets and intraclasts grains. The microbial boundstone is a dominant process of formation the microbial grains that include the trapping and binding processes of the detrital sediment. In addition, the microbial framestone process has appeared in the same zones, which are under the impact of the biogenic.

Finally, Mishrif includes mudstones, wackstone, packstone, grainstone and bindstones microfacies based on detail of the petrographic microfacies and sedimentological criteria. These microfacies have deposited in the interior platform of the rimmed shelf carbonate in the evaporitic, restricted and patch reef of open marine environments. In this chapter, the sequence of the described grains confirms that carbonate grains have interrelated each other.

2.2 Sampling

In this study, the Mishrif Formation has been investigated from four wells in the Nasiriyah oil field located in Thi Qar Province (SE of Iraq) about 38 km northwest of Nasiriyah city, between latitude 34°80'-34°60'N and longitude 57°50'-60°10'E (Figure 23).



Figure 23 : Location map shows the Nasiriyah oil field modified after (Al-Khafaji, 2015)

151 samples were collected from cores of the four drill cores, NS-1, NS-2, NS-3 and NS-5. All these wells are exploratory. The company that has drilled the wells has taken around 50 m cores from each well, at different depths of the Mishrif Formation. The sampling protocol is therefore systematic and very dense (approximately, one sample each meter) (Figure 24). The thickness of the Mishrif Formation is around 170 m to 180 m in each well (Figure 3).

The first problem that appeared was the difference concerning the thickness of the Mishrif between SOC and other sources. The second problem was the discrepancy between

results of direct studies on the cores and results obtained from well log analysis, especially with regard to unit thickness. For that reason, the best way is to take one sample each meter along the 4 drill cores and to compile data about the nature of the unit. The most important units for diagenetic studies are the shale layer, reservoir unit #1 and reservoir unit #2. Moreover, reservoir unit #1 probably represents the best target to characterize the diagenetic conditions, as it records the effects of fluid circulation and the evolution of secondary porosity as well as the diversity of cement composition.

In addition, the diagenetic evolution has the most important effects on porosity. The dominant porosity is a secondary type, included the dissolution, vuggy, moldic, stylolite, channel, microfracture, fracture porosity. The compaction process played a major role in the diagenetic processes, included cementation, micritization, neomorphism, dolomitization, pyritization, stylolitization, fracturing and dissolution that influenced the petrographic properties.

Major and trace elements were analyzed by the EDS technique, combined with SEM, in order to identify chemical changes by diagenetic processes in carbonate rocks. Finally, the fluid inclusion analysis by microthermometry and Raman spectroscopy was used to identify the responsible fluids of the changes of rock properties.



Figure 24 : Example of cores drilled in the Nasiriyah oil field during the collection process of samples

Table 1: Distribution of samples is related to reservoir units

Units of wells	Minmum thickness (m)	Average thickness (m)	Maximum thickness (m)	No. of samples
Khasib Formation (above cap rock)	/	/	/	10 (NS-5)
Cap rock	4.5	7	12.5	/
Upper Mishrif	52	56	62	7 (NS-3)
Shale layer	10	12	13	5
Reservoir unit #1	11	14	23	28
Barrier rock	2	3	6	6
Reservoir unit #2 (high saturated oil)	36	44	52	64
Reservoir unit #2 (high saturated water)	30	35.5	40.7	31
Total Samples				151

First, 100 hand specimens were observed under a binocular Olympus SZX12 to prepare more than 50 thin sections, which were studied to understand the microfacies, paleodepositional environments, exotic mineral studies and diagenetic processes (Table 2). Microscopic observations were carried out using an optical microscope Olympus BX60. In addition, cathodoluminescence, fluorescence, Raman microspectrometry and Scanning Electron Microscope (SEM) were applied to thin sections.

The existence of various groups of organisms in the Mishrif requires a particular method to infer paleoenvironmental proxies. We have adopted a sequenced method. This method is a type of microfacies approach that is based on the relationships among interrelated components (fossil grains). For example, the relationship between some types of algae and corals is parasitic in nature. Another example is the coexistence between algae and microbial grains that could reflect a shallow water environment. For that reason, the microfacies study was divided into three stages. Firstly, skeletal grains were categorized depending on their abundance. Secondly, microbial grains were determined as a function of their effects on the observed area. Thirdly, non-skeletal grains (microbial or abiogenic grains) were interpreted depending on the natural distribution and chemical composition.

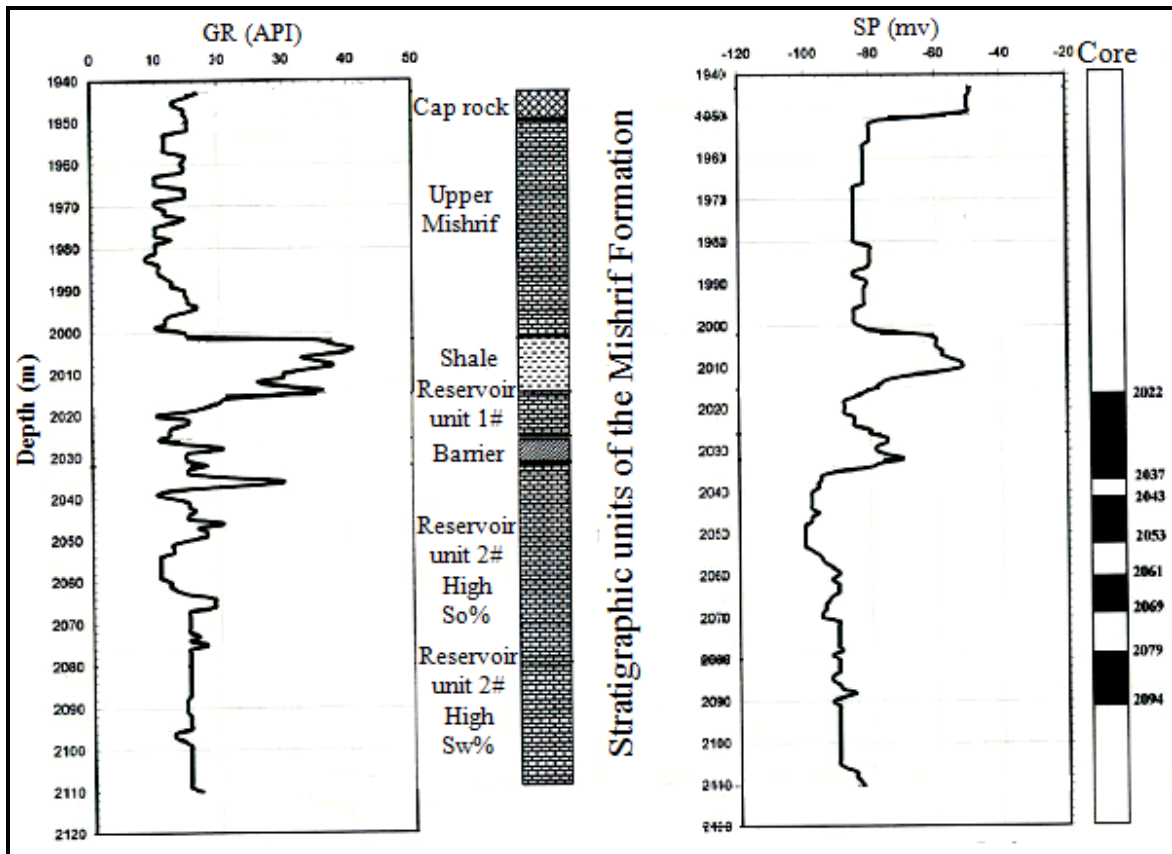


Figure 25 : Samples are collected based on the stratigraphic units of the Mishrif Formation in the NS-1 well (source: South Oil Company, SOC)

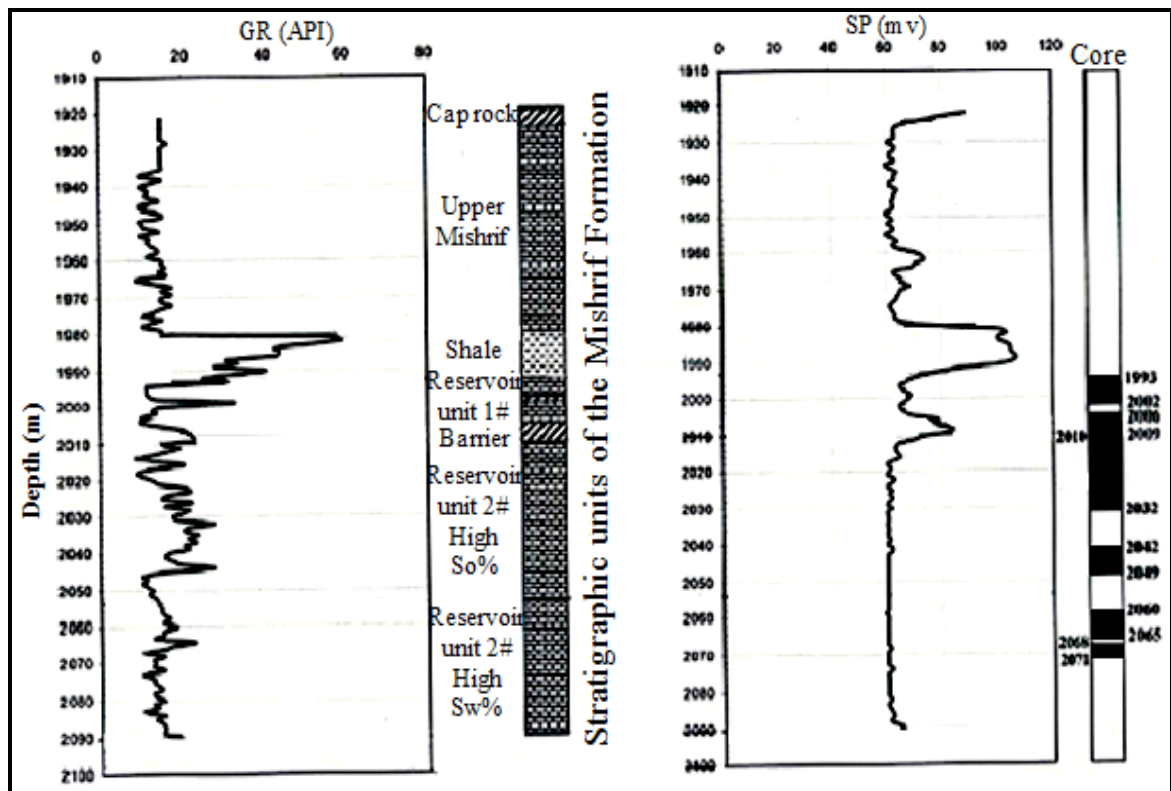


Figure 26 : Samples are collected based on the stratigraphic units of the Mishrif Formation in the NS-2 well (source: South Oil Company, SOC)

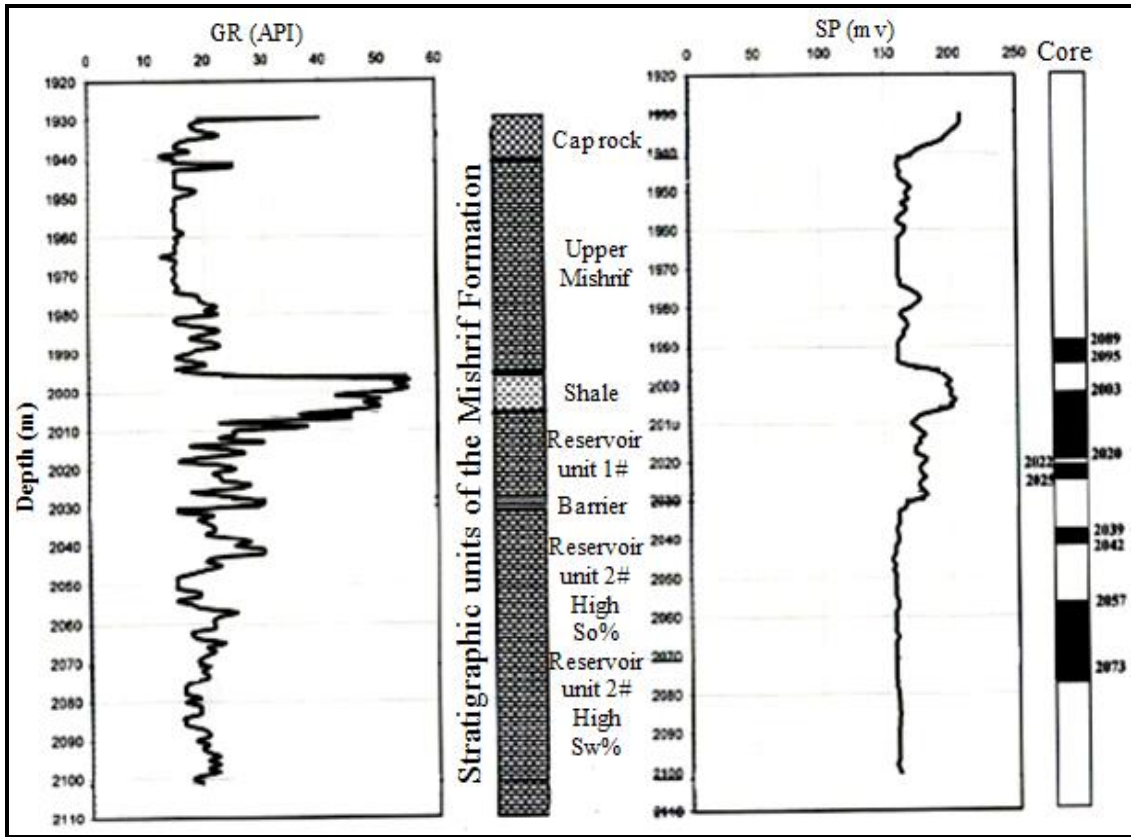


Figure 27 : Samples are collected based on the stratigraphic units of the Mishrif Formation in the NS-3 well (source: South Oil Company, SOC)

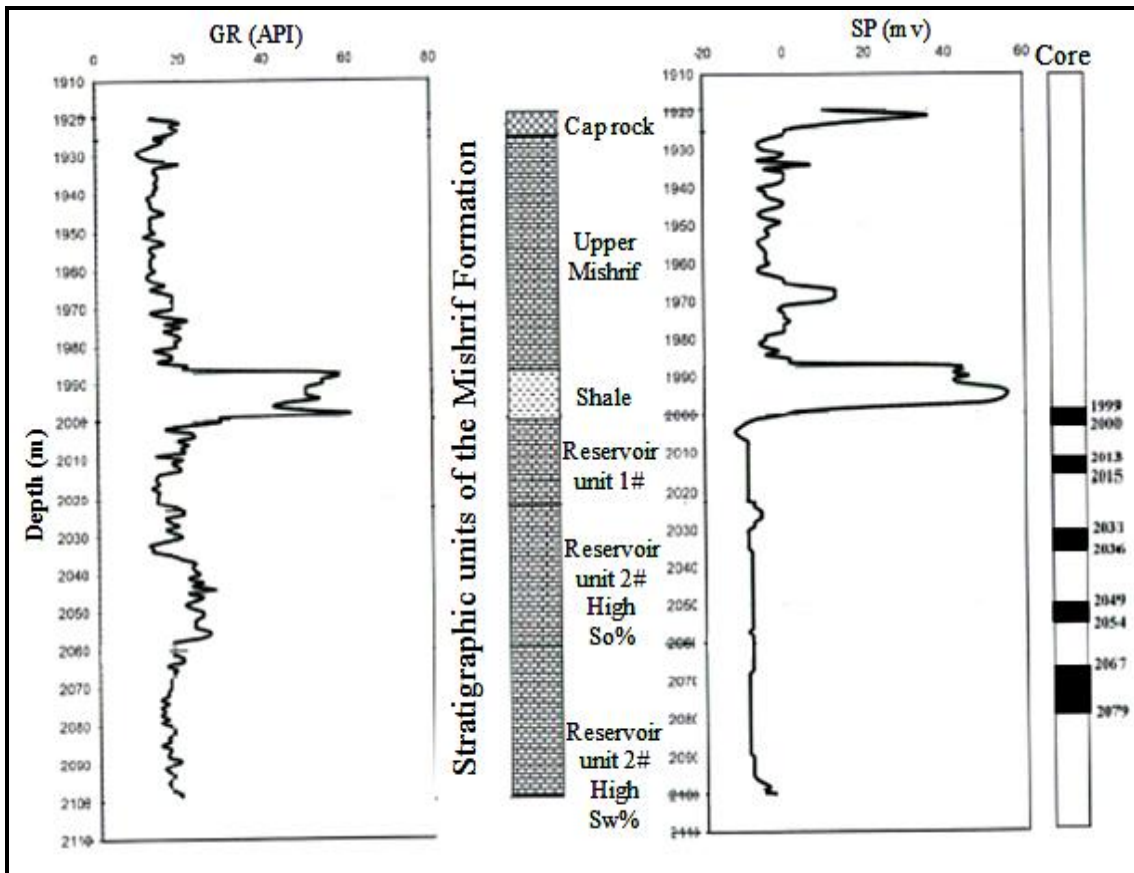


Figure 28 : Samples are collected based on the stratigraphic units of the Mishrif Formation in the NS-5 well (source: South Oil Company, SOC)

Table 2 : Thin sections of samples prepared for microfacies analysis

No.	Depth references m	Well No	Units of Mishrif Formation in the Nasiriyah oil field
1	2024.60	NS-1	Reservoir unit #1
2	2027.42		Reservoir unit #1
3	2033.80		Reservoir unit #2 high saturated oil
4	2043.42		Reservoir unit #2 high saturated oil
5	2048.95		Reservoir unit #2 high saturated oil
6	2052.90		Reservoir unit #2 high saturated oil
7	2064.50		Reservoir unit #2 high saturated oil
8	1993.10	NS-2	Reservoir unit #1
9	2002.52		Reservoir unit #1
10	2005.55		Reservoir unit #1
11	2014.66		Reservoir unit #2 high saturated oil
12	2023.05		Reservoir unit #2 high saturated oil
13	2042.65		Reservoir unit #2 high saturated oil
14	2048.26		Reservoir unit #2 high saturated oil
15	2062.60		Reservoir unit #2 high saturated water
16	2070.80		Reservoir unit #2 high saturated water
17	1992.70	NS-3	Upper Mishrif Formation
18	2003.53		Shale
19	2007.32		Reservoir unit #1
20	2011.66		Reservoir unit #1
21	2014.67		Reservoir unit #1
22	2018.86		Reservoir unit #1
23	2024.25		Reservoir unit #1
24	2039.91		Reservoir unit #2 high saturated oil
25	2062.58		Reservoir unit #2 high saturated oil
26	2065.85		Reservoir unit #2 high saturated oil
27	2070.21		Reservoir unit #2 high saturated oil
28	2075.90		Reservoir unit #2 high saturated water
29	1897.48	NS-5	Shale
31	1902.87		Shale
32	1999.60		Shale
33	2014.10		Reservoir unit #1
34	2031.65		Reservoir unit #2 high saturated oil

No.	Depth references m	Well No	Units of Mishrif Formation in the Nasiriyah oil field
35	2032.30		Reservoir unit #2 high saturated oil
36	2033.80		Reservoir unit #2 high saturated oil
37	2049.47		Reservoir unit #2 high saturated oil
38	2051.77		Reservoir unit #2 high saturated oil
39	2067.53		Reservoir unit #2 high saturated water
40	2075.19		Reservoir unit #2 high saturated water

2.3 Petrographic Description

In this chapter, we will highlight the grain and matrix types in the Mishrif, the modification, and changes that operated on the grains during their formation. Microfacies are identified according to the classification of (Dunham, 1962). This classification is based on the concept of grain-supported rock texture. Grains are sedimentary particles arising before sedimentation.

2.4 Characteristics of grains

Variations of grain types reflect the variety in the paleoenvironments for both marine and non-marine carbonates because the grain types result from paleoenvironmental factors (e.g. water temperature, water energy levels, sedimentation rates and variation of spatial distribution of grains). The compositional maturity is the extent to which a grain-rich carbonate sediment approaches the constituent end-member such as intraclasts, ooids, fossils, peloids, micrite matrix, and terrigenous minerals (Smosna, 1987). The constituent endmembers reflect the complexity of the processes operating in carbonate sediments.

2.5 Skeletal grains and microbial grains

Examination of thin sections shows that the studied formation contains a proportion of benthic Foraminifera or pieces of structures (shell), planktonic Foraminifera or floating Foraminifera, corals, molluscs (Rudists) and green algae (Chlorophyta). In addition, the grains have a biological origin but they can not be attributed to any known skeletal structures that are called microproblematica, including microbialites grains and *Favreina* microcoprolite grains.

The abundance of skeletal grains and microproblematica grains are controlled by several factors such as the abundance of the benthic organisms, light (shallow water levels), water temperature, salinity, the rate of carbonate production versus the rate of siliciclastic input and spatial variations in the distribution of grains related with latitude.

Comparison of the biotic composition of the Mishrif Formation in the Nasiriyah oil field with common microfossil groups and Flugel's observations for a similar period indicates strong similarities in fossils distribution except for corals in the edge shelf.

The important point of skeletal grains and microproblematica grains is the mineral composition. All these grains in the first glance are composed of minerals such as aragonite and high magnesium-calcite. Note that those grains are essential features to describe the

depositional environment in addition to representing a high potential to infer diagenetic conditions.

2.5.1 Foraminifera

Foraminifera are present in the various units of the Mishrif Formation. Benthic Foraminifera exist in the upper and middle parts and planktonic or floating Foraminifera are in the lower part of Mishrif.

2.5.1.1 Benthic foraminifera

Foraminifera are common in restricted lagoon at shallow inner platform environments from Late Paleozoic to Early Tertiary (Flügel, 2010).

Foraminifera represent the second group of shells protists in importance inside the Mishrif Formation of the Nasiriyah oil field. Most foraminiferal tests found in the upper and intermediate parts, particularly benthic foraminifera, have a large size from 0.6 to 3 mm and more, but smaller shells of size less than 0.6 mm are abundant. Note that the complexity of the internal structure of benthic Foraminifera increases with increasing size, particularly the number of chambers (Figure 30 and Figure 31).

Benthic foraminifera have a great importance because they are considered as index fossils for Cretaceous carbonate platform. Currently, benthic foraminifera allow discriminating the detailed stratigraphic zones in shallow-water limestones of early and middle Cretaceous. In addition, oxygen isotopes can be used to identify the stratigraphic zones as a biozonation or paleoceanographic zones by using the water temperature as accurately determined tool. Oxygen isotopes carried on calcite tests of benthic Foraminifera provide accurate temperature estimations.

Benthic foraminifera present in the Mishrif formation that include a large variety of genus and families (e.g. Miliolids, Alveolinids, *Discocyclina*, and *Textularia*). This abundance indicates very good conditions for living at that time.

Miliolids (Figure 29) and Alveolinids represent some valuable paleoenvironmental indicators. Miliolids live in shallow warm waters of normal salinity. They occur in different microfacies formed in shallow lagoonal platforms and sometimes in close association with reefs. Their tests lack pores and they have multiple chambers. The type of wall composition (porcelaneous, hyaline and agglutinated) can be used as an accurate tool to determine the paleodepths and salinity by plotting in triangular diagrams (Miracle, 2002). They are composed of calcite needles that have a significant proportion of magnesium with organic material. This proportion of magnesium is responsible for the abundance of dolomite.

Textularia exists in various marine environments. They are often dominant in transitional environments with brackish and marsh conditions as well as in the bathyal and abyssal depths.

However, in the case of Mishrif Formation, the benthic foraminifera have large shells suggesting formation in the transitional environment instead of in deep marine (bathyal zone or abyssal zone) environment where shells are predominantly of small size below the photic zone. The coexistence of Miliolids and Alveolinids suggest a deposition environment in lagoonal environments.

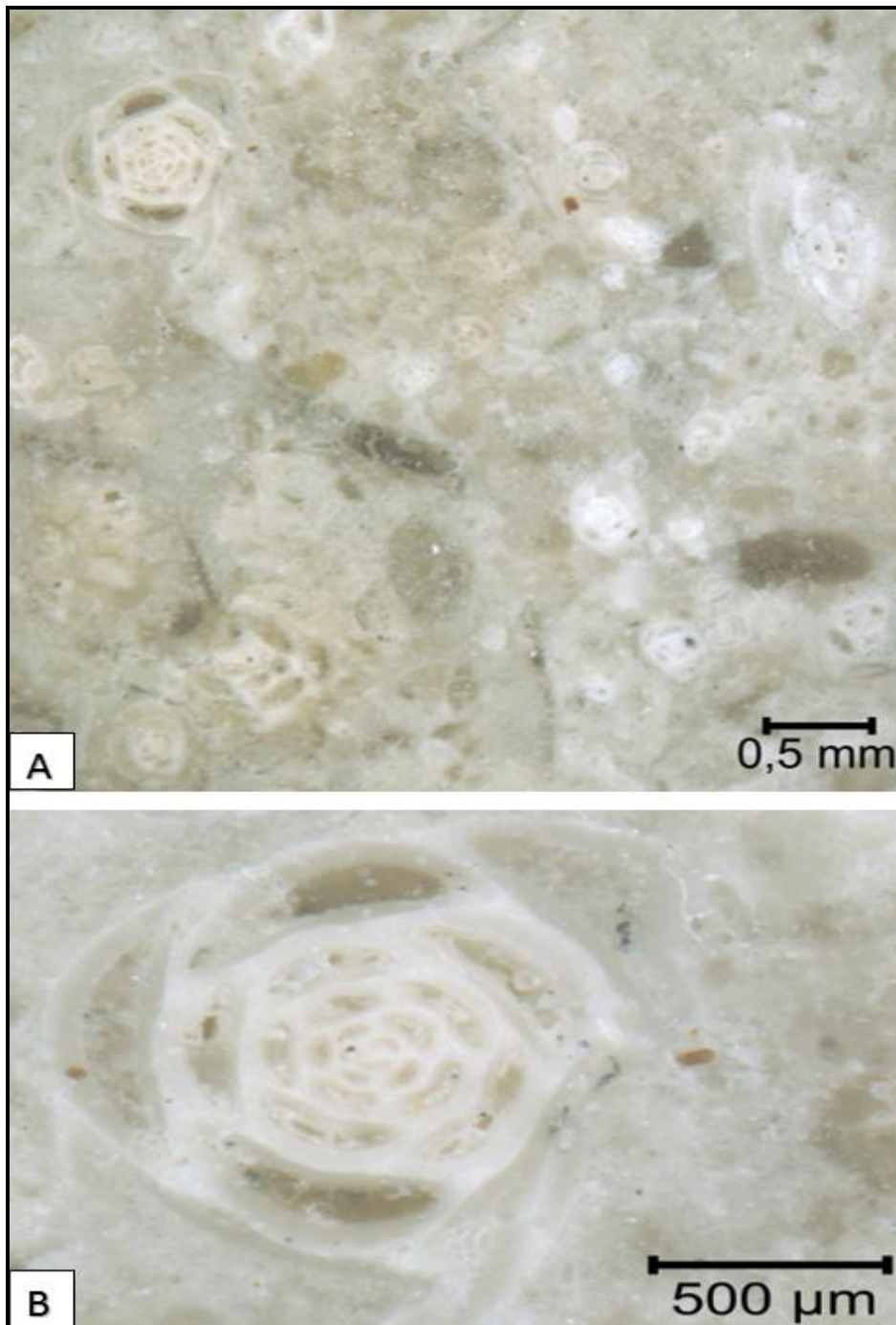


Figure 29 : (A) The abundance of Miliolids (B) Typical chambers of Miliolid (NS-2 well at depth 2014.66 m, Mishrif Formation, SE Iraq)

Figure 30.

A. Core No. NS-1 (Sample Depth 2052.90m): Cretaceous Foraminifera Superfamily Alveolinidae: The longitudinal section of alveolinidae, known from the Early Cretaceous up to today (Flügel, 2010). They have calcareous unperforated tests. The chambers are divided into numerous chambers by septula and they are arranged in many rows. Coiling is ovate but appears as planispiral in section. This genus was the largest found in the Mishrif Formation, size could be as large as 3 mm.

B. Core No. NS-1 (Sample Depth 2064.50m): Cretaceous Foraminifera Superfamily Alveolinidae: Cross section of genus *Cisalveolina fallax* found in the deeper part of the Mishrif formation. The chambers appear semi-perforated and coiling is fusiform. Whereas dissolution is very important at this depth it does not significantly affect the tests of the *Cisalveolina fallax*. (Saint Marc, 1979) has given an age of Late Cenomanian to Early Turonian for *Cisalveolina fallax*.

C. Core No. NS-5 (Sample Depth 2051.17m): Cretaceous Foraminifera Family Fusulinida: Cross section of the common fusulinid, shells exhibit the morphological criteria that allow an age determination. The chambers are organized in many rows and coiling is fusiform. Fusulinids live in the clear-water, offshore environment, and reef shelf. The brown colour indicates a large proportion of organic matter.

D. Core No. NS-1 (Sample Depth 2064.50m): Cretaceous Foraminifera Superfamily Alveolinidae: Large fragments of Alveolinidae. The matrix is composed of sparite, which is rich in fine fossil debris.

E. Core No. NS-1 (Sample Depth 2033.80m): Cretaceous Foraminifera family Gavelinellidae: The specimen resembles *Gavelinella*. The genus has many chambers with perforated walls. Coiling is fusiform and the base reveals a high proportion of organic material. Age given by (Tyszka, 2006) is Cretaceous.

F. Core No. NS-1 (Sample Depth 2033.80 m): Cretaceous Foraminifera Superfamily Discocyclina: univalve kind of shells. The laminated test has orientation. The form of Discocyclina reveals the compaction process and the area has thin stylolites, indicated to late compaction with low capacity. It contains small fragments of bioclasts with the high ratio of the organic material.

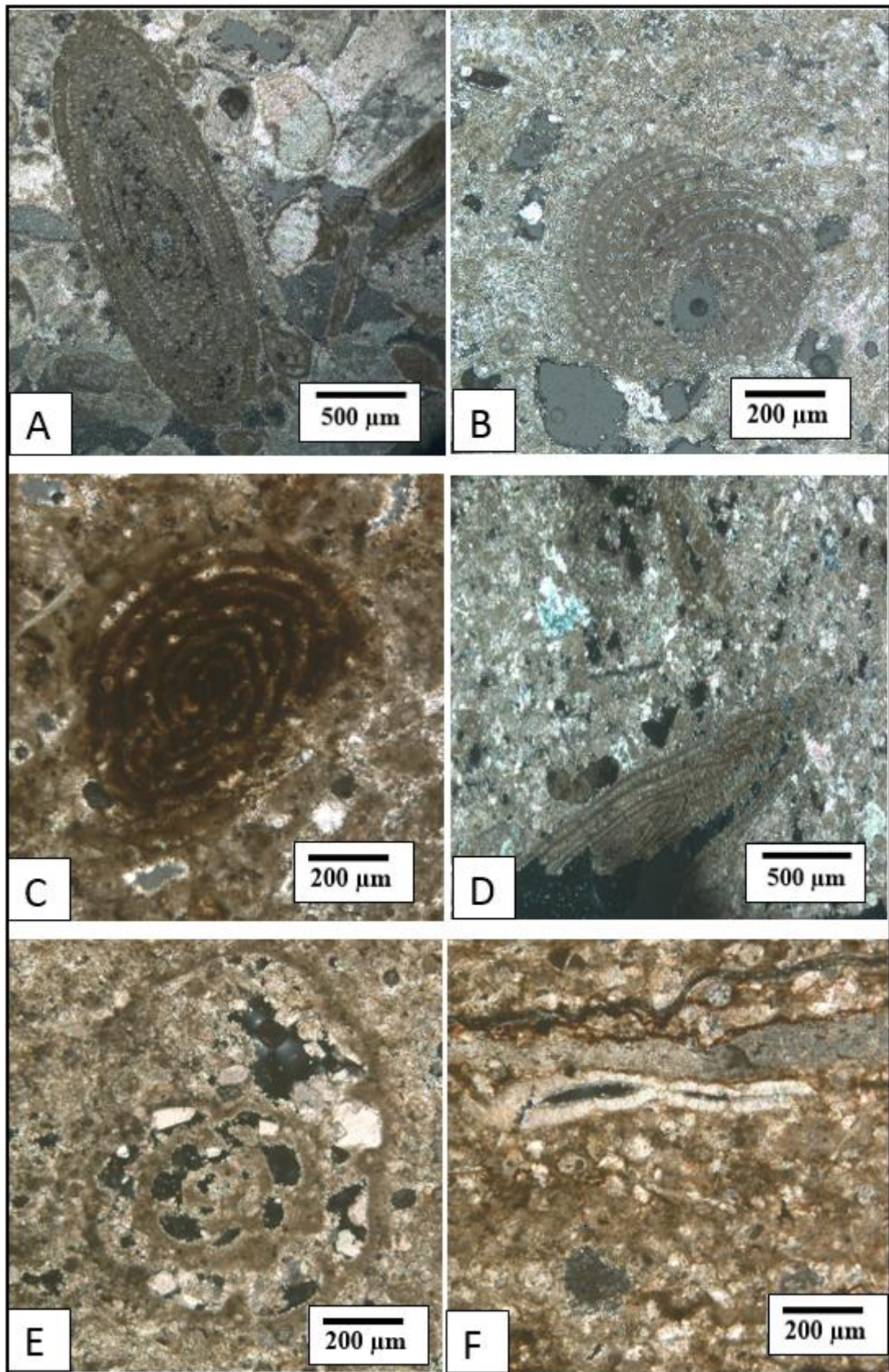


Figure 30 : The diversity of benthic Foraminifera exists in the NS-1 well at depth from 2033.80 to 2064.50 m (Mishrif Formation, SE Iraq)



Figure 31 : Longitudinal section of *Chrysalidina* belongs to benthic Foraminifera. Chambers are arranged on the form of triserial with decrease of the number of chambers towards the end of the shell. Chambers are strongly overlapping. The final three chambers are occupying one-third to one-half of the shell length. Cenomanian-Turonian age exists in the NS-3 well at depth of 2024.25 m (Mishrif Formation, SE Iraq)

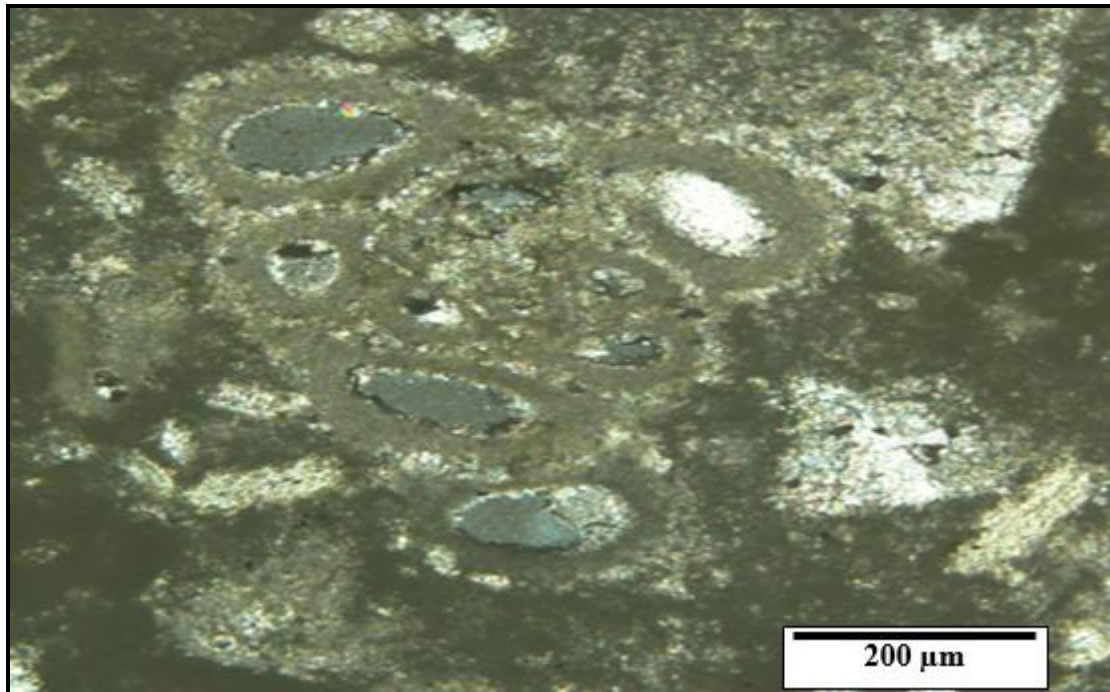


Figure 32 : Cross section of microplanktonic Foraminifera composed of many chambers in carbonate mud with a low proportion of cement. Coiling is fusiform. Chambers are arranged like grape clusters, existed in the NS-2 well at depth of 2014.66 m (Mishrif Formation, SE Iraq)

2.5.1.2 Planktonic foraminifera

Planktonic foraminifera are considered as organisms living in the upper part of the open oceans as a pelagic depth zone or photic zone (Flügel, 2010). Further, these organisms are the best indicators for the basinal environment or they are usually found in the ooze deposited on the deep-sea bottom. They are very important tools for interregional correlations for Cretaceous and Cenozoic (Bolli et al., 1985) terranes.

Planktonic foraminifera (*Globigerina* ooze, *Oligostegina*, and *Globotruncana* assemblages) are abundant in the Mishrif Formation in the NS-5 well from the depth ranging from 1897.48 to 1999.60 m in a fine-grained carbonate mud. These levels are considered as critical to differentiate a Cenomanian-Early Turonian or Late Turonian-Early Campanian age. Moreover, they are best indicators of the transgression process (flood scenario).

The distinction between the two sequences (Cenomanian-Early Turonian and Late Turonian-Early Campanian) is based on the sediment colour. Indeed, the dark gray to greenish gray colour is the distinctive colour for sediments of the deep shelf environments (Flügel, 2010) (Figure 32 A & D) whereas the light brown colour would correspond to shallow marine environments with the euphotic zone (Figure 32 B & C). For that reason, we consider that depth 1999.60 m coincides with the transition between the Khasib and Mishrif formations in the NS-5 well. The Khasib Formation overlies Mishrif in NS-5 and NS-3 wells whereas, in NS-2 and NS-1 wells, the Kifl overlies Mishrif.

Deep inner shelf and lagoons represent potential formation environments of the Khasib Formation (Jassim and Goff, 2006) based on oligosteginal fauna. Assemblages include *Globotruncana*; it is another argument for the open marine environment.

In the NS-3 well at depth 2062.58 m, the presence of planktonic Foraminifera indicates the boundary between Mishrif and Rumaila. The Mishrif Formation in the Nasiriyah oil field can be considered as a sandwich of organic matter with fossiliferous limestone surrounded by carbonate mud of the overlying Khasib and the underlying Rumaila formations.

Planktonic foraminifera are found in the Rumaila Formation in the section type of the Nasiriyah oil field. The list of fossils contains Oligosteginal fauna was published by (Bellen et al., 1959).

The presence of planktonic Foraminifera in the Mishrif Formation is not considered as a critical indicator of the marine environments. The deposition conditions of the planktonic foraminifera are determined by an intense presence of planktonic foraminifera. The planktonic foraminifera have lived and died during a short time, could be considered as typical conditions of the deposition.

The concept of sea transgression interprets the presence of planktonic foraminifera specifically in NS-5 well. The flood scenario plays important role in the transition process of planktonic foraminifera. The factors of environment include water salinity, temperature, nutrients supply and photic zone also support the reproductive process in the planktonic foraminifera. Finally, could say the planktonic foraminifera exist in the different microfacies, formed in deep inner shelf and sometimes in close to margins reef.

Figure 33.

The evolution of the planktonic foraminifera during Late Cretaceous is shown in (Figure 32 & Figure 33) through the number of chambers, which have perforated walls.

A&C: Core No. NS-5 (sample depth 1999.60 m): Late Cretaceous Phylum planktonic Foraminifera, Genus: *Globigerina* with fragments of benthic Foraminifera

Planktonic Foraminifera mixed with fragments of benthic Foraminifera, molluscs and corals in the light to brown carbonate mud reflects the euphotic zone deposits of shallow marine inner platform environments in the upper part of the Mishrif Formation in the Nasiriyah oil field, SE Iraq.

B: Core No. NS-5 (sample depth 1897.48 m): Late pelagic Cretaceous Phylum planktonic Foraminifera, Genus; *Globigerina* with Genus *Oligostegina*

Planktonic Foraminifera in the dark gray shale reflect the outer shelf to basinal deposits in the lower part of the Khasib Formation in the Nasiriyah oil field, SE Iraq.

D: Core No. NS-5 (sample depth 1902.87 m): Late pelagic Cretaceous deposits Phylum planktonic Foraminifera, Genus; *Globigerina* with Genus *Oligostegina* and *Globotruncana* assemblages

Sediments represent the lower part of the Khasib Formation (Figure 33 D). The fossils presented a very well preserved, which reflects a very quiet environment. The correlation between (Figure 33 C & D) is very clear and it may be used to establish a regional correlation between Cretaceous (Cenomanian-Early Turonian and Turonian-Late Campanian) regardless the sediment differences.

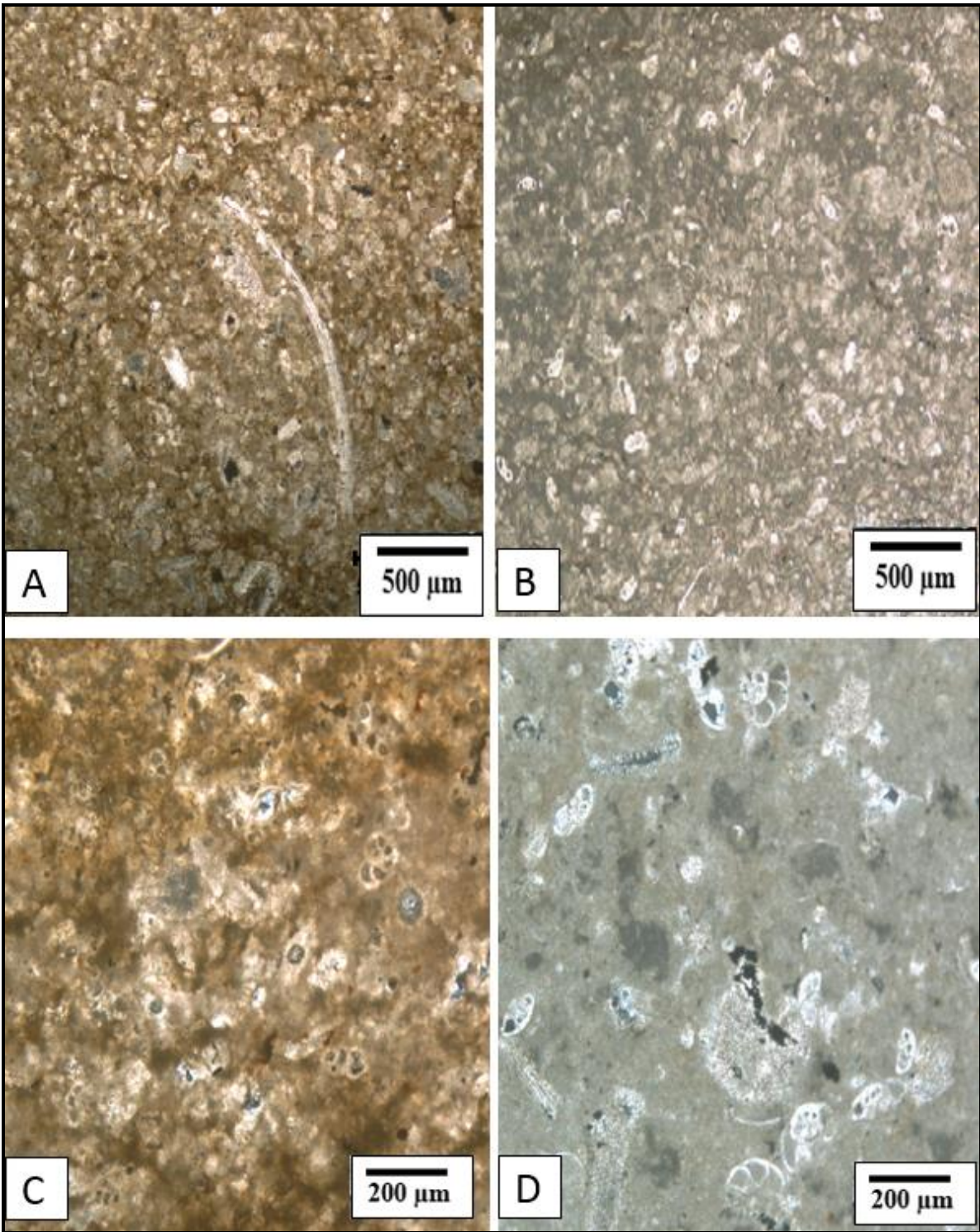


Figure 33 : The correlation of Upper Cretaceous is inferred from the microfacies analysis of the Mishrif Formation and of the lower part of the Khasib Formation in the NS-5 well at depth from 1897.48 to 1999.60 m, SE Iraq

2.5.2 Corals

Corals represent the first major group in limestones of the Mishrif Formation in the Nasiriyah oil field. Corals (Anthozoa) are classified into two types in terms of natural living: Colonial and solitary coral. Colonial corals consist of large numbers of polyps cemented together by calcium carbonate produced by themselves (Figure 35.F). They have erect-branched shape. Each polyp has (0.5-2) millimeters in diameter and a few centimeters in length. Corals exclusively live in the marine environment and are usually sedentary. They are important reef builders in tropical oceans, subtropical, warm water but also in cold water. Distribution of corals starts from Paleozoic as rugose and tabulate corals and goes on to Cenozoic as scleractinian corals, which are subdivided into numerous families depending on their morphology and skeleton (Flügel, 2010). The subclass Zoantharia of order Tabulata is mentioned in (Scholle and Ulmer-Scholle, 2003) and it has existed from Ordovician (Cambrian?) to present. They were contributors of stromatoporoid, microbial reefs, and biostromes. These bioherms are built as small isolated biostromes widely distributed in muddy, open shelf carbonate environments. Corals sometimes do not grow continuously because they are covered by mud, oncoids or bioclasts.

The most abundant corals are erect-branched corals, which can be distinguished according to their cylindrical or crescent shape or forming polygonal tubes (Figure 34.A & Figure 35). The coarse-bedded form is significant characteristic in this environment (Figure 35.A, B). The less abundance of coral in the Mishrif Formation is microtabulate hexa-polygonal (Figure 34.B).

Noteworthy, corals in the Mishrif are classified within the euphotic zone of the interior platform in open marine. As well as, the ecosystem of open marine is connected with the open sea to keep on the same salinity and the temperature. The local reef patches or organic banks widely distribute in the attached platforms. They occur in different types of microfacies, mainly formed in the reefs, shallow lagoons platforms and in upper slope settings.

The corals have framework porosity. The economic importance of the Mishrif Formation comes from the corals because this site of corals produces the high ratio of calcium carbonate. In addition, the site of corals always contains the high diversity of the organisms, lived in the patches-corals reef. The high porosity of the corals reef and possibility to preserved organic matter due to coexistence between corals and other organisms that exist in the corals reef, made this site is an important petroleum reservoir.

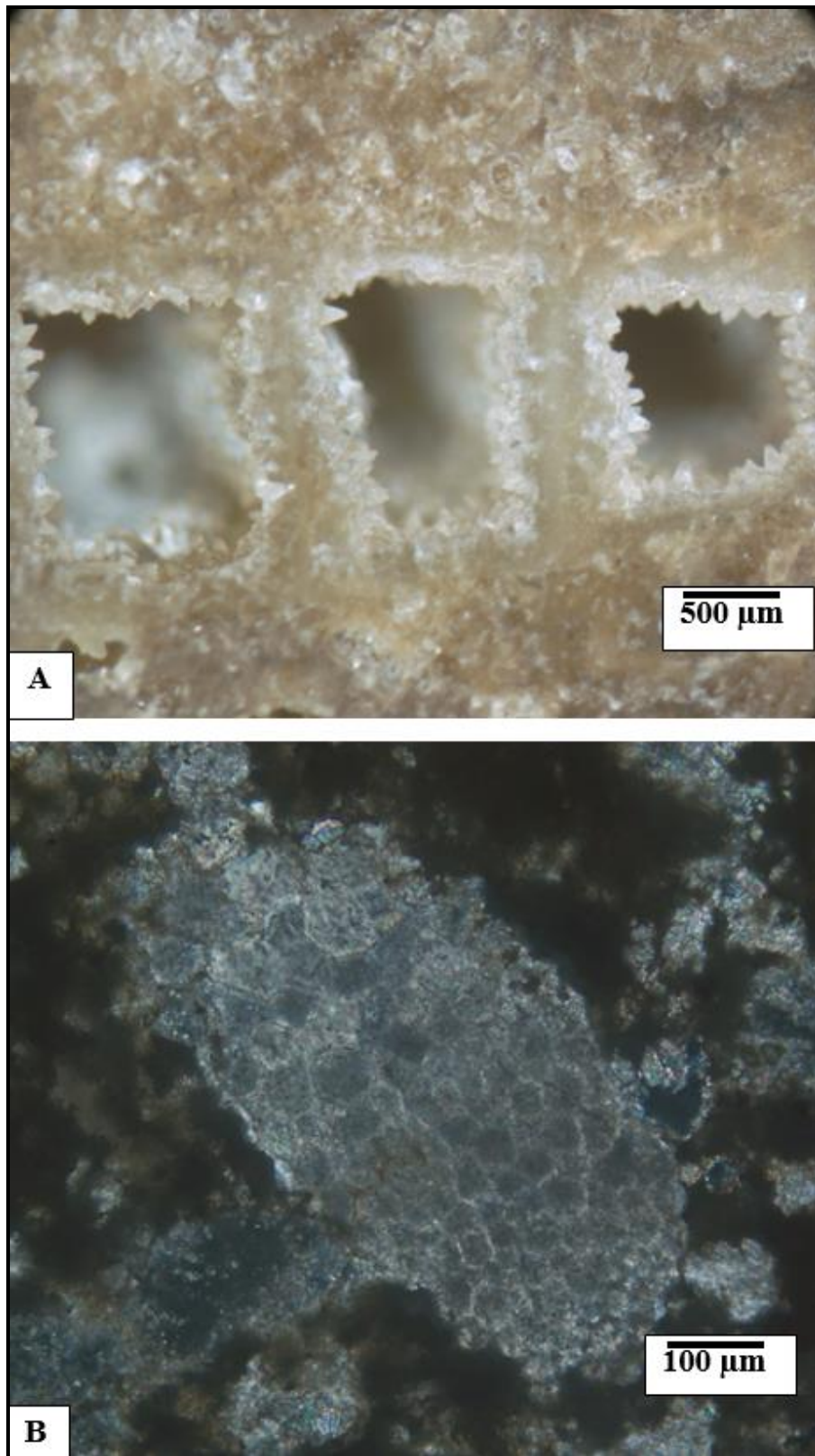


Figure 34: Polymorphous bodies of colonial corals (A) Colonial corals exist as a polygonal shape (cubic to rectangular), with framework pores (NS-5 well, depth 2031.65 m). (B) Microtabulate coral is a coral honeycomb (NS-5 well, depth 2051.77 m) (Mishrif Formation, Nasiriyah oil field, SE Iraq)

Figure 35.

The preservation stages of the erect-branched corals compare with diagenetic stages in sketch after (Flügel and Flügel-Kahler, 1997 cited in Flügel, 2010) (Figure 36). The diagenetic stages enhance the effect of the diagenetic process in change the exterior form of the erect-branched coral particularly in the figures C and D. All the changes on coral skeletons are determined under Binocular SZX12 in (Figure 35). Finally, the effect of compaction process has relatively increased but it does not depend on the increase of depth.

A: The corals show the typically cross-bedding layers. The organisms appear as a pack of erect-branched corals without any curvature because the small size of colonies allowed them to undergo a high degree of compaction without deformation. Preservation can be enhanced by coral structures cross-bedding, by the pre-cementation process of fine crystals of calcite cement that exist between the members of colony corals (polyps). The gray colour shows the ratio of organic matter. The size of colonial coral is about three cm³ at depth 2078.32 m in the NS-5 well.

B: Sticks-coral underwent an important compaction in this zone and the cross-bedding was removed. Cylindrical shape and the small fragments of corals still conserved. The thickness of coral wall clearly appears and the white colour reflects the sample, which is relatively free from organic matter. The corals show the molds without the interior structures such as corallites and these molds are not opened. The sample was taken from the depth of 2032.30 m in the NS-5 well.

C: The cylindrical shape of corals still protected but the increase of effect compaction leads to make its crescent shape. In some cases, chemical compaction leads to close some coral molds. Hence, corals have elastic degrees depend on the force of compaction process (the effect of pressure) and depend on the size of space between the polyps (members of the colony). The sample was taken at depth 2031.65 m in the NS-5 well.

D: The corals shape underwent to change its exterior form. Polygonal shape appears during reduce the intergranular porosity among the polyps. Some of the coral polyps have completely closed by blocky burial cement, which led to reduce the intragranular porosity. The coral molds are filled with blocky calcite cement and rhombohedral dolomite. The corals have multiple shapes in the same depth so they have cylindrical, crescent and the polygonal shape (Figure 35). The effect of overpressure zone the degree of compaction and the effect of polyps density in the space of colony reflect the multiform of corals. Livid colour represents dolomite grains, formed from reworked on the residual calcite crystals. Dolomite mineral can be the best indicator of the pathway of diagenesis process.

E: This stage characterized by the deformation of corals. The transverse section in the coral colonies occurred by the effect of degassing fractures. The gray colour indicates to dolomite grains, which are rich in residues organic materials and they replaced calcite cement. The sample was taken at the depth 2014.10 m in the NS-5 well.

F: Deformation of corals increases by increasing the effect of the compaction process. However, corals produce the amorphous materials of pure calcium carbonate from some microcracks. The effect of tectonic activity is a very important to increase the compaction process regardless of the depth level. The calcium carbonate is transparent or colourless to the white colour. Benthic microbial communities, chemical and mechanical compaction processes

are involved in the secretion process of the pure calcium carbonate. The sample was taken at depth 2051.77 m in the NS-5 well.

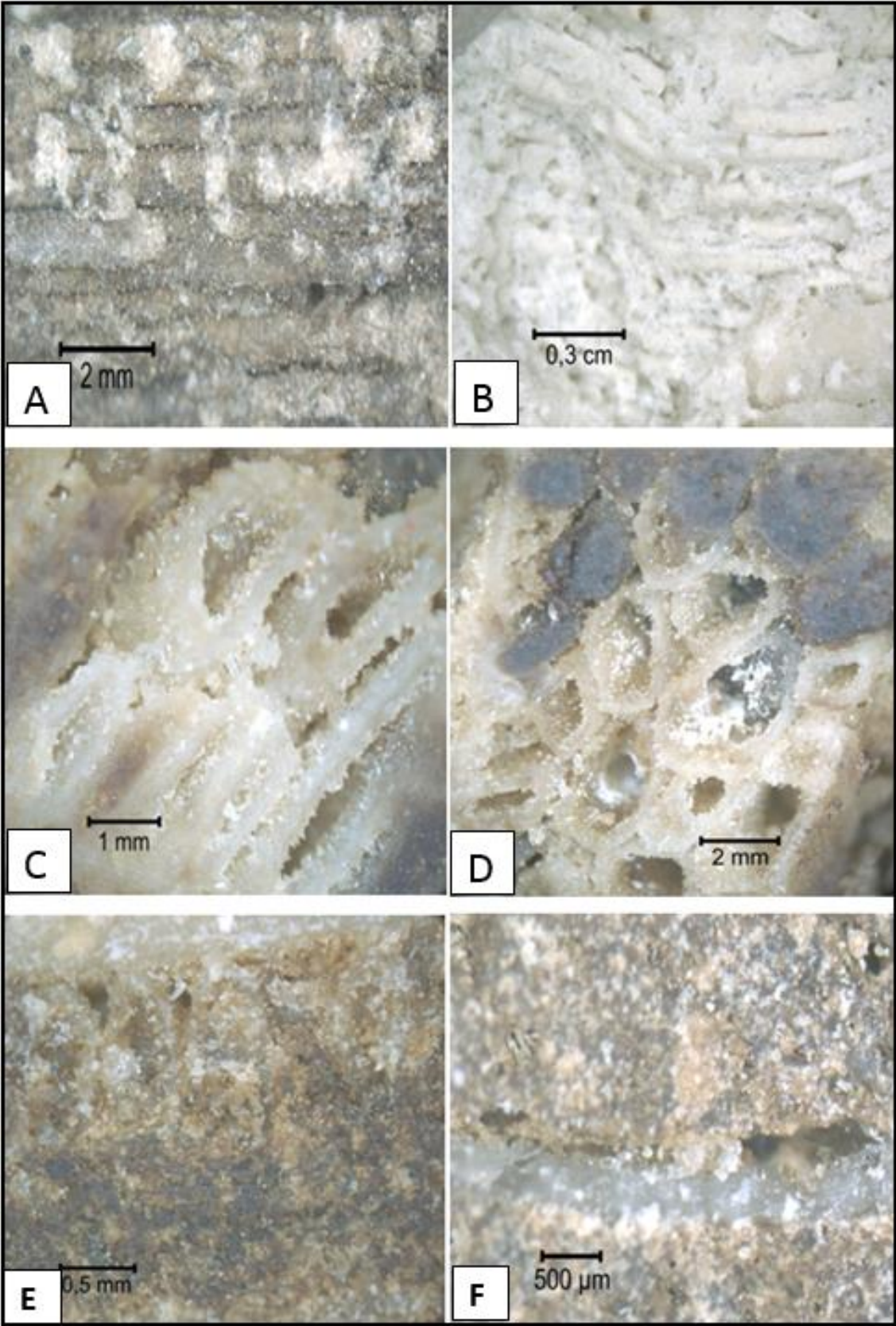


Figure 35 : Evolution of preservation stages of framestones (coral skeletons) in the Mishrif Formation in the NS-5 well at depth 2014.10 to 2078.32 m, SE Iraq

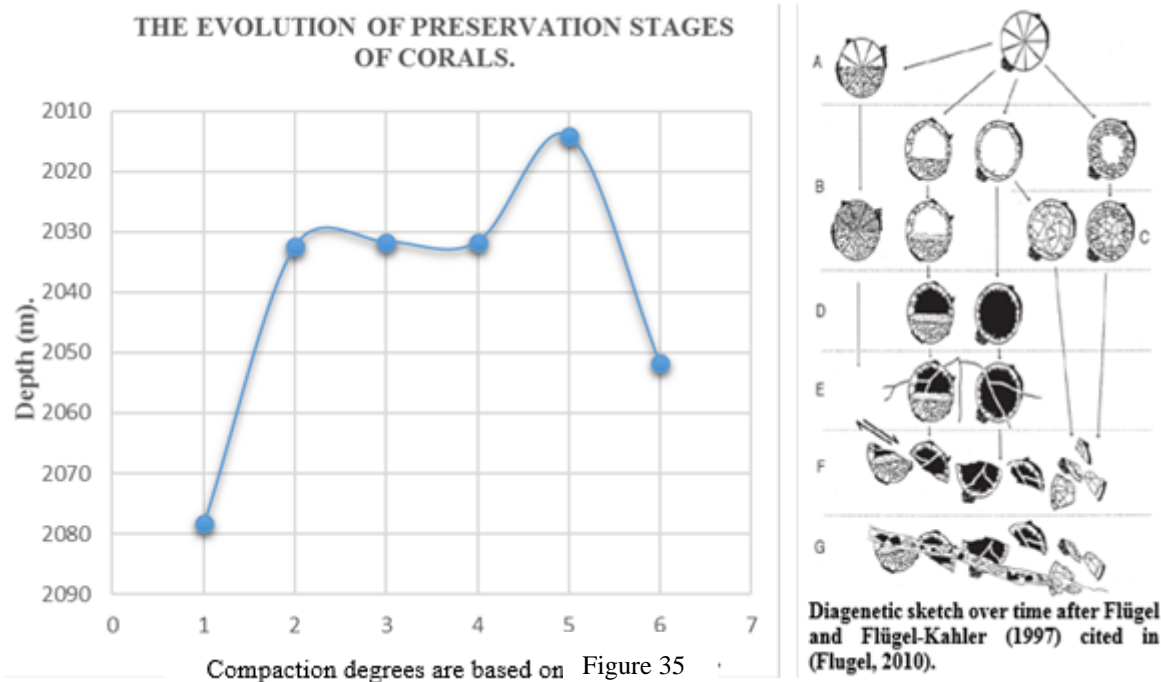


Figure 36 : Similarities and differences between the evolution of preservation stages of corals and diagenetic sketch over time.

2.5.3 Rudists

Cretaceous carbonate platform of the Tethys Ocean contains the major reef builders, *i.e.* sessile rudists, which dominated in shallow marine environment within benthic communities (Ross and Skelton, 1993; Gili et al., 1995). Rudists were amongst the most important carbonate producers in the calcareous depositional system (Steuber, 1998 and Steuber and Löser, 2000). Rudists had a worldwide distribution, and they are particularly represented in the Middle East and around the Gulf of Mexico (Simo et al., 1993).

The Mishrif Formation has fewer rudist buildups as compared with the Aptian Shuaiba Formation that is considered as an important hydrocarbon reservoir in the Arabian Gulf (Al-Sharhan, 1995).

Rudists in the Mishrif Formation have different characteristics from the coral reef and algae. Rudists existed as an individual body, while corals existed as a gregarious organisms of erect shape or elevator shape and they rarely found as individual organism. Rudist reef is usually of low relief. Corals grew as a superstratal fabric while rudists always grow as a contractual fabric (Figure 37).

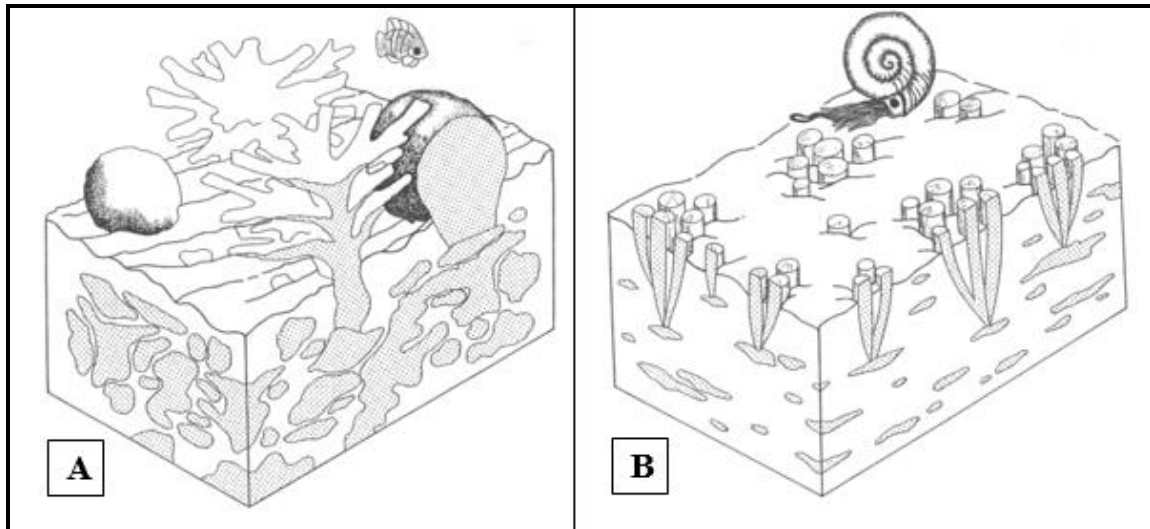


Figure 37 : The growth of superstratal fabric (A) versus the growth of constratal fabric (B) (Gili et al., 1995)

Bivalve skeletons vary in composition from aragonite to calcite. Most of them are composed of pure aragonite, but some have interlayered calcite and aragonite and a few ones are completely made of calcite. Calcite contains less than 1 mol% Mg (Moore, 2001). The less ratio of rudist in the Mishrif represented the aragonite mineral in the predeposition process. Aragonite helped the first stage of the interaction process between fluids and rocks. Aragonitic layers have well preserved under certain circumstances only in modern or relatively young deposits or in special cases in which diagenetic alteration is inhibited.

Mollusca exist in the Mishrif (Figure 39.C, D & E). The complete body of rudists found in the muddy limestone (Figure 39.A & B). It may be gradually filled with dolomite or/and calcite converted into the dolomite. Hence, the geopetal structures underwent diagenetic process because of the fluids passing through their structures (Figure 39.C, D and E).

Figure 38.

A: Core No. NS-5 (sample depth 2051.77 m): Cretaceous Bivalves Superfamily, Rudist: In general, the arcuate shape is a dominant one on the other shapes patterns. Rudist contains of calcite mineral and it shows ribbed edge.

B: Core No. NS-3 (sample depth 2018.86 m): Cretaceous Bivalves Superfamily, Rudist: Elevator morphotypes of rudist, which were supported by accumulated sediment during their vertical shell growth. Rudists contain the primary calcite and they have well preserved with framework porosity.

C&D: Core No. NS-2 (sample depth 2014.66 m): Cretaceous Bivalves Superfamily, recumbent Rudist: Cathodoluminescence observations show the conversion of aragonite into dolomite in the radial lid of rudists. Rudists appear as recumbent fine rectangular structures. Generally, aragonite maybe dissolved and the resulting porosity maybe filled with sparry calcite.

E&F: Core No. NS-2 (sample depth 2014.66 m): Cretaceous Bivalves Superfamily: Encrusted Rudists observed by SEM, show the resistant of purely calcite convert to dolomite mineral. Encrusted rudists have calcite structure contoured by matrix of crystals dolomite.

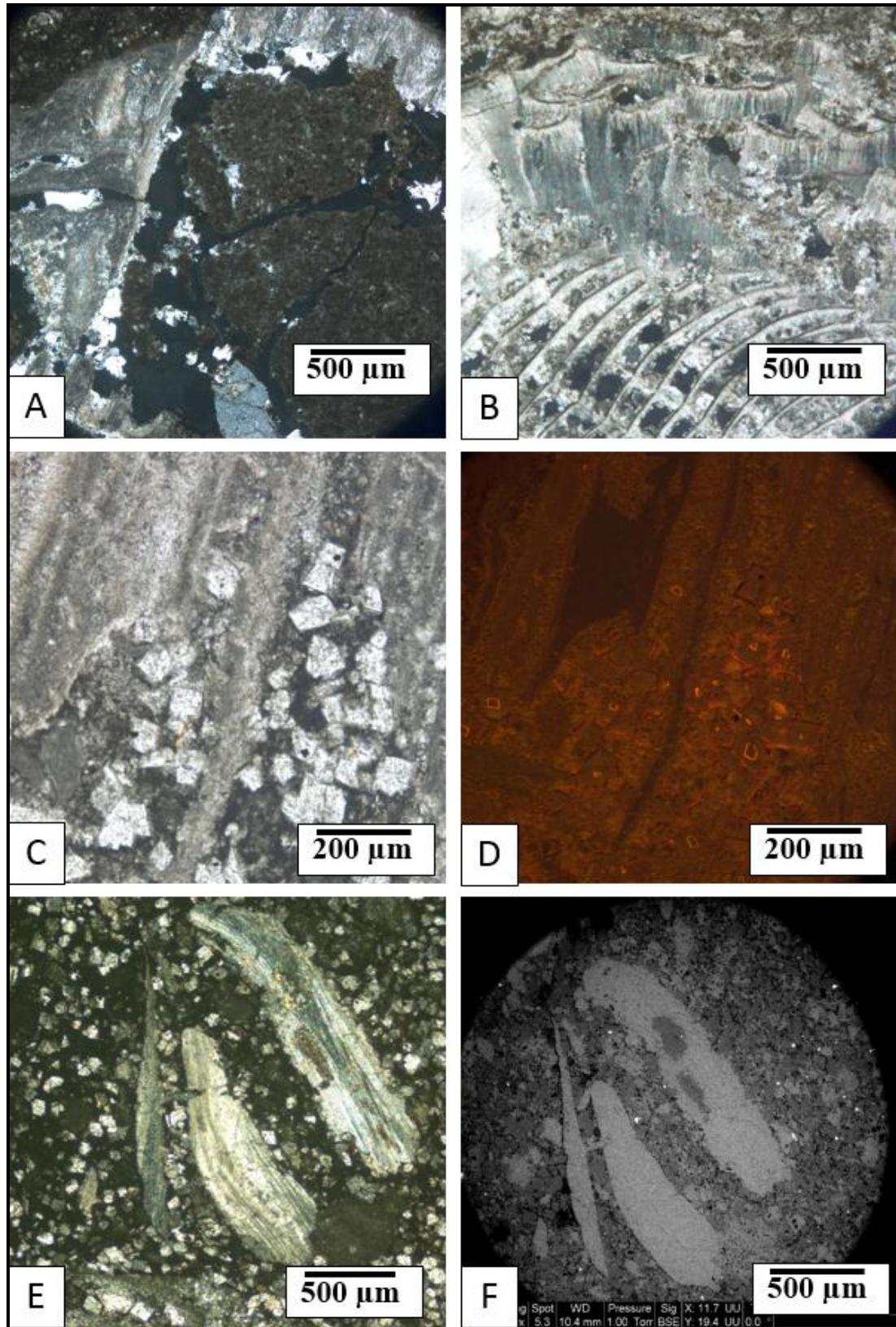


Figure 38 : Enlarged view of different rudist morphotypes. (A) Remnant of arcuate shape. (B) Framestones of vertical morphotypes of rudist were supported by sediments, which have accumulated during growth of their shells. Photos (C & D) show radial lid, which is recumbent as a fine rectangular structure. Photos (E & F) show encrusted rudists with calcite cover and dolomite crystals, which are surrounded them

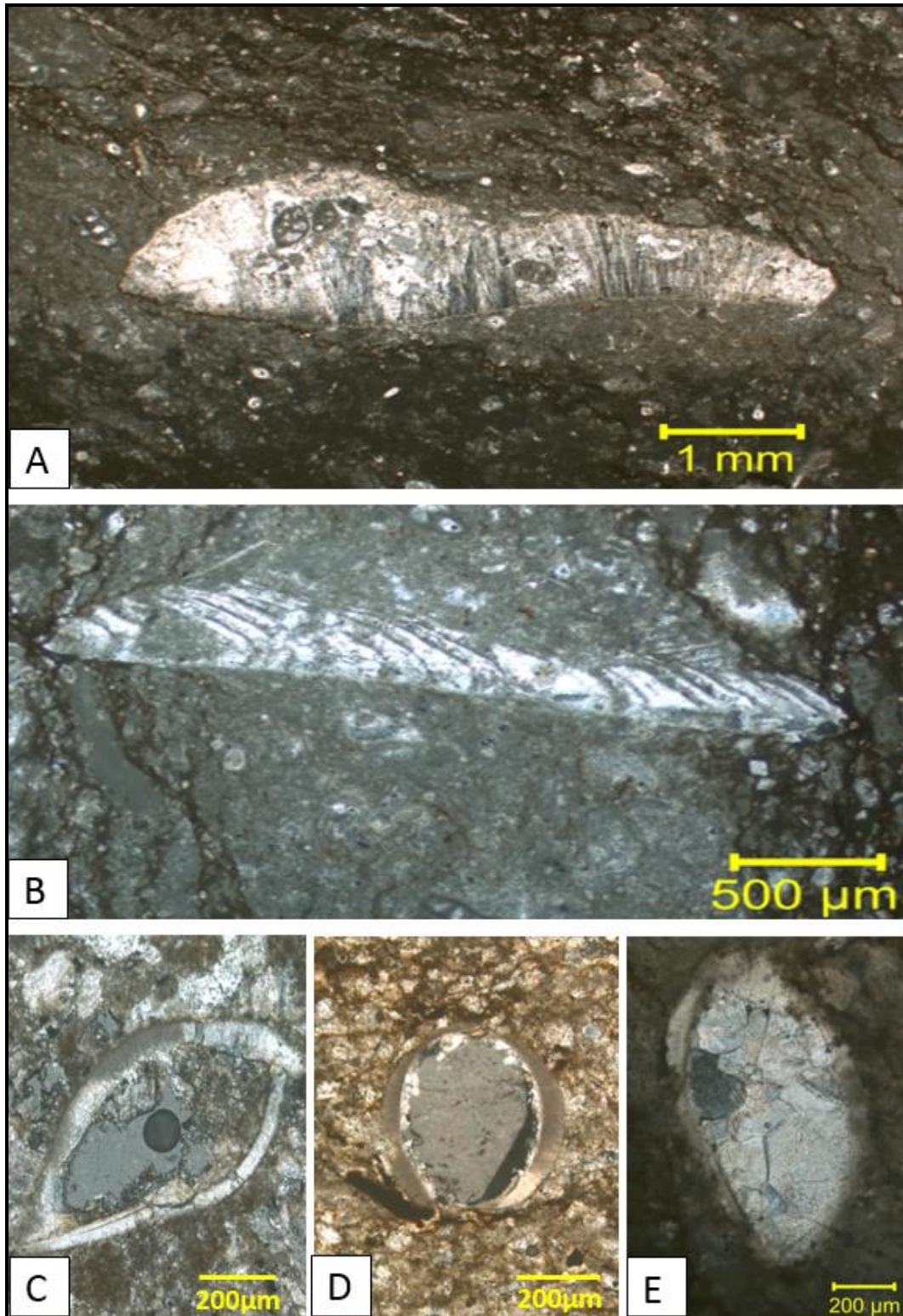


Figure 39 : The compositional maturity of grains reflected matrix type, conditions of environment and diagenetic process. (A) Rudist is encrusted and slightly ribbed, Miliolida joins with rudist and there are many wispy stylolites (NS-3 well 2024.25 m). (B) Rudist is encrusted and distinct ribbed (NS-3 well 2024.25 m). Normal bivalves have represented geopetal structures in the images (C) NS-2 well 2002.52 m, (D) NS-1 well 2033.80 m and (E) NS-3 well 2024.25 m respectively

2.5.4 Mixed algae zone (*Phylloid*, *Dasyclad* and Charophytes)

Mishrif Formation contains algae as important constituents in the upper part of Formation. Algae group have different types such as *phylloid* algae, *dasyclads* and charophytes (Figure 41). They exist in different environments, mainly from reef to back-reef and shallow lagoons platforms. They also have appearance in different microfacies such as lime wackestone submicrofacies bearing algae (MF2-3) and lime bindstone microfacies (MF5) (Figure 42).

Charophytes are a group of green algae that appeared the more widespread distribution in the Late Mesozoic and Tertiary and they represented the important fossils in that period. *Gyrogonite* is a calcified part of the oogonia, represented the reproductive parts of charophytes that are calcified in comparison with other parts of organism himself. (Flügel, 2010), describes the erected body of the thallus and their branched parts by “a regular succession of nodes with whorls of small branches and internode.

The name of *phylloid* algae refers to a descriptive approach rather than a genetic frame. It means platy or leaf-like form of the part of thallus or biomass (Flügel, 2010). *Phylloid* algae grew in very shallow water. Sometimes, they are found in abundance at depth greater than 50 m. They therefore live in the photic zone (photosynthetic) (Moore, 2001) and in the environments characterized by normal salinity. Typically, they have length from 2 to 10 cm and their thickness is about 0.5 to 1 mm. They are mainly composed of aragonite, but a few forms are known to include high-Mg calcite.

Some *dasycladaceans* and *codiaceans* green algae are shown as a filamentous structure, elongate plates, consisted of segmented grains with well-developed tubular form (Figure 41. D). The segments are composed of extremely small grains, probably formed by a major source of carbonate mud (micrite) (Figure 40).

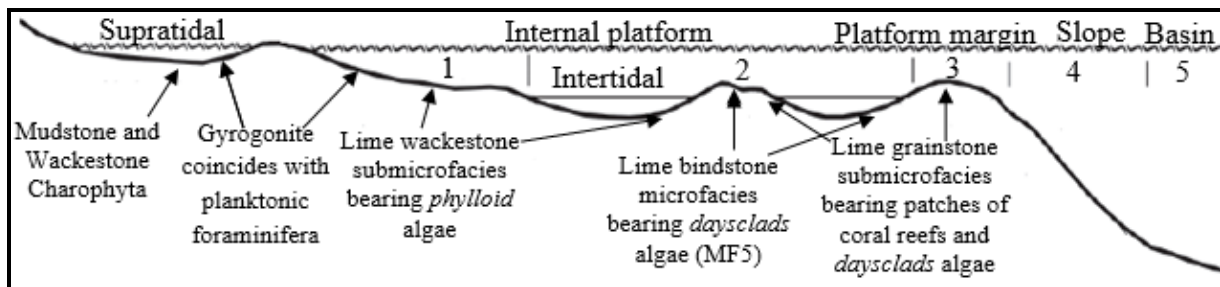


Figure 40 : The Distribution of *Phylloid*, *Dasyclad* and *Charophytes* algae during upper Cretaceous carbonate platform in the Nasiriyah oil field.

Charophyta include the same characteristics like other green algae living in the shallow water zone. They require light for growth (photosynthetic organisms) and they are usually found in the lacustrine water and in the zone from fresh water to brackish water. Their widespread distribution in marine as well as non-marine environment made them very useful organisms for correlations between marine and non-marine sediments. Moreover, charophytes fossils represented by elliptic gyrogonite, well preserved (Figure 41.F) and oogonia represented by almost dolomite mineral with edges of calcite in the Mishrif Formation.

The substantial points represented by non-marine environment that have been integrated with Coral distribution in the NS-5 well. Moreover, the distribution of gyrogonite

associations in the upper part of Mishrif Formation detects the huge amounts of planktonic foraminifera, that supports the involving of fluctuation sea level in the distribution process of organisms and their sediments in that time.

In addition, the existence of planktonic foraminifera accompanied with gyrogonite bodies (Figure 41.F), supported the hypothesis that indicate to rudists underwent of the final demise before the green algae in the final mass extinction. Usually, the common microfacies that associated with charophyte are mudstone microfacies and microbial packstone microfacies.

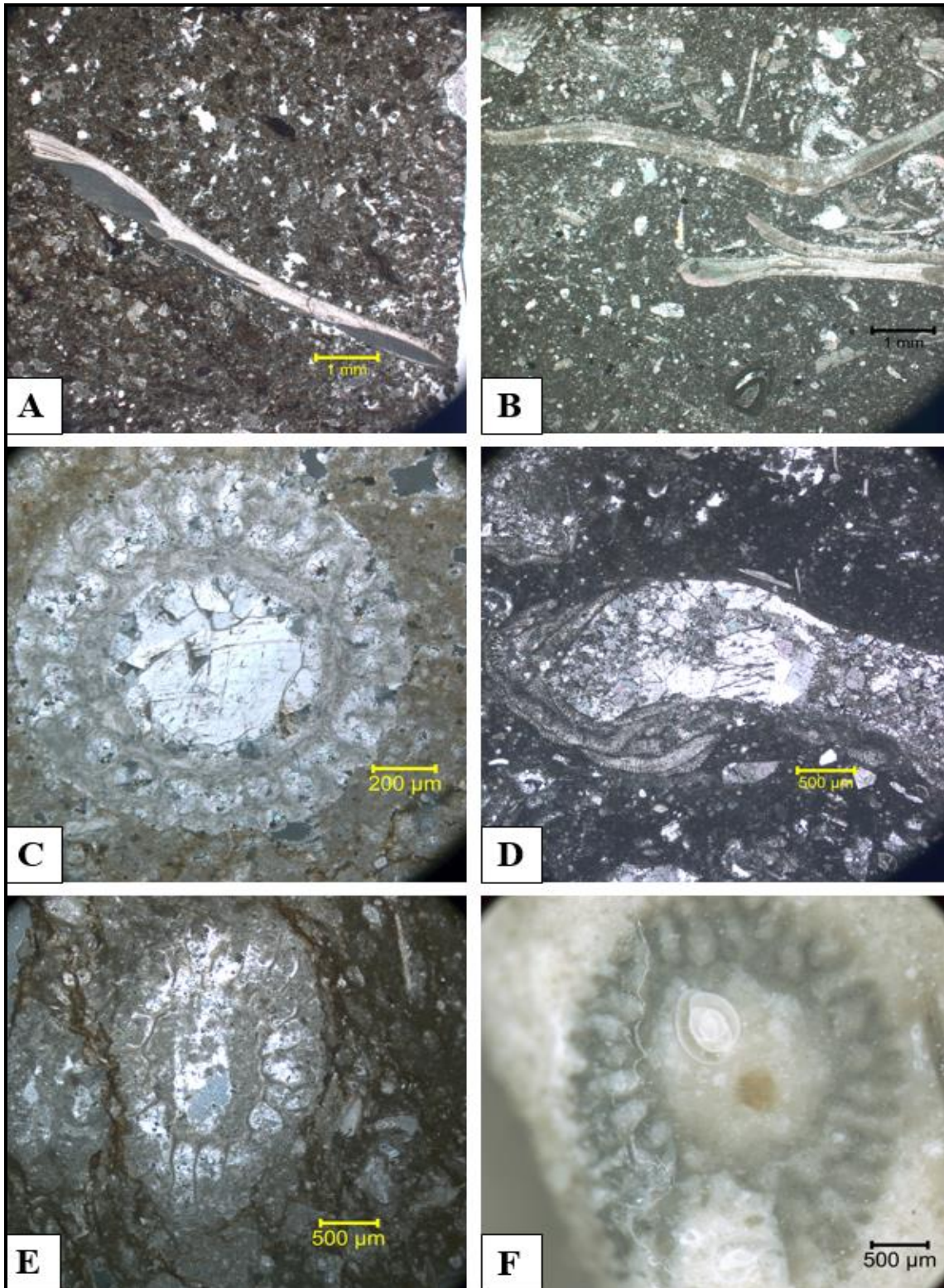


Figure 41 : Algae grains are significant grains in the Mishrif Formation. (A) Upright *phylloid* algae seems leaf-like in the NS-5 well at depth 2049.47 m. (B) Branched *phylloid* algae in NS-1 well at depth 2027.42 m. (C) *Charophyte* was a major sediment and produced near back-reef setting in NS-3 well at depth 2014.67 m. (D) *Dasycladaceans* green algae are shown as a spiral shape of filamentous structures in NS-3 well at depth 2011.66 m. (E) Gyrogonite is well developed in NS-3 well at depth 2024.25 m. (F) Gyrogonite coincides with planktonic foraminifera that reflects the transgression of sea in NS-2 well at depth 2014.66 m

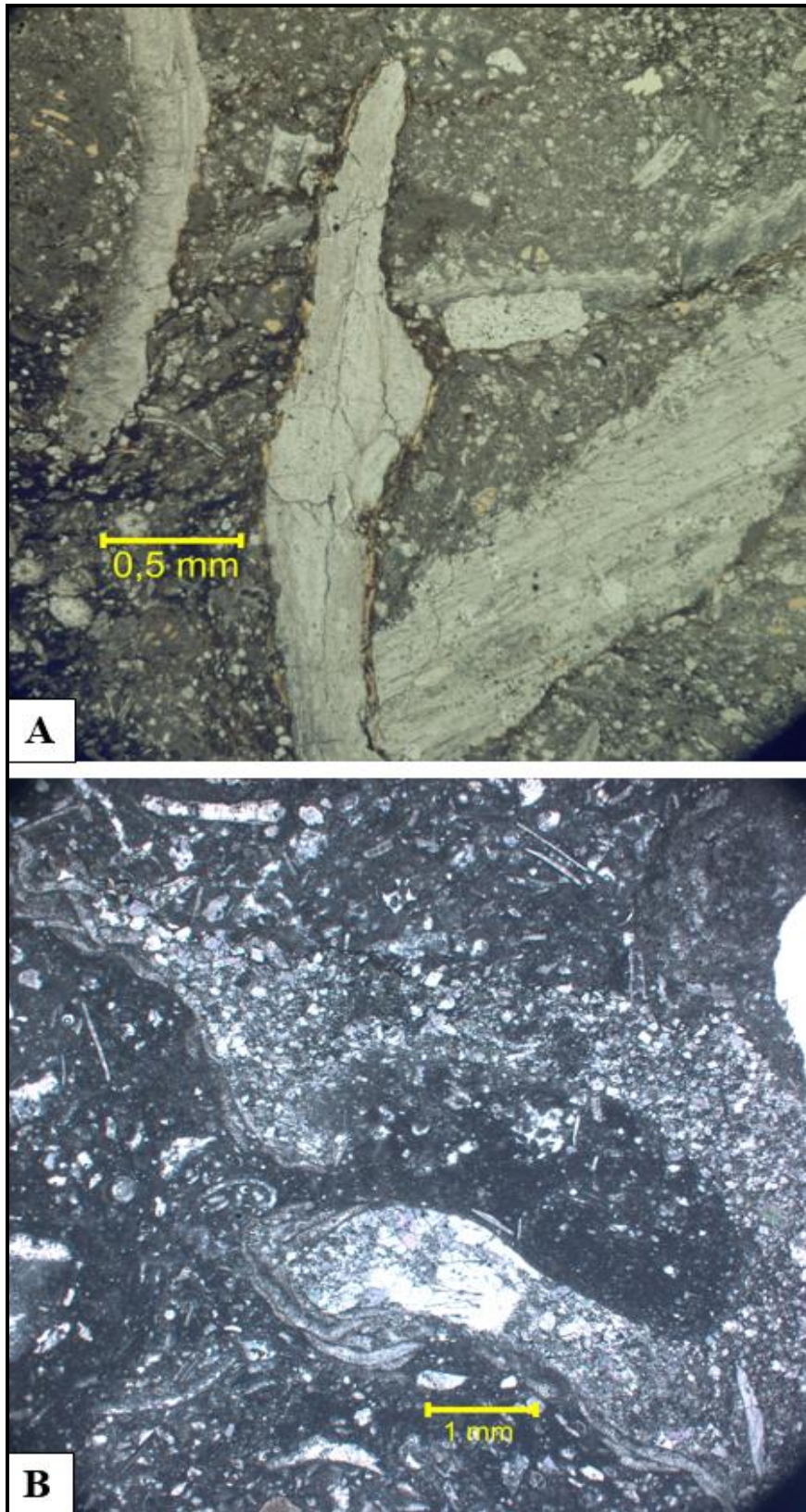


Figure 42 : Lime bindstone microfacies (MF5). (A) Some *phylloid* algae are difficult to distinguish their origin, because they have poorly preserved and the calcareous grains are covering all remains of *phylloid* algae in NS-3 well at depth 2024.25 m. (B) Crown form of *dasycladacean* green algae is related to fluctuation of sea level in NS-3 well at depth 2011.66 m

2.5.5 Microproblematica

Microproblematica is a group of microfossils with uncertain biological nature, (Hughes, 2013). The microfossils include Microbialites as species of Cyanobacterial *stromatolites*, crustacean fecal pellets of the genus *Favreina* and maybe certain types of peloids. In general, the Microproblematica consist of the Prokaryotes, included bacteria and cyanobacteria. The Cyanobacterial stromatolites usually belong to the phylum Cyanophyta and Prokaryotes, which are photosynthetic or non-photosynthetic microbes (Moore, 2001).

The importance of the Microproblematica comes from the main role of the cyanobacteria and bacteria in the transformation the organic matter to generate the hydrocarbon (Słowakiewicz and Mikołajewski, 2011). The hydraulic characteristics of the pellets indicate to great cross-section of pellet tends to fall perpendicular in the settling path (Briggs et al., 1962 and Wanless et al., 1981).

In this study, microproblematica are located in the Mishrif, belonged to the shallow water zone that reflected four important facts. Firstly, microproblematica require light. Secondly, they coexist with algae microfossils and they include same characteristics. Thirdly, they are integrated with effect of the fluctuation sea level. Fourthly, the scattered fossils in NS-1 and NS-2 wells underwent to the redistribution process (Figure 47 to Figure 50).

Microproblematica differentiated from other biological fossils by it has not any skeletal remains. The vertical distribution of Microproblematica in NS-1 and NS-2 wells contributes to construct the paleoenvironmental interpretations within a series of very shallow water environment (Figure 60).

Microbialites are interpreted as fossilized of cyanobacterial stromatolites of upper cretaceous age. They are well represented within packstones microfacies of supratidal zone or very shallow intertidal or lagoonal paleoenvironments. The crustacean faecal pellets of the genus *Favreina* is locally present in NS-1, NS-3 and NS-5 wells that found within packstones microfacies in intertidal zone to patch-reef paleoenvironments. The relation between *Favreina* and *microbialites* has defined based on the (written communication, Vachard, 2012), who states that structures *Favreina* are composed of microbialites and not micropellets cited in (Hughes, 2012). Cathodoluminescence microscope detected the high distribution of biostructures, found encrusting biocomponent fragments, which appeared in the dark red colour. The study of microbialites contains two of an important information channels, included biologically studies and mineralogical studies. For that reason, the microbialites study maybe considered a best method to track the old trace in the life of carbonate rocks.

2.5.5.1 Microbialites

Microbialites are “organosedimentary deposits formed by interaction between benthic microbial communities (BMCs) and detrital or chemical sediments”, those structures organosedimentary grew by accretion process, described as a gradual accumulation of benthic microbial community (Burne and Moore, 1987). Microbialites include a dual nature as mineral and microbial roles, which are highly interrelated; That is the reason why they constitute the oldest reliable traces of life (Couradeau et al., 2017).

The growth and evolution of Microbialites particularly in the NS-1 and NS-2 wells reflected the effect of the sea level fluctuation and the effect of environmental setting of

Mishrif. The Microbialites structures show a variety of microbial carbonate grains, included domal, columnar, planar, spherulitic, lumpy *stromatolites* structures. They represented the lagoonal settings (Figure 44). The variety of Microbialites structures (Morphogenesis) reflected the diversity of environmental conditions (Figure 43).

The stratigraphic columns of the NS-1 and NS-2 wells show the evolution of the microbial lithostromes (Figure 47 to Figure 50). Microbialites were coexisted with green algae that lead to confirm the shallow-water environments because the green algae are often lived in the shallow-water environments. Microbialites passed through stage of flourish with regression of sea level and under high salinity.

Figure 44.

The dominant process of microbial grains formation in the Mishrif Formation often is the microbial boundstone, which include trapping and binding of detrital sediment. In addition, the microbial framstone process appears in the same zones, which contain the biological calcification.

A: Core No. NS-1 (sample depth 2052.90 m): Domal Microbialites, clotted thrombolites: In general, the shape of the domes seems dominant on the other shapes of Microbialites. Domal Microbialites contain of calcite, covered by quartz and they show the effect of the fluctuation sea level on the dome edges.

B: Core No. NS-1 (sample depth 2024.60 m): Planar Microbialites, *stromatolites*: Planar morphotype of *stromatolites* were supported by spots of quartz as a spherulitic form, accumulated during regressive sea level. They included the well preserved layers of calcite.

C&D: Core No. NS-1 (sample depth 2052.90 m): Lumpy Microbialites with the framework porosity: The primary framework of the microbialites became the place of secondary cementation. They reflected moldic porosity as result of dissolution process. They contain of spherulitic forms.

E: Core No. NS-1 (sample depth 2052.90 m): Full lumpy form Microbialites: They show the resistance of encrusted calcite to dissolution process. The encrusted grooves contained calcite, contoured by organic materials, under Cathodoluminescence.

F: Core No. NS-3 (sample depth 2018.86 m): Laminated *Stromatolites*: The different morphotypes reflected the pathway of sea level and the environmental conditions. The morphotypes of calcite included high concentrations of fluid inclusions.

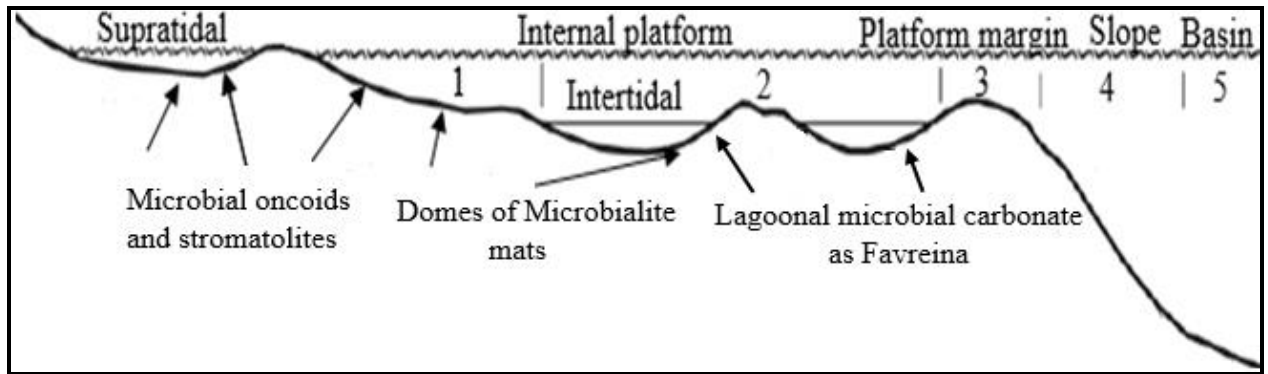


Figure 43 : Microbial carbonate grains distribution in Upper Cretaceous in Mishrif Formation at Nasiriyah oil fields

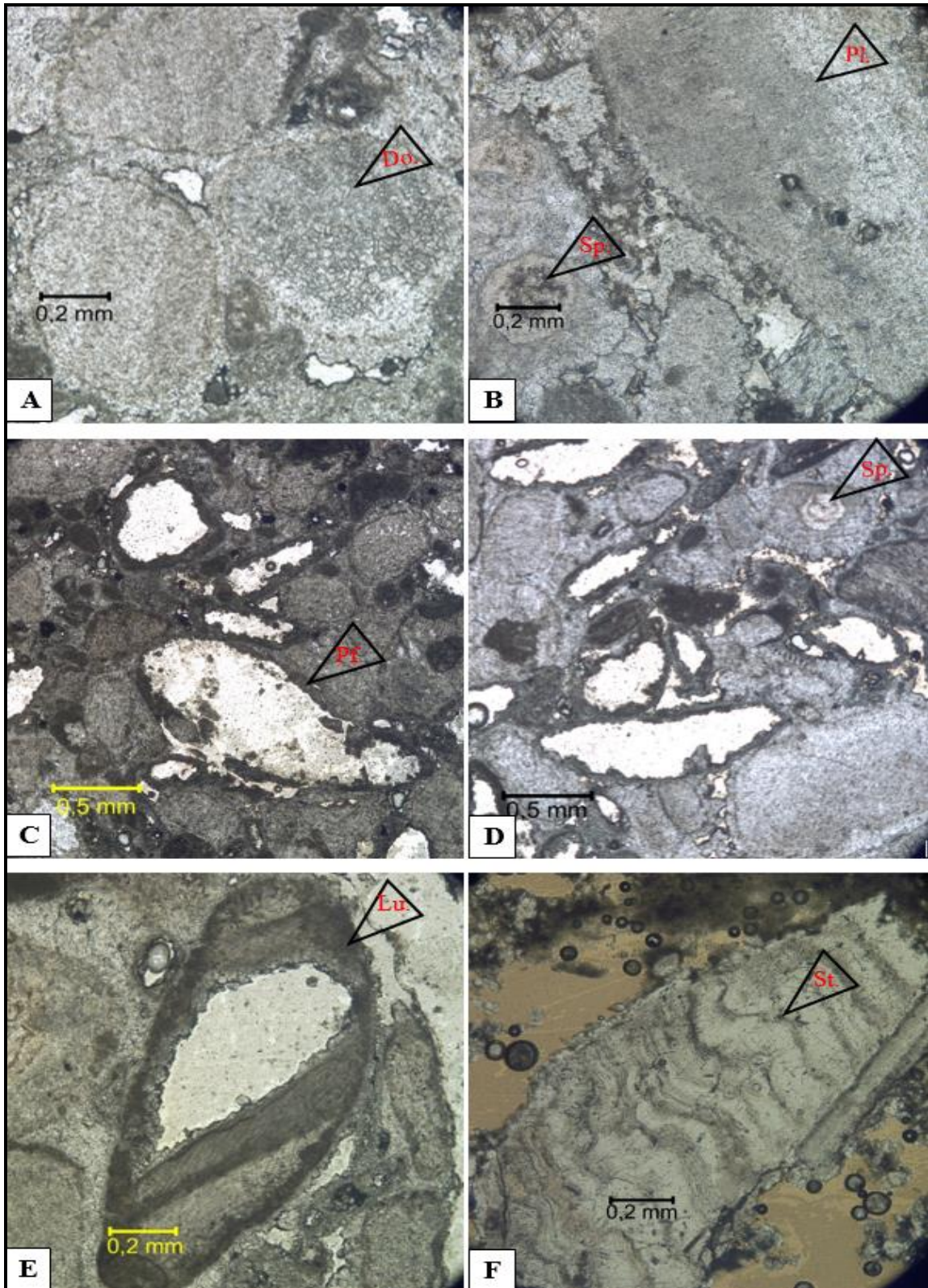


Figure 44 : Microbialites structures are in NS-1 well at depth 2052.90 m as a first cycle of the Microbialites deposition and the second cycle of the Microbialites deposition is at depth 2024.60 m in the same well

2.6 Non-Skeletal grains (microbial genetic and abiogenic grains)

The overwhelming majority of carbonate grains are biological in origin and they form in tropical marine environments (Reid et al., 1990). The strict differentiation between skeletal grains and non-skeletal grains could be very visible than the overlapping differentiation between microbial grains and abiogenic grains. Mishrif includes two types of the wells, first type contains the NS-1 and NS-2 wells as an overlapping differentiation between their layers. The second type includes the NS-3 and NS-5 wells as a strict differentiation between their units (Figure 47 to Figure 50).

On the one hand, non-skeletal grains have evolution stages based on the sea level fluctuation, which influence the microbial grains to overlap abiogenic grains. On the other hand the effect of biological processes is very wide in carbonate rocks, side by side with effect of microbial processes, included high distribution in the very shallow environments. For that reasons, the microbial grains and abiogenic grains are deeply affected by biotic processes, which render very difficult the differentiation between their origins.

(Folk, 1959) has defined abiogenic grains as grains that are formed by chemical precipitation within the depositional basin, organized into discrete aggregated bodies and probably undergoing some transport process. Abiogenic grains of the Mishrif have three types peloidal, aggregated and rounded clastic grains. Regardless, on the terms of grains evolution and the interrelated boundaries between microbial grains and abiogenic grains.

2.6.1 Pellets and Peloidal grains

Pellets are fine-grained fecal particles that are composed of carbonate mud with micrite internal structure. They have a high content of organic matter and iron sulfides because the organisms eat and digest organic matter from the mud and excrete the undigested lime-mud as fecal pellets. They have typically size from 0.03 to 0.3 mm in length. Their shapes commonly are elongated, ovoid, rod-like shaped and even rounded grains. Pellets commonly are separate into micrite grains during the dewatering and compaction processes in shallow burial but they are well preserved when early cements harden them.

Peloid is a “comprehensive descriptive term for polygenetic grains composed of micro- and cryptocrystalline carbonate” (McKee and Gutschick, 1969). Peloid is a term that refers to allochems. They have smaller size than other carbonate grains. The term peloid includes genetically different grains of variable size, produced from reworking, recrystallization, microbial activities and from early and late products of diagenetic processes. Peloids are abundant in the shallow water environment but can be found in other types of environments because of redeposition process and they can transport because of their small sizes.

Pellets often occur in shallow-marine environments particularly in lagoonal carbonates for that reason they consider as an important member in the Mishrif formation. They often diffuse as the sequential nests in the NS-2 well.

Comparison between the origins of peloidal grains in the Nasiriyah oil field requires to analysis bacterial decomposition, which allows to identification the origin of peloidal grains and the type of intragranular cement. The distinction between fecal pellets and microbial peloids is very difficult. They have a dark colour under microscope and appear vague or

indistinct under cathodoluminescence (Figure 45). In the studied site, the diameter of peloidal grains is a $< 200 \mu\text{m}$ and in the strict sense, they include diverse sizes; irregular shapes and their internal fabric are vague (Figure 46).

The mass appearance of the pellets and peloidal grains could be interpreted as autochthonous constituents, especially in NS-1 and NS-2 wells (Figure 47 to Figure 54). Therefore, the mass occurrence of the pellets and peloidal grains emphasizes shallow-water environments, which have a low energy from subtidal to restricted marine environment. Taking into account, the fluctuation of sea level and the microfacies characteristics of the NS-5 well reflect much more open marine environment.

Dolomite disappears in the zone of pellets and peloidal limestone because, this zone has undergone to early calcite cementation, which rapidly occurred and this zone became like aggregate grains in the characteristics. The early cementation worked as a barrier to preserve the carbonate pellets and/or peloidal limestone.

The effect of sea level fluctuations seems very clear in the stratigraphic columns of NS-2 and NS-1 wells (Figure 47 to Figure 50), which show peloidal grains have alternate deposition from microfacies packstone to grainstone microfacies. The cyclic deposition interpreted as the peloidal packstone microfacies deposited in the zone of subtidal to low intertidal, included the lack in abundance and the diversity of organisms. These organisms maybe limited by some species of benthic foraminifera and green algae as well as, high salinity and the abundance of the sulfate minerals.

The peloidal packstone microfacies deposited in the zone, included the abundance of biotic constituents, which represented by burrowing microorganisms and fecal pellets. For that reason, we can say the zone of peloidal grainstone microfacies represents the ebb tide (regressive situation) and the zone of peloidal packstone microfacies represents the high tide (aggressive situation). For that reason, the peloids and pellets have an important role to determine the paleoenvironments conditions especially in the subtidal and low intertidal zones of the inner platform.

Figure 45.

A: Core No. NS-2 (sample depth 1993.10 m): Fine-grained fecal pellets: In general, they usually include high content of organic matter for that reason, they have vague image under cathodoluminescence. The grains have a black colour under transmitted light. The bright colour under cathodoluminescence results from the high intensity of the backscattered emissions, which are generated from sulfate.

B: Core No. NS-2 (sample depth 1993.10m): Fecal pellets with inorganic precipitate: In situ, the accumulated sulfate minerals are represented by anhydrite (anhydrous calcium sulfate mineral in the center of image), which confirmed the involvement of sulfate-reducing bacteria. These microfacies include anhydrite remains, which are well preserved. The effect of anhydrite and pyrite minerals clearly seems in the evolution of secondary porosity in the NS-2 well.

C: Core No. NS-2 (sample depth 2048.26 m): Lithic peloids: In NS-2 well, the inorganic and organic matter had chemically precipitated in forms of microcrystalline grains, which have poor sorting. Morphologically, they are elongated and/or rod-like shaped and their

accumulations like aggregate grains. Here, the effect of microbial cementation (biocementation) obviously appears by cathodoluminescence.

Figure 46.

A: Core No. NS-2 (sample depth 1993.10 m): Peloids result from postdepositional alterations of grains: In general, the peloidal grains characterize by an exterior edge, which reflect the recrystallization process after paleofluids, which invaded the formation. Interaction between acidic fluids and calcitic pellets of the matrix produces an excellent secondary porosity. Morphologically, the subangular to angular of peloidal grains and angular pores seem dominant on the all formation after dissolution process. Cathodoluminescence reveals that fluids are super-saturated in calcium carbonate after they invade the formation and these fluids assisted to precipitate the edges of peloidal grains.

B: Core No. NS-1 (sample depth 2048.95 m): Mud peloids with clotted-grayscale micrite: Morphologically, subrounded and subangular micritic grains characterized by poor sorting and a vague internal fabric because of the presence of clotted mud (gray cloud). They have very small size around 200 μm and they have various shapes.

C: Core No. NS-1 (sample depth 2048.95 m): Fine-grained mud peloids: very small peloidal grains characterize by cryptocrystalline granular texture. On one hand, the grains have size around 50 μm in length and they have different shapes, indicated to the reworking of weakly lithified carbonate mud in the place. On the other hand, their textures reflect numerous intragranular pores with visible clotted-forms.

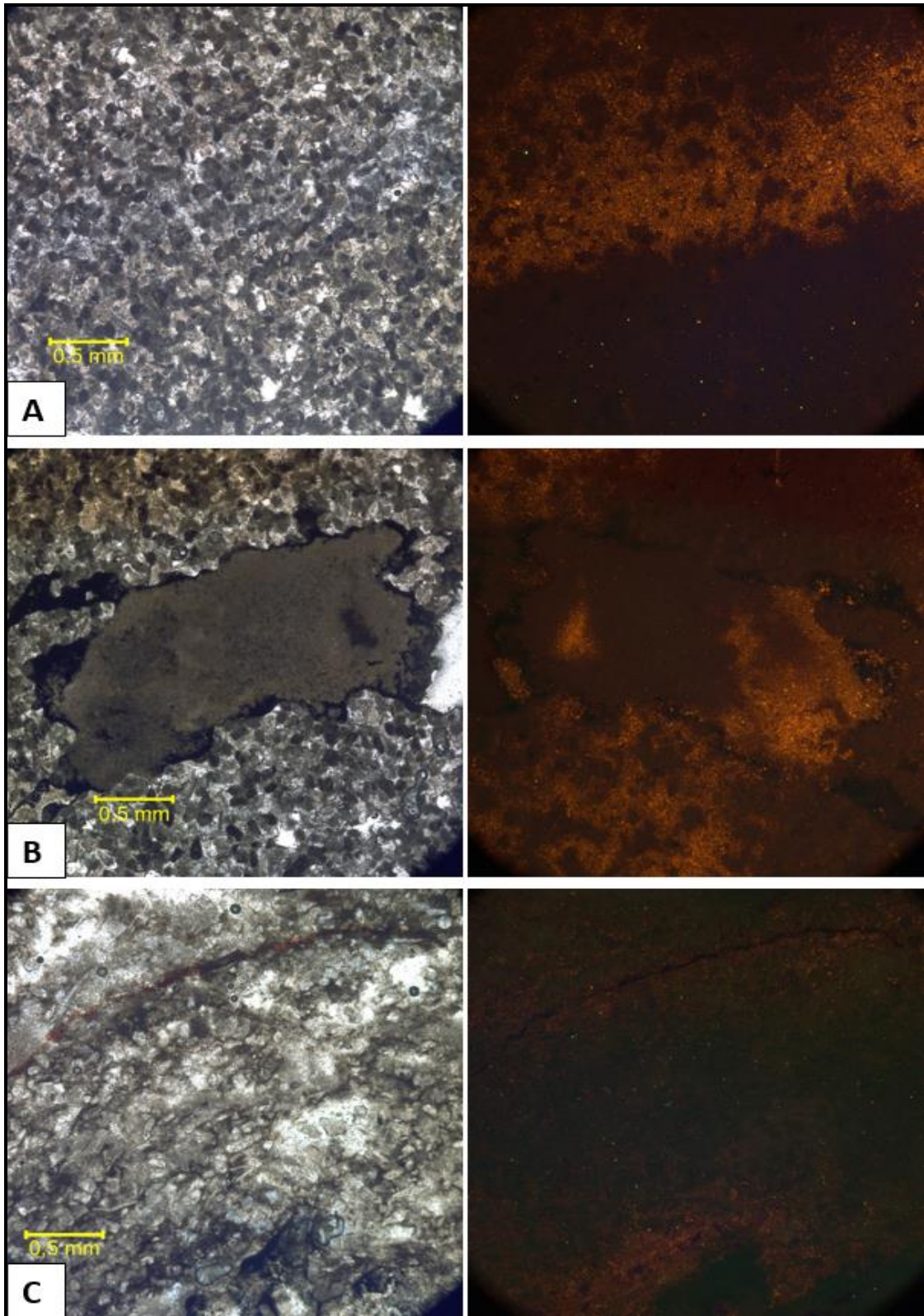


Figure 45 : Faecal pellets contain high content of organic matter and iron sulfides for that reason, they give grayish colour under transmitted light and they have indistinct photos under Cathodoluminescence microscope

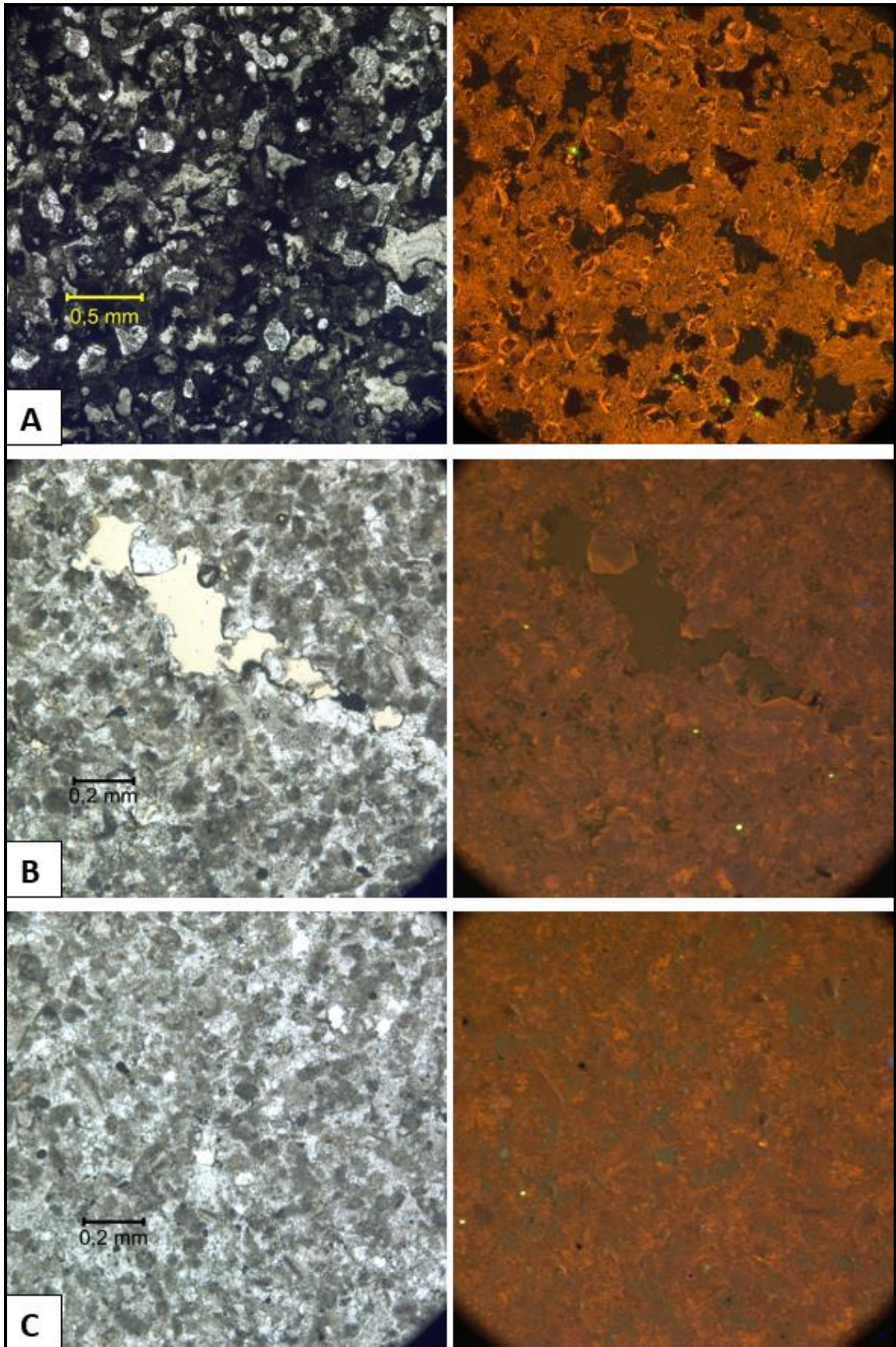


Figure 46 : Peloids display different sizes and irregular shapes of grains

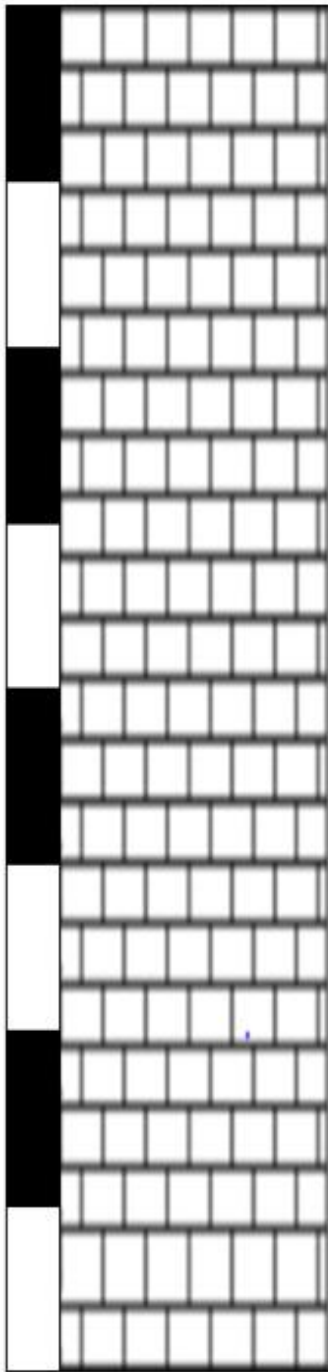
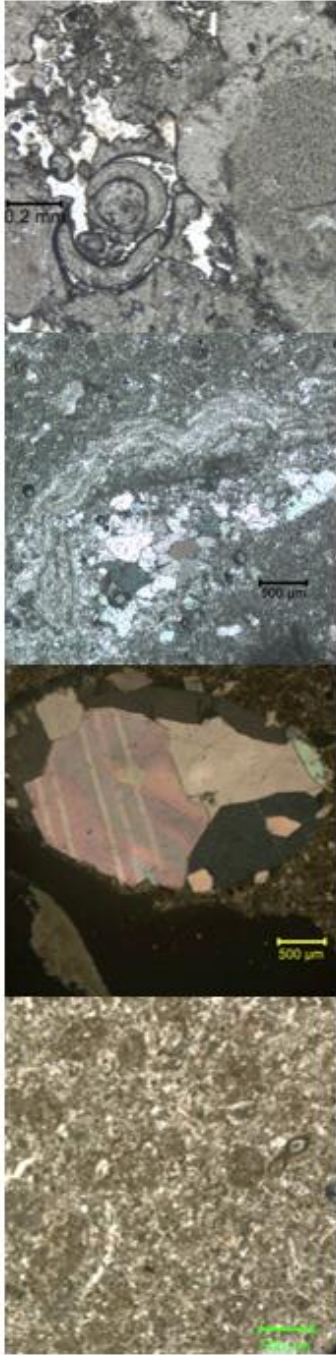
Erathem.	System.	Stage.	Samples.	Depth (m).	Profile.	Microfacies.
Mesozoic.	Cretaceous.	Cenomanian - Early Turonian.	S1	2024.60		
			S2	2027.42		
			S3	2033.80		
			S4	2033.80		

Figure 47 : Upper part of the stratigraphic column reflects the evolution stages of microfacies in the Mishrif Formation in NS-1 well

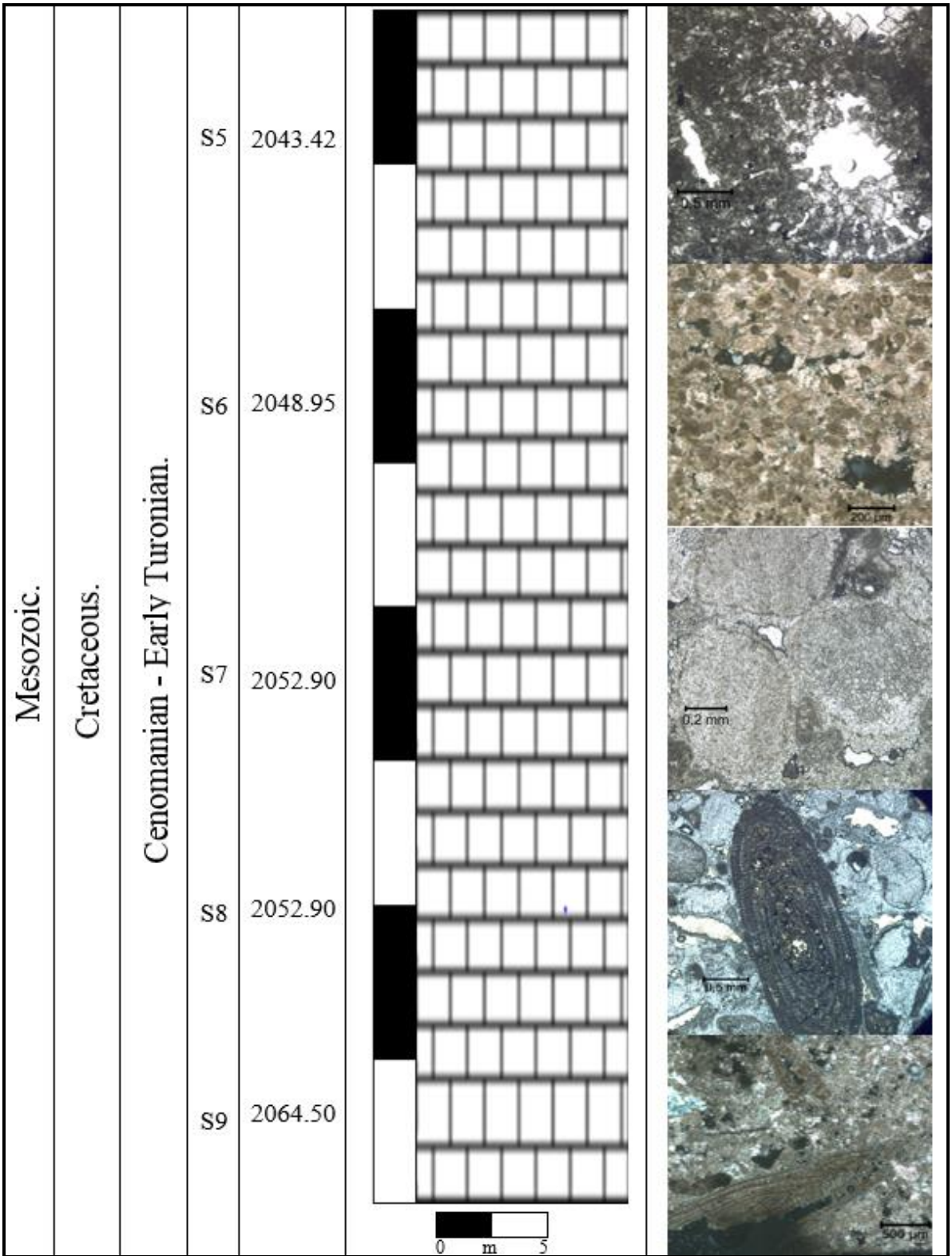


Figure 48 : Lower part of the stratigraphic column reflects the evolution stages of microfacies in the Mishrif Formation in NS-1 well

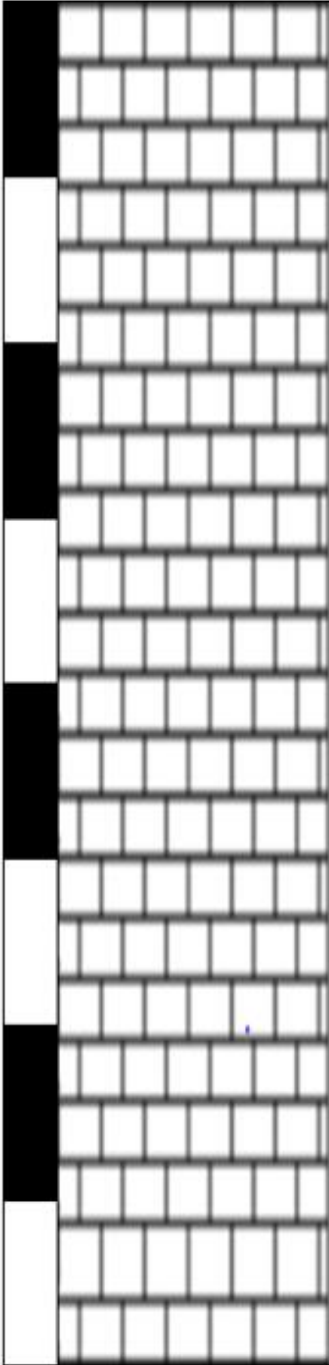
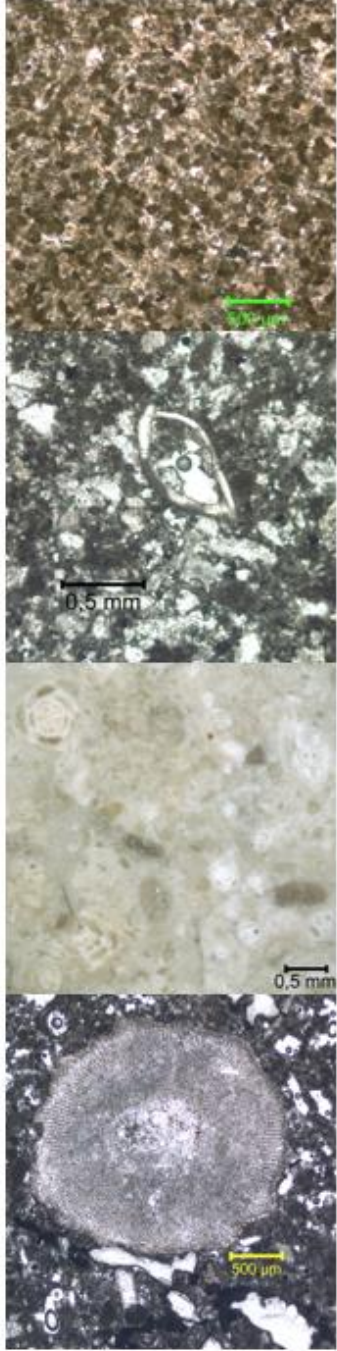
Erathem.	System.	Stage.	Samples.	Depth (m).	Profile.	Microfacies.
Mesozoic.	Cretaceous.	Cenomanian - Early Turonian.	S10	1993.10		
			S11	2002.52		
			S12	2014.66		
			S13	2023.05		

Figure 49 : Upper part of the stratigraphic column reflects the evolution stages of microfacies in the Mishrif Formation in NS-2 well

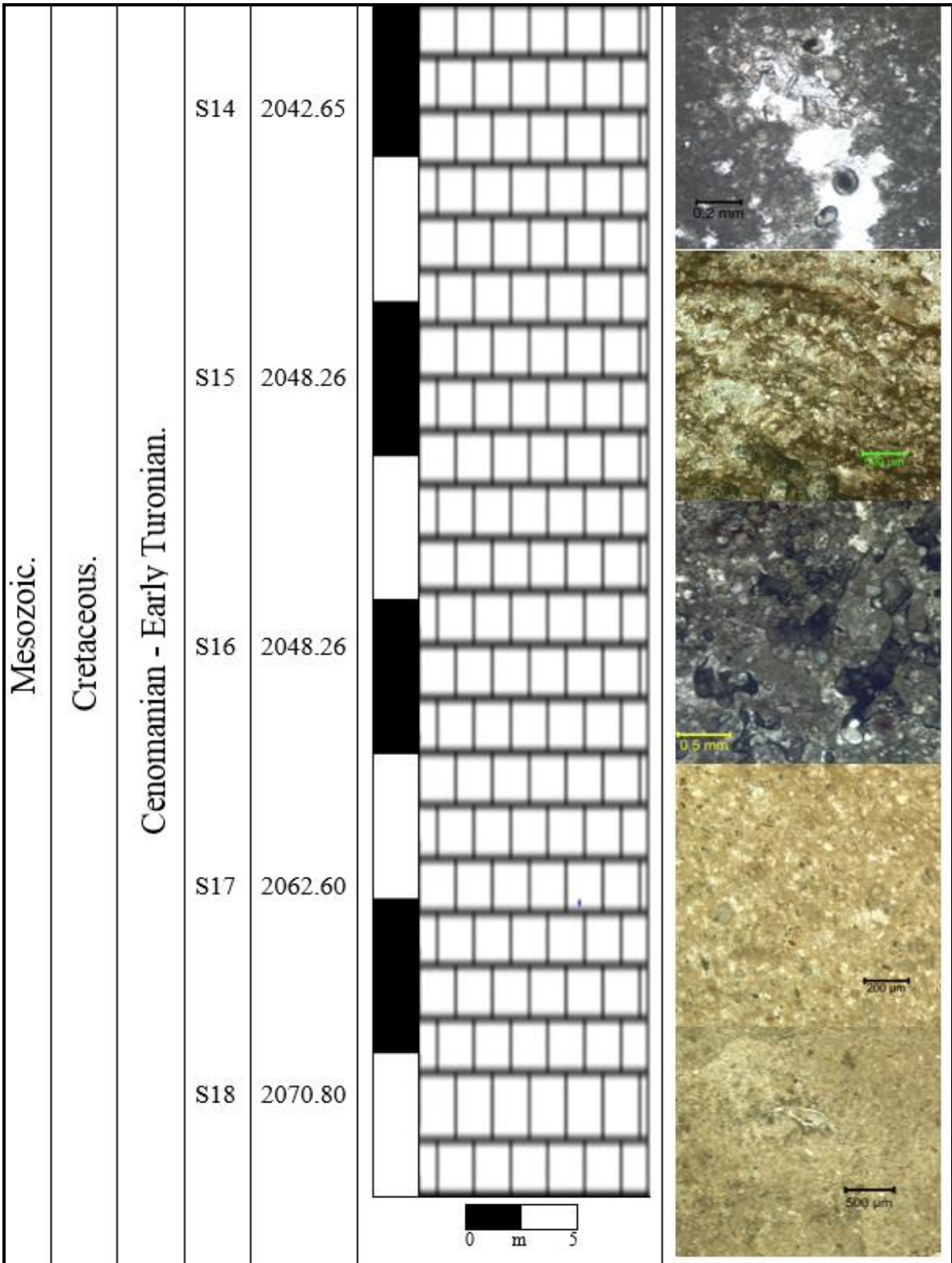


Figure 50 : Lower part of the stratigraphic column reflects the evolution stages of microfacies in the Mishrif Formation in NS-2 well

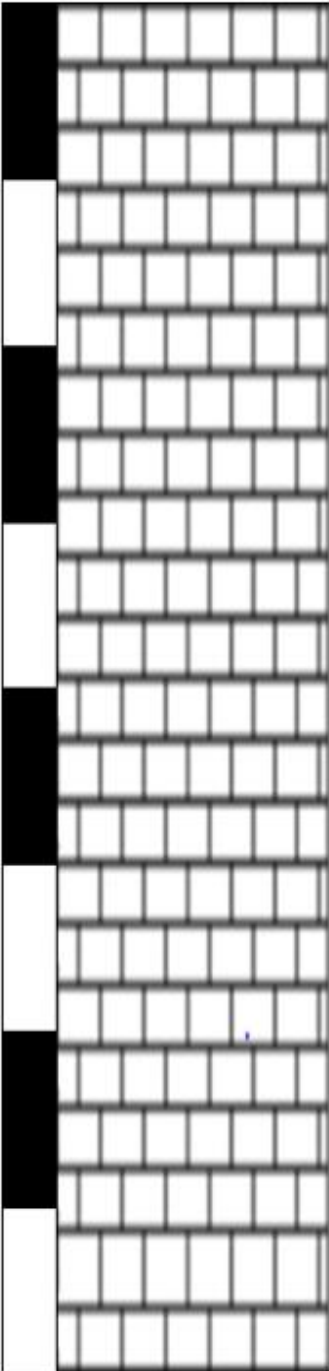
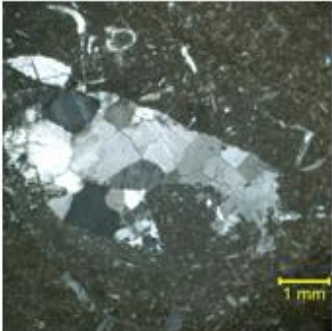
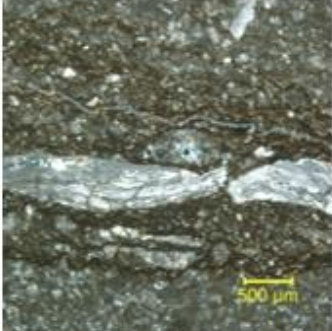
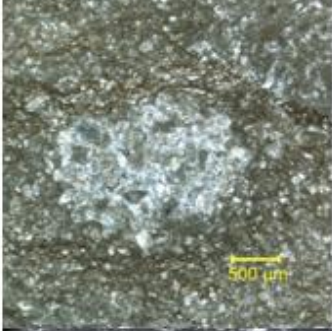
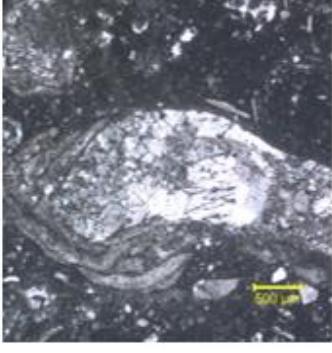
Erathem.	System.	Stage.	Samples.	Depth (m).	Profile.	Microfacies.
Mesozoic.	Cretaceous.	Cenomanian - Early Turonian.	S19	1992.70		
			S20	2003.53		
			S21	2007.32		
			S22	2011.66		

Figure 51 : Upper part of the Stratigraphic column reflects the evolution stages of microfacies in the Mishrif Formation in NS-3 well

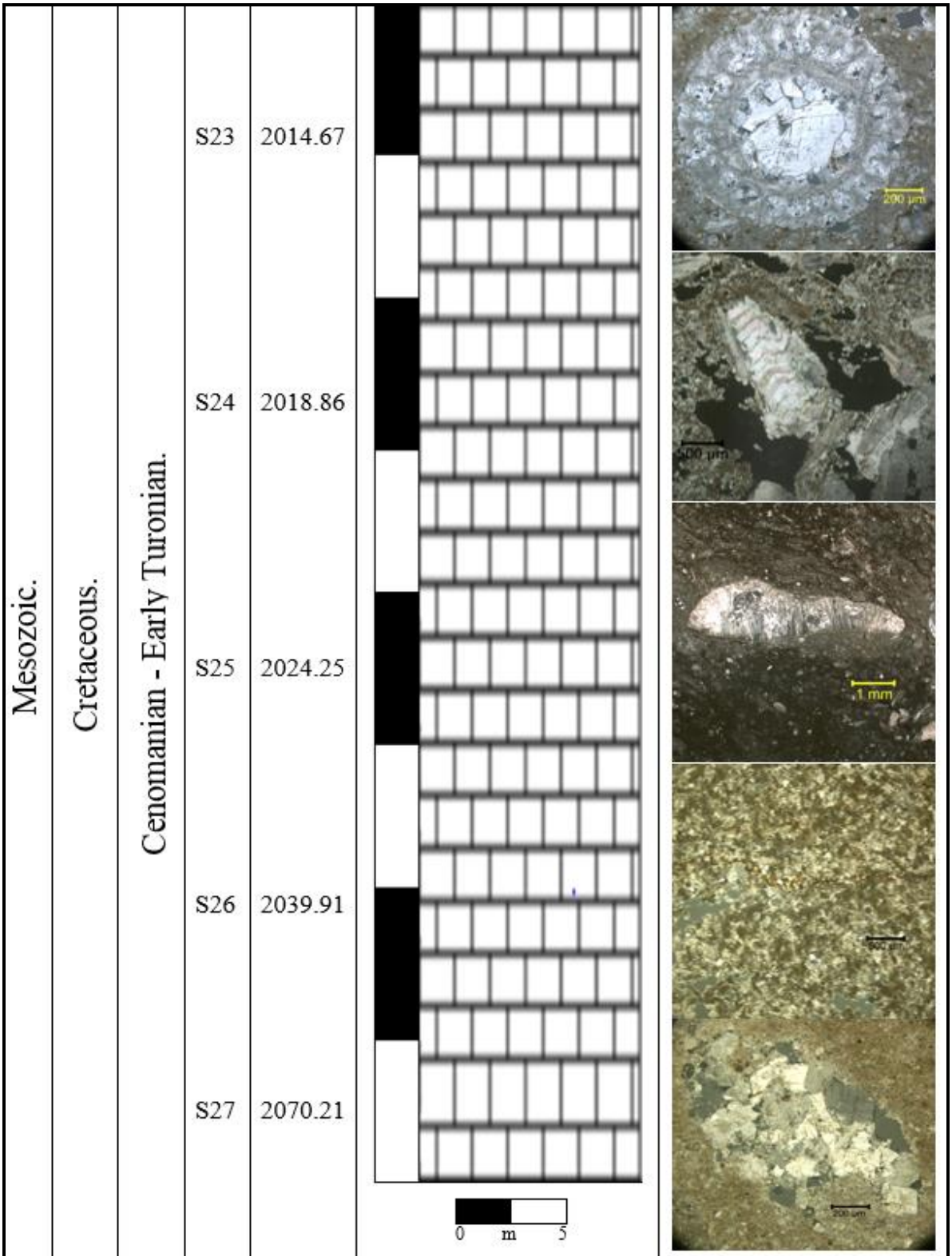


Figure 52: Lower part of the stratigraphic column reflects the evolution stages of microfacies in the Mishrif Formation in NS-3 well

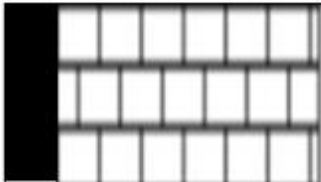
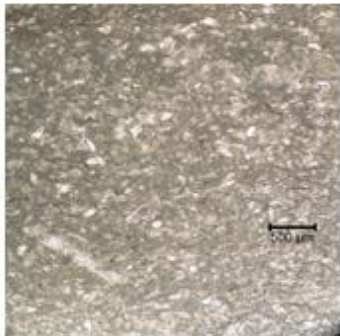
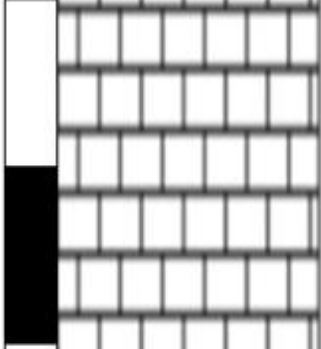
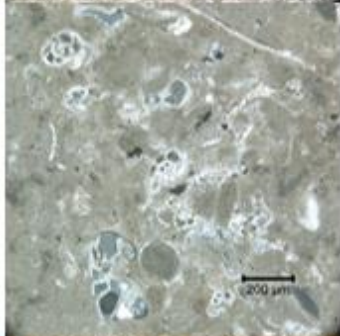
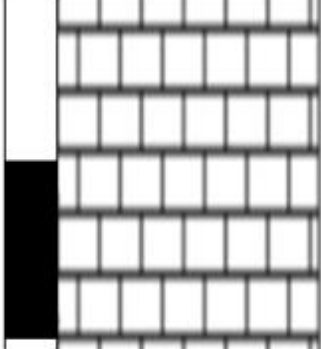
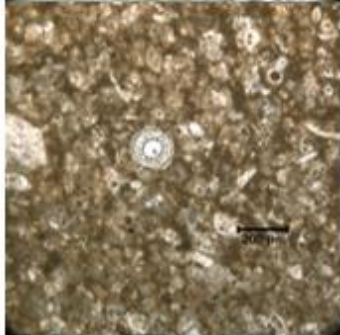
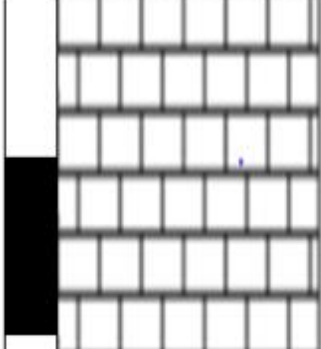
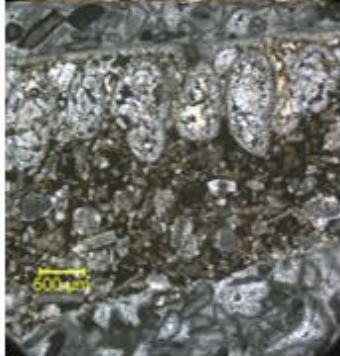
Erathem.	System.	Stage.	Samples.	Depth (m).	Profile.	Microfacies.
Mesozoic.	Cretaceous.	Cenomanian - Early Turonian.	S28	1897.48		
			S29	1902.87		
			S30	1999.60		
			S31	2014.10		

Figure 53 : Upper part of the stratigraphic column reflects the evolution stages of microfacies in the Mishrif Formation in NS-5 well

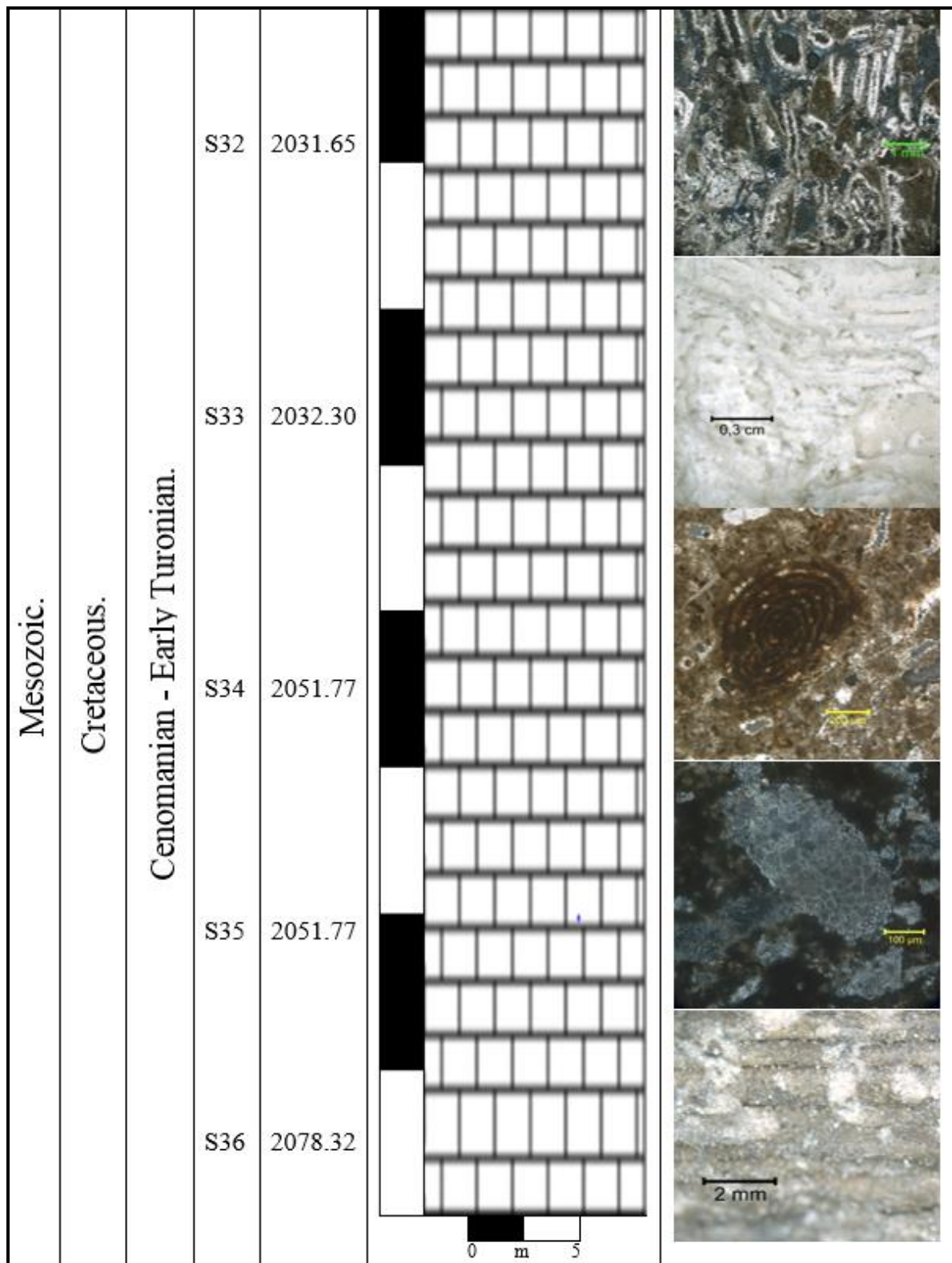


Figure 54 : Lower part of the stratigraphic column reflects the evolution stages of microfacies in the Mishrif Formation in NS-5 well

2.6.2 Aggregate grains

Aggregate grains are invaluable proxies, which help to reveal the paleoenvironments conditions, most aggregate grains form in very shallow environments where marine currents and water waves are sufficient to remove fine-grained sediment, but not sand (Flügel, 2010).

The aggregate grains contain grapestones, lumps, microbial/algal aggregate grains, encrusted/coating aggregate grains and other types of the composite grains. The aggregate grains in Mishrif Formation have size > 1mm to a few mm in the long.

The significant correlations exist between the stratigraphic columns (Figure 47 to Figure 54) and the distribution of the current wells on the contour map. On one hand, most of the mature aggregate-grains belong to lumps type in the NS-2 and NS-3 wells. On the other hand, the microbial aggregate grains and encrusted aggregate grains distributed in the NS-1 and NS-5 wells sequentially. In the strict sense, the effect of fluctuating sea and the effect of microbial mat are clearly responsible on the formation aggregate grains of NS-1 well (Figure 55.A). The grains maturity in the NS-1 well passed through different stages from Microbialites stage to peloidal stage and finally the microbial aggregate stage.

Therefore, there are many depositional cycles, detected in the NS-1 well corresponding to the sea level fluctuation. The Microbial aggregate grains in the NS-1 well resulted from progress of the sea level. Simply, the grains of Mishrif formation underwent to the compaction process, led to produce high amounts of peloidal grains. These grains played important role to form the depositional cycles of the aggregate grains. By presence the main factors that are syn-cementation, the effect of microbial film in the shallow water environment and the effect of saturated fluids of CaCO₃ (Figure 55). The remains of traces of microbial films detect the relationship between the aggregate grains types of the NS-1 and NS-2 wells in pre-lumps stage. This feature leads us to say the microbial origin of these wells is one. In general, when we take glance on the (Figure 55), the aggregate grains have the diverse shapes but the mature aggregate grains have an irregular shape.

2.6.3 Rounded clastic grains

Rounded clastic grains contain several types of minerals. For example, calcite evidently shows twinning. Euhedral dolomite reflects the mineral transformation process. Rounded clastic grains are not transported grains because they deposit from the fluid pores in the end of the migration process. Therefore, the final shape of pores is rounded that indicates to deep burial environment.

Textural patterns and compositional maturity of rounded clastic grains are best indicators on moderate and persistent marine currents in the shallow subtidal conditions. Rounded clastic grains are available in the restricted environment only; it might be able to become the best indicator on the restricted environment. In addition, they can provide several informations on evolution of porosity, complete the oil migration process and the abundance of the fluid inclusions. Note that, the NS-2 and NS-5 wells do not have any rounded clastic grains (Figure 56).

Figure 55.

In the Cretaceous of the Near East, carbonate with aggregate grains are produced limestones, included the important resources of chemically high-quality carbonate rocks (Flügel, 1977 and 1981). In the Mishrif, the relationship between paleoenvironment proxies (aggregate grains) and the host of paleoenvironments include specific stages.

A: Core No. NS-1 (sample depth 2052.90 m): Microbial aggregate grains are associated with microbial mats. The first stage of aggregate grains reflects main role of restricted water circulation, sediments mobilization, distribution of microbial films lead to agglutination of sedimentary particles with each other. Usually microbial mat induced early cementation between the sedimentary particles. Finally, the microbial aggregate grains resulted in the formation of Microbialites and especially oncolites. The first stage of microbial aggregate grains indicates to a fluctuating water circulation in the subtidal to intertidal with low terrigenous sediments input.

B: Core No. NS-5 (sample depth 2014.10 m): Encrusted /Coating aggregate grains: The second stage of aggregate grains takes shape between calcite zone on the left angle and dolomite zone on the right angle during compaction process. This stage reflects biogenic precipitation, which contains CaCO_3 mineral from saturated fluids. The evolution between first stage and second stage of aggregate grains is clearly visible here. The second stage of aggregate grains is an important one to increase the periods of stabilization and cementation (Wanless et al., 1981). This stage of aggregate grains found between lagoonal environment and open marine environment.

C: Core No. NS-2 (sample depth 2014.66 m): pre-lumps aggregate grains: The mature aggregate grains have two periods. Firstly, during a pre-lump stage, the aggregate grains became like lump but these aggregate grains are characterized by a few of lobes and the cementation took place around these lobes. There are remains traces of microbial films in this stage and this feature resulted from the NS-2 well, which is located in the lagoonal environment. The existence of microbial genetic indicates to shallow water environment and it indicates to quiet water level in that time too.

D: Core No. NS-3 (sample depth 2007.32 m): lumps/lobate aggregate grains: The second period of mature aggregate grains characterizes by the absence of mud, absence of microbial trace, increasing the compaction and agglutination among the lobes. Chemically, this stage is important because it chemically indicates to high quality of carbonate rocks. The later cementation may be occurred by bacterial degradation of calcium sulphate, which exists in the NS-2 well at depth 1993.10 m.

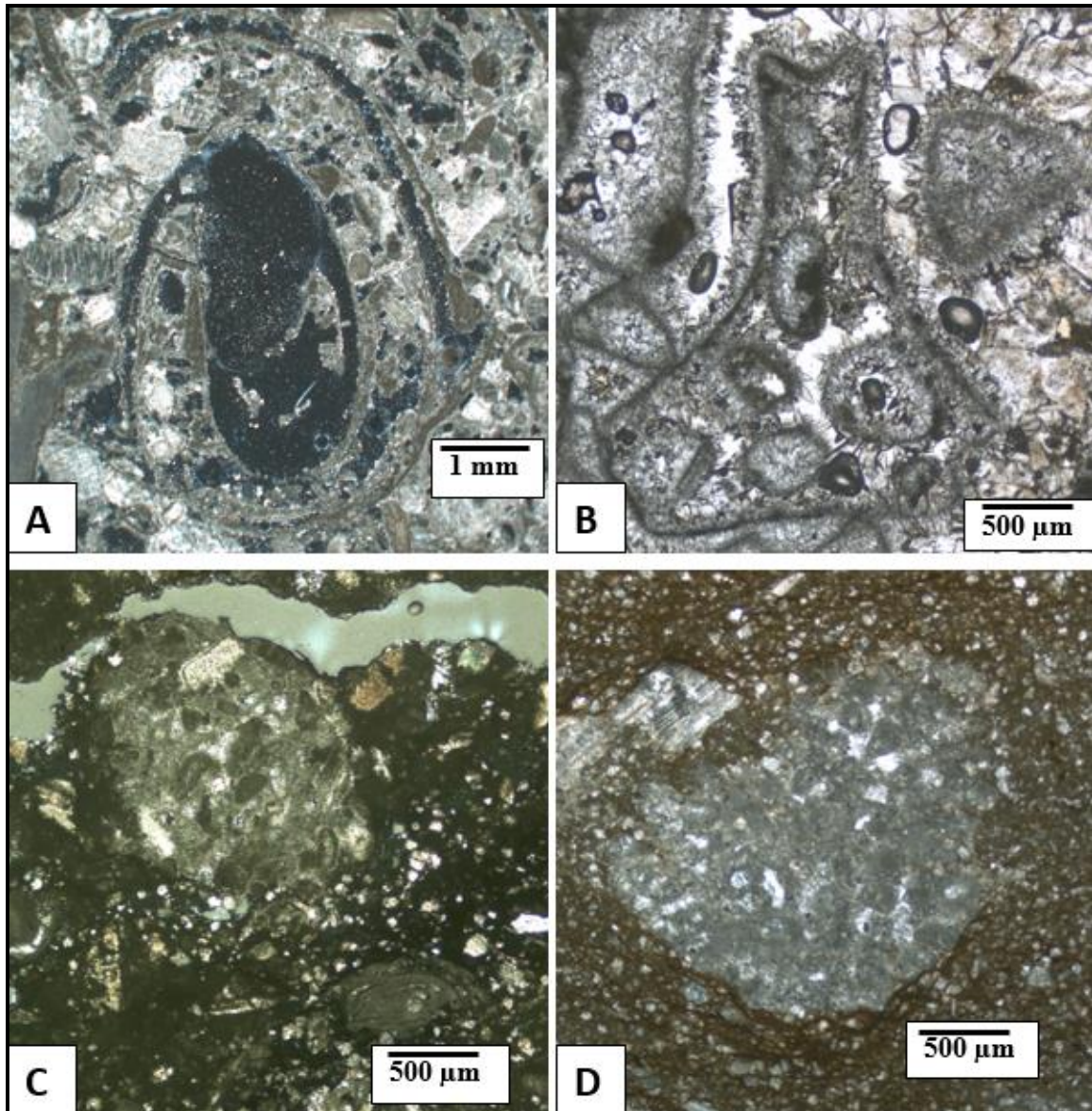


Figure 55 : The Mishrif Formation shows the different stages during forming of aggregate grains, which are used as differentiated standards to explain the paleoenvironments characteristics. Each of stage has different type from the shape, size, effect of microbial film, ratio of cement comparison of the absence of carbonate mud and the absence of terrigenous sediments

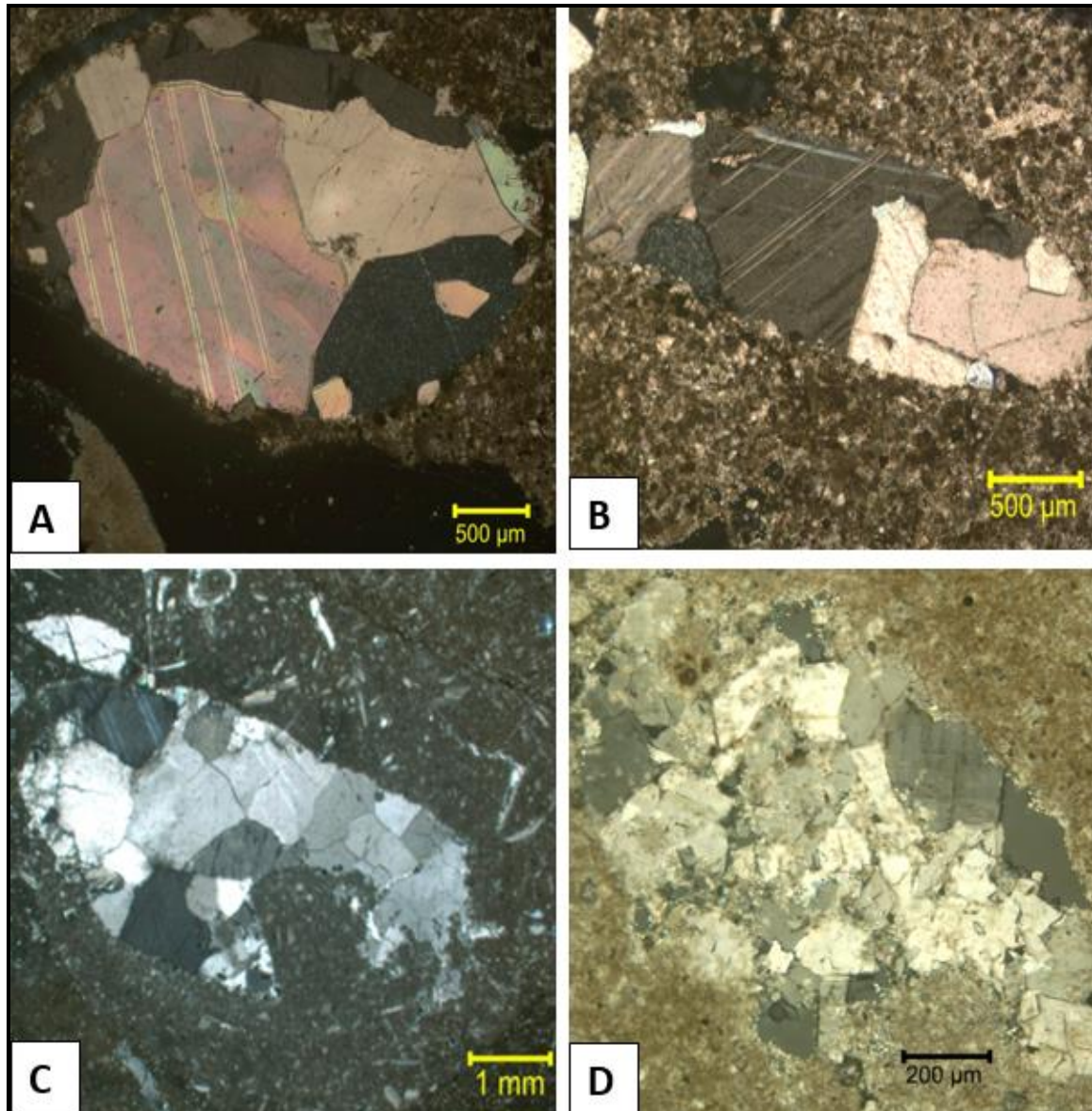


Figure 56: (A and B) Rounded clastic grains are existed in the NS-1 well at depth 2033.80 m. Calcite evidently exhibits several twinning, with pieces of euhedral Dolomite. (C) Large rounded clastic grains exist in the NS-3 well at depth of 1992.70 m. (D) Accumulated dolomite in the rounded clastic grains is in the NS-3 well at depth of 2071.21 m

2.7 Matrix or groundmass

Matrix or groundmass is a descriptive term, used to describe the fine-grained sedimentary materials including microcrystalline carbonate mud (micrite) and sparry carbonate cement (sparite), enclosed by allochems. The matrix nature is also used to classify the rocks based on the ratio between the matrix and grains.

2.7.1 Micrite

Micrite is a descriptive term for microcrystalline carbonate mud (Folk, 1959). It includes crystal size below $4\ \mu\text{m}$ such as clay or silty. Micrite is a component of the carbonate rocks that can be found as a matrix, envelope (Figure 44.C&D), or as peloidal grains. All

these types of micrite can be produced by micritization, chemical precipitation, or desaggregation of peloids into smaller fragments.

The shallow water environment of the Mishrif Formation facilitated the formation of mud grains, mainly as micrite envelopes around grains or as peloids. Micritization occurs due to the action of endolithic algae or other organisms, which live inside rock, coral, or shell of organisms. The micrite envelope is the first stage of micritization process that can be help to preserve the shape of bioclastic grains. The shape of envelope determines the final shape of sparry calcite that maybe fills the envelope after dissolution process has occurred (Figure 58).

2.7.2 Sparry calcite

Sparry calcite is a descriptive term for coarse-grained calcite or aragonite that either accumulated during deposition or was introduced later as cement by diagenetic process. It is coarser than micrite and their size exceed 10 μm . Individual crystals are easily recognizable with an optical microscope (Figure 58). Sparry calcites are dominated in the limestones of the Mishrif Formation. Crystals have polygonal, subhedral and often-prismatic forms.

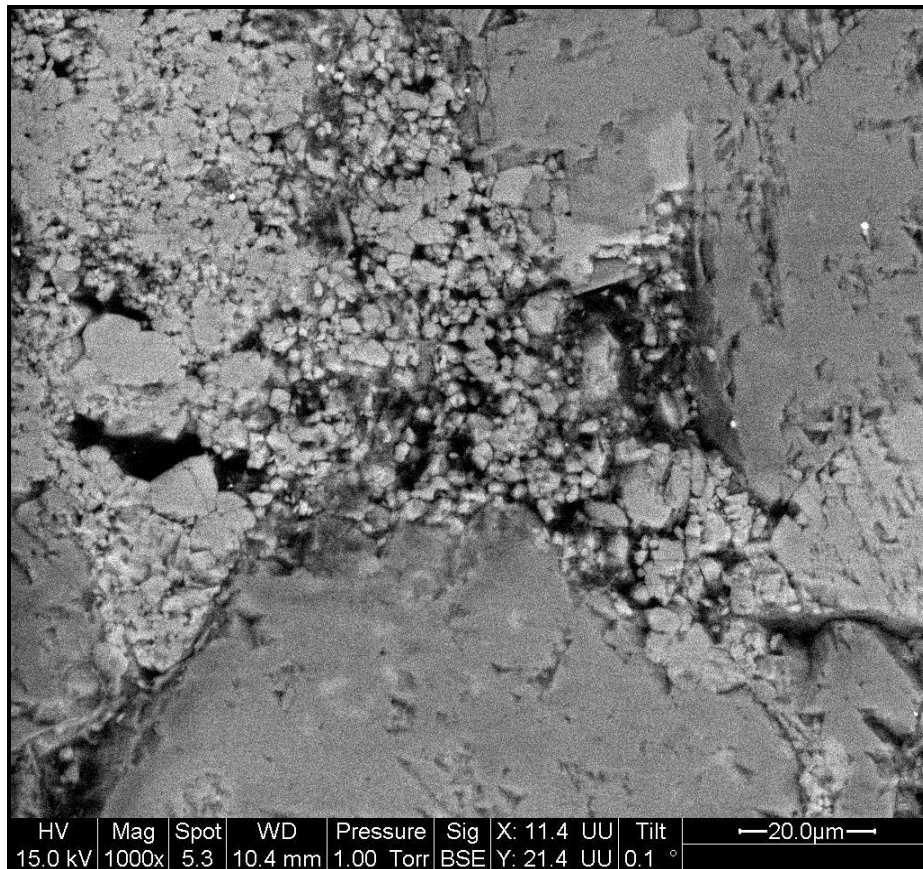


Figure 57 : Microporosity of micrite reflects a typical microporous of carbonate reservoir in the Mishrif in the NS-2 well at depth of 2014.66 m

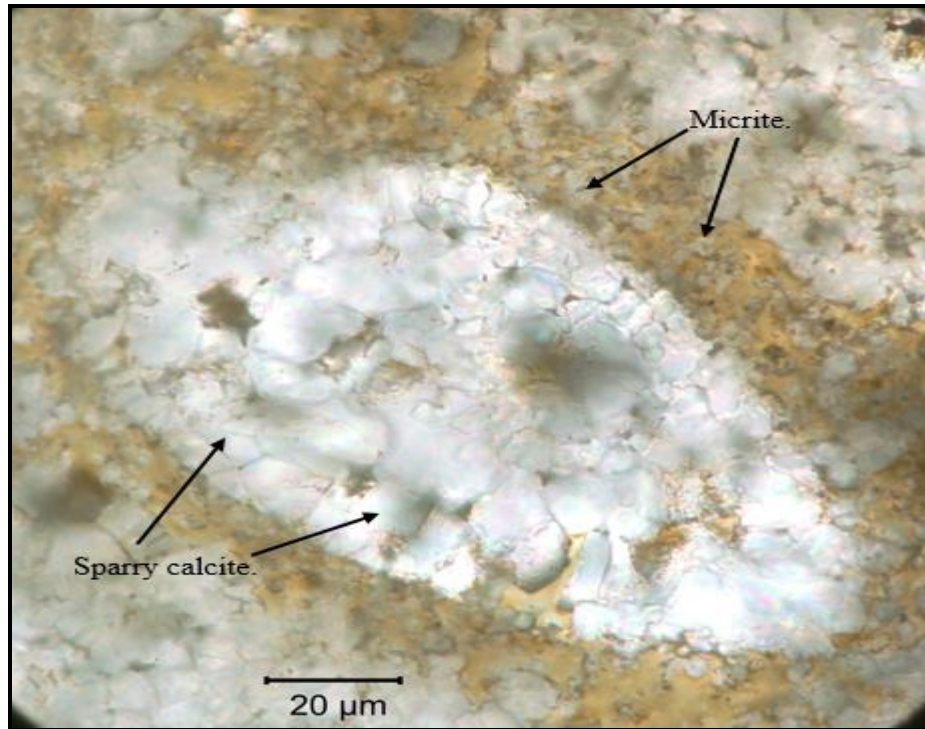


Figure 58 : Sparry calcite is dominated crystals in the paleopores, surrounded by micrite during micritization. Sample from the NS-1 well at depth 2033.80 m

2.8 Major criteria are used to differentiate among carbonate microfacies

Microfacies are local frameworks, described paleoenvironments across evaporitic-restricted and open marine environments. These microfacies are differentiated according to the changes of sedimentological and biological criteria with impact of the environmental factors such as light, water temperature and sediment influx. There are many criteria, used in this study to distinguish amongst carbonate microfacies in the Mishrif Formation. Depositional microfacies are deposited based on the following criteria:-

The grain nature is the first criterion to infer microfacies. The different types can be divided in three main categories: Skeletal grains, microbial grains and non-skeletal grains. Skeletal grains include Foraminifera, themselves divided into benthic and planktonic Foraminifera, corals, bivalves (rudists), and algae (Chlorophyta). Microbial grains include Microproblematica, divided into Microbialites and *Favreina* (microcoprolite grains). Non-skeletal grains are composed of two categories: Firstly, non-skeletal grains are related to microbial origin consisting of pellets, peloidal grains and aggregate grains. Secondly, abiogenic grains consisting of rounded clastic grains. The grains nature has many of factors, which worked as group under the umbrella of grains nature for example.

The rate of grains frequency is an important factor that clearly shows redeposition process, number of cyclic depositions and the similarities between environmental factors. The second important factor is the living type, included parasitic living, solitary living and mass living. The third factor is the dominant fossil groups, used to understand the nature of paleoenvironments. In this study, we used the factor of dominant group to distinguish between the major potential-paleoenvironments (Figure 62.D).

The fourth factor is the abundance of fossils which is responsible on the arrangement style of the fossils in this study. This factor is represented by overlapping relationship between fossils types. For example, the relationship between the biogenic and microbial fossils is determined by the role of algae in the deposition of microbialites under conditions of the shallow water environment. In addition, the genesis of microbial fossils and the abiogenesis fossils revealed the origin of the genetic peloids and the origin of the genetic aggregate grains.

The groundmass/matrix is the second criterion that includes micrite and sparry calcite, used to distinguish local microfacies. The matrix included following factors: The matrix ratio (micrite/sparry calcite) is an important factor to determine the type of depositional textures based on the classification of Dunham. The important relationship is between matrix and the nature of allochems, which represented in this matrix (the abundance of grains).

The dolomite ratio exists in the matrix. The dolomite form and type pose the following questions. Does dolomite has a rhombic shape? Are there zonation patterns in dolomite? What is the size of the crystals of dolomite? Are there any remains of microcrystalline calcite inside dolomite crystals? Is there any increase of the clay proportion along the stratigraphic column? Are there abundance of stylolites in the clay matrix?

Pyrite exists along the stylolites. Quartz mineral distribution takes place along the old fracture as the belts of the fracture fillings. The distribution of anhydrite crystals in the restricted environment from intertidal to supratidal is very important. Indeed, anhydrite reactivates the secondary porosity and changes the depositional textures. The matrix included the proportion of organic matter, occurred under the condition of bacterial reduction; maybe increase the role of bacterial reduction, produced high mature sediments.

The composition mature /flourishing grains maybe indicate to the good environment conditions. For example, the abundant corals with abundance of green algae indicate to the photic zone. Demise period has characteristics of the minimum rate of O₂ comparison by growth of CO₂.

Some types of grains determine the levels of tides based on the distribution of these grains. In addition, some of grain types determine the paleoseawater levels, included the processes of transgressive and regressive seawaters (Figure 60).

2.9 Depositional microfacies

Standard classification (Dunham, 1962) with grains size 0.25-2 mm and Extended classification of Dunham (GeoMika, 2013) have been used. The late classification included Floatstone, Rudstone, Bafflestone, Bindstone and framestone microfacies, used to determine the bindstone microfacies. Microfacies Types are equivalent Dunham textures, determined the matrix and the abundance of the fossil-supported textural types.

2.9.1 Lime mudstone microfacies (MF1)

The lime mudstone microfacies deposited in an environment, characterized by the quiet water currents (Bathurst, 1975). Lime mudstone microfacies dominated underlying Rumaila Formation (Aqrabi et al., 1998). This microfacies is common in the lower parts of Mishrif Formation in the transitional zone between Mishrif and Rumaila formations. This

microfacies is widespread and it is diagnosed in the zones, separated between Mishrif units. It is a best impermeable layer.

Lime mudstone microfacies occur in the various levels throughout the studied sections. It is found in the NS-2 well at depth of 2005.55 m, in the NS-3 well at the depths of 2062.58 m, 2070.21 m and 2075.90 m. In addition, it existed in the NS-5 well at depths 1897.48 m, 2067.53 m and 2075.19 m. It is an autochthonous microfacies. It belongs to SMF 23.

Micrite is the main component with very low rate of benthic and planktonic foraminifera. Porosity represents microporosity type, channel, stylolite and seams or pressure solution. The chemical compaction process in the lime muddy sediments reproduced new shape of the pores by process of outgassing in the NS-1 well at depth of 2033.80 m (Figure 118).

Cementation is dominated by early cementation process. Calcite and dolomite crystals contain of evident rims, included multi-zonations. There are two interpretations of mudstone microfacies origin. Firstly, the layers deposited as a scenario of the sea level fluctuation. Secondly, the layers reproduced by effect of chemical compaction process.

2.9.2 Lime wackestone microfacies (MF2)

This microfacies has been observed at various levels of the wells. It represents one of the most common microfacies in the Mishrif Formation. It consists of specific types, such as large benthic Foraminifera, benthic Foraminifera, algae, rudist, echinoderms, bioclastic grains and lithoclastic grains.

This microfacies is characterized by abundance of the stylolites. Usually solitary moldic porosity because the less abundance of fossils in this microfacies. It represents the brackish water to restricted environments and some parts of open marine environment. In this study, this microfacies will be divided based on the type of grains due to the large distribution of this microfacies in Mishrif Formation.

2.9.2.1 Lime wackestone submicrofacies bearing large benthic Foraminifera

This microfacies consists of some genuses of foraminifera such as *Praealveolina* and *Cisalveolina fallax*, reached their sizes more than 3 mm in length. It exists in the NS-1 well at depth of 2052.90 to 2064.50 m and in the NS-3 well at depth of 2003.53 m, 2007.32 m, respectively. Stylolite occurs through this microfacies. The expansion of the stylolite network resulted of the effect of dissolution process, produced large stylolite systems. There are many grains of pyrobitumen, considered as best indicators for thermal degradation process. In addition, many patches of the mature oils in this microfacies included blue colour under fluorescence microscope. It is an autochthonous microfacies. It belongs to SMF 8.

2.9.2.2 Lime wackestone submicrofacies bearing Foraminifera

This microfacies consists of some genuses of benthic foraminifera such as *Textulria*, *Alveolina*, with Echinoid and Mollusca. Porosity represents vugy, moldic, micro-channels and intercrystal porosity. This microfacies is characterized by brown colour because it includes the organic materials. The grains seem surrounded by an envelope of micrite. It is an autochthonous microfacies. It belongs to SMF 9.

2.9.2.3 Lime wackestone submicrofacies bearing algae

This microfacies consists of some divisions of algae such as *phylloid* algae, which mean platy or leaf-like, dasyclad algae and chlorophyta green algae. It exists in the upper part of Mishrif in the different wells. Calcite is dominated and it contains multizoned rims. Dolomite is appeared as euhedral and massive crystals, existed in the center of charophytes. The major extension of this microfacies is between the NS-1 and NS-3 wells. The proportion of mud is fluctuation due to increase the fluctuations of sea level. Stylolites are considered an important feature in this Microfacies. It belongs to SMF 9.

2.9.2.4 Lime wackestone submicrofacies bearing bioclastic

This microfacies represents one of the more important microfacies; it is a widespread in the most studied sections because of the compaction process, dominated in the burial environment. It consists of the parts of skeletons. It includes vuggy, moldic porosity and large stylolite systems with residue of the organic materials. The ideal examples of this microfacies exist in the NS-1 well at the depth of 2033.80, 2043.42 m and in the NS-2 well at depth of 2023.05 m. In addition, it exists in the NS-3 well at depth of 2018.86 m. This microfacies presents a high porosity due to the effect of dissolution process and in this microfacies, the calcite is usually dominated with multigenerated rims. All pores are fully covered by calcite. It belongs to SMF 10.

2.9.2.5 Lime wackestone submicrofacies bearing rudist

This microfacies is different from the microfacies bearing bioclastic because it contains the complete fossil structures. The elevator and encrusted shells of the rudist are dominated. It contains also the benthic foraminifera such as miliolids (Figure 78.A). There is an evidence of oil and the brown colour represents the organic materials. Therefore, increase the proportion of mud carbonate in this microfacies is necessary to preserve the rudists.

Calcite is dominated mineral and the dolomite crystals are existed. Pores are characterized by moldic pores. This microfacies belongs to SMF 8.

2.9.2.6 Lime wackestone submicrofacies bearing lithoclastic

This microfacies contains of the lithoclastic grains as very important grains. It represents the transition case between the biogenic-microfacies and the microbial-microfacies. On the other words, it represents the transitional boundary between lime wackestone microfacies and lime packstone microfacies based on the amount of grains. It appears less abundance of the complete structures and stylolites.

This microfacies exists in the various levels of the studied wells as well as, it exists in the NS-1, NS-2 and NS-3 wells at depth of 2043.42, 2002.52 and 2070.21 m respectively. The absence or rare this microfacies in the NS-5 well leads to say the paleodepositional environment of the NS-5 well is a different from other wells. This microfacies includes vug pores as the major pores. It contains a high proportion of fluid inclusions. It is an autochthonous microfacies. It belongs to SMF 24.

2.9.3 Lime packstone microfacies (MF3)

This microfacies includes the microbial carbonate grains (Oncoids), Miliolids and peloids of microcoprolite with patches of the corals. This microfacies was seen in the specific levels of the wells as a vertical distribution that means the depositional environment passed through different conditions. A lateral distribution shows fluctuated distribution of the packstone microfacies throughout the studied wells, because of less abundance of the fossils such as Miliolids, oncoids and peloids of microcoprolite.

It represents one of the most important microfacies in the Mishrif because it includes moldic porosity and it has high rate of organic materials. This microfacies is characterized by less abundance of the stylolites or rare. It represents the restricted to open marine environment. Based on a lateral distribution of this microfacies, will be divided into three types, which are:

2.9.3.1 Lime packstone submicrofacies bearing Microbial carbonate grains

The microfacies is dominated on the peritidal area as partially protected lagoons and it belongs to the subsiding coastlines of passive tectonic margins (Scholle and Ulmer-Scholle, 2003). Microbial carbonate grains are called Oncoids grains also, as very important grains because this microfacies contains of the Microbialite domes, indicated to the effect of tidal currents and the fluctuation of sea level. On one hand, the origin of microfacies sediments is the biogenic-microfacies included the cyanobacteria effect. On the other hand, the origin of microfacies sediments is abiogenic-microfacies because some of authors are considered these microfacies sediments not carry any microbial effect after deposition. Indeed, the microfacies sediments are empty from any nucleus.

Based on the ratio of micrite and sparite, this microfacies includes proportion of micrite as a micrite envelope. For that reason, it represents the first stage of the lime packstone microfacies. This microfacies exists in the NS-1 well at depth 2052.90 m as a first cycle of the deposition and in same well at depth of 2024.60 m as a second cycle of the deposition (Figure 81). It includes high ratio of the moldic porosity. It is an autochthonous microfacies. It belongs to SMF 22.

2.9.3.2 Lime packstone submicrofacies bearing Miliolids Foraminifera

This microfacies includes miliolids as important components. It exists in the NS-2 well at depth 2014.66 m between the peloidal microfacies, characterized by high rate of the sparry cement that reflects the tongue shape between the studied wells. This microfacies reflected the transgression of sea water.

In addition, it is considered as a link between open marine environment, represented by the NS-5 well and the evaporitic environment, represented by the NS-2 well. It contains of moldic porosity and stylolites. The dolomite crystals are dominated with abundance of the quartz. It is an autochthonous microfacies. It belongs to SMF 18.

2.9.3.3 Lime packstone submicrofacies bearing Favreina (microcoprolite grains)

The microcoprolite grains are often called Favreina, as microcoprolite grains of the decapod crabs. Favreina indicate to Pelsparite, characterized by moderate energy deposition from open marine to shallow restricted lagoons. It contains an uncertain internal structure.

Carbonate rocks in the NS-5 well contain high abundance of microcoprolite grains (dung). It represents one of the common microfacies in the Mishrif. In addition, these grains have accompanied by a fragments of corals.

This microfacies diagnosed in the NS-5 well at depth 2031.65 m and it is common in the upper part of the Mishrif Formation. It includes moldic and vug porosity. Calcite and rhombohedral dolomite are dominated with abundance of pyrite because of the dissolution process is followed by cementation. This microfacies represents the transitional boundary between lime packstone microfacies and lime grainstone microfacies based on the first appearance of sparite as pelsparite grains. It belongs to SMF 16.

2.9.4 Lime grainstone microfacies (MF4)

This microfacies contains coral patches, round coated grains (peloids) and aggregate-grain. This microfacies diagnosed in the NS-5 well, exception of the aggregate-grain appeared in the NS-2 and NS-3 wells. The vertical distribution of this microfacies clearly appears in the NS-5 well only that means the depositional environment is differentiated among the wells of the study area.

The moldic porosity is dominated that underwent to the effect of fluids to develop into vug porosity. Sparry calcite is the main component, dolomite rims contain multi-zones and pyrite is existed. The effect of the chemical and mechanical compaction processes is very distinguished. This microfacies is characterized by less abundance of the stylolite. Fractures are present maybe because of the effect of hydro-pressure, resulted from increase the litho-pressure. This microfacies usually represents the open marine environment.

This microfacies represents less common microfacies in the Mishrif because of the Mishrif deposits represent the inner rimmed platform environments. The inner rimmed platform contains wide belts of the wackestone microfacies and it contains very narrow belts of the grainstone microfacies (Figure 59). Based on the type of grains in this microfacies, will be divided it into three types of sub-microfacies, which are:-

2.9.4.1 Lime grainstone submicrofacies bearing patches of colonial corals

This microfacies contains of the coral patches and bioclastic, which are various in size. This microfacies is diagnosed as a first time in this study. This microfacies reflects the correlation between an ancient shelf characterized by less abundance of the corals and modern shelf high abundance of the corals. It represents one of the most common microfacies in the NS-5 well at depths 2014.10, 2031.65, 2032.30, 2033.80, 2051.77 and 2078.32 m. This microfacies is characterized by high porosity and the abundance of the organic matter as well, the existence of several microfractures ranged from 2 mm to > 2 cm in diameter. All these characteristics make this microfacies an important part of the potential reservoir. The main porosity is the moldic and growth framework porosity together.

Corals cross-section shows spherical, subspherical, rectangle and cubic shapes of the pores. These pores are ranged from 0.5 - 2 mm in diameter. Sparry calcite is the main component and the dolomite exists in the fractures as fraktur lining as well as, rhombohedral dolomite crystals found in center fracture. This microfacies includes evidences of oil. It is an autochthonous microfacies. It belongs to SMF18.

2.9.4.2 Lime grainstone submicrofacies bearing peloidal grains

This microfacies is densely packed of the subrounded, ovoid and irregular peloidal grains. The distance between the center of grains and the rims of grains are indistinct. These grains are ranged from 0.02 mm to 0.05 mm (Flügel, 2010). Subrounded peloids contain of macrosparry calcite, occurred by the diagenesis process. The well-sorted process of subrounded peloids reflects the moderate energy of the sea currents in the deposition environment.

The deep gray colour or darkening colour in this microfacies particularly in the envelope graines (circumference of grains) reflects the reducing conditions, which removed O₂ and produced H₂S. In addition, these colours occur due to the high content of the organic matter. These reducing conditions represent the conditions of the shallow lagoons environment. This microfacies also indicates to high diagenetic process particularly the effect of compaction, cementation and high effect of dissolution processes. These processes led to change the shapes of pores as well as, they impacted on the final fabric of the calcite crystals cement, composed of Prismatic spar fabric and Syntaxial overgrowth fabric. This microfacies is represented in the NS-1, NS-2 and parts of NS-3 and NS-5 wells at different depths. This microfacies may be resulted from overlap between microfacies of Kifl Formation and microfacies of the Mishrif Formation. It belongs to SMF 16.

2.9.4.3 Lime grainstone submicrofacies bearing aggregate-grains

This microfacies contains of the aggregate-grains. It represents one of the most common microfacies in the Mishrif particularly in the upper part of the NS-3 well at depth 1992.70 m. It represents various sizes range from 1 mm to more than 1 cm. This microfacies includes early cementation, protected grains from the compaction process. Many stylolites include passages around aggregate grains. It often uses as a best indicator to early cementation and it includes the mature grains by compare these muture grains with other grains are outside the aggregate grain. It belongs to SMF 17.

2.9.5 Lime bindstone microfacies (MF5)

This microfacies represents the filamentous *dasycladacean* algae and *phylloid* algae, surrounded the crystals of calcite and dolomite to isolate these crystals from its surrounding. This microfacies maybe reflects the relation between existence of algae and the fluctuation of sea level. This microfacies appears as a crown form. It occurs in the all wells of study area but especially it exists in the NS-2 and NS-3 wells at depth of 2014.66 and 2011.66 m respectively.

On one hand, this microfacies resembles a large spot to isolate the restricted lagoon zone from platform margin or it represents a best indicator of the partition process of the shelf reef. On the other hand, it maybe represents a new small shelf or a new small mound in the

lagoon environments. It is a very important due to it represents the boundary between high mud zone and early cementation zone. Calcite is dominated and the intergranular porosity is existed. It is an autochthonous microfacies. It belongs to SMF 19.

Table 3 : Synopsis of the microfacies data has built from various samples took from the Mishrif Formation. These samples reflected microfacies type (MFT), represented the equivalent textures of the Dunham and they determine type of the depositional environments

No	Microfacies Types are equivalent Dunham textures	Description of microfacies types is based on the sediment compositions	Related to SMF	Type of Depositional Environment (Interior Platform)	
1	Lime mudstone microfacies (MF1)	Micrite/Bioclasic fragments of foraminifera, bivalves and algae, 1:3 fragments. Generally lime muddy/dolomite. It is an autochthonous microfacies	SMF 23	Shallow lagoon	
2	Lime wackestone microfacies (MF2). It is an autochthonous microfacies except microfacies W6.	1	Lime wackestone submicrofacies bearing large benthic Foraminifera. Micrite/ some genuses of foraminifera such as <i>Praealveolina</i> and <i>Cisalveolina</i> . Fossil structures range more than 3 mm in the length	SMF 8	Open marine
		2	Lime wackestone submicrofacies bearing Foraminifera. It consists of some genuses of benthic foraminifera such as (<i>Alveolina</i> and <i>Textulria</i>) with Echinoid and Mollusca. The grains seem surrounded by an envelope of micrite	SMF 9	Open marine
		3	Lime wackestone submicrofacies bearing algae. It consists of some genuses of algae such as Charophyta green algae and <i>Phylloid</i> algae. Calcite/Dolomite	SMF 9	Open marine
		4	Lime wackestone submicrofacies bearing bioclastic. It consists of the fragments of skeletons	SMF 10	Open marine
		5	Lime wackestone submicrofacies bearing rudist. This microfacies is different from microfacies bearing bioclastic because it includes complete or semi-complete shell structures of rudist. It contains also of benthic foraminifera such as miliolids with some of bivalve shells. Mud/Calcite and rhombohedral dolomite	SMF 8	Open marine
		6	Lime wackestone submicrofacies bearing lithoclastic. Lithoclastic grains represent the transition case between the bio-microfacies and the non bio-microfacies such as a microfacies-bearing Peloids. It seems as a start of change of the grains ratio. It represents the transitional boundary between lime wackestone microfacies and lime packstone microfacies based on the ratio of fossils. Calcite and dolomite	SMF 24	Shallow lagoon (restricted)

3	Lime packstone microfacies (MF3). It is an autochthonous microfacies	1	Lime packstone submicrofacies bearing Microbial carbonate grains. Microbial grains (Oncoids). It represents domes of Microbialite that indicates to the effect of tidal currents and the fluctuation of sea level. It contains of the micrite envelope that means it represents the first stage of the lime packstone microfacies based on the ratio of micrite to total grains	SMF 22	Shallow lagoon (restricted) and Tidal flats
		2	Lime packstone submicrofacies bearing Miliolid Foraminifera. Miliolids foraminifera represent the whole this microfacies. This microfacies exists in the NS-2 well at depth 2014.66 m between the peloidal microfacies, contained of high ratio of sparry calcite. It reflects the tongued shape between wells of Mishrif. Dolomite, calcite and quartz	SMF 18	Shallow lagoon (restricted) to Open marine
		3	Lime packstone submicrofacies bearing of Favreina (microcoprolite grains). Microcoprolite grains (dung) are often called Favreina, which are related to decapod crabs. Favreina indicate to pelsparite, moderate energy deposition. It includes an uncertain internal structure. Favreina accompanies fragments of corals. Calcite and rhombohedral dolomite are dominated. It represents the transitional boundary between lime packstone microfacies and lime grainstone microfacies based on the first appearance of sparry as a pelsparite grains	SMF 16	Shallow lagoon (restricted) to Open marine
4	Lime grainstone microfacies (MF4)	1	Lime grainstone submicrofacies are bearing patches of colonial corals. It contains of the coral patches and bioclastic, which are various in sizes. This microfacies is diagnosed the first time in this study. Calcite/dolomite. It is an autochthonous microfacies.	SMF 18	Shallow lagoon (restricted) to Open marine
		2	Lime grainstone submicrofacies are bearing proids subrounded, ovoid and irregular grains. It represents densely packed of the peloids with some biomicrobial grains. This submicrofacies is resulted from overlap between microfacies of Kifl and Mishrif formations.	SMF 16	Shallow lagoon (restricted)
		3	Lime grainstone submicrofacies are bearing aggregate-grain. It contains of aggregate-grain. It represents one of the most common microfacies in the Mishrif. This microfacies includes various sizes, ranged from 1 mm to more than 1 cm. It has early cementation and many stylolites	SMF 17	Shallow lagoon (restricted) to Open marine

5	Lime bindstone microfacies (MF5). It is an autochthonous microfacies	It represents the filamentous green algae that surrounded by the crystals of calcite and dolomite to isolate these crystals from its surroundings. It appears as a crown shape. In addition, it resembles a large spot to isolate the restricted lagoon zone from platform margin or it represents a best indicator to partition process of shelf reef. In other words, it maybe new small shelf or new small ridge in the lagoon environment. This microfacies is very important due to it represents the boundary between high mud and early cementation zones	SMF 19	Shallow lagoon (restricted)
---	---	--	--------	-----------------------------

2.10 Carbonate platform types and facies models

During Cenomanian-Early Turonian, rimmed shelf platform marked by a well developed in the inner platform especially deep lagoon to open marine with numerous patches of coral reefs. The Cenomanian-Early Turonian sequence characterizes by the reactivation of longitudinal ridges and transversal blocks (Cretaceous orogenesis) with effect of transgressive sea. Cretaceous orogenesis influences the paleogeography evolution in several places. The evolution of paleogeography started from the Albian up to the Cretaceous (Buday, 1980a). In the southwest part of the miogeosynclinal area, considered as a part of deep basin sediments (Balambo-Tanjero Zone). Shelf reef divided the basin into small basins due to the differentiation in sedimentological and biological facies criteria. Mishrif formed during formation the shelf reef, included Tikrit/Samarra-Amara ridge.

(Jassim and Goff, 2006), classified Mishrif based on the composition of the microfacies and they included the Mishrif in the Zubir wells into the rudist reef belts. However, they also were included the Kifl into evaporitic environment in the inner platform shelf.

Indeed, Mishrif in the study area belongs to the inner platform environments of the type rimmed shelf due to the Mishrif includes very wide facies belts, which are available in two positions according to the synopsis standard facies belts in the rimmed shelf (Figure 59). Inner platform includes very shallow water environments such as evaporitic, restricted and open marine environments. However, these environments are peritidal shallow water environments, reflectd two main types of the microfacies belts, which are:

1. The low-energy microfacies belt.
2. The high-energy microfacies belt.

Mishrif Formation in the Nasiriyah oil filed was deposited in the inner platform, which confirmed by the presence of the erect-branched corals. The erect-branched corals locally occur as a small patchy-reef, formed in the beds rich in grainstone with *Favreïnids* as microcoprolite, patches bryozoans and microalgae.

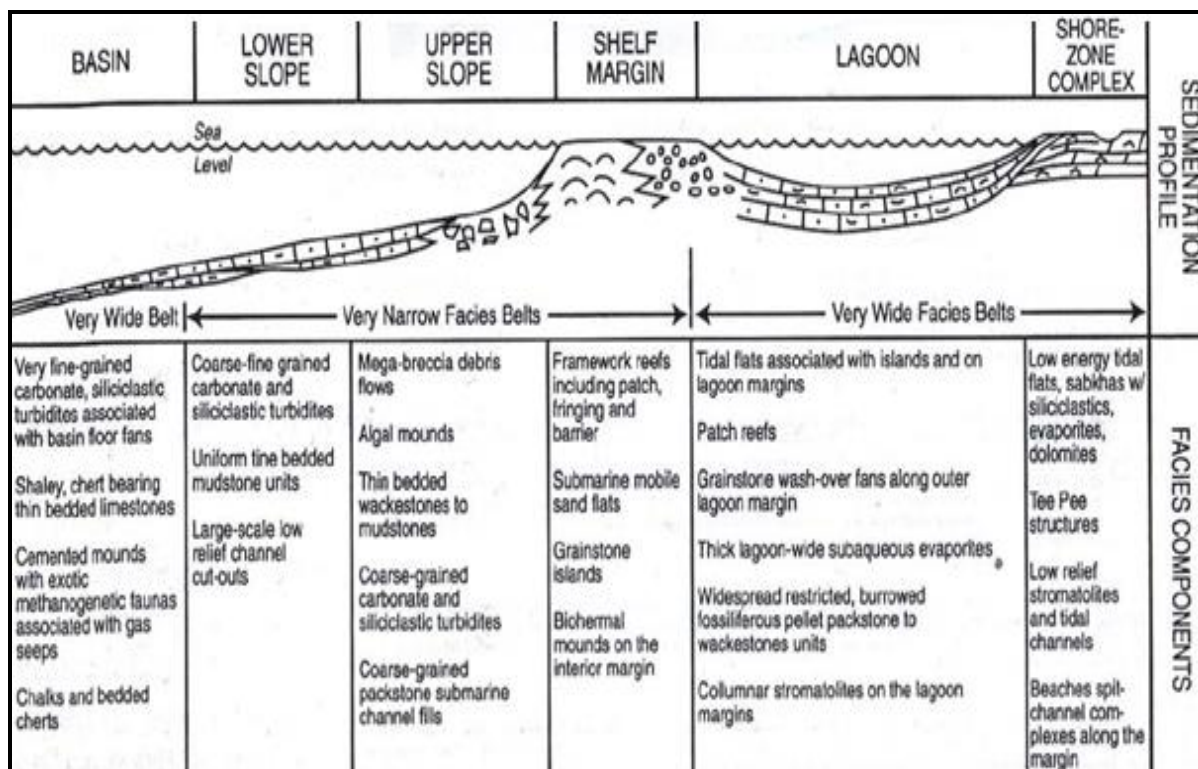


Figure 59 : Synopsis of the standard facies belts in the rimmed shelf (Wilson, 1975)

The lowest member of the low-energy belt characterizes by burrowed fossils, mud. This member consists of mudstone, wackestone with anhydrite beds across subtidal to intertidal evaporitic environment. The upper submember of intertidal-subtidal exhibits thin-bedded, variable green algae wackstone and bioclastic wackstone. The upper intertidal to supratidal submember of evaporitic environment characterizes by locally microbialites as stromatolites with usually a microbially argillaceous mudstone or bindstone with aggregate grainstone and peloidal grainstone.

The high-energy microfacies belt also exhibits the shallow subtidal in the NS-5 well as reef patches. The presence of the erect-branched corals is locally occurred as a small patchy-reef in the beds rich in organic matter and microalgae. The top of the shallow subtidal upward to open marine have planktonic foraminifera as a transgressive seawater with nests of packstone *favreina* microcoprolite. Previous indicators indicate the Mishrif Formation in the Nasiriyah oil field was deposited in the inner carbonate platform.

Composition nature of the rudist reefs characterizes by very narrow facies belts. The results of microfacies analysis of the Mishrif show the differentiation of the sedimentological and paleontological compositions between the wells. Results of the microfacies analysis give the strict interpretation about the paleoenvironment as shallow water (evaporitic-restricted environments) of the NS-1, NS-2 and NS-3 wells. The overlapping units are existed in these wells. The NS-5 well is represented by open marine/lower parts of the back reef.

There are many evidences, which emphasize the Mishrif belongs to inner shelf platform, including:

1. Abundance of the evaporitic microfacies.
2. Existence of the miliolids microfacies (Foraminifera).
3. Evolution of the microbial microfacies bearing excellent quality of the chemical carbonate rocks, started from pellets and peloidal microfacies to the microbialites microfacies passing through *Favreina* microfacies. These microfacies contain of the many deposition cycles in the Nasiriyah wells (Figure 47 to Figure 54).
4. The rudist microfacies very less distribution comparing with other microfacies, for example the NS-5 well, included coral reef microfacies.
5. Kifl gradually grew from Mishrif Formation by evolution of the bacterial reduction sulfate, worked on the decomposition of calcium sulfate that produce large amounts of microbial sediments, supported the platform in two points.
 - A) The evolution of microbial sediments produced many sediments cycles, observed in the stratigraphic sections (Figure 47 to Figure 54).
 - B) Decomposition of calcium sulfate increases the interaction between fluids and rocks, played important role in produce the secondary porosity, led to increase the porosity values in the Mishrif Formation.

On one hand, it is very difficult to recognize the boundary between Mishrif and Kifl formations because Kifl gradually grew from Mishrif. Nevertheless, it is very easy to realize the boundary between Mishrif and Khasib formations from uppermost unit of the Mishrif. On the other hand, the Mishrif and Rumaila boundary can be recognized in the lower unit of the Mishrif by observing the differentiation of mud microfacies. The mud in the Rumaila and Khasib formations characterizes by gray to blue colour, very fine grains and high concentration of the planktonic Foraminifera structures. These mud colours indicate to the marine environment (Figure 33 & Figure 60).

Finally, the microfacies analyses not indicate to the terrigenous sediments input, reflected the natural composition of the paleoenvironment and paleogeography. The changes of the sedimentological and biological criteria synchronize with the fluctuations of the sea level, confirmed the changing in the paleoenvironmental factors (Figure 60).

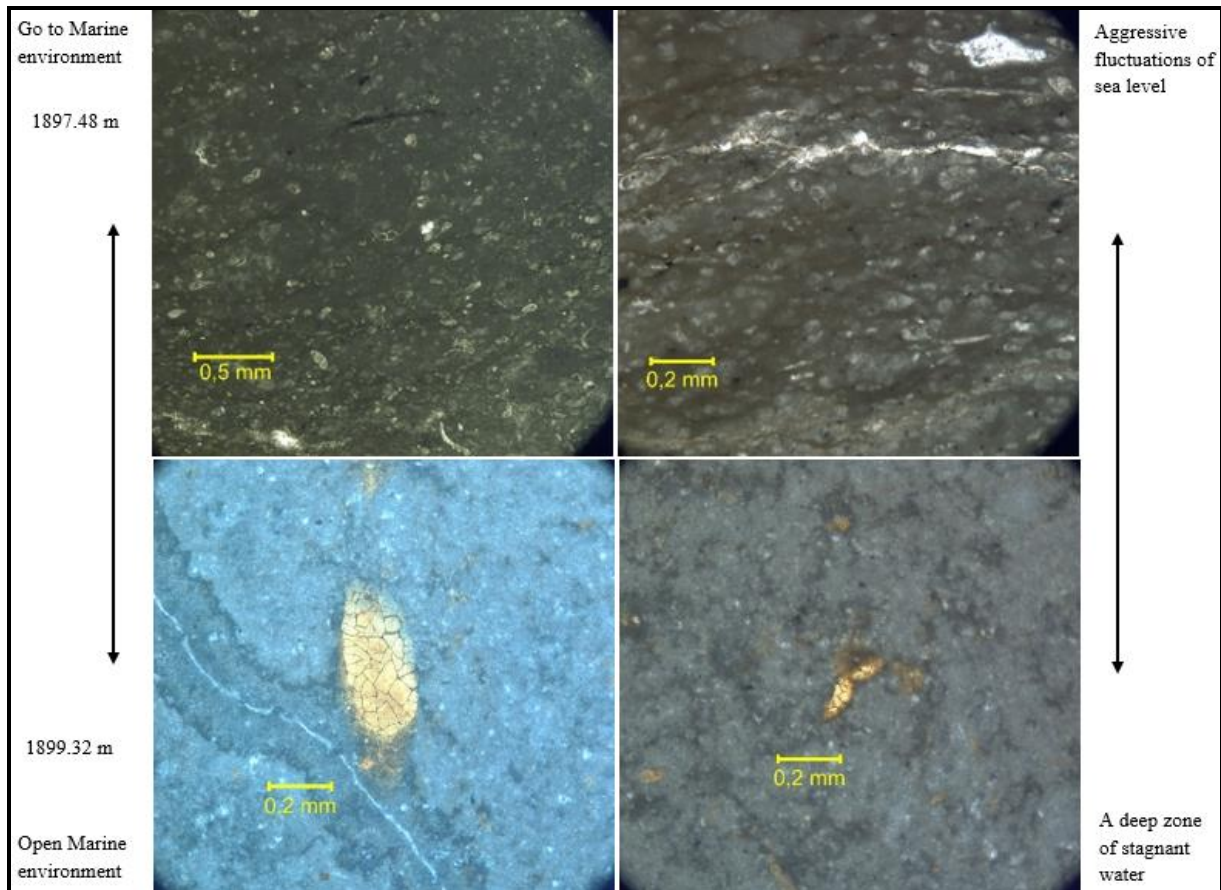


Figure 60 : Sedimentological and biological criteria determined the strict border between the Mishrif and Lower part of the Khasib formations in the NS-5 well at depth 1897.48 and 1899.32 m

2.11 Depositional environments

Study of depositional environments includes understanding of the fossil assemblages, sedimentary structures, their textures and mineral compositions, existed in each paleoenvironment of the inner carbonate platforms. Reconstruction of the depositional paleoenvironments by rock properties requires identify the sedimentary processes in each depositional setting over time distinguish the depositional successions (Ahr, 2011).

Microfacies analysis give huge information about the fossil groups, sedimentary structure, textures, types of lithofacies and matrix. The information interpreted based on the statistical method. However, the statistical method is established by the reclassification these grains based on their concentrations in the vertical distribution (frequency) in their wells. The most highlighting grains in this case study are peloidal grains, miliolids, coral patches, rounded clastic grains, green algae, calcimicrobial grains, *favreina*, rudist and gastropods respectively based on their concentration and their distribution (Table 4).

Note that, Mishrif is heterogenic formation, but here in this study we adopted the high concentrations grains with high frequency of their lateral and vertical distributions.

Table 4 : The values of vertical distribution of the fossils include high frequencies in the wells

Type of grains	Depth in the wells (m)				Microfacies	Environment
	NS-1	NS-2	NS-3	NS-5		
Peloidal grains	2043.42 & 2048.95	1993.10 2002.52 2042.65 2048.26 & 2062.60	2018.86 2039.91 2061.73 2062.58 2065.85 207021 & 2075.90	2033.80	MF4	Restricted shallow water
Foraminifera (Miliolids)	2024.60 & 2033.80	2014.66	2003.53 2007.32 & 2011.66	2049.47	MF3	Restricted shallow water to open marine
Coral patches	—	2014.66	—	2014.10 2031.65 2032.30 2049.47 2051.77 & 2078.32	MF4	Restricted shallow water to open marine
Rounded clastic grains	2033.80	—	1992.70 2024.25 & 2070.21	2051.77	MF2	Restricted shallow water
Green algae	2027.42	2014.66	2011.66 & 2014.67	—	MF2 & MF5	Open marine & Restricted shallow water
Microbial carbonate grains	2024.60 & 2052.90	—	—	—	MF3	Restricted shallow water to tidal flats
Favreina	—	—	—	2031.65	MF3	Restricted shallow water to open marine
Mollusca (Rudist and gastropods)	—	2014.66	2024.25	2033.80	MF2	Open marine

* The sign (—) means not available grains.

We have two groups depend on (Figure 61) that found in the data of (Table 4) that shown below. First group includes some types of the fossils, characterized by high degree of frequency. The frequency increases more than 10 meters in the depth. Second group includes frequency less than 10 meter in the depth of same wells.

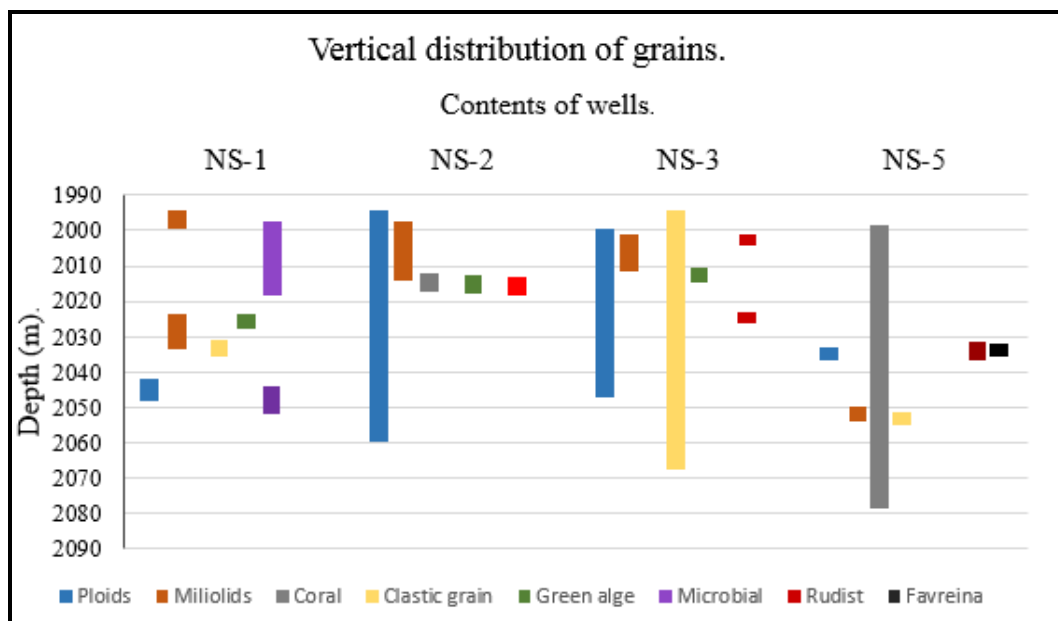


Figure 61 : Vertical frequency of the grains distribution is in Mishrif according to data of (Table 4)

Nevertheless, the vertical distribution reflected the rate of the carbonate mud in the end of any well in (Figure 61). The most important objective of carbonate mud appears as sandwich shape and it plays main role to form mound mud or bioherm reservoir. The ends of first group grains reflected the start of transitional boundary between Mishrif and Rumaila formations in the depth around 2078.32 m with increase the rate of the carbonate mud. The details of the grains of first group and their environments are in (Table 5).

Table 5 : First group of the grains includes high frequency of the best indicators of the paleoenvironments

Type of grains	Well n°	Depth m	Grains are best indicators on their environments
Microbialites	NS-1	2024.60 2052.90	Cenozoic microbial carbonate deposits are predominantly peritidal environments (Scholle and Ulmer-Scholle, 2003)
Peloids	NS-2 NS-3	2059.5 2047	Open marine to restricted or coastal settings (Scholle and Ulmer-Scholle, 2003)
Miliolids	NS-2	2014	Miliolids are main constituents of the protected environments (Hallock and Glenn, 1986)
Clastic	NS-3	2067.5	Rounded clastic grains are best indicator in the restricted environment
Corals	NS-5	2078.32	Photic zone in the shallow marine. An analogous symbiotic relationship clearly determines the environment, here it is <i>Favreina</i> (Scholle and Ulmer-Scholle, 2003)

The second group is less concentration of the grains as shown by the results of microfacies analysis and the details of (Figure 61). The second group of grains can help us to interpret some of scientific clues such as the coexistence of organisms or parasite living. Nevertheless, the second group can use to show the lateral distribution of the microfacies. The grains details of second group and their environments are shown in the (Table 6).

Table 6 : Second group of the grains includes frequency less than 10 m in the depth

Type of grains	Well n°	Depth m	observations
Green algae	NS-1 NS-2 NS-3	2027.42 2014.66 2011.66	Green algae generally are most common in depths of 2 to 30 m of sea level. Wide salinity ranged from brackish to strongly hypersaline. Green algae are common in reef and near back reef areas and can even form thick bioherm or mud mound (Scholle and Ulmer-Scholle, 2003)
Charophytes	NS-3	2014.67	Charophytes are most common in lacustrine settings, especially clear-water, alkaline/calcium-rich lakes. Fossil forms are widely distributed in non-marine rocks especially in shales and limestones. Nevertheless, they are also extend into rocks, deposited in brackish and perhaps even more saline environments (Racki, 1982)
Molluscs Rudist	NS-2 NS-3 NS-5	2014.66 2024.25 2033.80	The vast majority inhabits in shallow-marine settings; Rudists are especially bivalves, but now-extinct and even were important bioherm and reef builders (Scholle and Ulmer-Scholle, 2003)
Microcoprolite <i>Favreina</i>	NS-1 NS-3 NS-5	2024.60 2018.86 2031.65	<i>Favreina</i> exist in the restricted environment of the inner carbonate platform environment, produced by decapod crabs as fecal pellets (Flügel, 2010)

The lateral distribution of grains shows a new correlation among the fossils depend on thickness of their shells (Figure 61). In the other words, the thick shells exist in the environments, included high energy of the water currents. Coral, rudist and algae represent thick shells fossils in open marine environment, characterized by high energy levels. While, the farthest interpretation of the potential environment is the back parts of reef environment. The carbonate mud rate increases from NS-5 pass through NS-3, NS-2 until NS-1 respectively. Mud rate reflected the quiet environment such as restricted shallow water, generated large amounts of the mud in the NS-1 and NS-2 wells and the high-energy environment such as open marine produced low amount of the carbonate mud in the NS-5 and NS-3 wells (Figure 65).

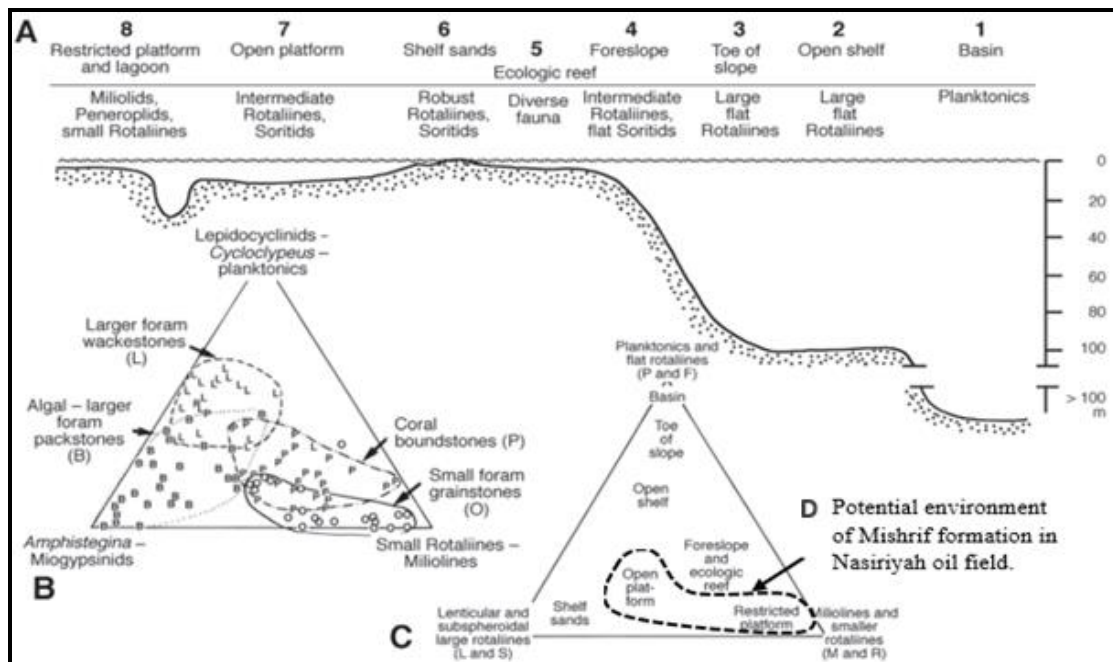


Figure 62 : The potential environments of the Mishrif Formation, modified after (Hallock and Glenn, 1986)

Characteristics of fossils show the inner shelf platform environment as a major setting of the Mishrif, contained of open marine, restricted shallow water and evaporitic/brackish environments. The coral, algae and rudist fossils are exceptionally indicated to their membership in the bioherm builders that may be indicate to back reef environment based on their concentrations. All the results are applied on the model of (Hallock and Glenn, 1986), obtained from the microfacies analysis side to side the results generated from vertical distribution of the grains. The model shows the potential paleoenvironments of the Mishrif based on the relative distribution of the grains (Figure 62. D).

(Hallock and Glenn, 1986) model reveals the impact of grains distribution on the interpretation of potential palaeoenvironments. A) The Standard Facies Zones (FZ) are classified by (Wilson, 1975) for a rimmed carbonate shelf. B) Triangle model contains foraminifera with other grains assemblages from Standard Facies Zones. C) The model is adopted the relative percentages of three diagnostic environments depend on the distribution of these grains. D) Potential environment of the Mishrif Formation in Nasiriyah oil field.

The abundance of grains is indicated to the accurate paleoenvironment of the Mishrif. The accurate paleoenvironment is restricted environment in the NS-1, NS-2 and NS-3 wells. Nevertheless, in the NS-5 well is a different equation, the open marine is an accurate environment. The results of microfacies showed the differentiated compositions in the Mishrif such as the diverse fossils, dominance of the microbial sediments, various lithology, depositional textures and distribution of the rounded clastic-grains. The previous characteristics clearly explicate the imaginary boundaries between these environments. Finally, three environments played a major role in the Mishrif Formation deposit that are:

2.11.1 Open marine environment-interior platform

The open marine environment is determined by (Wilson, 1975) that is located in natural straits (waterway), open lagoons and in the bay behind the outer platform edge. The abundant fossils of the open marine environment existed in the Zubair oil field in the SE Iraq as the Cretaceous rudist reefs were detected. Lithology is variable carbonates and terrigenous sediments are absent in the open marine environment. Open marine environment includes moderate energy levels because; it is well preserved the fossil structures, represented by coral, residue of the rudist structures and algae. The existence of algae grains indicates to depth, which do not exceed tens of meters in deep zone.

The open marine environment is a very narrow environment in the Mishrif Formation. It interbedded with restricted environment because of the previous depositional proxies. It is indicated to the ecosystem included different benthic organisms, a few of planktonic organisms and a microbial-dominated communities. However, the Mishrif fossils of the open marine environment characterize by presence of large foraminifera, residue of the echinoderms, patches of coral reefs and mollusca (Figure 63). Furthermore, the echinoderms exist as a very low rate compare with other grains, reflected the paleoenvironment conditions. The low rate of the echinoderms existence reflects the fluctuation of seawater level. The carbonate deposits in the NS-5 well and some units of NS-3 well represent this environment.

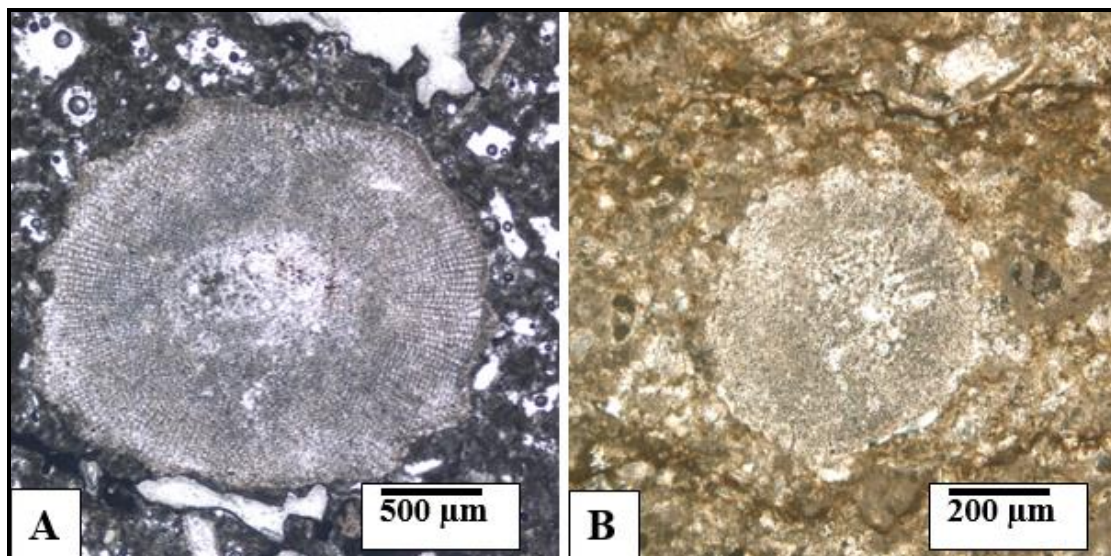


Figure 63 : Some types of the echinoderms exist in the different paleoenvironments in the Mishrif

Figure 63.

A) The NS-2 well at depth of 2023.05 m: Echinoderm includes high ratio of pores, interpreted under transgression conditions of the sea water.

B) The NS-1 well at depth of 2033.80 m. Echinoderm exists in the brown sediments with planktonic organisms, interpreted the existence under the fluctuation sea level.

2.11.2 Restricted environment-interior platform

The sediments of very shallow water of the lagoon environment are represented in the Mishrif that exist between the evaporitic environment as the terminal facies in the SE of Rutba high (terrigenous clastic facies) and the emergence of open marine in the NS-5 well and some units of NS-3 well. The restricted paleoenvironment is significantly contributed to reactivate diagenetic processes. Because, it included the high degree of salinity water and the strong existence of microbial grains with reduce the rate of the skeletal grains that lead to euxinic sediments. Euxinic sediments occur in the isolated parts in the deep lagoon environment, for this reason, the spots of the black shale have appeared (Figure 65).

The important fossils in this environment are foraminifera (miliolids), algae (charophytes) and microbial grains. Increased rate of presence algal grains and the microbial grains grows towards the subtidal zone. Depositional texture is clotted microbialites, lobate aggregate grains (grainstone) and peloidal grainstone. Lithology is dominated by dolomitic limestone. The restricted environment characterized by emergence the coarse cement of calcite especially in the NS-2 and NS-1 wells (Figure 64). The restricted environment of the Mishrif is a widespread; it covered most of the Formation especially in the NS-1, NS-2 wells, some layers in the NS-1 and NS-2 wells are interbedded with layers of NS-3 well.

2.11.3 Evaporitic or brackish environment-interior platform

The sediments of the evaporitic environment in the Mishrif are gradually deposited from the interactions, led to form anhydrite crystals. The fossils in the evaporitic environment characterized by not indigenous fossils, but there are a lot of microbialite (stromatolitic algae). This environment totally is represented by the Kifl Formation. Evaporitic environment is located in the zone of peritidal environment at the upper parts of NS -1 and NS-2 wells while, the upper parts of the NS-3 and NS-5 wells represented the Khasib Formation as open marine environments in the interior platform. It is a very narrow environment in the Mishrif. It is located between Rutba high (terrigenous clastic sediments in the west) and the restricted environment in the east. For that reason, it is considered as a terminal facies in the Mishrif.

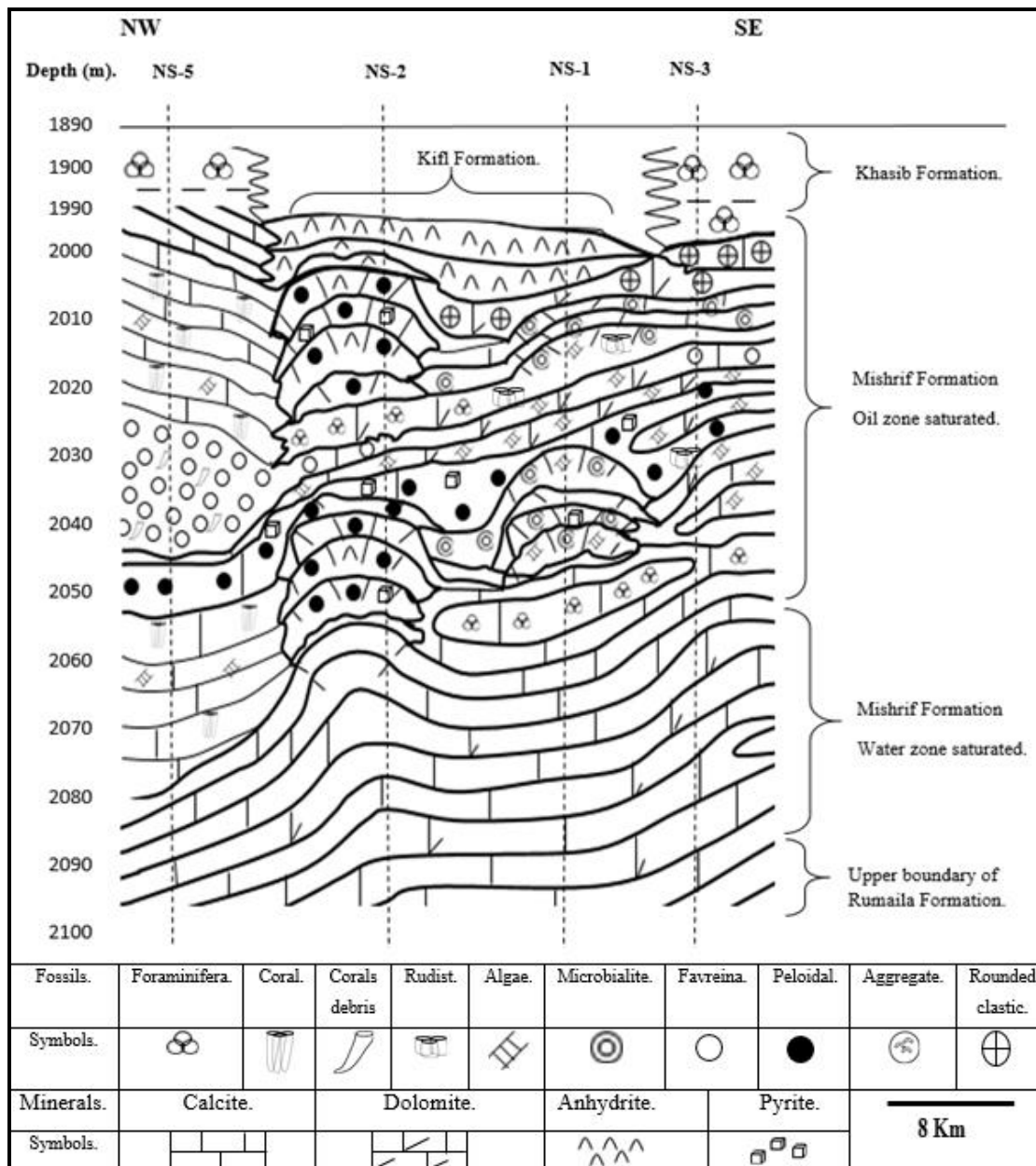


Figure 64 : The potential sedimentary model shows the horizontal distribution of the microfacies in Mishrif Formation in the Nasiriyah oil field, southeast Iraq

The hydrogen sulfide causes the precipitation of ferrous sulfide, which blackens the rich accumulations of organic matter (Pettijohn, 1957). The bacteria reduce the sulfates that are generated to important concentrations of the hydrogen sulfide, found in the fluid inclusions analysis. In the strict sense, sulfate-reducing bacteria provide pyrite, which provided more bicarbonate for filling the pores as a sparry marine cement (Figure 64).

The depositional model of the Mishrif (Figure 65) corresponds with the wells distribution in the contour map that reflects the paleoenvironments types. The NS-3 and NS-5 wells are represented by an oxic environment conditions. The NS-1 and NS-2 wells are represented by the suboxic environment conditions according to the results of microfacies.

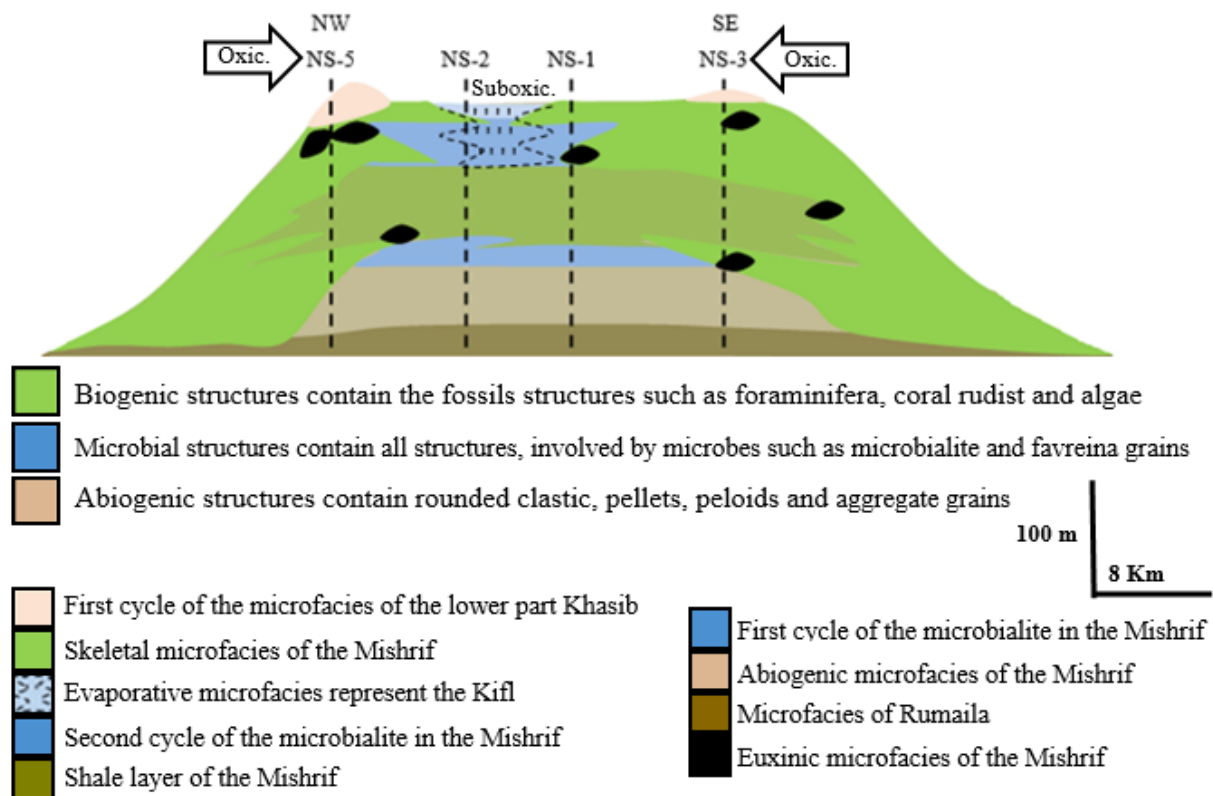


Figure 65 : Depositional model reflects the types of microfacies of the Mishrif reservoir in Nasiriyah oil field.

2.12 The maturity and evolution stages of the grains demise

The microfacies studies show the path of mass extinction that reflected the grains abundance and the relation is between the depth and the grains existence. It occurred in the steps based on the interpretations of the abundance and distribution of grains with the depth (Figure 61).

The grains include diversity in the shape and the size (morphotypes) that are shown in the stratigraphic column of the Mishrif for each well. Stratigraphic column shows two stages of typical fossils existence. Firstly, the fossils are more resistance to crisis of oceans in the upper Cretaceous, included corals, green algae and miliolida, existed as gregarious fossils. Secondly, the less resistant fossils to crisis of oceans are mollusca (rudists), large foraminifera (*alveolina*) and echinodermata. They are appeared as a solitary existence, reflected the drastically decline of their existence (Figure 47 to Figure 54).

Drastically decline of the fossils bodies passed through two stages of the demise. The first stage of demise represents the solitary existence of the rudists, large foraminifera (*alveolina*) and echinodermata. The second stage of demise represents the presence of planktonic foraminifera (*Globigerina ooze*, *Oligostegina* and *Globotruncana* assemblages) associated with absence of all types of previous fossils except the charophytes green algae (Figure 40.F). These interpretations are based on the grains abundance. Indeed, the relation is between the grains distribution and the depth, (Figure 61) showed the decreasing of the grains size that took place in the depth approximately 2000 m upwards to the emergence of the planktonic foraminifera. This emergence is represented by the Khasib Formation.

The grains distribution with the depth indicated to the most majority of the fossils bodies, existed in the depth of 2000 m to 2050 m. While, the coral grains appeared until in the last sample of the Mishrif core of the NS-5 well at the depth 2078.32 m. This interpretation is according with (Figure 62. B) Triangle model, contained of foraminifera with other grains assemblages in the Wilson standard facies zones.

According with report of the AD oil field (Zhao et al., 2012), the fluctuation of sea level in the (Figure 21 & Figure 22) and the results of (Figure 61); The maturity and evolution stages of the grains are responsible of the forming the platform carbonate during (Cenomanian- Early Turonian), included Mishrif, Kifl formations and the first emergence of lower Khasib Formation.

The maturity and evolution stages of the grains demise include four stages of the sea level fluctuation, represented by:

1. Regression of sea level less than 150 m that formed Mishrif Formation.
2. Transgression of sea level to approximately to 300 m led to demise of rudist, large foraminifera and echinodermata (first demise).
3. Transgression of sea level still continues; according to change of sediments colour with remain same fossil grains (Figure 75). The transgression of sea level led to destruction of rudist bodies and large foraminifera (final demise). The transgression of sea level is simultaneous with emergence of planktonic foraminifera, formed the lower part of the Khasib.
4. Regression of the sea level to a little over of 100 m led to emergence the second cycle of the grains, represented by green algae packstone, formed the upper part of the Khasib in the AD oil field.

Kifl mainly characterizes by anhydrous facies. Kifl in the Nasiriyah oil field represents the degradation stage of Mishrif sediments during the late period of the regression of the sea level because of the emergence of the anhydrate facies. The sea level fluctuation led to extreme increase of the rate of salinity in the shallow water. For that reason, the existence of the NaCl crystals in the both sides of stylolite and the calcitic joints interpreted under the fluctuation conditions. In addition, the appearance of microbial carbonate microfacies (oncoids) exists with demise the green algae (charophytes). The emergence of microbial carbonate microfacies detected the reason why the Kifl does not include recorded fossils in the wells of the Nasiriyah field.

The emergence of the microbial carbonate rocks (Oncoids) in the NS-1 well represents two times. The first emergence is in the depth of 2052.90 m and the second emergence is in the depth of 2024.60 m. The two emergences interpreted under umbrella of the sea level fluctuation. The chemical composition of seawater, the sea level fluctuation, the deposition process continuance and the increase of the burial column led to the evolution of the compositional maturity of the grains (Figure 66).

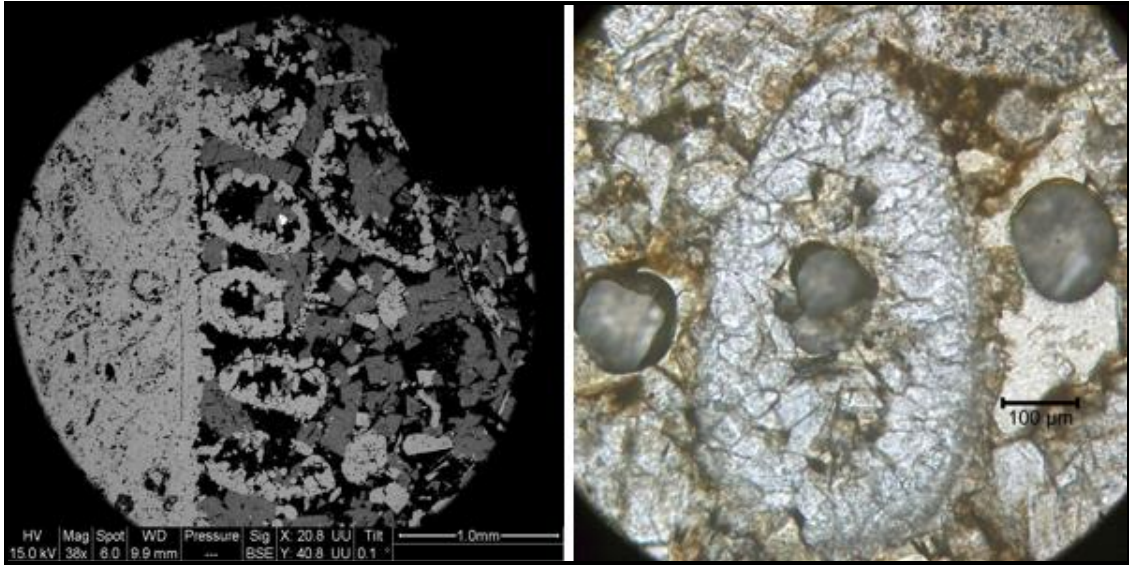


Figure 66 : Compositional maturity of the grains is in NS-5 well at depth 2014.10 m

Third chapter
DIAGENETIC EVOLUTION OF THE MISHRIF FORMATION

3.1 Diagenetic processes

Diagenesis includes any physical and chemical changes in the sediments during the conversion to the sedimentary rocks that occurs after deposition process in the seafloor with impact of the organic processes. Chemical processes are widespread in carbonate rocks that represented by chemical compaction, dissolution, cementation, neomorphism, dolomitization or dedolomitization and replacement. Two processes can work together; for example, compaction and dissolution produce pressure solution and stylolitization in the carbonate mud.

3.2 Factors affecting the efficiency of diagenesis processes

3.2.1 Pressure

Grains size of the Mishrif Formation decreased with increase the depth, which resulted to increase the lithostatic pressure (Figure 67). Mishrif includes carbonate mud layers, resulted from the rapid burial or increase of the weight of the rocks column. The rock column of Mishrif displays two impermeable layers. These impermeable layers are able to create a geopressure zone. Moreover, the differential compaction immediately leads to create fractures. Hydrostatic pressure clearly appears in the pore spaces as a fluid column. It affects the pores shapes depend on the difference between the degrees of hydrostatic pressure and lithostatic pressure (Figure 68).

The hydrostatic pressure is affected by salinity and temperature. In the study area, most of pores display a round shape that mean the degree of hydrostatic pressure is enough to keep the pore shape. Sometimes, the hydrostatic pressure is somewhat less than lithostatic pressure; in some cases, when the hydrostatic pressure is higher than lithostatic, the degassing pores are existed (Figure 70).

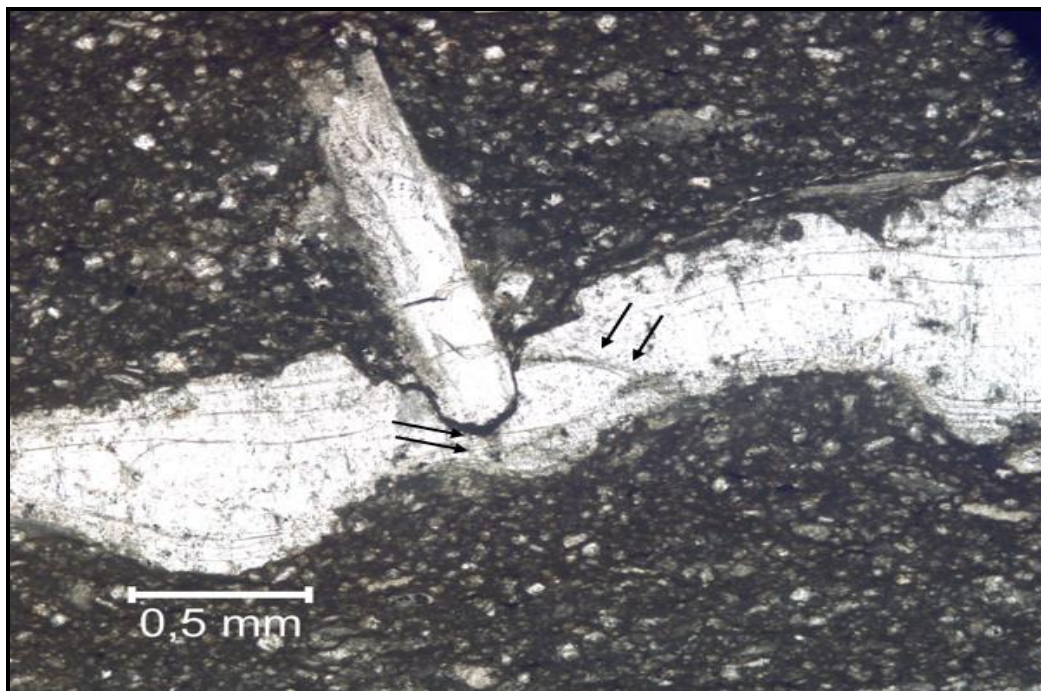


Figure 67 : Microbial bioherm likes semi-ductile calcite cement in the Mishrif. The quantity of carbonate mud increases by increase the effect of pressure. Fractures occur by the effect of differential compaction in the calcite belt. The black arrows indicate to these fractures. The sample is taken from the NS-3 well at depth of 2007.32 m

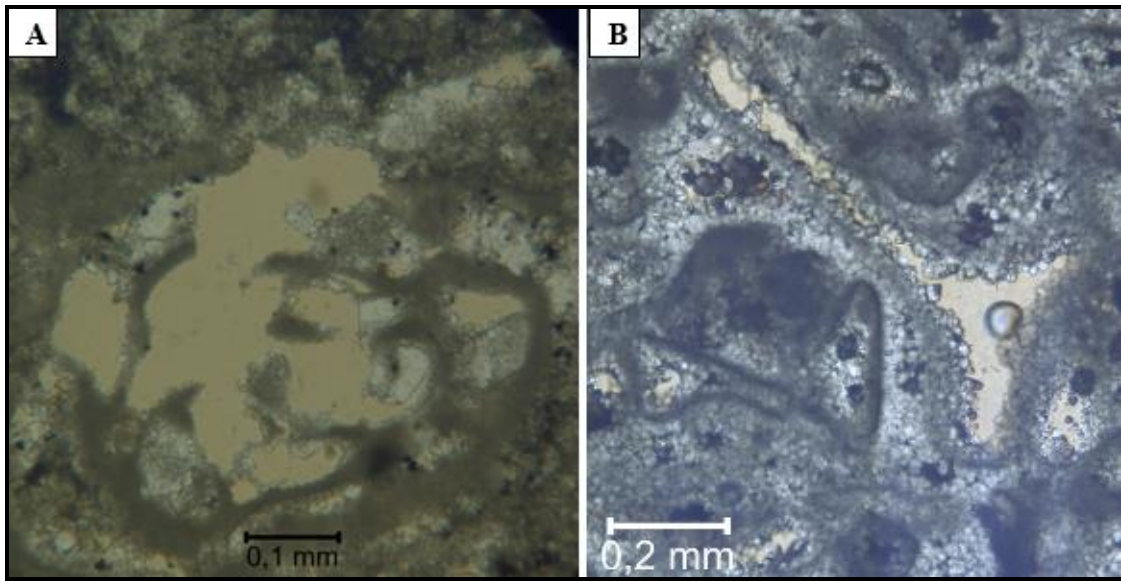


Figure 68 : Pressure affects the shapes of moldic pores. (A) Biomoldic pores represent round shape in the NS-3 well at depth 2024.25 m. (B) Biomoldic pores are elongated shape in the NS-5 well at depth of 2014.10 m

3.2.2 Temperature

The temperature effect can be determined on the basis of mineral diversity with depth, such as the dolomite crystals in case of the Mishrif. The changes of the metastable minerals can be occurred by the temperature effect. For example, the distribution of pyrite and the size of the dolomite crystals will increase with rise of temperature of the fluid inclusions (Figure 80). In addition, the residue of solid pyrobitumen leads us to guess the process of thermal degradation, occurred after the generation and migration processes of oil with increase the temperature in the reservoir rocks (Figure 69).

Regardless, the contemporary brine is affected by the precipitation of calcite or dolomite. The homogenization temperature (T_h) of fluid inclusions includes range from 120°C to more than 250°C.

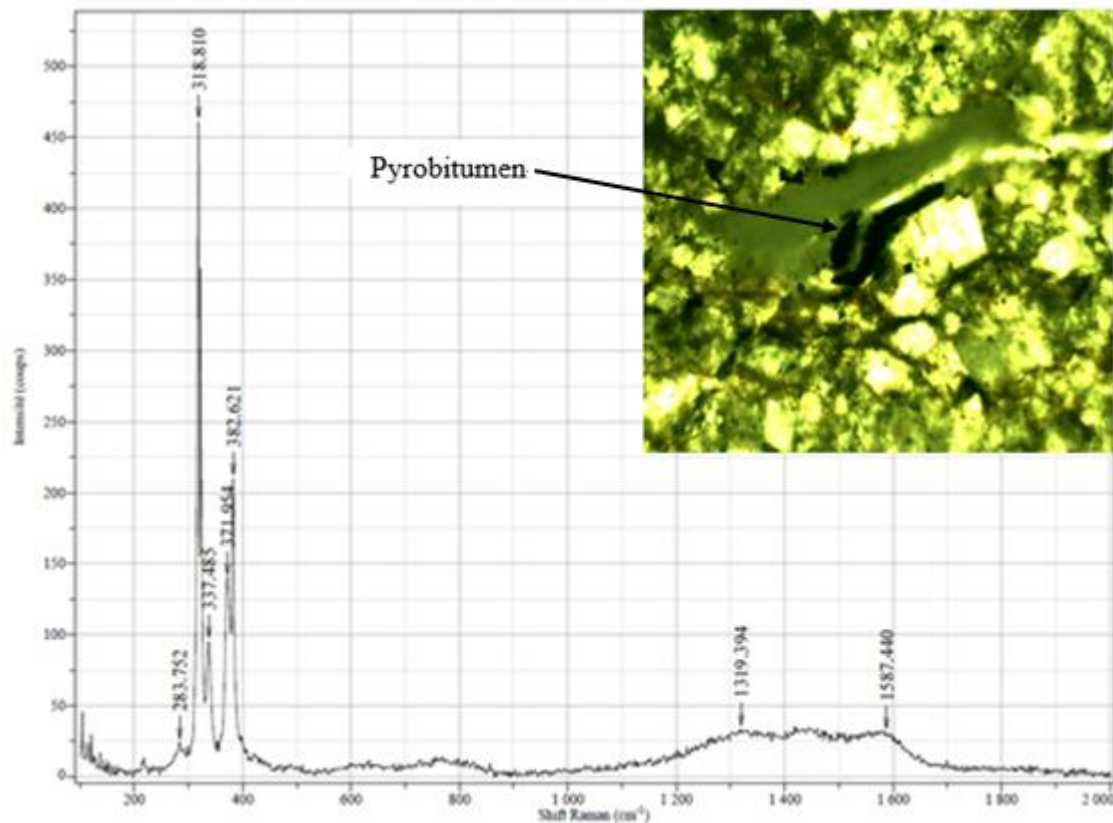


Figure 69 : Solid pyrobitumen is in the NS-3 well at depth 2003.53 m

3.2.3 Diagenetic fluids

The fluids origin of the deep burial environment depended on the salinity ratios by standard seawater. On the one hand, fluids with salinity less than that of seawater are meteoric, marine or original basin fluids (Land and Prezbindowski, 1981). On the other hand, fluids are included more than 100,000 ppm of the dissolved solids, these fluids classified as a part of brines and their origins are related to evaporite.

The chemical compositions of diagenetic fluids are very complex. The wide differences between paleofluid compositions arise from the continuous interactions between rock-water and/or mixing between dissimilar waters. Nevertheless, the elemental proportions of the deep burial fluids include $Na > Ca > Mg$ and the ratio of Mg/Ca is a very low (Collins, 1975).

3.2.4 Location of the reservoir

The site of reservoir reflected an important relationship with the previous three factors, affected the properties of reservoir rocks. The location of basin contains of the several subfactors, included hydrologic system as a first subfactor such as characteristics of flow. The second subfactor is a tectonic system such as movement of plates, the effect of fault systems, fractures systems and the differential compaction. The location of reservoir forms the pathways of diagenesis processes in the burial environment.

For determining the effects of tectonic burial regimens, (Heydari, 1997a) has determined three basis of the hydrologic regimens, related to tectonic burial regimens are:

1. The passive margin.

2. The collision or active margin.
3. The post-tectonic regimen.

Moreover, in the passive setting there are three regimens of the hydrologic flow, determined by (Harrison and Tempel, 1993). For example, the density of fluids depends on the temperature and salinity of fluids. It controls the rate of velocity of fluids flow. The hydrologic flow regimens are:

1. Meteoric system characterizes by the high velocity, near surface and under the effect of driven gravity.
2. Compaction system includes moderate velocities in the depth greater than 1km.
3. Thermohaline system reflected the rate of velocities according to the density in the depth less than 3 km.

In the Mishrif Formation, permeability analyses are shown the anisotropic values of permeability 23-775 md (Jreou, 2013b). The study area represents the characteristics of passive margin, related to the distribution of the main depositional microfacies of the Mishrif across the Middle East region.

Based on our analyses by the SEM, Cathodoluminescence, Raman spectroscopy and Microthermometry Mishrif represents the characteristics of the compactional hydrological flow regime with impact of the brines in the different places of reservoir.

3.3 Understanding the diagenetic environment by studying the final forms of pores

3.3.1 Introduction to the evolution stages of porosity

The concept of porosity modification and evolution is very useful to understand the classification of the diagenetic environments and to determine the tectonic burial regimens. Indeed, the primary porosity evolved into post-secondary porosity. The required time to develop primary to secondary porosity is very vast. The required time contains three stages, included the eogenetic, mesogenetic and telogenetic stages (Choquette and Pray, 1970).

The eogenetic stage is the period that concerned of the deposition of initial sediments to the deposition of final sediment under the effect of surficial diagenetic processes. The eogenetic stage contains two zones. The first zone is in the vadose environment above the water table, it can be either subaerial or subaqueous. The second zone is in which point, the surface of recharged water is started. For example, the meteoric water, normal marine water and evaporated marine water.

Mineralogically, the eogenetic stage includes unstable minerals. The important diagenetic processes are dissolution, cementation, and dolomitization, produced meteoric phreatic, meteoric vadose, shallow marine, deep marine and evaporative marine environments (Moore, 2001).

The mesogenetic stage is the second period that their sediments are undergone to compaction process. The mesogenetic stage is characterized by very slow processes, which are responsible of the porosity modification. However, diagenetic processes in mesogenetic stage are taken a long time, supported the concept of porosity evolution. The diagenetic environment of the deep burial environment occurred during the mesogenetic stage.

The telogenetic stage is the third period, occurred when the rock sequences were in the mesogenetic stage and then the rock sequences exposed to uplift to the surface because of the unconformities. These rock sequences will again affect by the surficial diagenetic processes. The definition of the telogenetic term precisely means the old rocks, contained high stability of their minerals such as calcite and dolomite, undergone once again to the effect of the surficial diagenetic processes such as erosion and weathering on the old rocks. The telogenetic includes the meteoric vadose and meteoric phreatic zones as the most common diagenetic environments.

3.3.2 Primary porosity

Previous diagenetic stages of (Choquette and Pray, 1970) re-explained by (Moore, 2001). The porosity classification of Mishrif Formation follows both of them. However, most of the primary porosity completely occluded by blocky calcite cement or partially occluded by the growing of drusy calcite and dolomite crystals, resulted to reduce the volume of primary pores in the Mishrif (Figure 71). Primary porosity includes two types that are interparticle and fenestral porosity.

Interparticle pores are the pore spaces that existed between peloids grains. This porosity is developed in the peloidal grainstone microfacies but it is again undergone to occlude by the drusy and equant calcite cements. In the grainstones microfacies, mechanical compaction reflected a large impact on the interparticle pores (Figure 71).

Fenestral porosity is a pore space, developed by dewatering within the bioturbated wackestone microfacies (Figure 118). In some cases, fenestral porosity is partially filled by drusy calcite cement and it is richly found in lime packstone microfacies bearing microbial carbonate grains in the NS-1 well at depth of 2052.90 m (Figure 44).

3.3.3 Secondary porosity

Mishrif includes several forms of the secondary porosity. All secondary porosity forms of the Mishrif belong to the mesogenetic stage, indicated to deep burial environment (Figure 70, Figure 71 & Figure 72) (Moore, 1985; Sassen and Moore, 1988; Heydari and Moore, 1989 and Heydari, 1997). The secondary porosity represents the abundant types of porosity, covered all Mishrif reservoir. Most of these porosities classified as the dissolution pores, vuggy, moldic, outgassing, intercrystalline, post-stylolite and fracture porosity.

Vuggy porosity finds in the NS-1, NS-2 & NS-3 wells. Vuggy porosity is a kind of pores, formed as a result of the dissolution process, accompanied with the second oil migration. Vuggy porosity still opens without any cover by the sealed materials such as blocky calcite cement that means the open vuggy pores occurred after the huge distribution of the blocky calcite cement. Vuggy porosity is interconnected pores and it includes few centimeters in the size. For that reason, vuggy porosity supported the permeability in the Mishrif.

Moldic porosity generally occurred in the NS-5 well (Figure 71). Moldic porosity resulted because of the effect of dissolution process on the metastable fossil fragments. Moldic porosity includes characteristics such as they furnished by beautiful calcite crystals in the regular shapes (Figure 71). Dolomite crystals invaded some of moldic pores that lately

occurred. Moldic porosity is not interconnected pores and it is less enhanced permeability in the Mishrif.

Degassing/outgassing porosity also occurs after dissolution process, taken place in the different levels from stratigraphic column of the Mishrif (Figure 70 & Figure 118). This type of pores attributed to release the CO₂ gas and/or methane gas during presence of the acidic fluids. Degassing porosity reflected the activity of chemical compaction process in the Mishrif.

The intercrystalline porosity is a type of the secondary porosity that occurs due to richly distribution of the euhedral dolomite crystals. Intercrystalline porosity is interconnected in the first stage of the dolomitization process but it is semi-closed when increase the distribution of carbonate mud as a result of the continuation of dissolution process. Moreover, the small size of mud crystals leads to create the fabrics like a cobweb, infiltrated between the euhedral dolomite crystals. Usually, the intercrystalline porosity is enhanced the permeability in the Mishrif.

Post-stylolite porosity represents the post-stylolite systems, found especially within muddy facies in the NS-3, NS-2 & NS-1 wells respectively according to stylolite volume. The muddy fabrics like a cobweb shape inside the post-stylolite. The muddy fabrics increase the storage capacity of the post-stylolite systems (Figure 82, & Figure 114). These muddy fabrics act as an absorbent material to store the migrated fluids. Post-stylolite porosity represents the larger networks in size than fractures systems with some similarity in the characteristics especially the linings of the walls between stylolite systems and fractures systems (Figure 116).

Fracture porosity represents many generations of the fractures networks that found especially in the reefly facies in the NS-5 well. Especially, the secondary generations of fractures systems represent the fracture porosity in the Mishrif. Fracture porosity acted as pathways for migrated fluids and it cross-cut all cement types. Fracture porosity includes a few centimetres in size and it may be resulted by differential compaction process. Equant calcite cement and euhedral dolomite crystals fill most of the secondary fractures systems while primary fractures systems include the silicate belts on the walls lining, followed by calcite belts.

Some of the secondary porosities are completely closed by the cementation process (Figure 56), but other porosities are partially closed by the growth of calcite cement crystals (Figure 70). Som of pores are furnished by CaCO₃ that interpreted under term of the saturated fluids occurred by the dissolution process and these pore fluids are eligible to precipitate the calcite cement (Figure 71).

3.3.4 Porosity evolution is related to the paleofluids and natural sediments

Porosity evolution gets along with the fluids evolution in the reservoir, side to side with hydrocarbon maturation. Fluid inclusions analyses are given the realistic evidences of the involved fluids in the alteration of porosity forms (Figure 73). Mesogenetic stage is a very vast period of the fluids evolution, existed between the final depositions of the sediments until

the present day in the deep burial environment. The distribution patterns of the secondary porosity correspond with the microfacies distribution. Mostly, the last forms of dissolution porosity indicate to the basic tectohydrologic regime as a passive regime and the flow regime is a compactional system.

The dissolution and dolomitization processes are responsible to form the new patterns of pores (Figure 70). Mishrif wells can be divided according to the nature of sediments, determined the values of porosity into: The NS-1, NS-2 and NS-3 wells reflect the effect of diagenetic process more than the nature of their sediments. The NS-5 well depends on primarily on the nature of sediments and secondary on the fractures network. The different values of porosity can be attributed to the type of sediments in the wells. Because, the NS-5 well includes reefly carbonate facies and the mean of porosity reaches up to 13 % in this study, while other wells include muddy carbonate facies and the mean of the porosity of the NS-3 well reaches to 10%.

The high values of porosity in the NS-3 well can be attributed to the vuggy porosity and the stylolite systems. The high values of porosity in the NS-5 well can be attributed to the moldic, interparticle porosity in the corals and the secondary fractures systems.

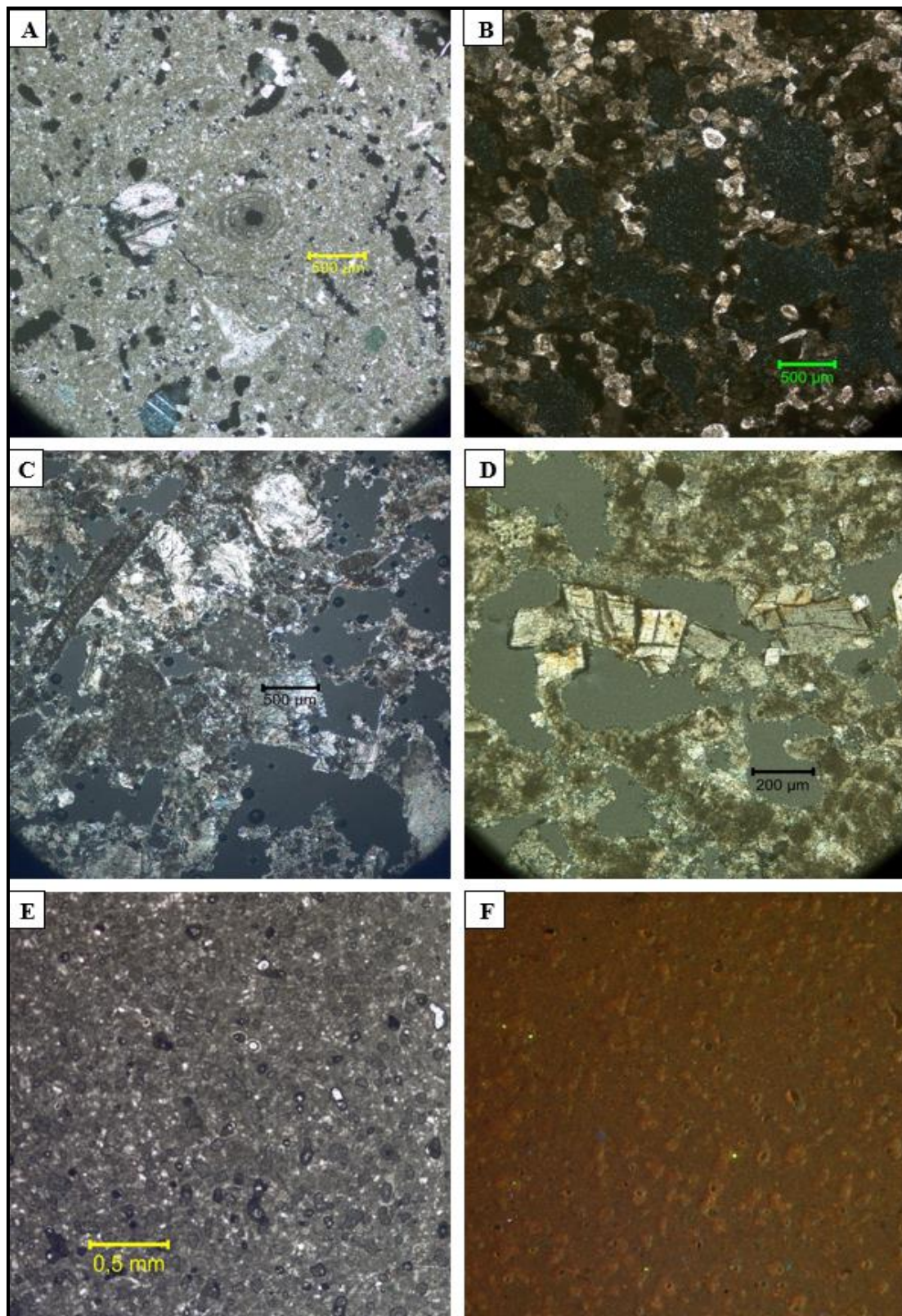


Figure 70 : The patterns of secondary porosity are used as a critical tool to determine the diagenetic environments. The dissolution pores (A, B, C & D) are dominant pores in the NS-1, NS-2 and NS-3 wells. Cathodoluminescence shows the degassing pores (E & F) in the NS-2 well at depth 2062.60 m

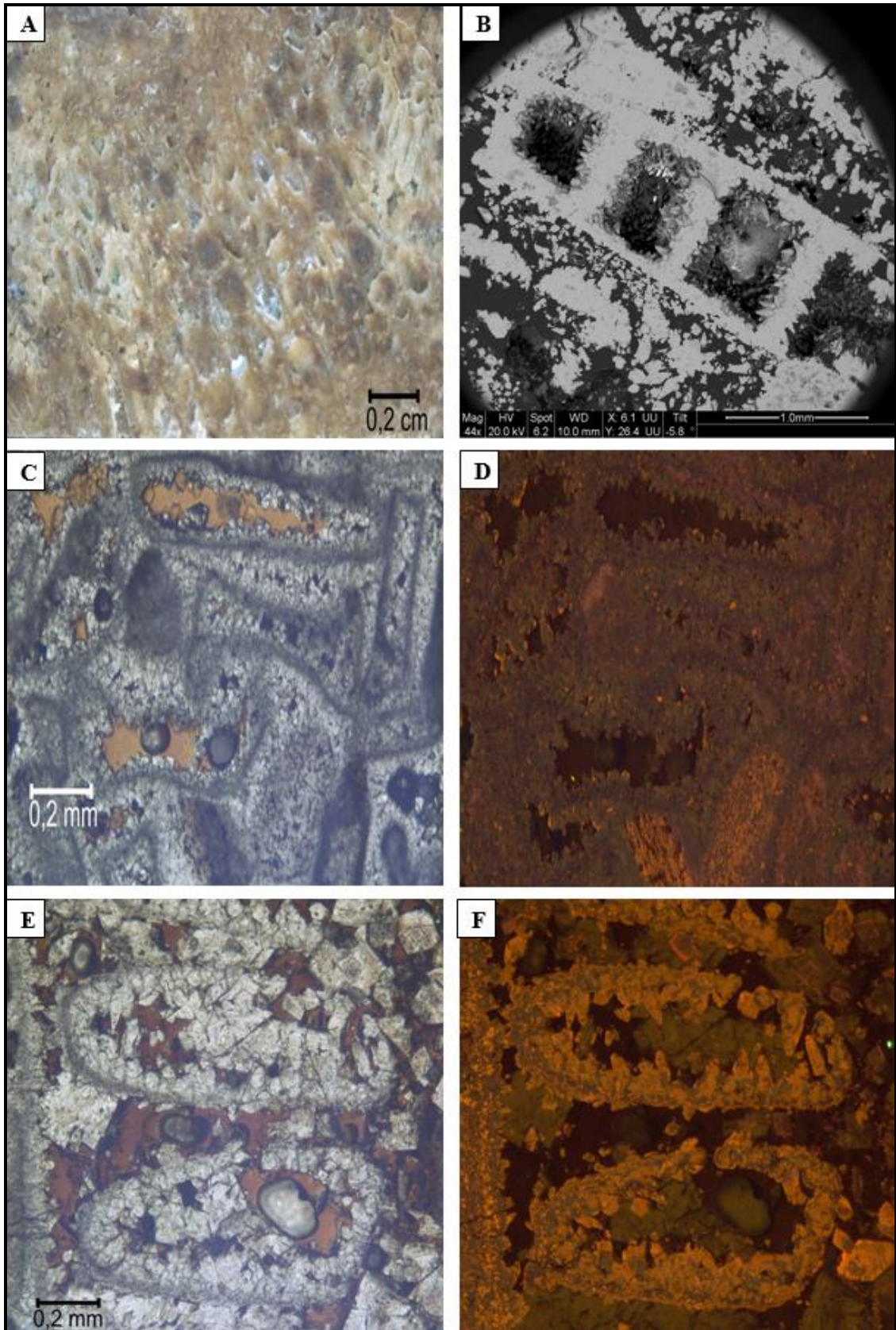


Figure 71 : Primary porosity includes two types as the fenestral porosity and interparticle porosity in (C & D). Moldic porosity evolved through diagenetic environment in the NS-5 well at depth of 2014.10 to 2031.65 m in (A, B, E & F)

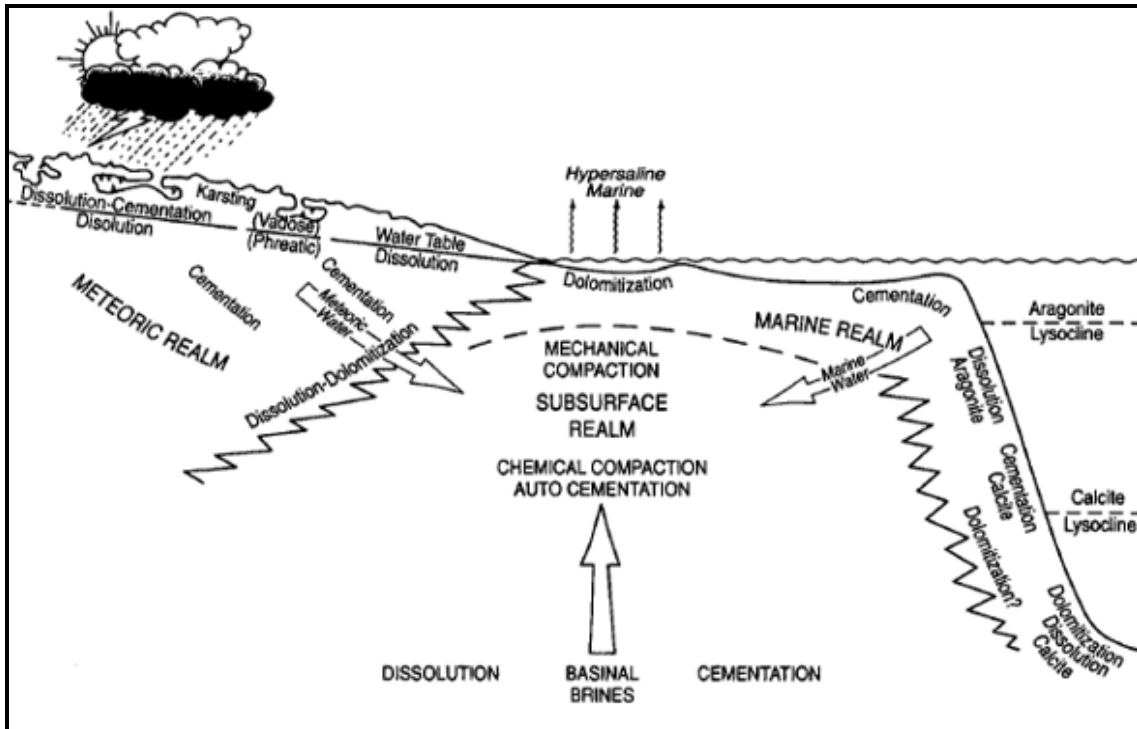


Figure 72 : The main diagenetic environments and the common diagenetic processes are drawn based on the concept of porosity modification and evolution (Moore, 1989)

Main diagenetic pores	Evolution of diagenetic fluids		
	Palaeofluids (CO ₂ dissolved in water)	migrating fluids high sulfide%	thermal degradation (hydrocarbons oil & gas)
Precipitated clastic grains 1	—————		
Rounded clastic grains	—————	-----	
Dissolution pores1	-----	—————	
Dissolution rounded pores		—————	
Furnished CaCO ₃ Moldic pores	—————	-----	
Dissolution pores after dolomitization.1		—————	
Outgassing or Degassing pores		-----	—————
Intragranular pores in the euhedral dolomite crystals (Genetic pores)	-----	—————	-----
Intergranular pores by euhedral dolomite crystals		—————	
Moldic pores fill in dolomite		-----	—————
Rounded pores have accompanied stylolite systems	—————	-----	-----
Pores have filled sulphide mineralization (pyrite & anhydrite).		-----	—————
Pores have filled by the pyrobitumen.			—————

Figure 73 : Paragenetic sequence of the porosity evolution shows the evolution of diagenetic fluids, found in the Mishrif Formation in the Nasiriyah oil field

3.4 The important methods are used for understanding the diagenesis processes

The petrographic studies and carbonate geochemistry analysis can be used together to understand the evolution stages of diagenesis processes in the deep burial environments. The diagenetic fluids are involved in the porosity modification. The petrographic studies include the compacted relationships existed between grains and cement, the relationships are between different types of cement, Distribution of paleofluid inclusions is in the host minerals. Patterns of cement distribution, the ratio of calcite to dolomite cement, the morphology of calcite crystals. The relationships are between carbonate and other exotic minerals such as the anhydrite, silicate, clay, pyrite and solid residue of pyrobitumen. All previous relationships show the paragenetic sequences and their influence on the diagenetic environment.

The geochemistry analyses of carbonate include the major, minor and trace elements analysis of the pore-filling cement, related to replace of the metastable minerals such as calcite and dolomite. On the one hand, the important study is an elemental analysis of the crystals residue, which filled the stylolite to guess the nature of transport systems. On the other hand, the results of this analysis led to reconstruct the pattern of fracture lining as well to build the paragenetic sequences of the Mishrif reservoir. Elemental analysis of the carbonate mud is also a very important to understand the type and shape of the crystals of clay minerals such as illite and smectite (swell of montmorillonite), reduced pore spaces. Finally, the temperature will be increased with the depth and it may be related to the alterations of the shape and size of these elements, led to generate new net of the porosity system (Figure 70).

Fluid inclusions analyses are important tools to estimate the formation temperature (homogeneous temperature). In addition, fluid inclusions analyses provide much information about the elemental concentration of the paleofluids. The stable isotopes analyses such as oxygen, carbon and strontium isotopes are very important studies to understand diagenetic environments. The results of the previous analyses will provide us by a better image of the diagenesis process, which affected the reservoir characteristics.

3.4.1 Petrographic studies

3.4.1.1 Morphology of the calcite crystals

The shapes of the calcite crystals are the useful tools to determine the origin of diagenetic environment. The calcite crystals include various shapes, belonged to the different environments. The shapes are related to the alterations of the elemental ratio, which resulted by the continuous interaction between fluids and rocks. In addition, the crystal shape explains growing process and precipitation process in the calcite crystals.

The concept of the sideway poisoning of the growing calcite crystals by substitute the Mg cation by Ca that is adopted by (Folk, 1974). The relation between small cation of Mg relative to Ca ion caused the lattice distortion at the end of growing calcite crystals. However, this lattice distortion led to the crystals elongation in the C-axis (Figure 74). On the one hand, the concept of Folk is represented by the performance of Ca ion, which prefers the incorporation with small cations such as (Mg, Fe and Mn). On the other hand, the Mg site in the calcite crystals is a great factor, which leads to produce the lattice distortion.

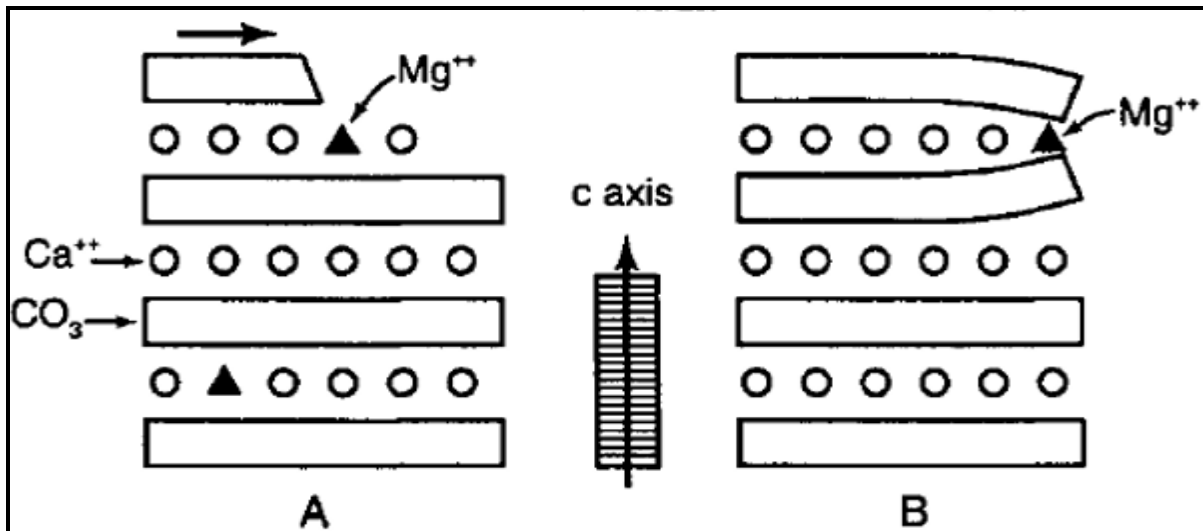


Figure 74 : scheme shows the growing calcite crystals under the theory of sideways poisoning by Mg cation (Folk, 1974)

According to concept of Folk, the high ratio of Mg/Ca leads to produce the elongated shapes of calcite crystals as marine environment, while low ratio of Mg/Ca leads to produce the equant calcite shapes as meteoric waters. Moore, 2001 has indicated to the poison effect of the Mg cation must be equally impacted with all directions of the growing surfaces in the calcite crystals this concept called (the differences in potential surface), which has early discussed from (Lahann, 1978).

Potential surface is an evolved surface from different crystal faces due to the calcite crystals determined by the group of faces, observed in the natural form of the calcite mineral. From this definition, the parallel crystal edge to the C-axis expose both Ca and CO_3 ions to the saturated fluid, while the growing normal face to the C-axis expose either Ca or CO_3 ions to the saturated fluid, but not both at the same time.

The diverse environments differentiated by the ratio of surface-active cations or surface-active ions that include the major role to create a strong positive potential surface on the C-axis face only. Because, the crystal edge is parallel of C-axis that shows both CO_3 and Ca to the saturated fluid, thus the normal faces of C-axis create a great positive potential surface from crystal edge (Moore, 2001).

The normal marine environment includes high concentrations of CO_3 at the C-axis face. The high concentrations of CO_3 lead to elongate the calcite crystals in a parallel way to the C-axis because, the normal face of C-axis will saturate with cations in normal marine environment (Moore, 2001). In this case, the face at the C-axis produces a strongly potential surface in the C-axis before the normal faces of the C-axis. For that, the calcite crystals included fibrous to bladed forms in the marine environment.

The meteoric water environment when both CO_3 and Ca concentrations are low, the difference in the potential surface between faces would be minimal (Moore, 2001). In this case, the calcite crystals produce an equant shape of the calcite cement because, the saturation of CO_3 ions and Ca cations are equilibrium or undersaturated. The calcite crystals include equant shape in the meteoric phreatic environment. Regardless, in the meteoric vadose

environment occurs the rapid degassing of CO₂, which led to elevate the saturation phase. This situation leads to elongate calcite crystals.

Although, there is a difference in the concentrations between Ca cation and CO₃ ions in the deep burial environment but, the crystal shapes include the equant calcite crystals to the complex polyhedral crystals. The concentrations of Ca cation contain of higher values than CO₃ ions, which are low availability. Thus, the ratio of CO₃ produces in the slow growth of the equant calcite crystals. The deep marine environment includes parallel case to the deep burial environment (Schlager and James, 1978 & Given and Wilkinson, 1985).

The rate of carbonate precipitation (the saturation by the carbonate ions in the environment) is the major factor that affects the calcite cement morphology. Nevertheless, the crystal shape of the calcite cement is a useful tool that indicates to the cementation history. On the one hand, in the same diagenetic environment it is possible to find different shapes of the calcite crystals, belonged to the different origins of the depositional environments. On the other hand, these crystals of calcite cement undergo to the conditions of meteoric environments or marine environments during their formation and then they have arrived to the burial environment. Perhaps, the difference between the concentrations of elements in the fluids and the rocks were responsible to continue interaction, which produced different shapes of the calcite crystals in the different times of this interaction. Mishrif Formation displays various shapes of the calcite crystals such as bladed and equant shapes to the polyhedral crystals in the same pore spaces (Figure 76 & Figure 77). Usually the endings of calcite crystals underwent to the deformation before transformation to the dolomite by the effect of paleofluids. The new dolomite grain preserves the same intragranular porosity of the calcite crystals and its deformations, which existed in the endings of calcite crystals (Figure 75).

That means the intragranular porosity in the dolomite grains is a genetic type, generated by conversion the calcite crystals to the dolomite grains. Otherwise, these deformations and intragranular porosity are slag, produced during the conversion process.

According with our observations through the petrographic study, there is a magnetic force, which is responsible on the directing the endings of the calcite crystals (the direction of C-axis) to transform these calcite crystals to the dolomite grains. This hypothesis states the Mg cation, existed in the endings of calcite crystals. Mg cation gravitates towards center of the dolomite grain. For same hypothesis, the generated data by EDS technique shows high concentration of Mg cation in the dark zone at the center of the dolomite grain in the NS-3 well at depth of 2011.66 m (Table 7).

Indeed, the deformation of the calcite crystals shows an unclear shape before conversion to the dolomite grains (Figure 75). Perhaps, these deformations are best reasons to convert the high-Mg calcite crystals to the dolomite grains, because the dolomite is a higher stability than high-Mg calcite. Generally, in the any diagenetic environment the fluids and the metastable minerals play the main role of the growth and conversion the cement crystals.

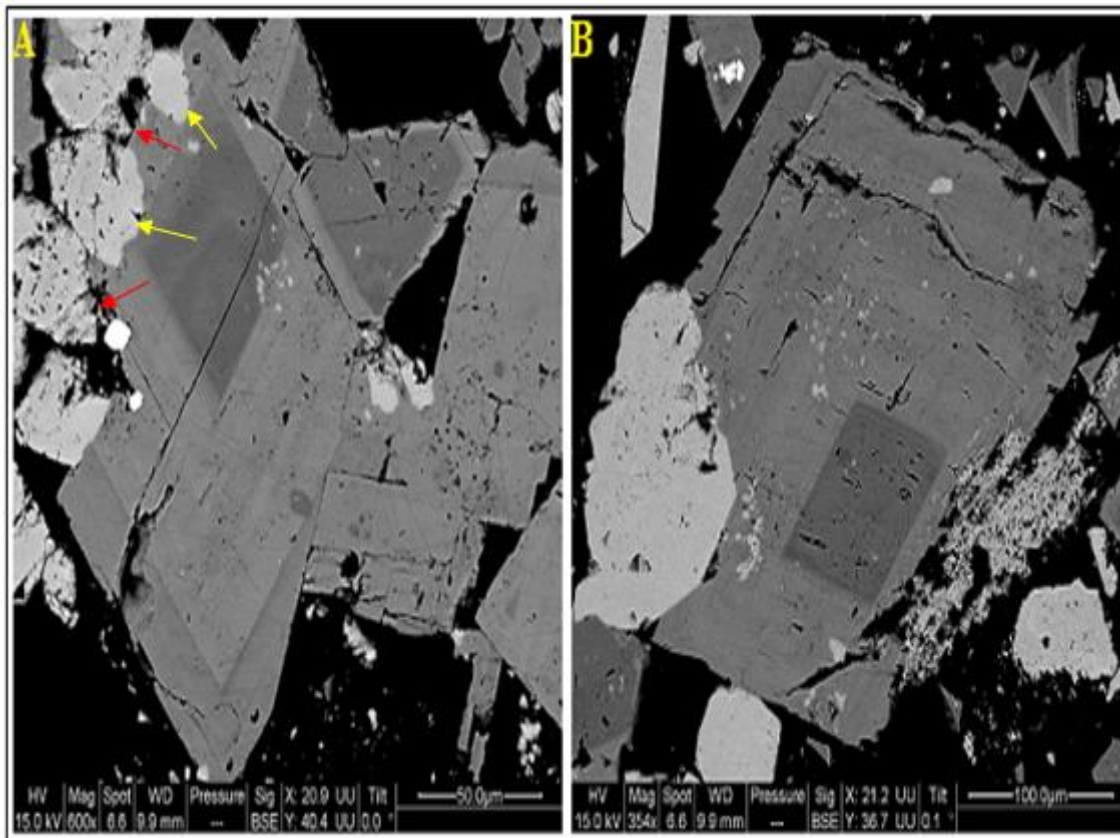


Figure 75 : SEM shows the transformation of the bladed calcite crystals to the dolomite grains. The red arrows indicate to the endings of the calcite crystals before the transformation process and the yellow arrows indicate to the endings of the calcite crystals during transformation process

Figure 77.

These different shapes of the calcite crystals lead to produce different fabrics of calcite cement particularly in the pore spaces.

A: Core No. NS-2 (sample depth 1993.10 m): Bladed crystals: They show the prismatic spar fabric or they reflect the scar shape after the microfractures have healed.

B: Core No. NS-1 (sample depth 2024.60 m): Bladed to equant crystals: They show the bladed to equant shape of calcite crystals, which are grown as the rim of cement in the intergranular pore spaces.

C: Core No. NS-2 (sample depth 1993.10 m): Equant crystals: They show the equant crystals of calcite cement, included syntaxial as an overgrowth fabric of the post-precipitated calcite, which indicates to the cementation history.

D: Core No. NS-5 (sample depth 2014.10 m): Bladed crystals: They show the bladed calcite and laminated dolomite grains. The bladed crystals show two patterns of fabric. First, they show dursy fabric on the exterior rims. Second, they also display poikilotopic spar fabric in the large crystal, included multisized crystals.

E: Core No. NS-3 (sample depth 2018.86 m): Polyhedral crystals: They reflect the syntaxial overgrowth calcite fabric.

F: Core No. NS-5 (sample depth 2051.77 m): Tubular crystals: They show microtubular shapes, displayed the beehive fabric of the calcite cement.

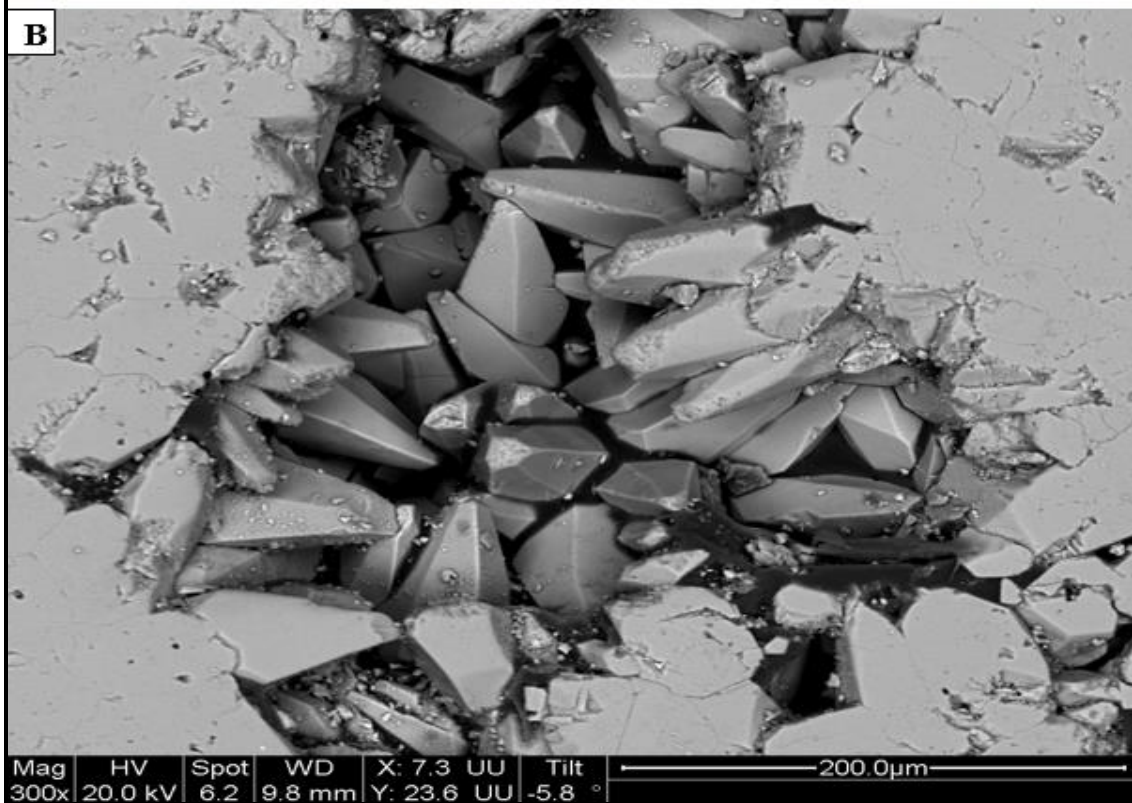


Figure 76 : (A) Bladed calcite crystals (arrows red) are like dogtooth spar, which evolved to equant calcite crystals (arrow black) in the NS-5 well at depth of 2014.10 m. (B) SEM image shows the form of the cement as the dogtooth spar, which is dominated as prismatic shapes in the most zone of Mishrif in the NS-5 well at depth of 2031.65 m

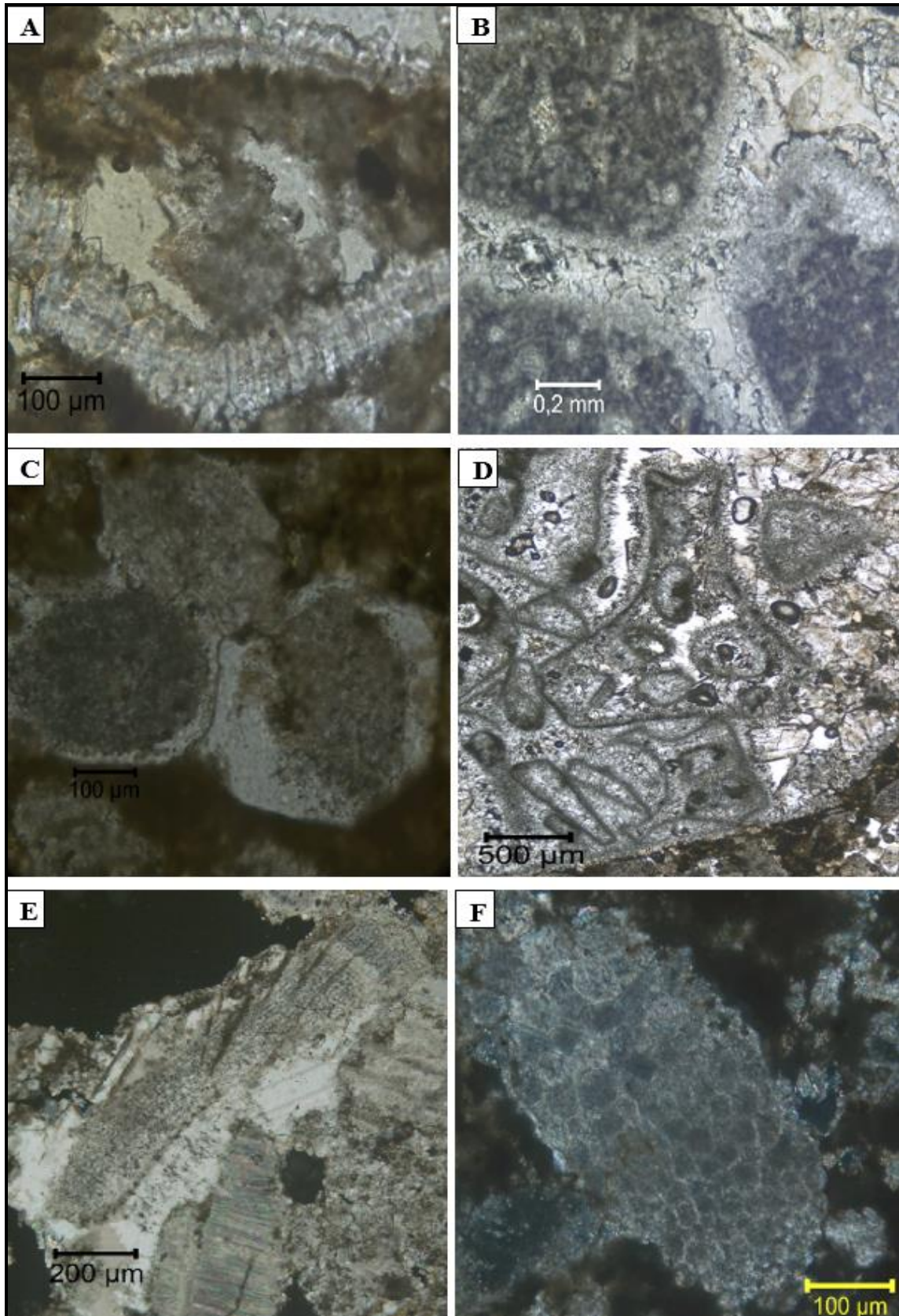


Figure 77 : PL Microscope shows the crystal shapes of the calcite cement and the final fabric of the calcite crystals

3.4.1.2 Patterns of the distributed cement in the Mishrif

Cement is the chemical sediments that precipitated from saturated solution. Cement grows in the pore spaces, which included the supersaturation degree of the pore fluids with respect to the cement type (Wolf, 1979).

The main factor in the distribution of cement patterns is a water quantity, existed in the any process of the cement precipitation. The cement exists around periphery (outer limits) of the pore spaces, thus the volume of water will give us the information on the type of the depositional paleoenvironment. As well as, the water volume reflects the volume of paleodiagenetic water, which is responsible of the heavy occurrence of diagenesis processes, produced the present diagenetic environment. Therefore, the depositional environment includes two sub-environments (vadose zone and phreatic zone) based on the volume of water.

The water table is a limit, existed between vadose zone and phreatic zone. The vadose subenvironment includes two zones, air zone and water zone, which is above the water table. The water held at the contact surfaces of the grains. For that reason, the water will show a curved surface, reflected the water curve at the time of the cement precipitation. The surface tension of water generated this curve shape of the cement, called meniscus cement (Dunham, 1971). Dolomite cement deposited as a meniscus cement (Figure 78. red curve). However, meniscus cement (red curve) is not represented the vadose subenvironment because this curve of dolomite cement formed around early round calcite grains.

In the vadose subenvironment, the water volume reflects low quantity that existed above water table. This situation will reflect new pattern of the depositional cement, represented by the droplets of cement and these droplets of cement were called microstalicitic (Longman, 1980).

The second part is a phreatic zone, which is under water table. The high quantity of water equally covered the peripheral area of the pore spaces. Cement precipitated as a circumgranular pattern and this type of cement pattern reflects the abundant quantity of water in the phreatic subenvironment during the time of depositional environment (Figure 78. red arrow).

The general characteristics of the burial cement are different from the surfacial counterparts. The burial cement is coarse, commonly poikilotopic and dully luminescent (Moore, 1985; Choquette and James, 1990 and Heydari and Moore, 1993). The existence of the fluid inclusions is not essential criterion perhaps these cement exposed to the potential re-equilibration (Moore and Druckman, 1981; Heydari and Moore, 1993 and Eichenseer et al., 1999).

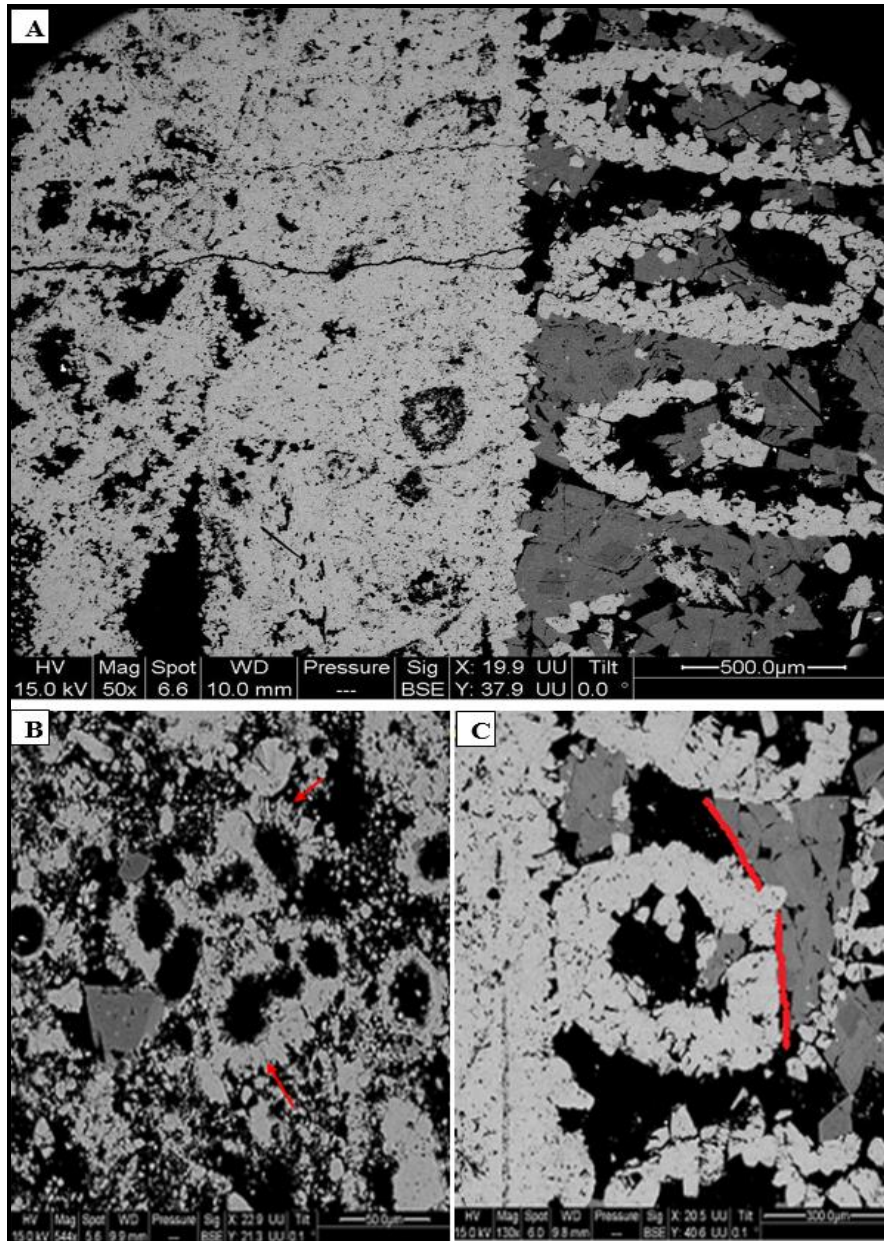


Figure 78 : SEM shows the coral spots, included the different types of distribution patterns of the calcite and dolomite cements in Mishrif in the NS-5 well at depth of 2014.10 m

The important factors that reduced the function of cement patterns are : First, the pressure (compaction process) particularly with increase of the burial column. Second, the unsaturated fluids are an important factor (dissolution process). However, the patterns of distributed cement in the Mishrif Formation in the Nasiriyah oil filed reflect a circumgranular pattern, indicated to phreatic subenvironment. Previous patterns of the distributed cement explicate under the effect of the natural phenomenon of the sea level fluctuation.

The burial cement includes commonly either calcite or dolomite with some low ratio of exotic minerals such as clay minerals, silicate minerals, sulphide minerals, hematite mineral and bitumen as an amorphous minerals etc. Other characteristics are clearly determined by the existence of the pressure solution and stylolite systems, reflected the transport and supply systems of the CaCO_3 along stylolite.

3.4.1.2.1 Calcite cement

The diagenetic record of the calcite cement in the Mishrif Formation shows several types of the calcite cement, grown through the interaction between fluids and rocks that are:

- 1) The calcite cement covered the events of diagenetic record, included early to late porosity (Figure 55).
- 2) The late stage of the calcite cement is represented by the growing recovery rates of the first stage (Figure 78).
- 3) Postdated stage of the calcite cement is represented by huge amount of the calcite cement along both sides of the stylolite systems.
- 4) Final stage of the life of calcite cement is represented by the partially transform of the calcite cement to dolomite cement especially in the lower part of the Mishrif Formation (Figure 79).

The effect of pore fluids is clearly determined by the different types of the cement texture, precipitated according to change in the composition of the pore fluids at that time. According to the results of Cathodoluminescence and transmitted light petrography, several types of calcite cement are identified and approximately, the important textures of the calcite cement are determined in the Mishrif Formation. Although, there are some problems of the overlapping events, interpreted under the concept of the geochemistry analyses.

- **Isopachous calcite cement**

The isopachous calcite cement includes many indicators, which indicated to the origin of texture type, precipitated in a phreatic marine environment (Folk, 1974; Lahann, 1978 & Steinhauff, 1989). This texture of calcite cement clearly determined in the many samples and the luminescent crystals range in size up to 25 μm . Under Cathodoluminescence, the crystals display a bright yellow to brown colour in the some cases; the crystals show a bright yellow to dark green colour that reflect the isopachous cement, which covered by the tectonic silicate. This cement is present in the packstone microfacies to grainstone microfacies. This type of cement forms in the rims of cement in the intragranular pores of the corals and around oncoids grains (Figure 71).

- **Drusy calcite cement**

Drusy cement linked with isopachous cement in the some linings of intergranular pores, this relation maybe reflected the common origin of the depositional environment. This type of cement is characterized by low degree of the luminescence than isopachous cement under cothodoluminescence. It contains of the large crystals compared with the isopachous cement. It is predominant in the intergranular pores especially between corals grains (Figure 76). Drusy cement shows in some cases the poikilotopic spar fabric, which indicated to a burial environment (Figure 77).

- **Equant calcite cement**

Equant cement represents the late stage to post-late stage of cementation. This type of cement is a signal to the advance stages of diagenetic processes in the burial environment. The equant cement in the meteoric environment is formed by the different causes. The crystals of equant cement include sizes, reached up to 500 µm and they have moderate abundance in the Mishrif Formation. Equant cement displays crystals zonation with yellow colour to bright brown colour under cathodoluminescence. Equant cement includes high rate of the recurrence because it occurred before and during emplacement oil and it appears on the both sides of the post-stylolite (Figure 77 & Figure 79).

- **Blocky calcite cement**

Blocky calcite cement represented the last stages of calcite cementation after the huge amounts of migrated oils, emplaced in the Mishrif Formation. It has range in size, reached up to 4 mm (Figure 56). This large size of the blocky cement reflected the volume of pores at that time comparing with the volume of present pores. On the one hand, the huge amounts of migrated oils were emplacement before this stage of cementation. On the other hand, the high abundance of petroleum fluid inclusions existed in the blocky calcite cement. In addition, we could say, this type of cement occurred after first migration of petroleum. The euhedral crystals of blocky calcite cement include yellow colour to the pale orange colour under cathodoluminescence. Blocky calcite cement includes two sub-stages depend on the relationship between blocky calcite and distribution of the syndolomite mineral. First sub-stage occurred before distribution the syndolomite euhedral crystals. Second sub-stage indicated to simultaneous occurrence of the blocky cement with distribution of syndolomite (Figure 56). The huge amount of blocky calcite cement is shown in the distribution of the vien calcite too. The fractures lining reflected huge amount of blocky calcite cement. This type of cement indicates to the youth period of the Mishrif Formation.

3.4.1.2.2 Dolomite cement

Dolomite classifies to three major groups based on the ratio of stoichiometry or non-stoichiometry of dolomite, related to brines and texture (Lumsden and Chimahusky, 1980). Dolomite of the Mishrif Formation includes two types depend on the time of their occurrence. First type is an early dolomite, which included dark green colour and dark red colour under the cathodoluminescence without any luminescent rims and it is very less occurrence in the Mishrif Formation. Second type is late dolomite to post-dolomite and it includes subhedral to euhedral shapes with luminescent rims. It is an authigenic grains because the dolomite grains precipitated after the pyrite minerals, which maintained the iron concentrations at low levels (Burns and Baker, 1987). The second type of the dolomite in the Mishrif Formation is classified under concept of (Sibley, 1982 & Sibley and Gregg, 1987) (Figure 80), into :

- 1) Fine size of dolomite crystals.
- 2) Medium size of dolomite crystals.
- 3) Saddle dolomite.

The second type of the dolomite cement represents the late stage of the Mishrif Formation in the diagenetic life. It started during the second substage of the blocky calcite cement. The existence of syndolomite in the stratigraphic units will modify the ratio of the porosity after it reduced by the effect of blocky calcite cement.

Mishrif considers in the youth period under concept of the metallic maturity of the diagenetic life, based on the volumes of the dolomite crystals, and also according with the type of fabric-destructive pore. This opinion gives us the ideas about the evolution steps and exploration in the future in the Mishrif. Dolomite cement includes many problems will explain in the geochemical analyses. The types of the dolomite cement in the Mishrif determined from the oldest to the youngest event.

The dolomite crystals disappear in the zone of pellets and peloidal limestone. Because, these zones include early cementation, occurred rapidly and these zones became like aggregate grains. The early cement worked as a barrier to preserve carbonate pellets and peloids grains in the limestone.

- **Fine size of dolomite crystals**

Fine size of dolomite crystals distributed and it dominated in the second unit of the high-saturated water at the limit between Mishrif Formation and Rumaila Formation (Figure 80). Usually, the crystals size of dolomite ranges from 50-100 μm . Under cathodoluminescence, the crystals exhibited the flat shapes, regular form (euhedral) crystals, multi-zonation form and they often have dark red colour in the center of the crystal with bright red colour in the rims. In general, the cathodoluminescence reflected the cloudy brown colour because the effect of the dull yellow colour of the crystals calcite cement. The destructive fabric is clear by the laminated forms without any residue of the fossils. The volume of the Fine crystals of the dolomite cement includes the 50% from the total dolomite cement in the Mishrif Formation. This type of dolomite cement occurred during the first stage of the stylolite systems due to these crystals of dolomite are evident by their existence on the both sides of the stylolite, synchronized with Blocky calcite cement and some of the pyrite crystals.

- **Medium size of the dolomite crystals**

Medium size of the dolomite crystals is an important stage of the dolomite cement in the Mishrif Formation. There is a link between distribution of the Medium size crystals of the dolomite cement and the evolution stages of the stylolite systems in the second stratigraphic unit of the high-saturated oil in the Mishrif Formation. It is worth pointing out here, the link between stylolite systems and Medium size of dolomite crystals is a mud-supported fabric, because they prefer mud facies to replace and distribute easily.

This type of dolomite cement is present in the late-stylolite systems to the post-stylolite systems with remains of the some shells. That means, some of the fabric-selective pores still exist that led us to say the Medium size of the dolomite crystals is a second stage of the dolomite cement (Figure 81). This stage includes the volume approximately reaches to the more than 40% from total dolomite cement in the Mishrif Formation. This type of the

dolomite cement includes many differences in the crystals forms and also in their colours with respect to the important difference in the number of their zones.

Basically, this type of dolomite cement displays reddish gray colour because it has zonation with different colours. The differences of colour under cathodoluminescence indicated to the different ratios of the trace elements (Boggs and Krinsley, 2006). This issue will discuss in the part of the geochemistry analysis. The mean of the crystals size reaches to more than 200 μm in the coarse cement texture, reflected the increase of the intergranular porosity. Thus, the Medium size of dolomite crystals will enhance the total porosity in the Mishrif Formation.

- **Saddle dolomite**

Saddle dolomite is characterized by the low ratio in the Mishrif Formation that reaches to 10% in the best situations. This type of dolomite cement found in the some large pores (Figure 79), also in the late stylolite and in late fracture with a low rate of their existence. Under cathodoluminescence, saddle dolomite shows the zonation, reflected the dull green colour in the cores and the bright yellow colour in the rims.

Mishrif Formation includes the large size of the curved crystals by overlapping and growing crystals of the Medium size of the dolomite cement. The natural size of the saddle dolomite is ranging from 1 mm to more than 2 mm that found in the Mishrif Formation (Figure 75). Curved crystals are clearly seemed in the late fracture (second stage), included the high distribution of Medium size of the dolomite crystals, which led to form the fracture-lining dolomite with some crystals of the saddle dolomite (Figure 78).

The second stage of the fractures systems occurred after the first process of petroleum migration that means after the blocky calcite cement occluded the pores. This interpretation leads us to say the saddle dolomite with fracture-lining dolomite reflect the roughly concurrent occurrence and this event will be widely explained in the Fluid inclusion analysis as a part of the geochemistry analyses. It is worth pointing here, the first stage of the fractures systems does not show any type of dolomite cement and especially, the fracture-lining dolomite. It could be said that the stylolite systems appearance launched the dolomite cement to form and transport in the mud-supported fabrics.

Dolomite occurred as a fracture-lining, maybe as a result to the degassing processes, released huge amounts of the CO_2 gas, which formed the fracture-lining dolomite. Degassing fracture occurred in the grainstone microfacies bearing patches of the corals and this fracture included the zigzag edges. Under cathodoluminescence, the fracture-lining dolomite reflects dark green colour without any zonation.

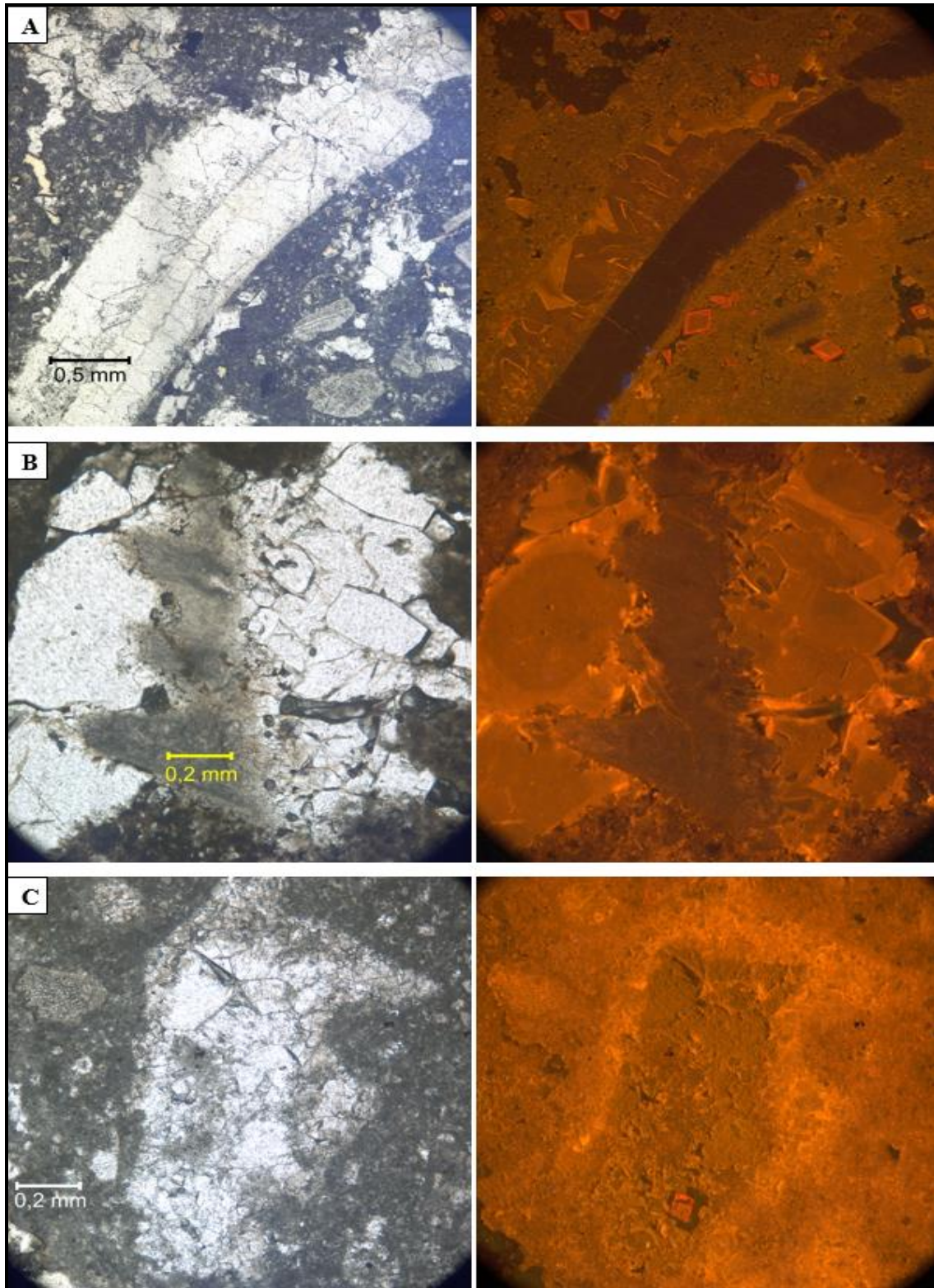


Figure 79 : Cathodoluminescence shows syntaxial overgrowth fabrics in the old pore spaces in the Mishrif Formation that may be reflected the nucleation patterns. (A) Phylloid algae grew as a calcite cement in the NS-1 well at depth of 2027.42 m. (B) Residue of the rudist calcite cement in the NS-5 well at depth of 2051.77 m. (C) Luminescent dolomite zone exists in the NS-2 well at depth of 2005.55 m

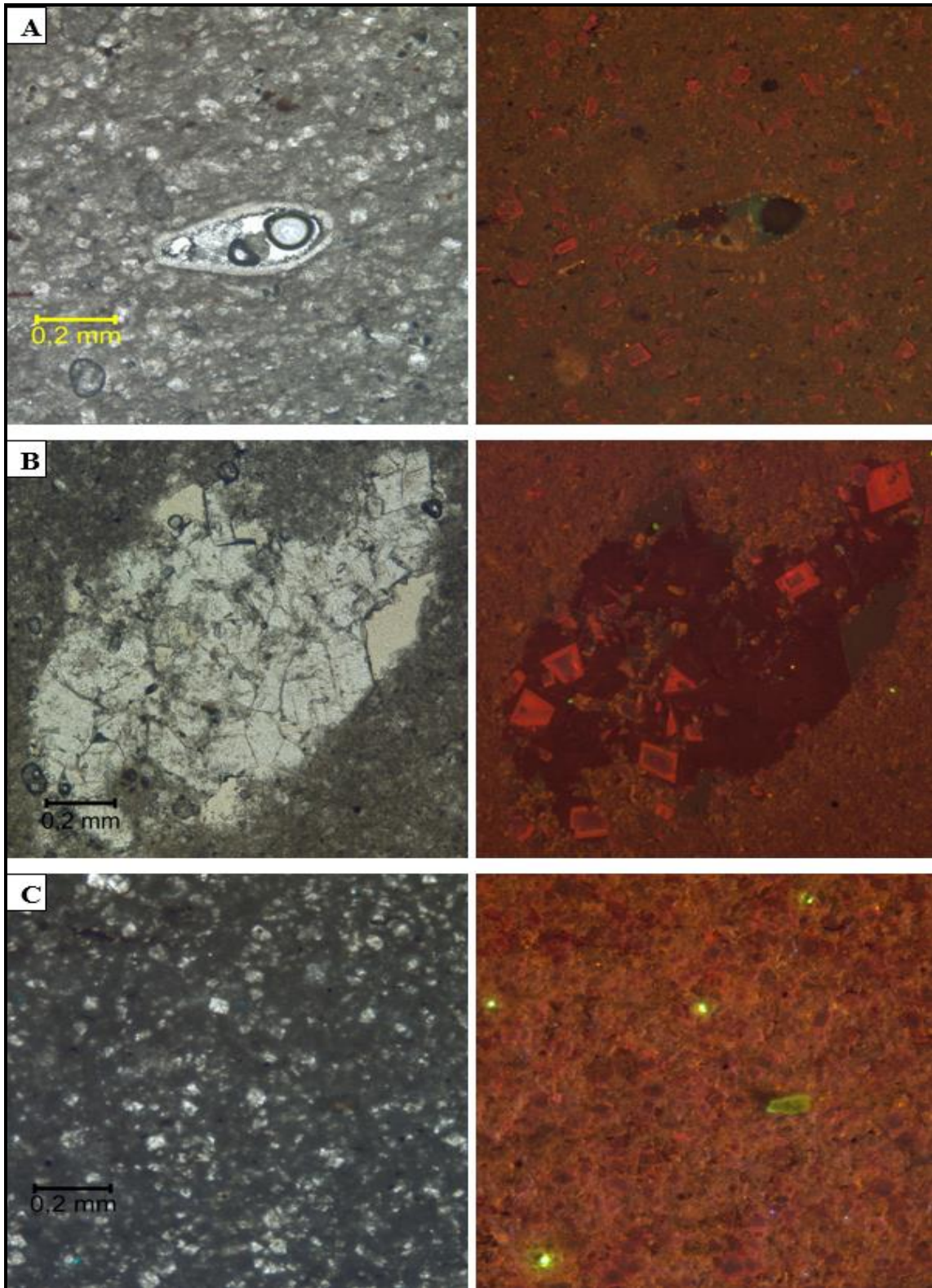


Figure 80 : Cathodoluminescence shows dolomite sediments, which increased with the depth in the NS-2, NS-3 and NS-5 wells at depths of 2062.60, 2070.21 & 2075.19 m respectively

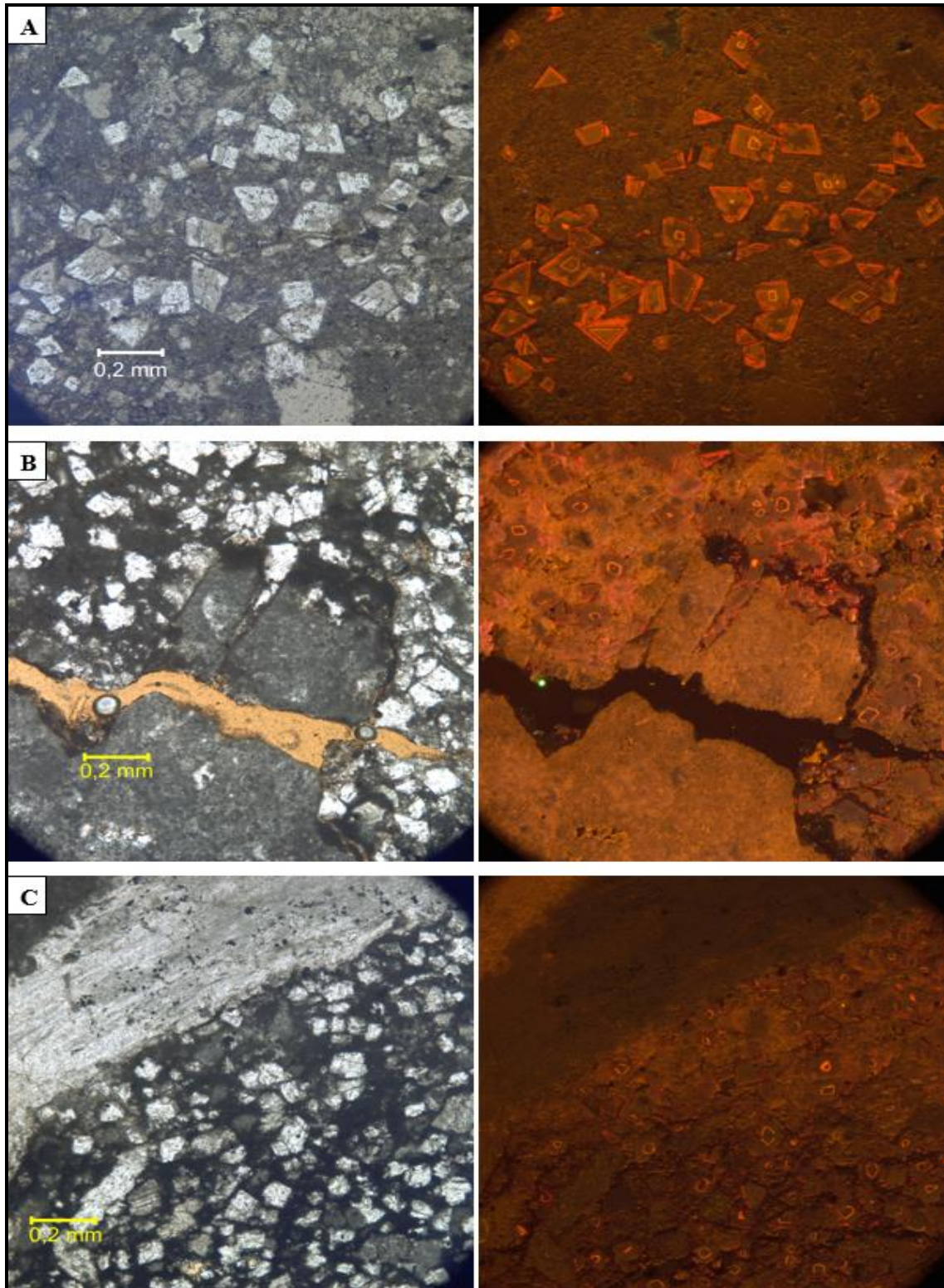


Figure 81 : Cathodoluminescence shows the Medium size of dolomite crystals, which synchronized with forming of stylolite systems in the NS-1 & NS-2 wells at depths of 2027.42 & 2014.66 m respectively of the Mishrif Formation at Nasiriyah oil field

3.4.1.2.3 Exotic minerals in the calcite cement

- **Clay minerals**

Micrite represented the potential source of the different types of the Mg element (Volery et al., 2011). The clay minerals include multi-impacts on the maturation of the source rocks and the evolution of the reservoir rocks. As well as, these multi-impacts controlled on the diagenetic processes (Jiang, 2012). Conversion process of the clay minerals by burial diagenetic burial could be a source of magnesium and dolomitization (McHargue and Price, 1982 & Sternbach and Friedman, 1984).

For previous reasons, the clay minerals could be used as a key to decipher the accompanying problems with the historical events of the geological record. The dissolution of clay minerals in the clays leads to produce new forms of the micropores. The coated grains by chlorite prevented the occurrence of quartz cementation.

The generated data by EDS analysis reflected the path of clay minerals during the life of the stylolite. The ghostly texture is the predominant texture in the fabrics of clays in the Mishrif (Figure 82). The clays precipitated in the beginning of the first deposition and during the last compaction process such as they formed from carbonate mud.

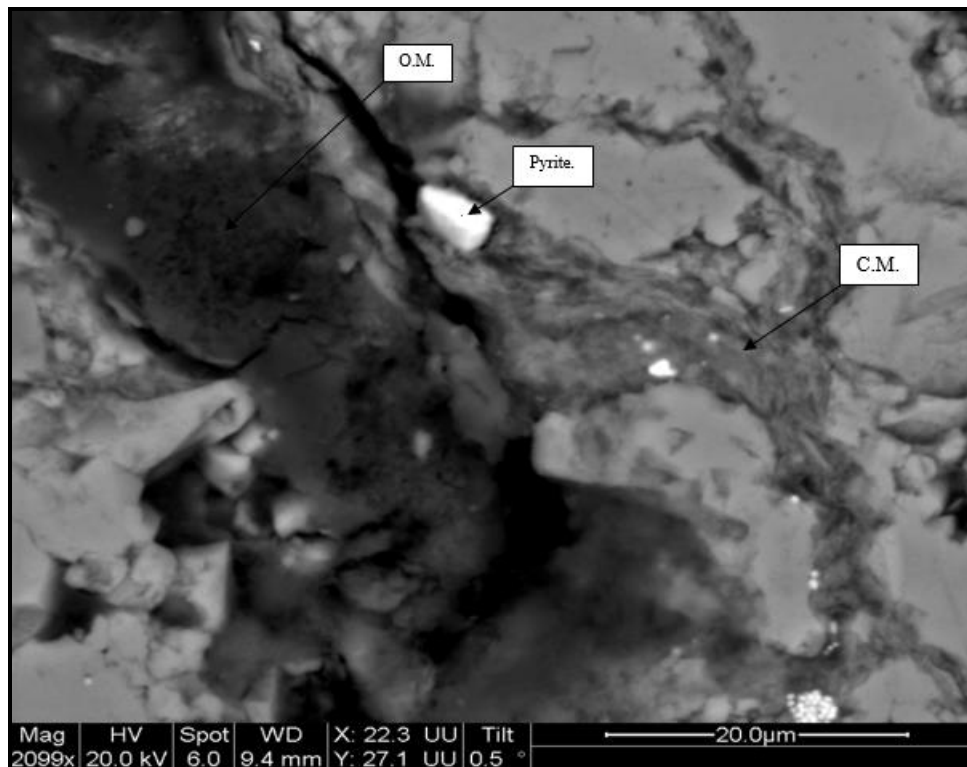


Figure 82 : Concurrent clay minerals evolved during the final product of the diagenesis processes. Clay minerals are engulfed in calcite cement that formed wispy fabrics in the ghostly texture (O.M means organic materials, C.M means clay minerals). This photo is taken under SEM and the sample belongs to the NS-3 well at depth of 1992.70 m

Clay minerals include important place in the Mishrif reservoir rocks, because they have transported in the pores, stylolite systems and fractures systems. In the other words, the evolution of reservoir rocks maybe was linked with the maturation of the clay minerals.

The clay minerals in the Mishrif Formation are concurrent with formation of pyrite and the residue of the organic materials. Clay minerals also cut all the textures of the calcite cement on both sides of stylolite and they are synchronous with final dolomitization process.

- **Silicate minerals**

Phyllosilicate cement was not affected by supplies of CaCO_3 as a major product by the late diagenetic cement (Kreutzberger and Peacor, 1988). Mishrif Formation includes different phases of the silicate minerals. First phase was represented by the distribution of the silicate minerals as a cover for the fossil structures. Second phase covered the both sides of the stylolites in the carbonate muds. Third phase was represented by the first stage of fractures systems as a fracture lining.

The distribution of the silicate minerals reflected the behavior of the silicification process, which has taken place during the first stage of the Mishrif Formation. Cathodoluminescence and Raman spectroscopy indicated to the early occurrence of the silicate minerals as a replacement of early calcite cementation (Figure 83). The silicate minerals include gray to dark green colour under Cathodoluminescence (Figure 81). The distribution of the sulfide minerals is clearly shown on the silicate cement (Figure 83).

The passive impact of distribution of the silicate minerals reduces the intragranular porosity. Quartz reflects the ductile feature with compaction process for that, it will protect the fracture walls when it represented as a fracture lining. Coarse grains of the quartz ranging from 200-500 μm have arranged as a vein, occurred before the first stage of the fractures systems. Therefore, silicate minerals reflected very early events in the first stage of the diagenetic record of the Mishrif Formation.

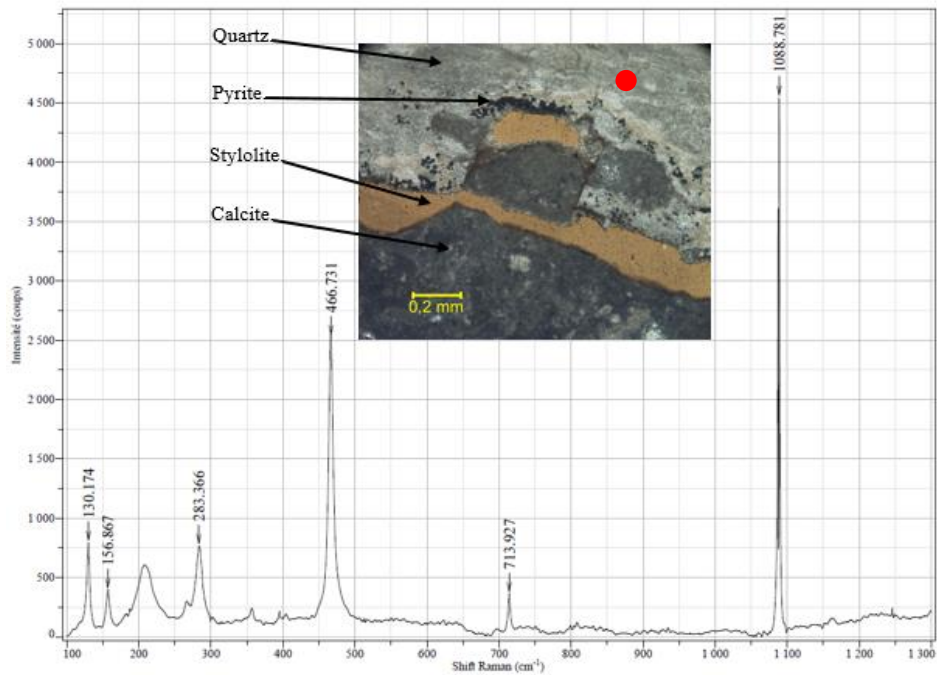


Figure 83 : Silicification process took place in the late stages of the diagenesis process in the NS-2 well at depth of 2014.66 m. Red point is a point of analysis.

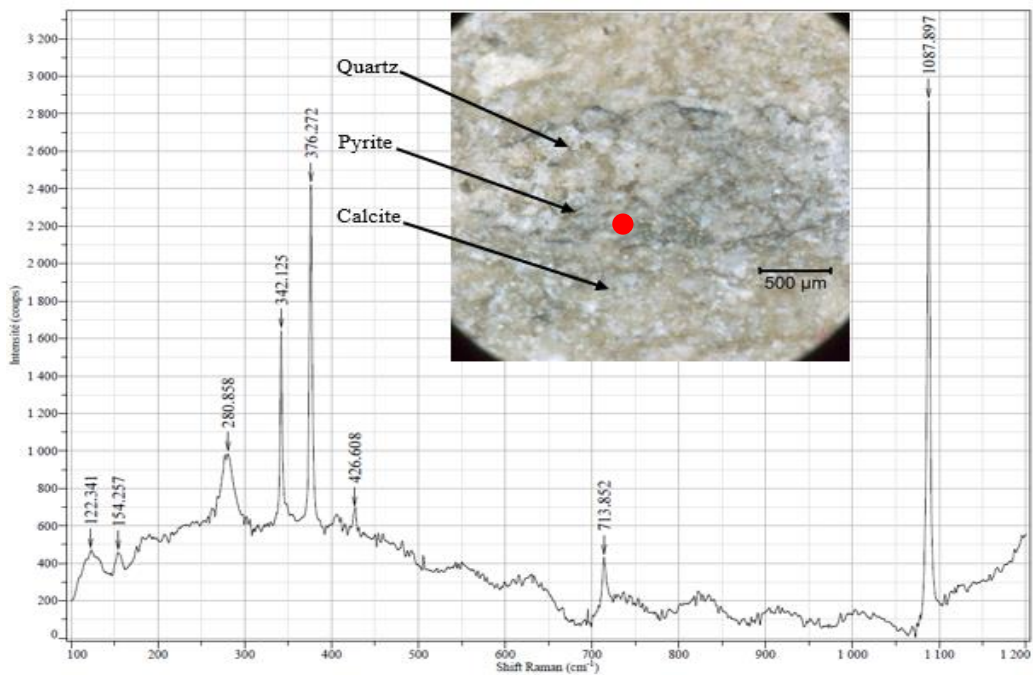


Figure 84 : First stage of pyrite covered the structure of foraminifer in the advanced stages of diagenesis process in the NS-1 well at depth of 2048.95 m. Red point is a point of analysis.

- **Evaporite minerals**

Early diagenetic reactions played important role in the zone of sulfate reduction, precluded the incorporation of Fe²⁺ in dolomite. For that reason, dolomite includes the luminescent rims (Berner, 1984; Raiswell and Berner, 1985; Burns and Baker, 1987 and Lyons and Berner, 1992).

The distribution of pyrite reflected the late stage of diagenetic processes in Mishrif. Pyrite is represented by product, occurred between sedimentary Iron and H₂S, which is supplied by sulfate-reducing microorganisms. Generally, this reaction also reflected the anoxic conditions of the organic degradation during subsurface environment (Strauss and Beukes, 1996).

The distribution of pyrite includes two stages in the Mishrif Formation. First stage represents the golden micro-grains of the pyrite, which covered all the fossil structures (Figure 42). Second stage reflects the subhedral to euhedral crystals, distributed along stylolite systems and around the final forms of the pores (Figure 83). The second stage of the black pyrite reflected the final points on the path of the reservoir evolution (Figure 85).

Evaporite minerals include anhydrite as a secondary mineral in the Mishrif Formation. Perhaps, the evaporite minerals occurred by leaching process after dissolution process takes place. The distribution of the anhydrite minerals represented the mid stage of the diagenetic fluids evolution in the Mishrif Formation (Figure 73). This distribution reflected the relation between anoxic paleoenvironment and abundance of the sulfate minerals. The passive impact of the anhydrite distribution includes destruction most facies of the NS-1 and NS-2 wells at the upper part between Mishrif and Kifl formations as a degradation of Mishrif facies. On the one hand, this impact largely appeared on the secondary porosity that led to produce the vug porosity. On the other hand, at the same time when the subsurface fluids included high content of the organic materials. The deposited calcite cement reflected dark colour under transmitted light and same cement displayed vague or indistinct photos under Cathodoluminescence (Figure 45).

- **Bitumen as an amorphous mineral**

Bitumen occurred after second stage of the luminescent dolomite (Medium size of the dolomite crystals). It may be reflected the final product of thermochemical sulphate reduction process (Machel, 1987). Bitumen distributed in the Mishrif Formation as an amorphous mineral that occluded some of the intragranular pores and intergranular pores. It reflects golden colour under Brightfield (BF) light (Figure 86).

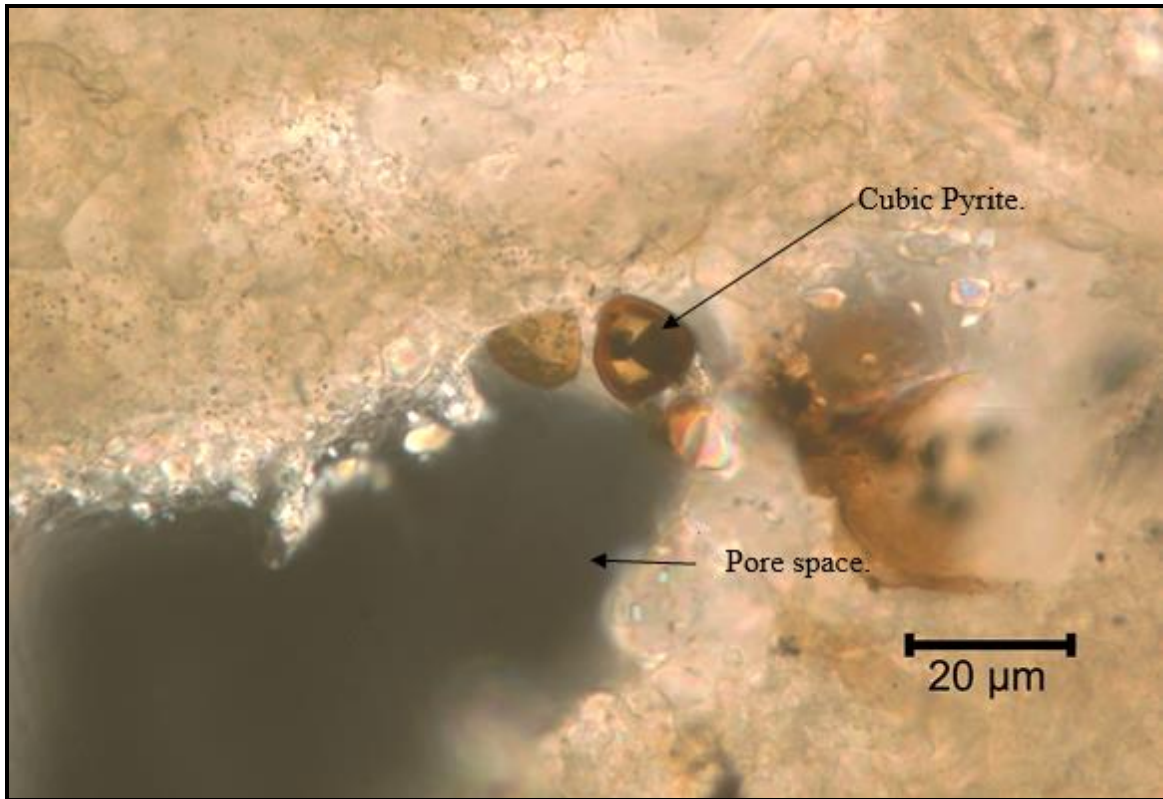


Figure 85 : Cubic pyrite reflects the final distribution around secondary porosity in the NS-3 well at depth of 2014.67 m

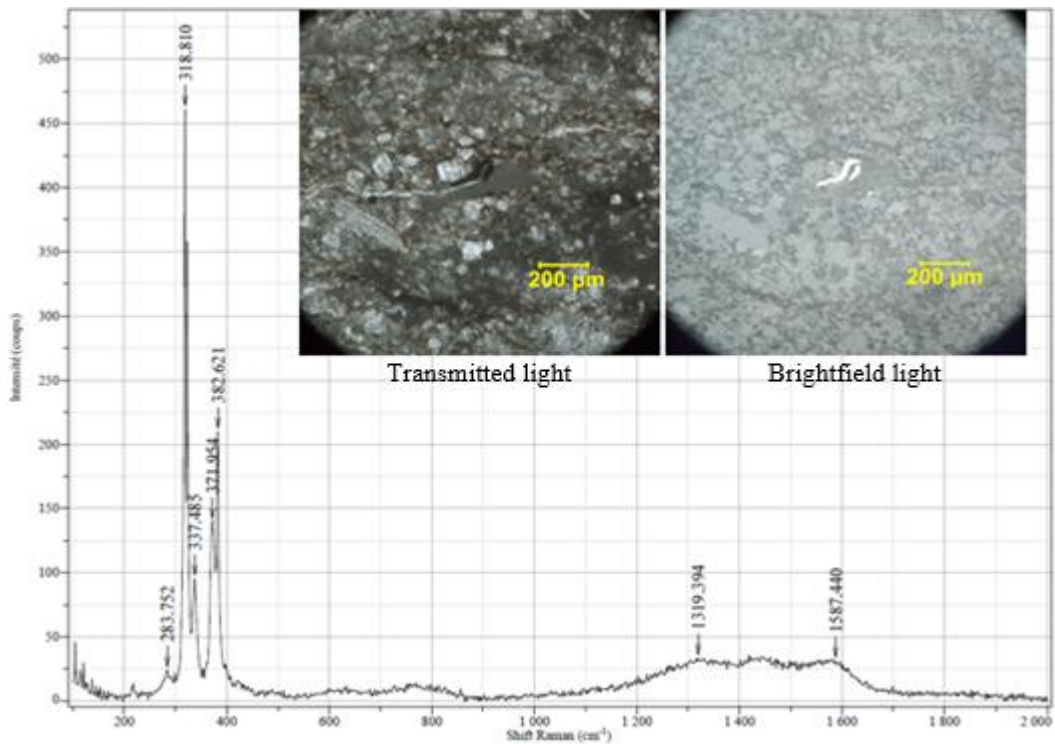


Figure 86 : Raman spectroscopy shows the integrated spectrum zone of pyrite and carbon minerals, reflected the solid bitumen according to transmitted microscope analysis of the same point in the Mishrif Formation in the Nasiriyah oil field at the NS-3 well of the depth 2003.53 m

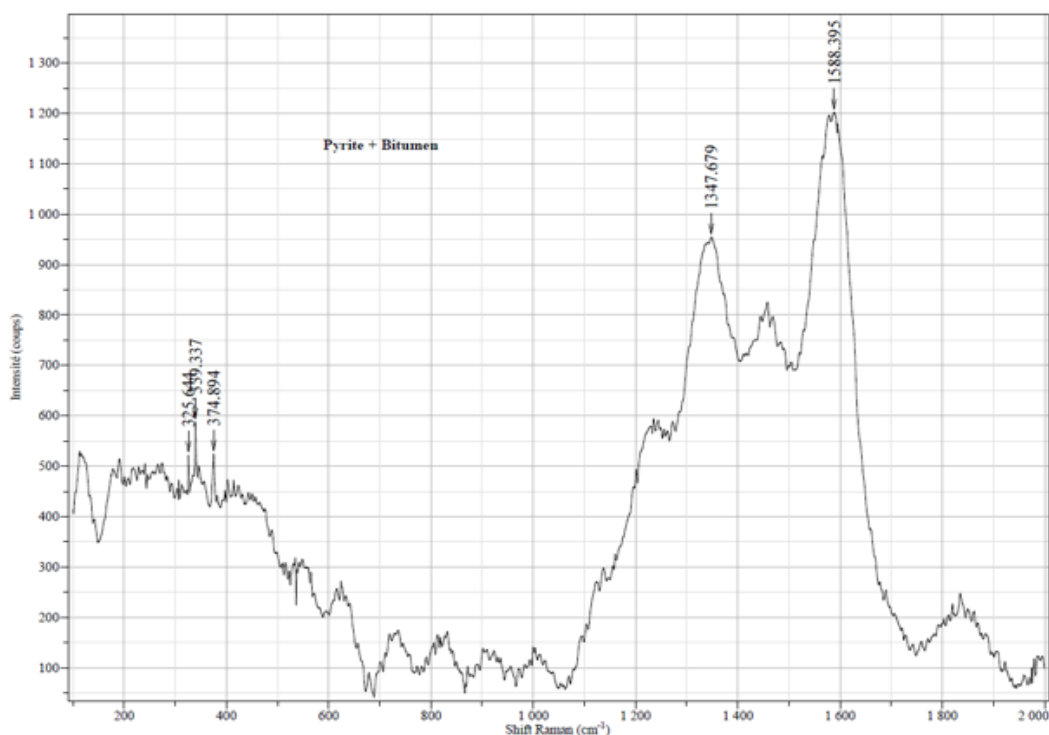


Figure 87 : Raman spectroscopy shows the integrated spectrum zone of the minor pyrite mineral and the large band of carbon mineral, reflected the bitumen in advanced stages of diagenesis process in the Mishrif Formation in the Nasiriyah oil field at the NS-1 well of depth 2033.80 m

3.4.1.3 The relationships between grains and cement are related to the compaction process

The petrographic relationships are among the grains themselves or between the grains and the cement or the relationships are between the cement to the compaction process. Petrographic relationships reflect many examples such as compacted grains, fractured grains, stylolites, fractures and pyrobitumen. All these relationships are used to detect the differences volume between early cement and late cement (Moore, 1985; Choquette and James, 1990 and Heydari, 1997a). Early cement is characterized by the highly dense-grains or interpenetrated grains without deformation of the cement and without evidences of the compaction (Coogan and Manus, 1975; Bhattacharyya and Friedman, 1984; Railsback, 1993; Goldhammer, 1997 and Moore, 2001).

Cement concurrently occurred with compaction process that is characterized by the deformation of their crystals and this cement includes some of the evidences on the compaction process. This cement is at least contemporary compaction process (Moore and Druckman, 1981 and Moore, 1985). Cement is enclosed in the both compacted grains with the early deformed cement and these new crystals of cement are not involved in compaction. This cement is a later post-compaction cement (Moore and Druckman, 1981 and Moore, 1985). Eventually, the major facts are a relative timing of the each cementation and replacement events that could clearly establish from cross cutting relationships, which are associated with fractures, stylolites and minerals replacement (Moore and Druckman, 1981).

All these relationships can be outlined by the evolution stages of the pores events, which are related to the major processes of the diagenetic environments. On the one hand, the

pore shapes show elongated shape in the Mishrif Formation at the zones, which display early cement. These pore shapes are very important indicators on the compaction process. On the other hand, this elongated shape indicates to the equilibrium situation or balance between hydrostatic pressure and lithostatic pressure (Figure 68).

Mishrif Formation includes grains and cement crystals, which are undergone to high deformation during the mechanical compaction (Figure 77). Stratigraphic column of the Mishrif appears high amounts of the carbonate mud, deformed structures and diverse fractures, which indicated to the impact of the mechanical compaction. The huge occurrence of the stylolite systems in the Mishrif is best evidence on the chemical compaction and pressure solution. However, the presence of microfracture indicates to increase the hydrostatic pressure (failure in the balance situation) to release the gases or fluids, which existed in the sediments or between grains.

Cathodoluminescence detect some of the clues, related to understand the diagenesis processes and to determine the diagenetic environment of the Mishrif Formation. Early cement protects grains from the compaction process and from the late stylolite systems. The intergranular pores include higher distribution in the early cement than late cement. The stylolite surrounds early cement zone but this zone of early cement reflects enough resistance. The stylolite transferred dolomite crystals, which undergo to the deformation because of the paleofluids passed through the transport systems (Figure 88).

In general, big shells reflect high hardness depend on the pressure in the burial column. The dolomite cement replaced early calcite cement and the coral patches reflect clear structures without deformation (Figure 88). Post-calcite cement appeared after the occurrence of the late-stylolite. The huge volume of the post-calcite cement reflects a bright golden colour under Cathodoluminescence because, the Iron element is not available in these sediments or this cement lately occurred after forming pyrite crystals. Perhaps, calcite cement locally occurs because the bio-fragments distributed in the post-cement. Perhaps, post-calcite cement concurrent occurs with Medium size of the dolomite crystals, included bright zones too (Figure 88).

Under subsurface conditions, the continuous interaction between fluids-rock results complex composition of subsurface fluids as well the mixture between chemically dissimilar water produces complex composition of subsurface water. All the previous cases will generate fluids rich in elements that enable to continue dissolution and precipitation processes. Generally, petrographic interpretations are insufficient to prove petrographic relationships. For that reason, these results must be compared with the results of geochemical analyses.

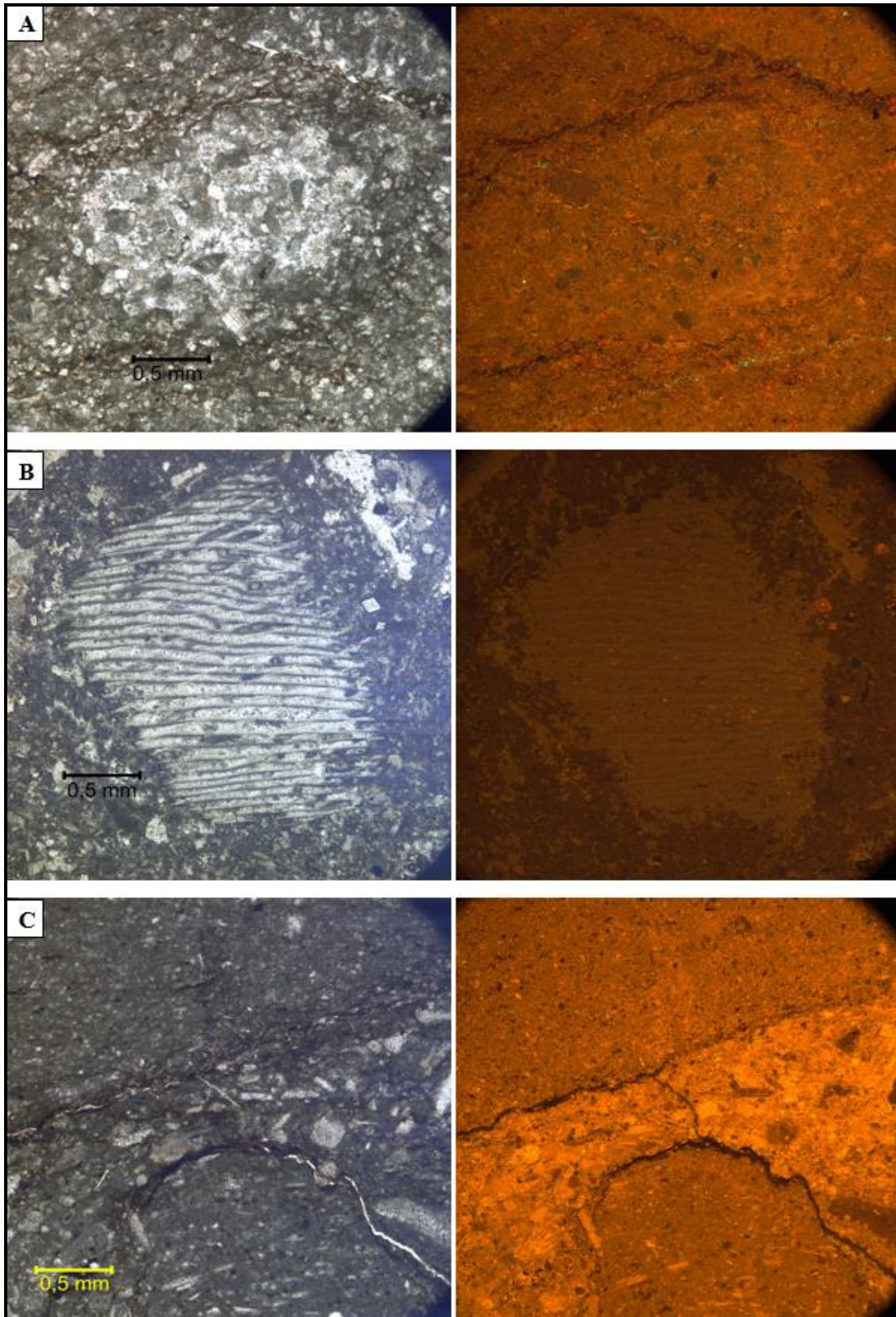


Figure 88 : Cathodoluminescence shows some of the differences between the early cement and the late cement that are related to redistribution process of elements in the Mishrif Formation in the NS-3, NS-1 and NS-3 wells at depths of 2003.53, 2027.42 and 1992.70 m respectively

3.4.2 Geochemistry analyses

3.4.2.1 Elemental analysis of the cement composition by EDS technique

Diagenetic evolution can be expressed by the alterations of the subsurface cements, precipitated from fluids, which are in the process of chemically evolving. However, the continuous rock-water interaction in the diagenetic burial environment over extremely long periods led to the diagenetic evolution. These rock-water interactions are not specifically confined to carbonates elements but commonly include basinal siliciclastics and evaporate.

Generally, when rock-water interactions have resulted mineralogically diverse rocks, which are often listed in the formation of progressively more concentrated brines, rich in metals such as Fe, Mn, Pb and Zn (Collins, 1975; Carpenter, 1978; Land and Prezbindowski, 1981 and Morse et al., 1997). Calcium, magnesium, iron, manganese, silica, aluminum, titanium, sodium, potassium and phosphorus elements have resulted from the elemental composition analysis of calcite and dolomite phases under EDS technique. Although though some of the others elements were not detected such as strontium under EDS technique. It is related to the performance of EDS technique and the amount of coefficient D. This study has aim to elicitation the relationship between stoichiometry; model of the basinal siliciclastics in carbonate reactions and explanation the paleofluid sources.

Dissolution and re-precipitation processes are responsible on the stability of carbonate phases by intervening diagenetic fluids (Bathurst, 1975). The most important process to incorporation trace elements into carbonate minerals is a substitution for Ca in the CaCO₃ structure (Veizer, 1983a). Other processes have less important in diagenetic studies such as interstitial substitution between structural planes, substitution at defect sites within the structure, adsorption by remnant ionic charges and present in non-carbonate inclusions (McIntire, 1963; Zemann, 1969 and Morse and Mackenzie, 1990). The substitution process for Ca⁺² is a major process, which is dominant on replacement trace elements, rather than interstitially between lattice planes at site defects, or as adsorbed cations, or within inclusions, this interpretation has outlined by (Moore, 2001), based on the results of (Veizer, 1983b) and (Banner, 1995).

However, the concentration of trace elements in the fluid, the water/rock ratio of the diagenetic system and the distribution of the coefficient (D) of the trace elements for a mineral-fluid system are the major factors. These factors have controlled on the incorporated process of trace elements into carbonate minerals (Tucker and Wright, 1990). The ions radii are represented the last factor, which has two options. First option, when ions with radii larger than that of Ca (>1.08 Å) are completely excluded from Mg sites. While second option, when ions with radii smaller than Mg (<0.80Å) are excluded from the Ca sites (Jacobson and Usdowski, 1976 and Kretz, 1982). However, Mn substitutes into both positions but it preferred the Mg site, especially at higher temperatures (Wildeman, 1970). For that reason, Mn element in dolomite cement has high ratio because in dolomite phase, trace elements can be incorporated into Ca and/or Mg structural positions. During fluid/rock interactions, trace elements from the carbonates have mixed with those from the fluid and then they will repartition during recrystallization, mineral precipitation and stabilization.

Energy-dispersive X-ray spectroscopy is a standard technique, which is widely used in the elemental composition analysis. EDS, EDX, or XEDS, sometimes it is called energy dispersive X-ray analysis (EDXA) or other researchers are called energy dispersive X-ray microanalysis (EDXMA). However, EDS is an analytical technique, used for decades already for the microlocal determination with high degree of the resolution to give reliable data of the chemical characterization of a sample. Generally, all SEM and TEM are attached with this technique. Therefore, the standard analyses are usually very fast and easy to get.

Typically, during EDS analysis we normally get elemental composition in both phases as an atomic percentage concentration and weight percentage concentration. Usually, the type of the presented data and their units depend on the type of research task. Definitely, one has to take into account that the information has given by the EDS technique that includes relative concentrations of total elements in the analysis point only. Total elements are quantifiable from the EDS spectrum. Nevertheless, the samples maybe have other elements, which are not detectable or quantifiable. For that reason, in the some cases we try to make up the normalized data to show the realistic data. In some cases, we have covered the samples by metallic carbon we will be going to remove the column of atoms C because this result indicates to the metallic carbon on the sample surface. Usually, the atoms that have reflected very weak light such as O₂ will be removing too.

The data have generated by EDS detector of the scanning electron microscope that have moderate to high magnifications. These data can be used to determine the different phases of cementation and dolomitization such as the luminescent cement and non-luminescent cement. Other reasons, to determine the paragenetic relationships of the minerals, which are growing in the pores systems or those minerals get along in both side of the stylolite systems or as belts of the natural fractures linings. The different types of the mineral fillings, which deposited through the transport systems in the Mishrif Formation, led us to study the multiple generations of the authigenic minerals under EDS technique (Figure 96).

During analysis of Cathodoluminescence microscope and Raman spectroscopy, some of the diagenetic phases have vaguely interpreted such as the zonation phases of dolomite crystals and some of growing phases in calcite cement. On the first place, to distinguish organic materials based on the weight percentage of the sulphur element (Figure 96). On the second place, we need to use EDS analysis to comparasion between weight ratios of the elements such as Mn/Fe ratio or Mg/Ca ratio. In addition, the elemental ternary plot shows the distribution of main carbonate elements in the calcite cement and dolomite cement (Figure 89).

Distribution of the coefficient D, is a responsible on the incorporation of trace elements by substitution process of the trace elements for Ca⁺², as noted by (Kinsman, 1969). The size of crystal plays a major role in distribution of coefficient D, where the magnitude of coefficient D for the carbonates is determined by the size of the crystal lattice (Moore, 2001). The small cations such as (Mg, Fe, and Mn) can be merged in smaller unit cell of the rhombohedral calcite, while the large cations such as (Sr, Na, Ba, and U) can receive from large unit cell of orthorhombic aragonite (Moore, 2001).

For this reason, the aragonite is responsible on distribution of coefficient Sr larger than the same coefficient in calcite. In our samples, we have not aragonite mineral and thus, we

have not found (Sr) strontium element. The incorporation of Mg and Sr into calcite is related to the Mg/Ca ratio in paleo-solution, but its distribution coefficient increases with decreasing Mg/Ca ratio (Mucci and Morse, 1983 and Zhong and Mucci, 1989).

The amount of the coefficient D can appear the deviations of the trace element/fluid ratios by determine if a trace element will be concentrated in the fluid or in the mineral phase and by any magnitude. When coefficient $D > 1$, the ratio of the trace element to Ca or (Ca + Mg) being incorporated into calcite or dolomite is greater than that of the fluid. When coefficient $D < 1$, the trace element will be partitioned preferentially into the fluid (Veizer, 1983a and Tucker and Wright, 1990).

As a rule, carbonate cements include various trace elements and minor elements, which existed in conjunction at the precipitating fluid. Cements are precipitated from the various liquids, which resulted from various diagenetic environments; these cements have different concentrations of the various trace elements and minor elements. The interpretations of the elemental composition of carbonate phases help us to reconstruction diagenetic environments and paleofluids. These chemical elements have the effects of the precipitation rate that enhance the transformation of aragonite or dolomite into calcite with help the conditions of the temperature, pressure and trace element composition.

During the dissolution–precipitation processes the changing in the Mn/Fe ratios have affected on the growth of patchy luminescence in Mg-calcitic particles. For that reason, there is an equilibrium relation between the elements, which existed in the precipitating fluid and the present elements in the precipitated cement (Figure 88). The elemental composition analysis uses to determine chemical gradients of the elements in the cement, related to paleo-fluid, which passed through this cement.

However, the information were gathered from the EDS technique, attached with scanning electron microscope have indicated to the atomic percentage and weight percentage that determined the predominant minerals. The detected elements are calcium, magnesium, iron, sulfur, manganese, silica, aluminum, potassium, sodium, phosphorus and titanium.

These elements have reflected the case of paleodiagenetic fluids, passed through the calcite cement, dolomite cement and poststylolite phases in the rocks. The paleofluids interacted with metastable minerals for example (aragonite and magnesium- calcite) in these rocks. The results of the atomic percentage in the (Table 7 and Table 8) show four phases.

3.4.2.1.1 Calcium and magnesium elements

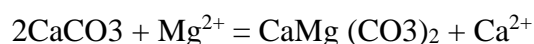
The relative values of Mg/Ca ratio include moderate values in range from 0.54 of the poststylolite to 0.65 of the calcite and dolomite phases comparing with the results of (Folk and Land, 1975), who indicated to the subsurface cement usually includes the range 0.04 to 1.8 of Mg/Ca ratio. The modern seawater value of Mg/Ca is around 5.2 molar, with high value of Mg/Ca but still the modern precipitations of seawater include aragonite because probably in large part kinetic (Warren, 2000). The Mg/Ca ratio indicates to the properties of the ancient subsurface fluids, which were responsible on the present-precipitated cement. As well as, these values of Ca and Mg concentrations are varied between ancient and recent dolomite cement. The recent dolomite cement includes high values of the Mg concentrations

comparing with ancient dolomite cement (Figure 96). The low Mg/Ca ratio of cement reflects an enrichment in calcium within the ancient dolomite (Morrow, 1990).

According to the distribution of main carbonate elements in the calcite and dolomite phases in the ternary plot (Figure 89) and depending on the degree of water-rock interaction, the typical subsurface cement shows a low range in the Mg and Ca concentrations when Si and Al concentrations have high range (Figure 90 to Figure 94). The blocky calcite cement shows high values of the Mg concentration that means the blocky calcite cement located in the zone of high Mg-calcite cement in the ternary plot (Figure 89). The values of Mg/Ca ratio of the all analyses of the Mishrif cements typically show the values lower than that of the modern seawater.

The problems of overlapping events of the Mishrif cement can be interpreted based on the results of EDS technique. Firstly, the blocky calcite cement concurrently occur with secondary dolomite (Medium size of the dolomite crystals), which reflect the high value of Mg concentration in the blocky calcite cement. Fluid inclusion analysis shows the average of the Eutectic temperature for the blocky calcite cement, which is around (-35.6°C). It indicates to high Mg concentration in the diagenetic fluids. These two types of blocky calcite cement and Medium size of the dolomite cement occur after petroleum migration with respect to the concentration of the sulfur element. Pyrite maintained on the iron concentration at low levels.

However, it is worth mentioning here that the most blocky calcite cement and Medium size of the dolomite cement existed in the zone of the sulfate-reducing bacteria at the NS-1, NS-2 and NS-3 wells. Exception the NS-5 well includes these types of cement in the degassing fracture. The dolomite equation can be resulted from dolomitization the limestone by modern seawater when the value of [Mg/Ca] is greater than 0.67 (Hsu, 1967).



The low Mg/Ca ratio produces non-stoichiometric dolomite. For that reason, paleofluids resulted from repetition of the dissolution-reprecipitation processes that are responsible on the modification of this ratio. The subject of the stoichiometry dolomite cement is very important to determine the stoichiometric phase in the dolomite cement.

Table 7 : First analysis of the elemental composition shows the atomic percentage of the elements concentration, generated by EDS technique from various samples of the calcite cements and the dolomite cements. Synopsis data are before normalization process

Samples n°	Well n°	Depth m.	Analysis n°	C	O	Ca	Mg	Fe	Mn	Si	Al	S	K	Na	P	Ti	sum		
1-	NS-2	2014.66	Pt 1	0	71,94	18,72	8,09			0,96	0,29						100		
			Pt 2	0	71,77	24,43	2,21			1,16	0,42							99,99	
			Pt 3	0	55,27	11,6	5,46	11,05		1,69	0,77	14,16						100	
2-	NS-3	2011.66	Pt 1	15,48	59,28	24,96	0,29	0	0									100,01	
			Pt 2	15,45	59,28	24,89	0,34	0,01	0,03										100
			Pt 3	15,68	58,44	14,75	10,13	0,98	0,02										100
			Pt 4	16,96	59,52	13,36	9,32	0,83	0										99,99
			Pt 5	17,9	60,42	11,88	9,6	0,2	0										100
			Pt 6	16,22	56,82	15,84	10,04	1,05	0,03										100
			Pt 7	16,34	56,72	15,48	11,4	0,05	0										99,99
			Pt 8	15,15	56,78	16,4	10,92	0,66	0,09										100
			Pt 9	16,04	57,1	15,33	10,79	0,67	0,07										100
			Pt 10	15,25	58,05	15,67	11,03	0	0										100
3-	NS-1	2024.60	Pt 11	9,91	10,24	27,09		52,76										100	
			Pt 12	17,32	54,59	28,03	0,06											100	
			Pt 13		56,82						43,18							100	
4-	NS-2	2023.05	Pt 14	0	60,83	1,66	1,02			36,49							100		
			Pt 15	17,66	57,77	24,05	0,47	0,05	0									100	
5-	NS-2	1993.10	Pt 16			3,24		44,3				48,01	4,45				100		
6-	NS-3	2014.67	Pt 17		7,85	0,61	1,07	31,62	0	0,84	0,8	54,59	0	1,25	1,29	0,08	100		
			Pt 18		16,49	0,51	1,44	19,01	0	1,01	1,01	57,21	0	1,88	1,41	0,03	100		
7-	NS-5	2014.10	Pt 12	22,36	53,42	15,62	8,59	0										99,99	
			Pt 13	25,23	52,24	13,92	7,44	1,17										100	
			Pt 14	23,74	52,7	13,94	8,66	0,96										100	

Table 8 : Second analysis of the elemental composition shows the atomic percentage of the elements in the poststylolite in the NS-3 well at depth of 1992.70 m. Synopsis data are before normalization process

Analysis n°	O	Ca	Mg	Fe	Mn	Si	Al	S	K	Na	P	Ti	sum
1	71,58			9,11				19,3					99,99
2	50	50											100
3	50,02	29,22	20,71	0,06									100,01
4	59,68	8,67	1,33	0,89		13,96	11,3	0,55	2,97	0,64			99,99
5	61,09	1,67	2,58	1,54		15,25	11,39	1,33	3,86	1,05		0,26	100,02
6	60,17	6,56	2,58	2,38		13,72	9,96	1,08	3,13	0,37		0,05	100
7	60,84	1,11	1,33	0,86	0,05	18,32	10,05	0,47	2,26	4,45	0,1	0,16	100
8	65,42	18,15	0,24	0,12	0,05	0,11	0,11	15,23	0,11	0,24	0,19	0,04	100,01
9	58,58	15,09	2	2,35	0,08	10,27	6,88	1,73	2,31	0,51	0,05	0,14	99,99
10	59,44	8,58	3,4	1,6	0,07	13,57	9,11	0,57	3,2	0,05	0,06	0,35	100
11	61,02	7,16	1,22	1	0,05	17,26	8,05	0,57	3,03	0,1	0,28	0,27	100,01
12	50,54	27,35	19,92	0,72	0,18	0,35	0,3	0,08	0,07	0,29	0,11	0,09	100

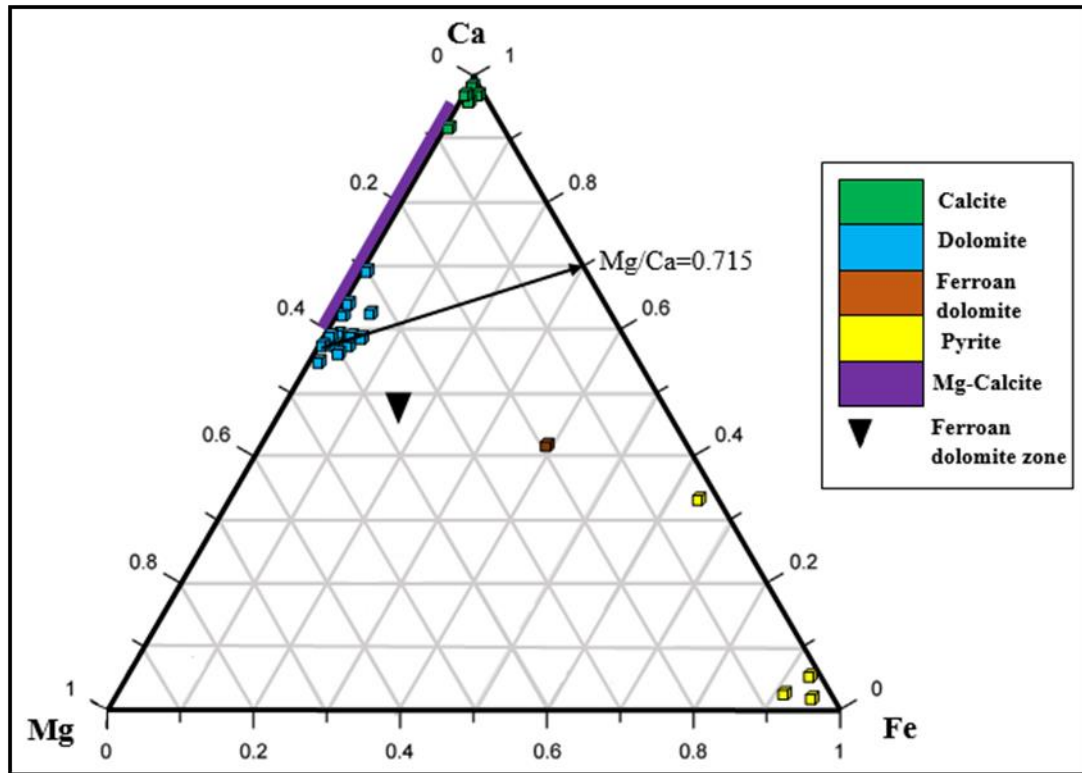


Figure 89 : Distribution of main carbonate elements in calcite cement and dolomite cement. The interpretations are according on chemical composition of carbonate cements

3.4.2.1.2 Iron and manganese elements

The similar behavior of the Iron and manganese affected on the properties of the carbonate rocks under Eh-Ph conditions. When fluids are oxidized, Fe^{2+} and Mn^{2+} are in the oxidized forms for that reason these elements are not available to incorporate into carbonate structures (Tucker and Wright, 1990). The relationship between Iron and manganese is very important feature under cathodoluminescence microscope because it can show the zonation boundaries of the calcite and dolomite crystals and their growing edges. The behavior of Mn and Fe detected the alterations and gradients in oxidation phases in ancient flow systems under cathodoluminescence microscope, which became a useful tool to determine the carbonate characteristics (Machel, 1985 and Hemming et al., 1989). The presence of the Iron and manganese elements reflects the Mn/Fe ratio, which almost includes low value especially in the ferroan calcite cement, contained low amount of Mg element and high amount of Fe element.

On the one hand, in a wider range of Eh conditions, Mn^{2+} is a little more soluble than Fe^{2+} and if Eh decreases, Mn^{2+} is preferentially incorporated into carbonates (Hams et al. 1985). On the other hand, the repetition of the dissolution-reprecipitation processes by paleofluids may be controlled the Mn^{2+} values. Fe^{2+} and Mn^{2+} include very low concentrations in seawater, but they exist in high concentrations in ground water and oil field brines (Veizer, 1983a).

Four cement groups are determined by (Budd et al., 2000) based on Mn/Fe ratio,, first group is luminescent calcite, second group contains both luminescent and nonluminescent cements, third group is dully-luminescent cements and fourth group is nonluminescent calcite.

The values of Mn/Fe ratio are very important to classify carbonate cement based on the luminescent degree. The low values of the Mn/Fe ratio indicate to the euxinic sediments (Figure 45).

During analysis of the mineral composition, calcite and dolomite cements of the Mishrif include many values of the Mn/Fe ratio in range from (3 to 0). The high values are clearly visible under Cathodoluminescence as the growing edges of the later calcite cement and in the zoning of the dolomite crystals (Figure 79 & Figure 96). The high values of the Mn²⁺ element exist in the later cement that led us to say the later cement probably is under condition of the decreasing Eh because Mn²⁺ is particularly sensitive to change the Eh-pH conditions in fluids.

Presence of the iron element includes three indicators in the Mishrif Formation. First, Iron element accompanies sulfur element, and this type of Iron element represents high concentration and maybe indicates to the secondary cement of ferroan dolomite as a species of ankerite after oil migration or this Iron element indicates to pyrite (Figure 89). Second, Iron element exists without presence silica element and sulfur element, this second type represents low concentrations of Iron. This case indicates to first cementation process in the normal euxinia environment. Third, Iron element represents high concentration, indicated to calcium sulfate or anhydrite cement in the euxinia environment (Figure 96). The inhibitor sulfur element usually affects the Mn/Fe ratio, which do not include specific relations with other elemental ratios such as Mg/Ca.

However, the high concentration of sulfur element resulted from two situations. First, the high concentration of the sulfur element can be gathered during diagenetic process, accompanied with anhydrite solutions or hypersaline brines. Second, the high concentration of sulfur element can be happened during degradation process of the petroleum in the reservoir rocks.

Dolomite cement displays reddish gray colour because it includes zonation with different colours. The difference of colour under Cathodoluminescence is indicative to the different ratios of the trace elements. However, hydrothermal sediments like dolomite and anhydrite occur often in the bulky samples in the Mishrif that led to increase hydrothermal elements such as manganese, iron, sulfur, silica, aluminum, titanium and sodium.

3.4.2.1.3 Silica, aluminum and titanium elements

Usually, silica and aluminium incorporate into the intracrystalline sites of the calcite cement by substitution of Si⁴⁺ and Al³⁺ for Ca²⁺ and other divalent elements, instead of they occur as silicate inclusions within nano scales (Nadoll et al., 2012). Hydrothermal fluids are generally enriched in Si, Na, Cl, and Fe, which buffered the calcite cement by silica and aluminium to block dolomite occurrence. Generally, hydrothermal sediments include enrichment of the aluminium element, which indicates to detrital input (Metz et al., 1988).

The similar behavior of the silica and aluminum is a contrast the main elements behavior Ca-Mg-Fe (Figure 90). However, Ca, Mg and Fe are the main carbonate elements, which reflected the negative relations with trivalent and tetravalent cations such as Al³⁺ and Si⁴⁺ (Figure 91 & Figure 92). Silica and aluminium directly substitute the Ca²⁺ or other

divalent elements. By the way, they indicate to the method of incorporation in carbonate elements.

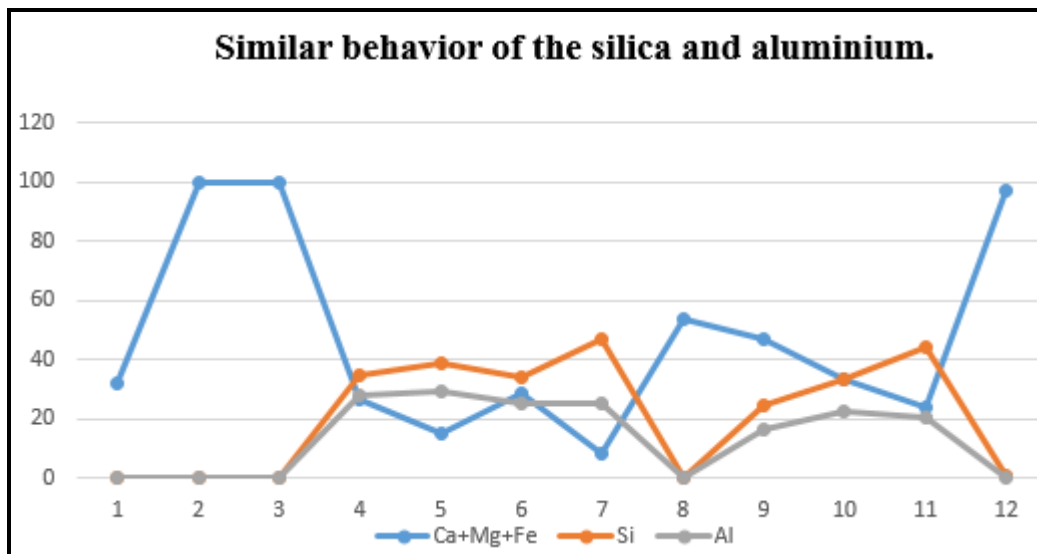


Figure 90 : The behavior of the silica and aluminium elements reflects the relation with main elements of carbonate rocks with respect to Eh-PH conditions

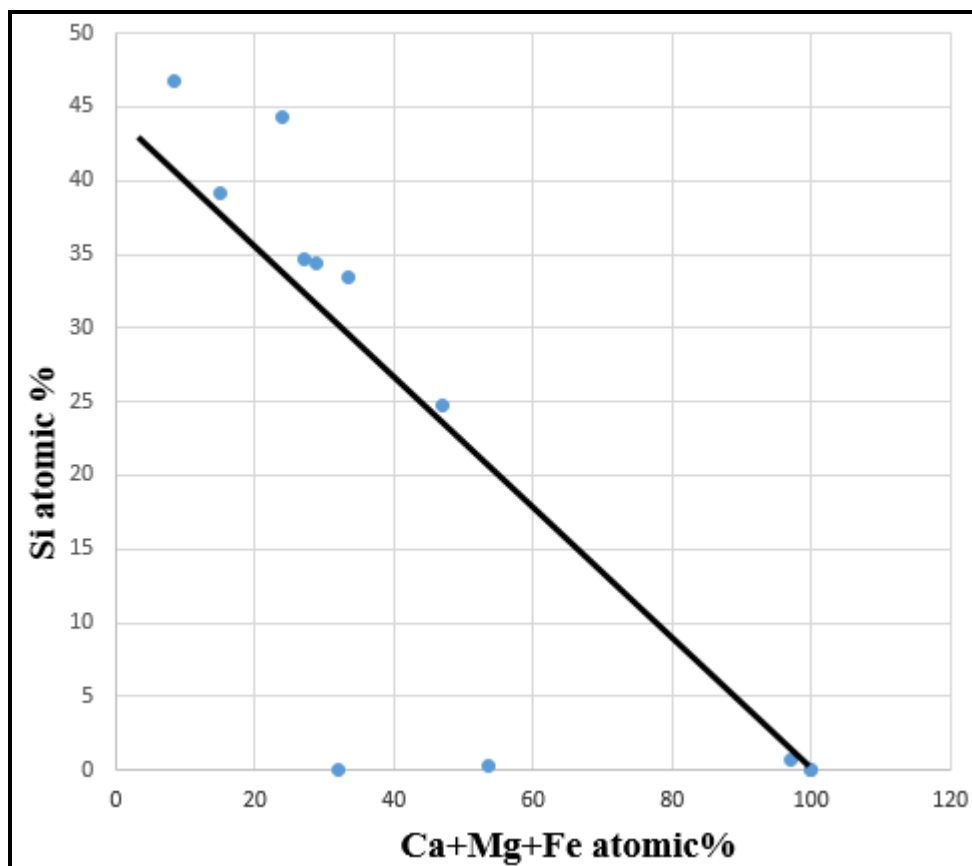


Figure 91 : Negative relationship is between silica and main carbonate elements

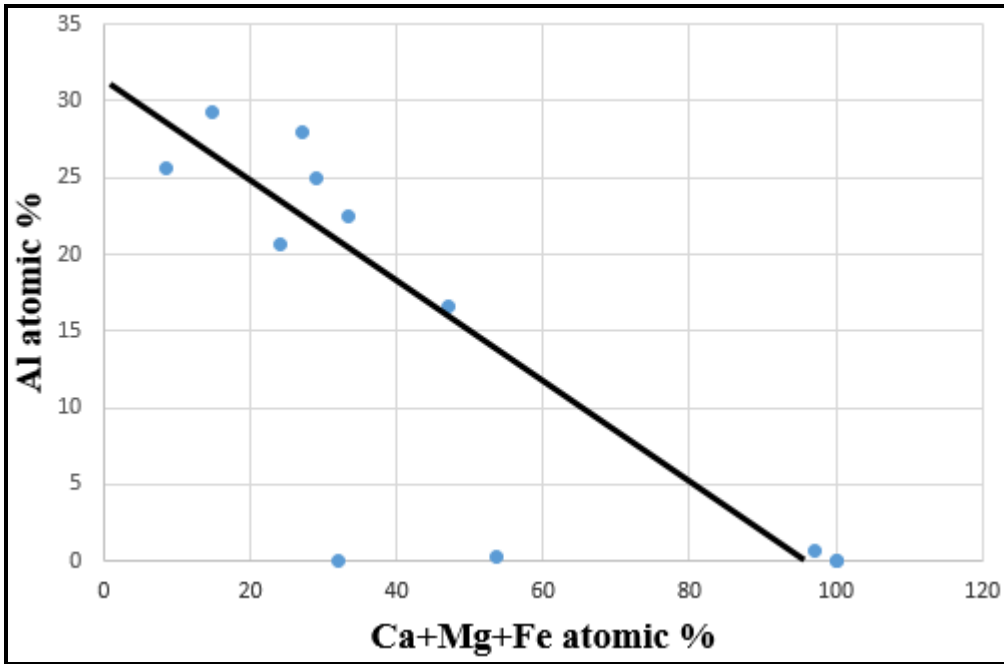


Figure 92 : Negative relationship is between aluminium and main carbonate elements

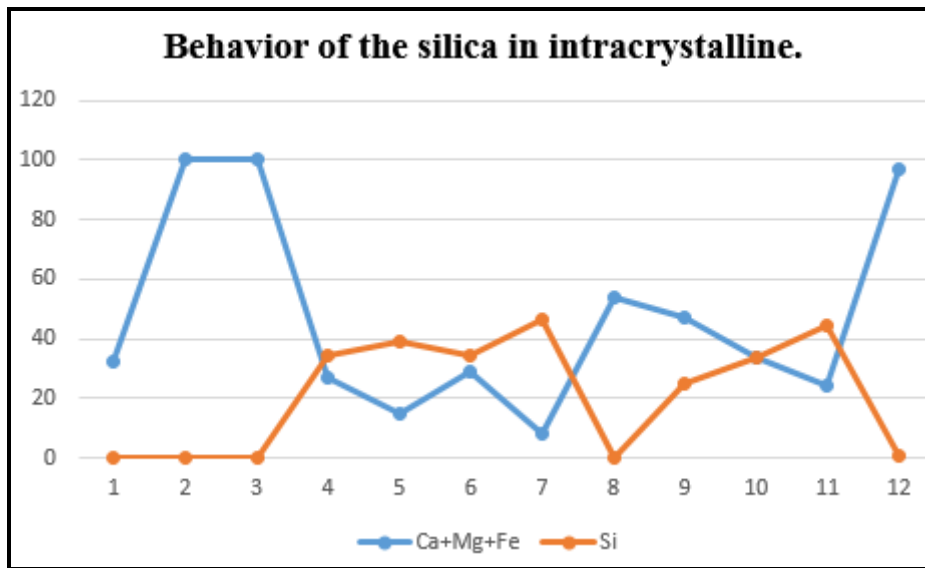


Figure 93 : Integrated zone of silica element reflects the intracrystalline zone in carbonate cement under Eh-PH conditions, maybe lead us to identify the zone of stoichiometric interaction of the calcium silicate mineral

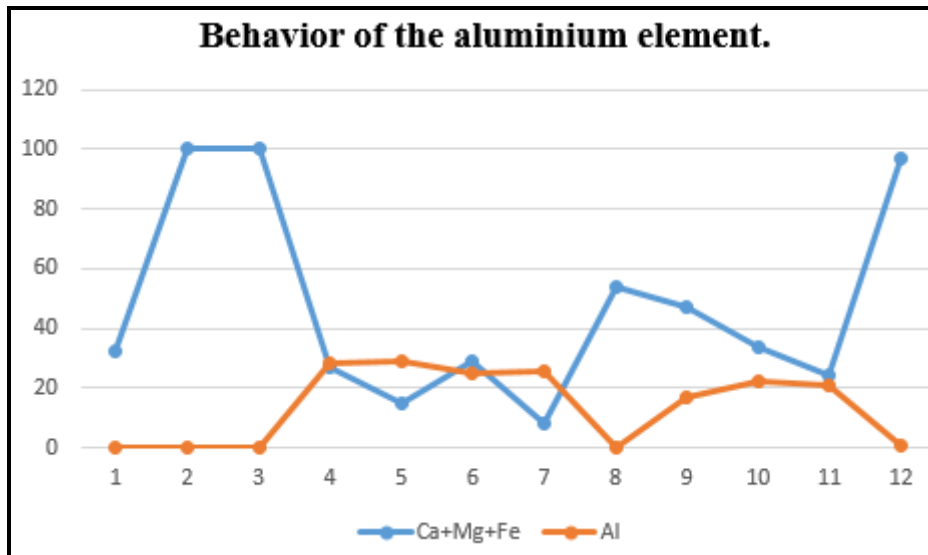


Figure 94 : Integrated zone of aluminium and carbonate elements reflects the high temperature conditions. It maybe leads to identify the zone of stoichiometric interaction of calcium aluminates groups

Al and Ti elements firstly reside in the detrital fractions in marine sediments (Taylor and McLennan, 1985). Most of the elemental composition analyses by EDS technique show the positive relationship between Al and Ti elements (Figure 95). Al and Ti behaviors are relatively conservative during subsurface processes. They are resistant to chemical weathering and diagenetic alteration.

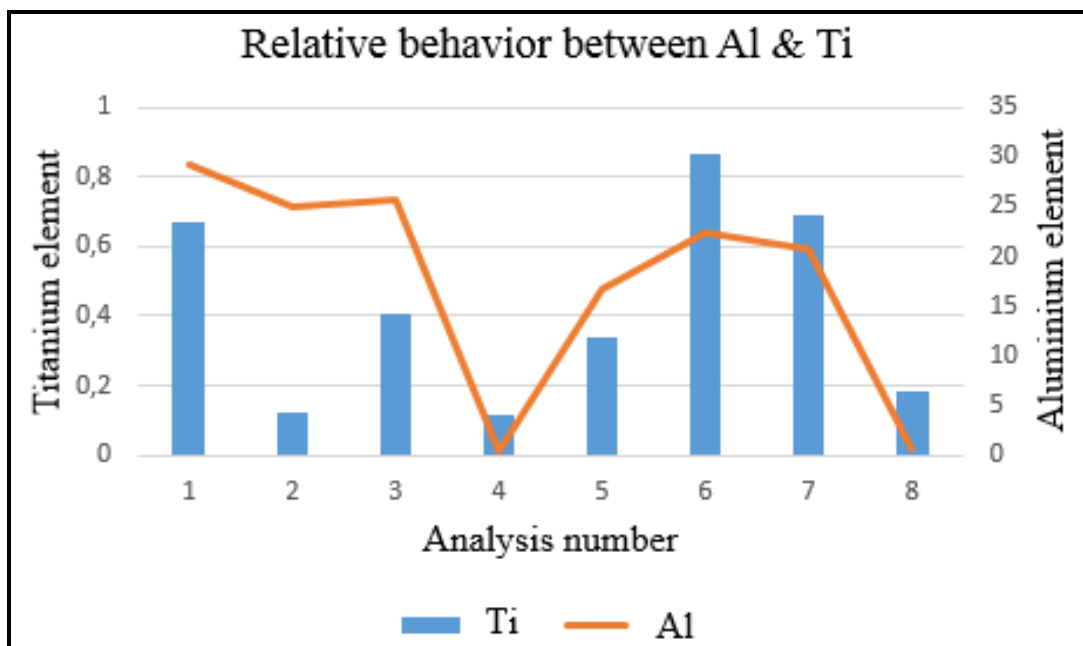


Figure 95 : The behavior of Al and Ti elements is relatively conservative in the carbonate rocks with respect to Eh-PH conditions

3.4.2.1.4 Sodium, potassium and phosphorus elements

The distribution coefficient of Na^+ indicated to fluid phase by his value of 0.00002, identified by (White, 1978) for two phases calcite and dolomite. Generally, the Na^+ substitutes Ca because their radii have almost same values 1.02 Å and 1.00 Å, respectively (Shannon and Prewitt, 1969 and Budd, 1997), described the location of sodium in dolomite.

The distribution of Na^+ in the Mishrif deposits indicates to evolution of the paleofluid towards the brines especially when phosphorus element and other evaporation elements include crude relationship. However, the high concentration of Na^+ exists in the poststylolite, which indicates to evolution paleofluid during interaction between fluids and rocks. Perhaps, these fluids reflected the presence brines. Furthermore, Na^+ is interested because it is relatively a major cation in seawater and brines.

Dolomite in the Mishrif Formation includes different relationship between Na^+ and Fe^{2+} elements. When Na^+ element increases, Fe^{2+} element goes to low value in dolomite and when Na^+ element decreases, Fe^{2+} element goes to high value. This phase of dolomite interprets under maturity conditions of dolomite, which gone towards saddle dolomite.

3.4.2.1.5 Conclusion

According with results of elemental composition analysis by EDS technique, Fluids evolved during their interactions with rocks. The compositional maturity of the dolomite cement reflects the semi-maturity towards to the saddle dolomite depend on the ratio of Fe^{2+} in the dolomite. High concentration of Na^+ can be attributed to the brines. As well as, the elemental data of the EDS technique reflects the effect of the hydrothermal solution, represented by the diagenetic alterations. Other ideas suggest the repetition process of dissolution-precipitation lead to effectively remove of the trace elements. Results of this study also highlight the utilization rate of the silicate carbonate and aluminium carbonate to determine the early hydrothermal alteration. Hydrothermal process blocks calcite cement to conversion into dolomite cement. The silica element existed in the primary fractures lining and in the poststylolite lining.

Elemental data of the EDS technique indicates to the location of Na^+ and location of Mg^{2+} in the same place that indicates to the common origin of the fluid as brines (Figure 97). The alteration of the host rocks can be resulted from the composition of hydrothermal fluids. As well, the physicochemical parameters of the hydrothermal fluids lead to the differentiation of hydrothermal alterations of the host rocks.

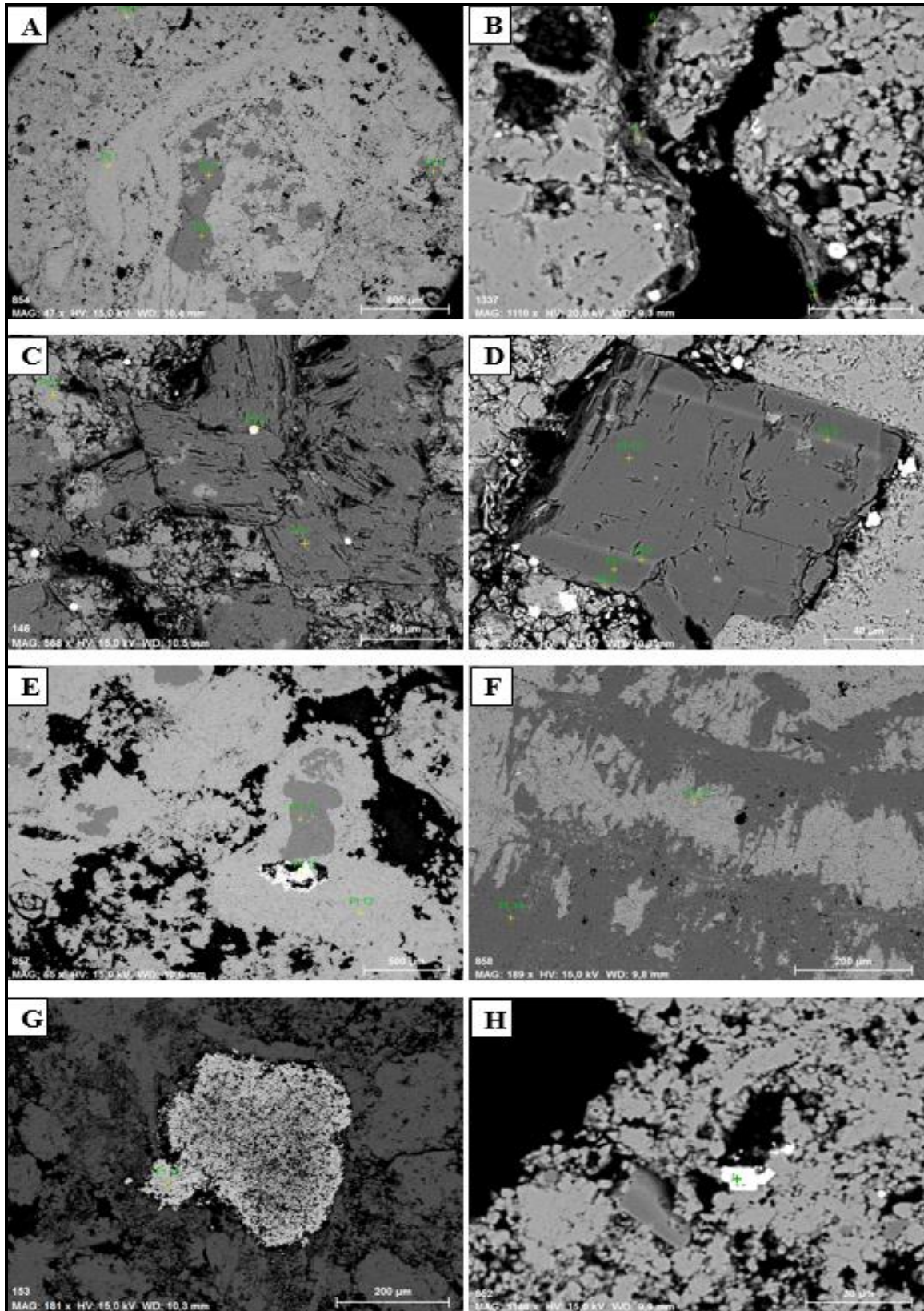
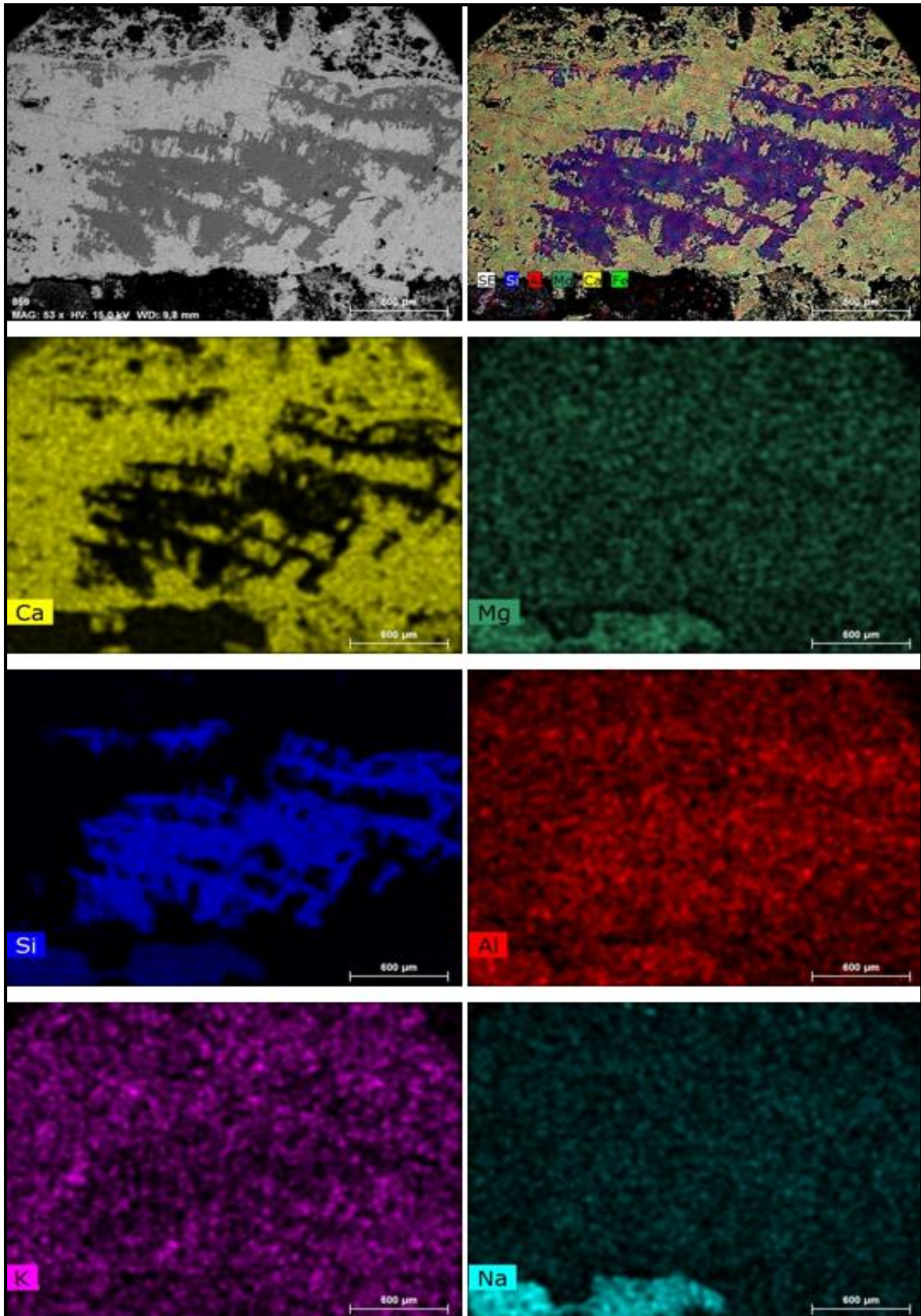


Figure 96 : SEM with EDS technique shows various types of the cement in the different distribution patterns at Mishrif Formation of Nasiriyah oil field in the wells of (A) NS-3 2011.66 m, (B) NS-3 1992.70 m, (C) NS-2 2014.66 m, (D) NS-3 2011.66 m, (E) NS-1 2024.60 m, (F) NS-2 2023.05 m, (G) NS-2 1993.10 m, and (H) NS-3 2014.67 m



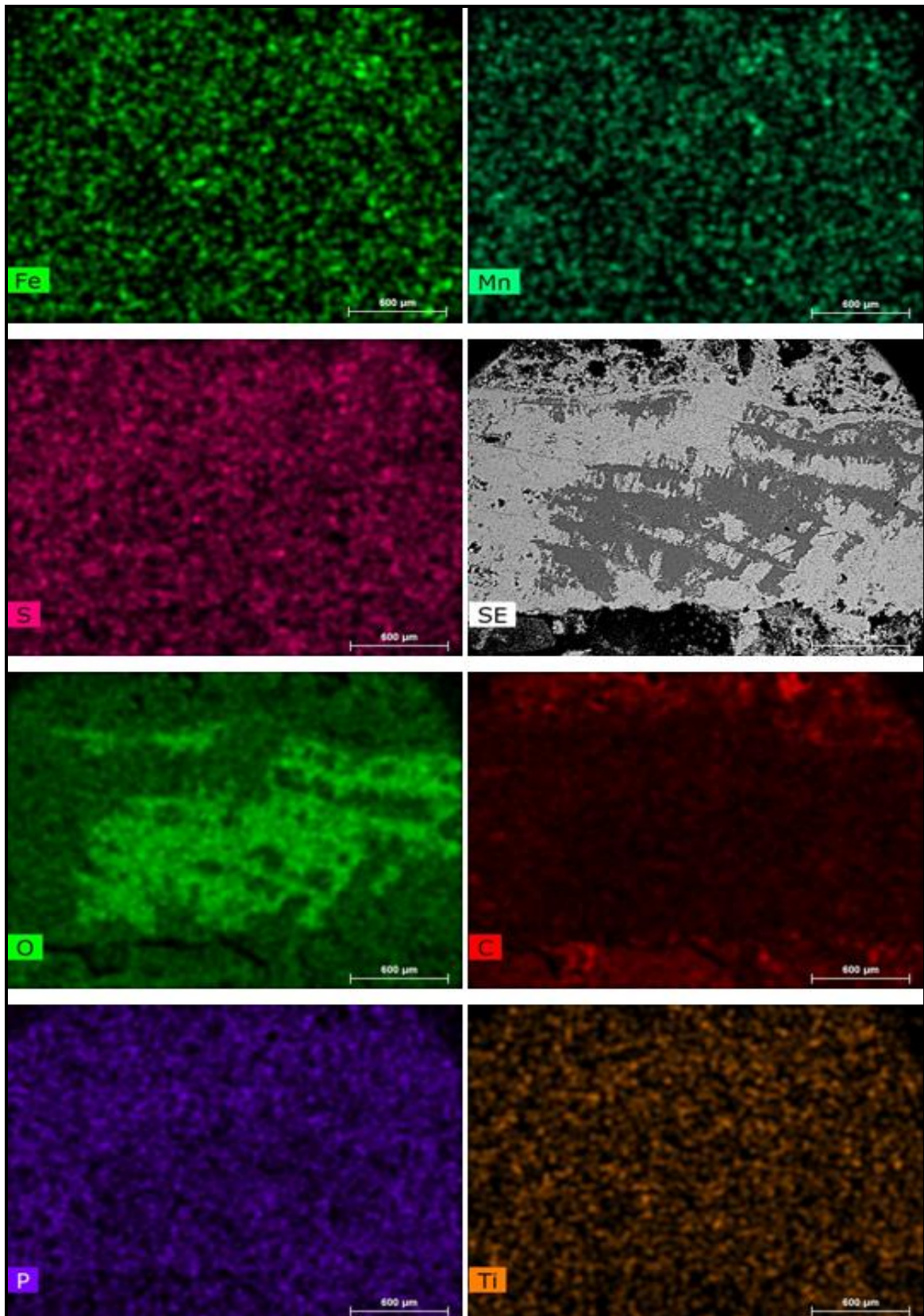
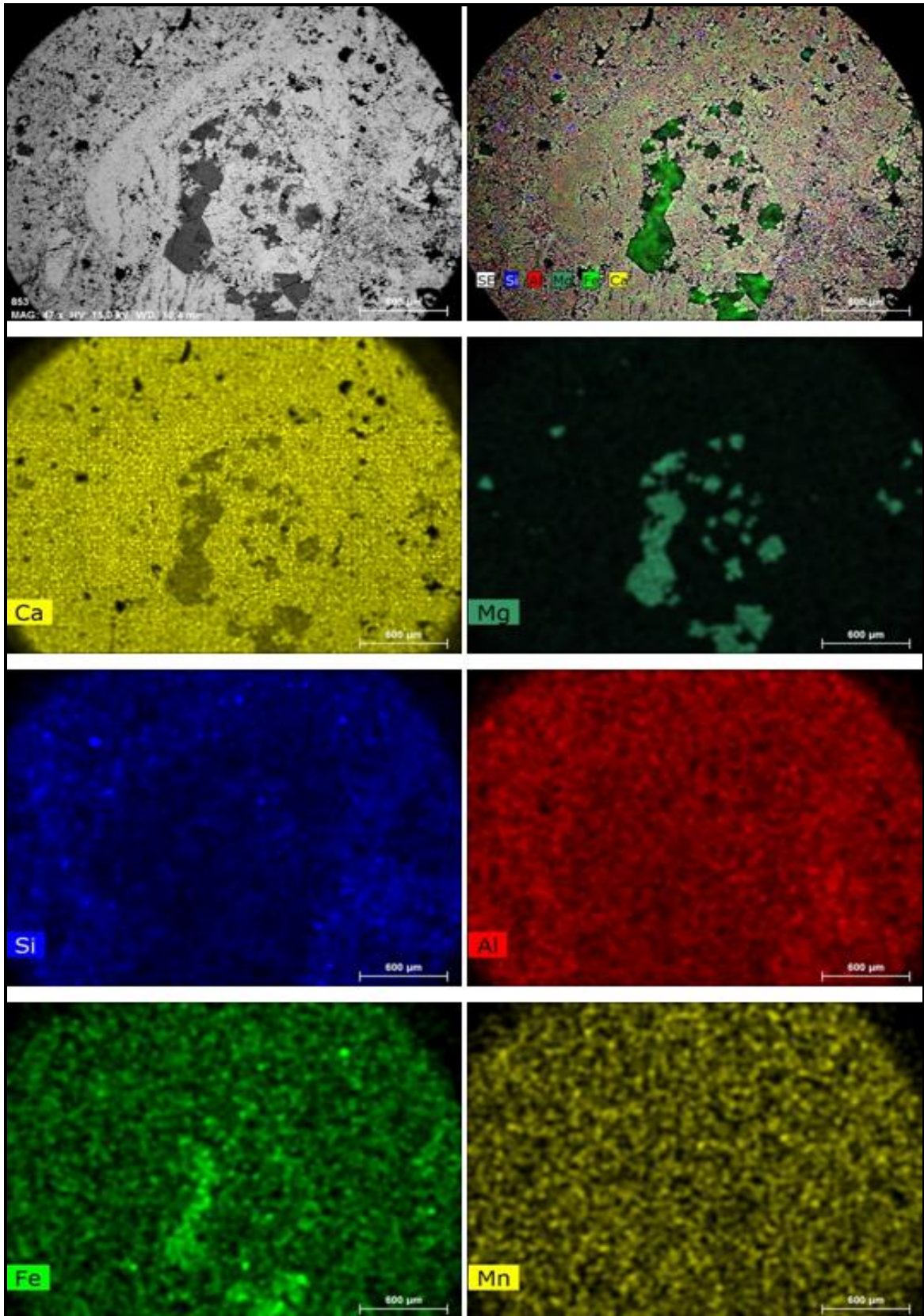


Figure 97 : EDS Cartography shows the elements distribution of the hydrothermal calcium-silicate cement in the (Figure 96) in the NS-2 well at depth of 2023.05 m



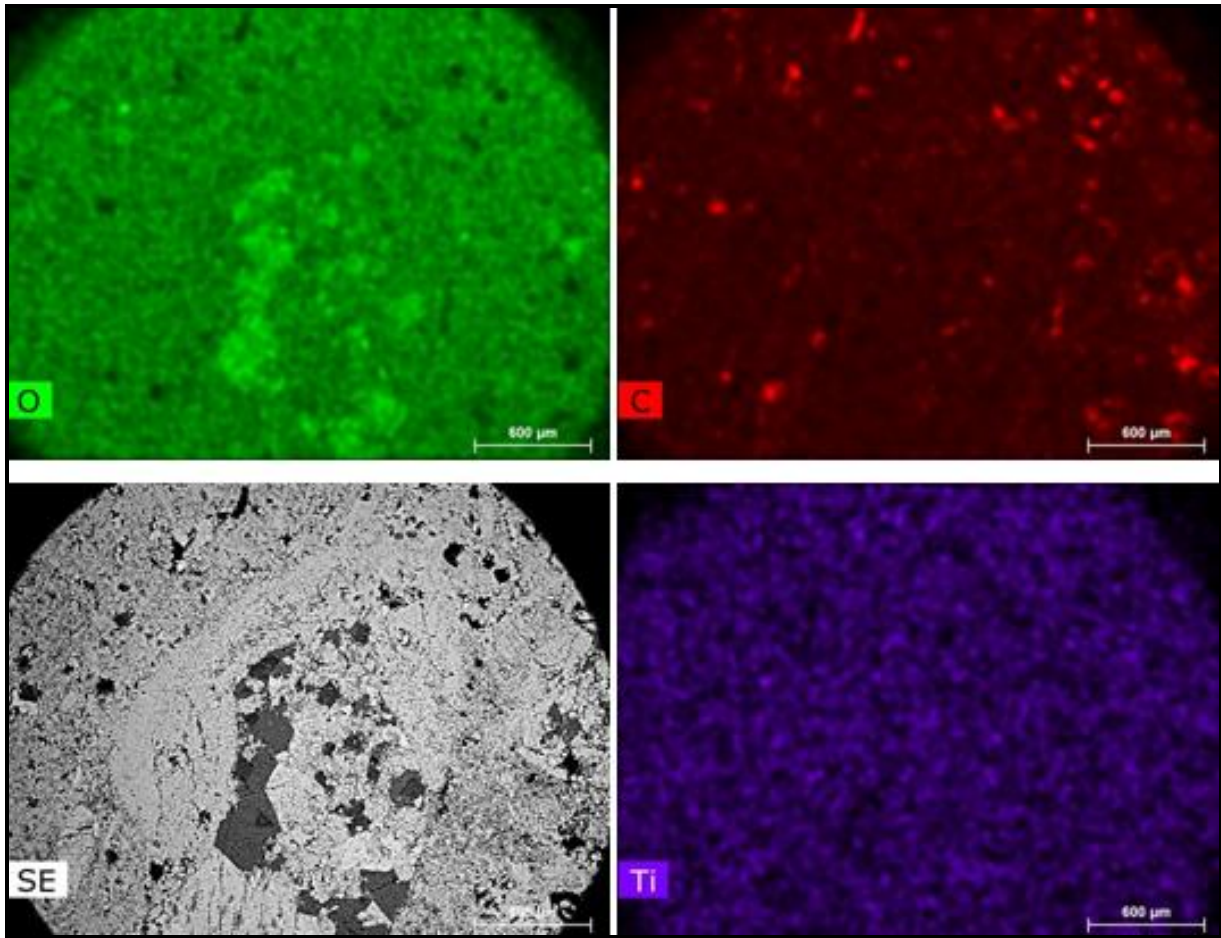


Figure 98 : EDS Cartography shows the elements distribution for later secondary dolomite cement in the (Figure 96.A) in the NS-3 well at depth of 2011.66 m

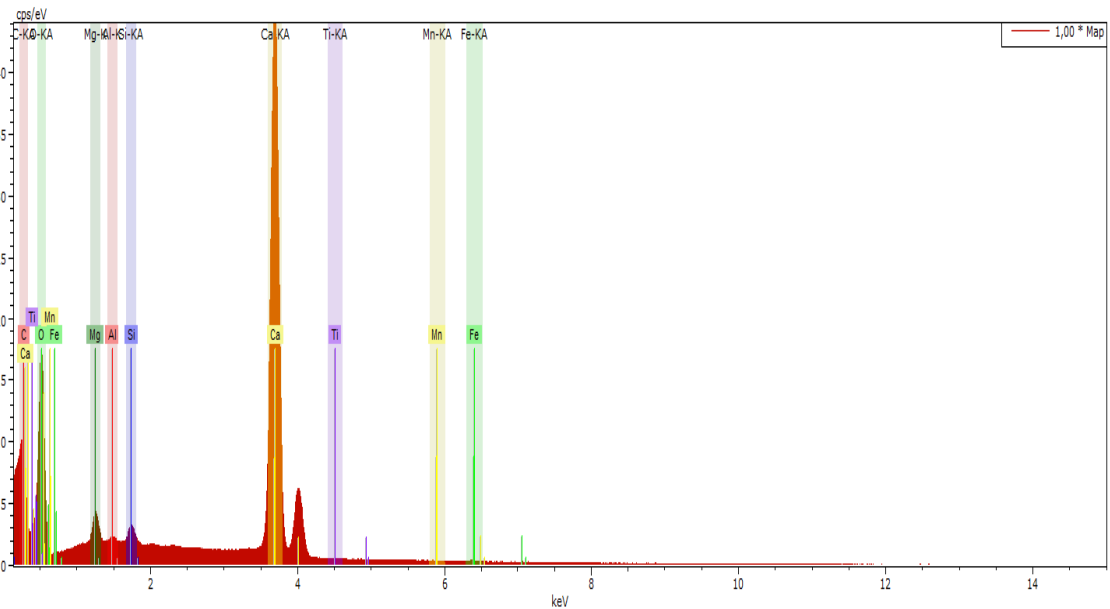


Figure 99 : EDS technique shows spectrum of the elemental composition in the NS-3 well at depth of 2011.66 m

3.4.2.2 Fluid inclusions

The study of fluid inclusions provides a wide range of data, some of which are unavailable right now from any other source in the various physical and chemical processes. Fluid inclusions studies are the clues to the many problems such as of the palaeotemperature, palaeopressure, palaeodensity of fluids and the ancient composition of the fluids.

Fluid inclusions are small volumes of palaeofluid trapped in minerals during growth or at a later time during fracturing. Sizes of fluid inclusions are usually ranging from 0.1-1mm but mostly between 4 and 10 μm .

The essential question is proving that the fluid trapped in cavities is representative of the ancient fluid. “Roedder’s rules” state that:

1. The inclusions trapped a single, homogeneous phase.
2. The inclusions represent an isochoric (constant volume system) or isovolumetric.
3. After trapping, nothing has been added to/removed from, the inclusions.

A wide variety of problems are encountered in fluid inclusion studies in carbonates, which are related to the size of fluid inclusions, the possible numerous generations of fluid inclusions in the host mineral. There are two ways to explain the fluid inclusion data. Firstly, the fine observation of textural relationships between fluid inclusion and host mineral will solve the problems of chronology. Secondly, the indispensable chemical data are deduced from microthermometry and Raman microspectroscopy.

Primary inclusion is trapped during the growth of the hosted crystals, in medium of free fluid. It is used for getting information on conditions of formation and chemical evolution of palaeofluid. Secondary inclusions are trapped by the healing of fractures in the host crystals at some unspecified time after its growth. Secondary fluid inclusions are generally distributed in trails. Pseudosecondary inclusions are trapped by the healing of fractures in the hosted crystal during continued crystal growth

3.4.2.2.1 Methods

3.4.2.2.1.1 Petrography

Petrography is the fundamental step for fluid inclusion studies. It is based on :

- Drawings and photos of selected groups of fluid inclusions defined as “Fluid Inclusion Assemblages” (FIA, Goldstein and Reynolds, 1994)
- Classification of fluid inclusions based on:
 - Number of phases at room temperature: monophasic (only liquid or gas), biphasic (liquid + vapour) or polyphasic (Roedder, 1984 & Goldstein, 2003).
 - Relative phase volumes (fill degree). Special attention will be paid on highly varying vapour filling ratios in a given FIA, as it could reflect heterogeneous trapping of an initially immiscible fluid
 - Inclusion size and morphology of fluid inclusion
- Relative age (primary, pseudosecondary, secondary) based on observations of the spatial distribution of the different populations of fluid

3.4.2.2.1.2 Fluorescence

Generally, a useful tool to distinguish aqueous inclusions and petroleum inclusions is the fluorescence microscopic technique (Guilhaumou et al., 1990). This study has used UV-light microscopy (Olympus U-RFL-T). Indeed, most of the petroleum fluid inclusions have fluorescence, while aqueous inclusions do not show this fluorescence (Burruss, 1981) and (Mclimans, 1987).

Axiomatically, petroleum fluid inclusions emit wide visible light range and each colour in this range will reflect the type of petroleum composition (Burruss, 1981). However, aromatic hydrocarbons are considered as main fluorescing components (Hagemann and Hollerbach, 1986 & Khorasani, 1987). The blue coloured petroleum fluid inclusion has behaved as aromatic hydrocarbons (Figure 102). Due to the bright blue colour of petroleum fluid inclusion reflects a greatest intensity in the low wavelengths (Khorasani, 1987). The red range of the NSO compounds reflects less intensity of fluorescence in the high wavelengths that represents the pseudosecondary fluid inclusion (Figure 102).

3.4.2.2.1.3 Microthermometry

Microthermometry is the basic method to study fluid inclusion. It consists in measuring temperature in a wide range of temperature (-200 to 600°C). The microthermometric stage used in the present study is the FLUID INC stage (USG patent). The thermometer was first calibrated with an ice bath until the 0°C value was. The other standards used were:

- Pure H₂O in synthetic fluid inclusions (0°C)
- CO₂ melting in H₂O-CO₂ natural fluid inclusion of Camperio (-56.6°C)
- Pure H₂O of critical density in synthetic fluid inclusions (374.1°C)

3.4.2.2.1.4 Microspectrometry Raman

Raman spectroscopy is a significant non-destructive technique for fluid inclusion analysis. It uses in the wide field from solid, liquid and gaseous phases for detection and identification the quality of materials. In this study, Raman technique is used to detect the type of mineral, the chemistry of aqueous fluid inclusion and the petroleum fluid inclusion. The minimal sample gives the huge information under this technique, which reflects the large advantages and uses of this technique.

The position of the peaks is obtained by the Raman spectroscopy can be determined the phase type based on this position of peaks and the spectra intensity. The study of fluid inclusions under Raman spectroscopy is carried out in the three steps:

- 1) Study of the gas phase has done by study the gas bubble.
- 2) Study of the liquid phase carried out on the aqueous and petroleum inclusions.
- 3) Study of the solid phase is represented by cubic pyrite.

3.4.2.2.2 Sample preparation

The 151 core samples were collected from four wells NS-1, NS-2, NS-3 and NS-5, which are located in Mishrif Formation at Nasiriyah oil field. The 48 thin sections were examined with conventional optical, fluorescence, scanning electron microscope with EDS technique, Raman spectroscopy and finally with microthermometry microscope to detect the diagenetic phases and paragenetic relationships among them. These thin sections were treated with special epoxy, which has standed 250 °C under heating stage of the Microthermometry. The 10 uncovered thick sections have double polished surfaces, which have been prepared.

Petrographic observations of petroleum inclusions were established based on the fluorescence behaviour colour, the number of phases at room temperature comparisonally with their relative proportions and the determination of fluid composition by microthermometry and Raman microspectrometry.

Table 9 : Thick sections samples prepared for fluid inclusion analysis

No.	Depth references m	Well No	Units of Mishrif Formation in the Nasiriyah oil field
1	2007.32	NS-3	Reservoir unit #1
2	2014.67		Reservoir unit #1
3	2039.91		Reservoir unit #2 high percent saturated oil
4	2062.58		Reservoir unit #2 high percent saturated oil
5	2070.21		Reservoir unit #2 high percent saturated oil
6	2014.10	NS-5	Reservoir unit #1
7	2033.80		Reservoir unit #2 high percent saturated oil
8	2051.77		Reservoir unit #2 high percent saturated oil
9	2067.53		Reservoir unit #2 high percent saturated water
10	2075.19		Reservoir unit #2 high percent saturated water

3.4.2.2.3 Results

Two types of fluid inclusions were identified in the Mishrif Formation. Firstly, aqueous primary and secondary fluid inclusions are present in both calcite mineral and dolomite. Secondly, petroleum fluid inclusions were identified using UV-fluorescence.

The huge abundance of aqueous fluid inclusions found in the blocky calcite cement with homogeneous temperatures range from 108°C to 175°C and the most frequency of homogeneous temperatures from 150°C to 175°C (Figure 104).

The aqueous fluid inclusions have mainly composed of H₂O-MgCl₂ system. The salinity rate of the fluid inclusions is shown according to the T_m ice values, which are plotted versus salinity of the MgCl₂ on the double-graph. Salinity ranges from 14.9 to 17.4 wt% of MgCl₂. The homogeneous temperatures of petroleum fluid inclusions in the latter fractures represent the high degrees from 225 °C up to 250°C.

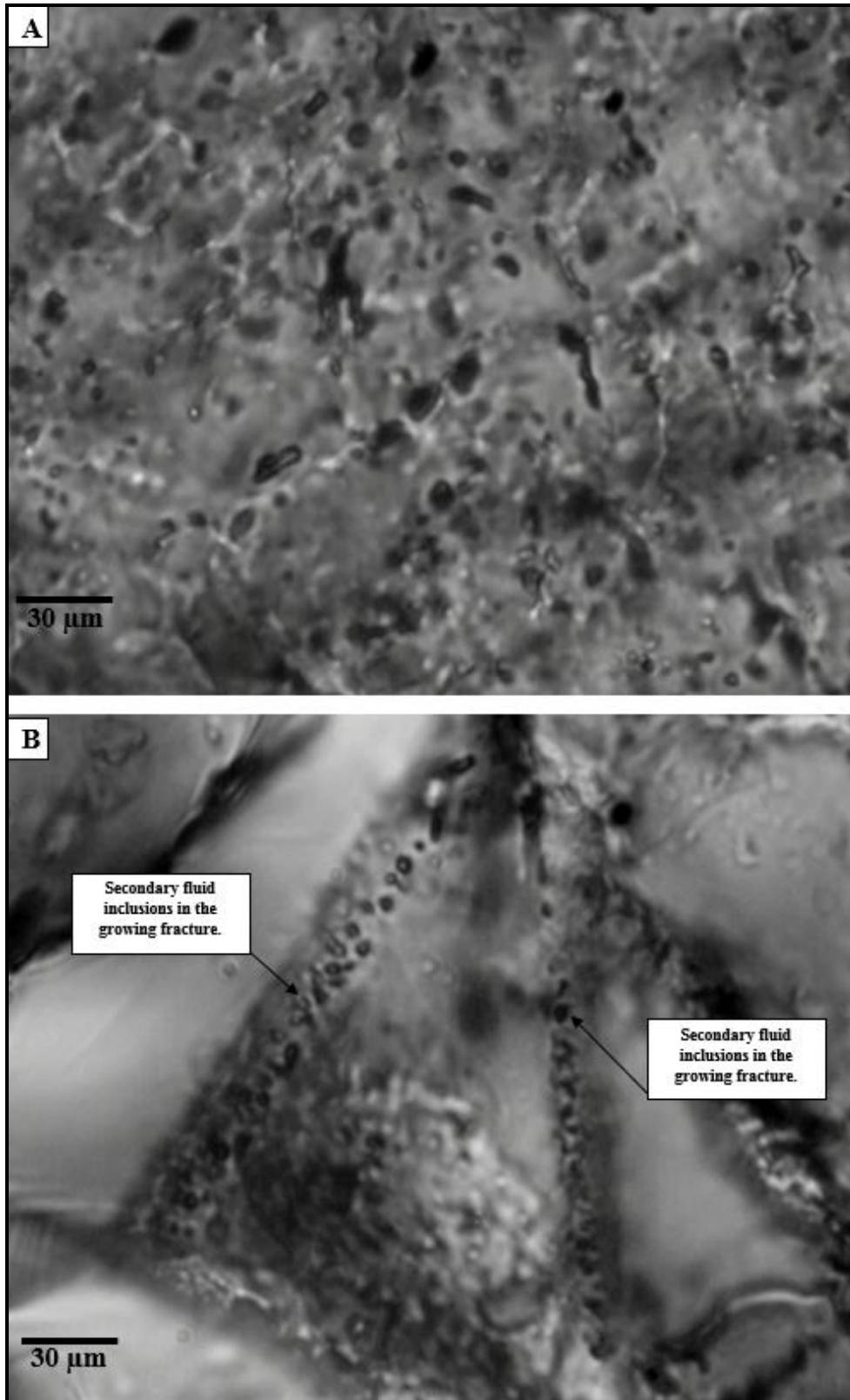


Figure 100 : Distribution patterns of many fluid inclusions are existed in the Mishrif Formation in the Nasiriyah oil field. (A) Petroleum fluid inclusions have filled some etches pits as a primary fluid inclusion in the NS-2 well at depth 2005.55 m. (B) Petroleum fluid inclusions have filled micro-fracture as a secondary fluid inclusion in the NS-5 well at depth 2014.10 m

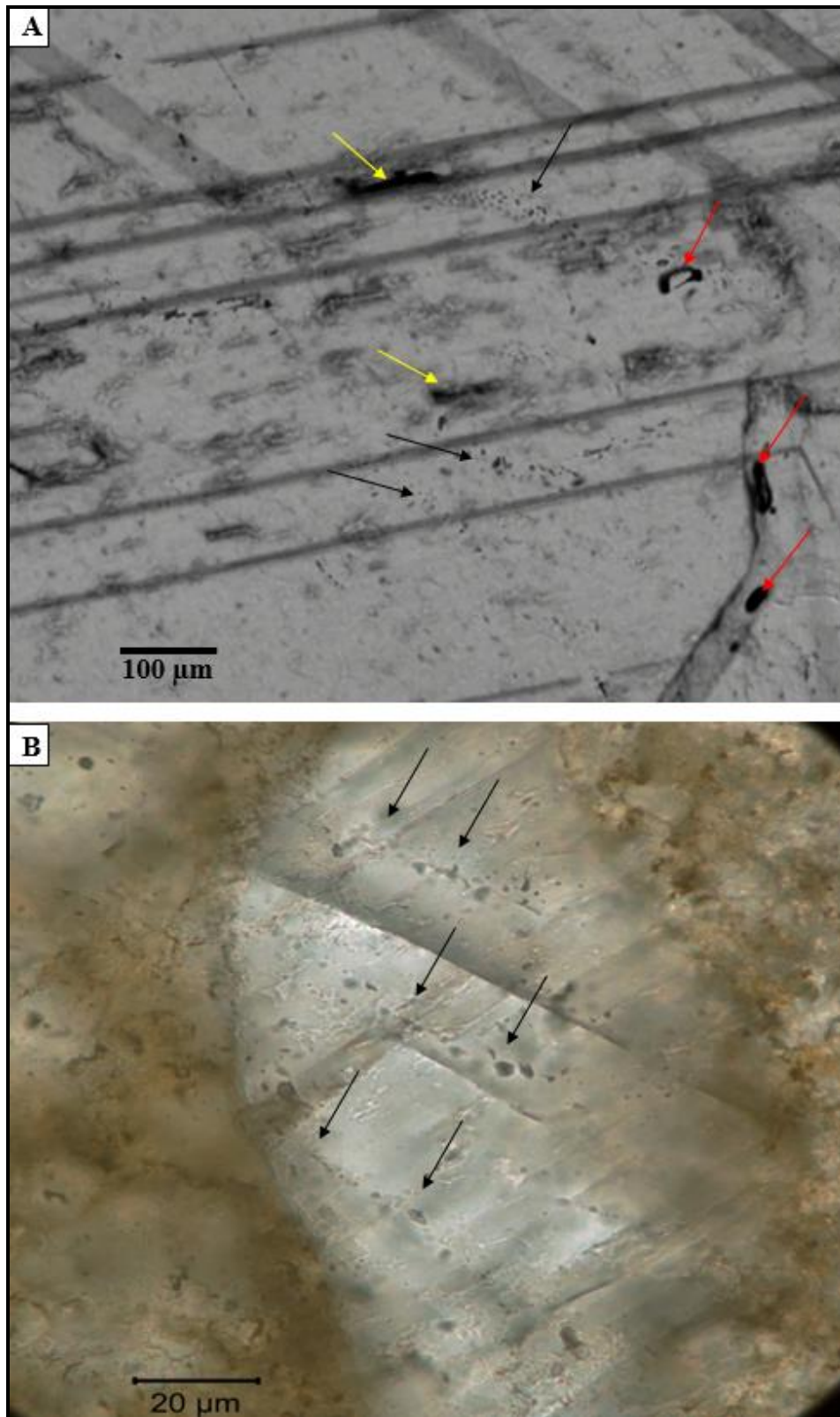


Figure 101 : Pseudosecondary petroleum fluid inclusions distributed as trails. (A). The red arrows have indicated to remains of bitumen, black arrows indicate trails of petroleum fluid inclusion and yellow arrows indicate locations of pores in well NS-1 at depth 2033.80 m. (B) Clear trails of the petroleum fluid inclusions in calcite in well NS-2 at depth 2048.26 m

Figure 102.

Primary petroleum inclusions are obviously identified as they appear with a large vapour bubble and a bright blue colour of fluorescent light. Homogenisation by liquid disappearance would be expected. The fluid in this type of inclusions would call as a condensate and their density is estimated at around 40 to 45° API.

The pseudosecondary inclusions show a relatively small vapour bubble, colourless in transmitted light and with a yellowish fluorescence colour in (Figure 102) at right side. The oil components are relatively less mature according to the yellow colour of petroleum fluid inclusions. Petroleum density is estimated at around 25 to 30° API.

Texturally, characteristics of poor sealing and necking down of the petroleum fluid inclusions at Mishrif Formation are less marked than in the aqueous inclusions, which characterize by very ragged shape. However, these primary petroleum inclusions have best features that are commonly excellent for microthermometry analysis.

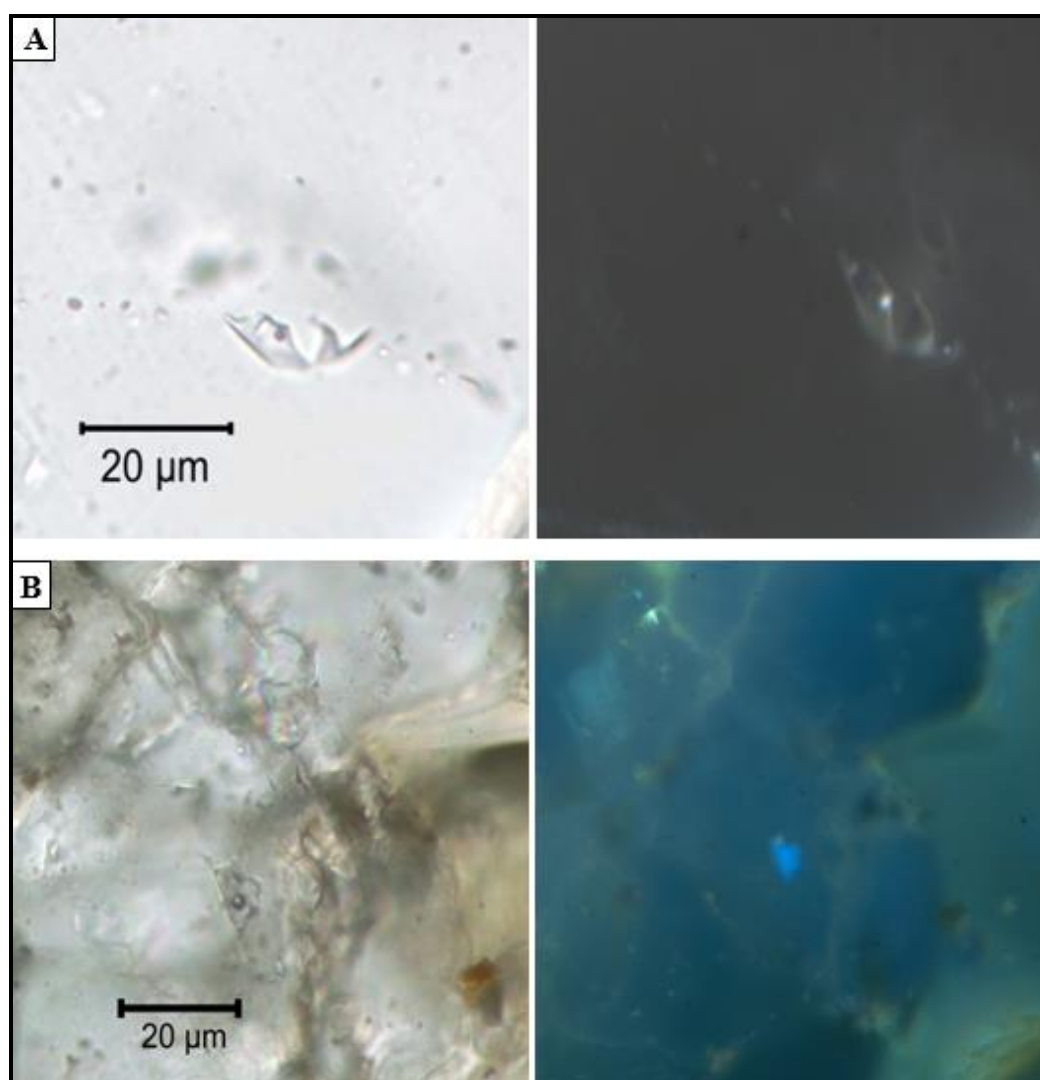


Figure 102 : The comparison between transmitted light colour on the left side and fluorescent light colour on the right side can be used as a critical tool to distinguish between aqueous fluid inclusions and petroleum fluid inclusions as well, to discriminate among the components of petroleum fluid inclusions too

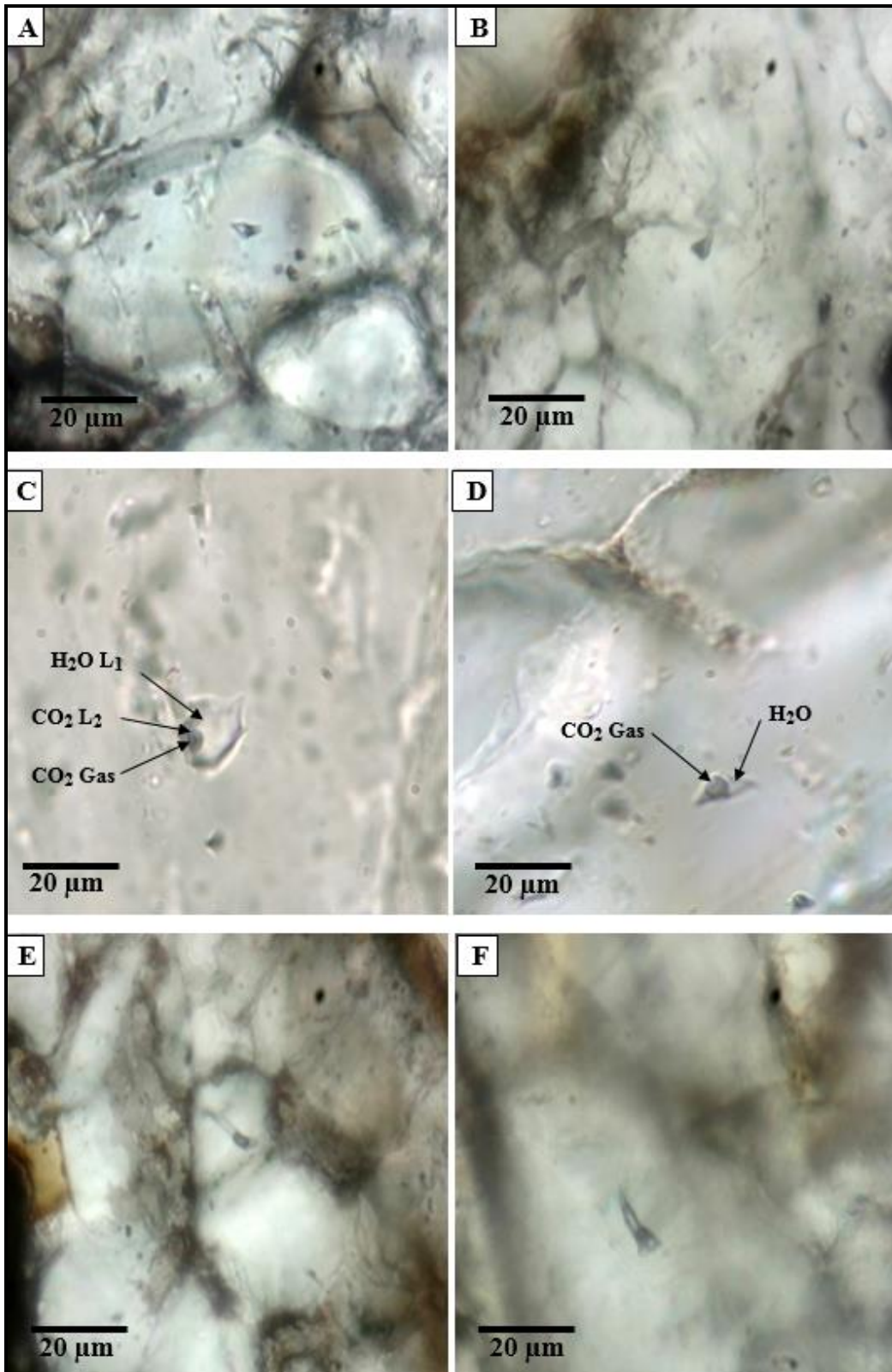


Figure 103 : Some of classical textures of the petroleum fluid inclusions are existed in calcite cement at Mishrif Formation. The proportion between liquid and vapour at room temperature can be used for identification the petrographic and chemical properties of petroleum fluid inclusions

3.4.2.2.3.1 Microthermometry

The whole procedure is outlined by (Shepherd et al., 1985). The best way to start microthermometry is by cooling samples before the homogenisation step, because of the risk of decrepitation.

Low temperature (transition phase) include the measurement of the eutectic temperatures, *i.e.* the first granulation of the frozen liquid and the final ice melting temperature (T_m ice) (Table 11).

The aqueous fluid inclusions have selected give eutectic temperatures between ranging from -31.6 to -40.1 °C, reflecting a fluid composition belonging to the H₂O-MgCl₂ system according to (Crawford, 1981). The range of T_m ice is between -16.4 and -22.9°C, which reflecting a very high salinity (from 14.9 to 17.4 wt% MgCl₂) (Dubois and Marignac, 1995).

Freezing tests down to lower limit of the stage (-185°C) have been tried on petroleum inclusions in a fracture of well NS-5 at depth 2014.10 m. For that reason, some sharp micro-cracks may occur during freezing tests in the diagenetic minerals such as a calcite, and this case may lead to leakage at inclusions. Nevertheless, we cannot achieve the complete solidification of petroleum fluid inclusions.

- Heating experiences and measurement of homogenisation temperatures (T_h °C).

Heating tests produce many decrepitations of petroleum fluid inclusions. The main types of the fluid inclusions have classified based on differences in the homogenisation temperatures (T_h) in the following (Figure 104).

1. Fluid inclusions have T_h from 108°C to 125°C that represent the first stage of calcite cement
2. Fluid inclusions have T_h from 125°C to 175°C that represent blocky calcite cement and all previous fluid inclusions in the first and the second points represent aqueous fluid inclusions.
3. Fluid inclusions have T_h from 175°C to 200°C that represent medium size of dolomite crystals cement; they represent the beginning of formation of the petroleum fluid inclusions.
4. Petroleum fluid inclusions have T_h from 200°C to 225°C that represent the immature petroleum fluid inclusions in the later blocky calcite cement.
5. Petroleum fluid inclusions have T_h more than 225°C that represent the mature petroleum fluid inclusions in the later fracture.

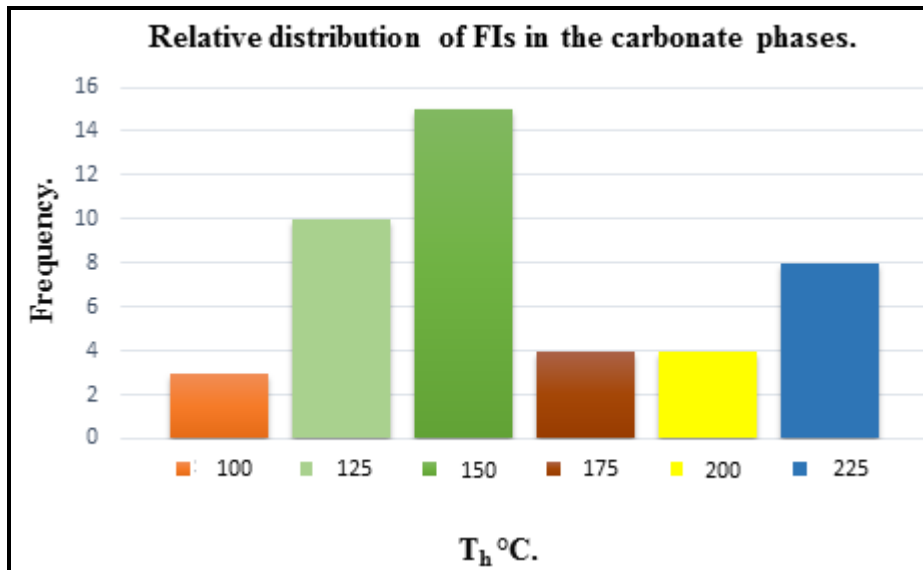


Figure 104 : Histogram of the homogenisation temperatures (T_h °C) shows the multi-generations of T_h (°C) aqueous and petroleum fluid inclusions based on their frequencies under microthermometer microscope

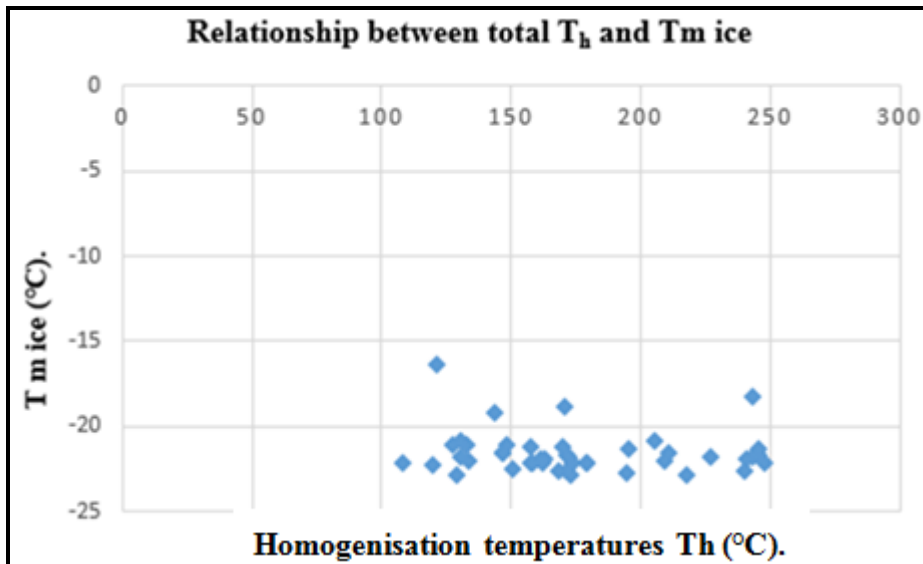


Figure 105 : Ice melting temperature (T_m ice) versus homogenisation temperature (T_h)

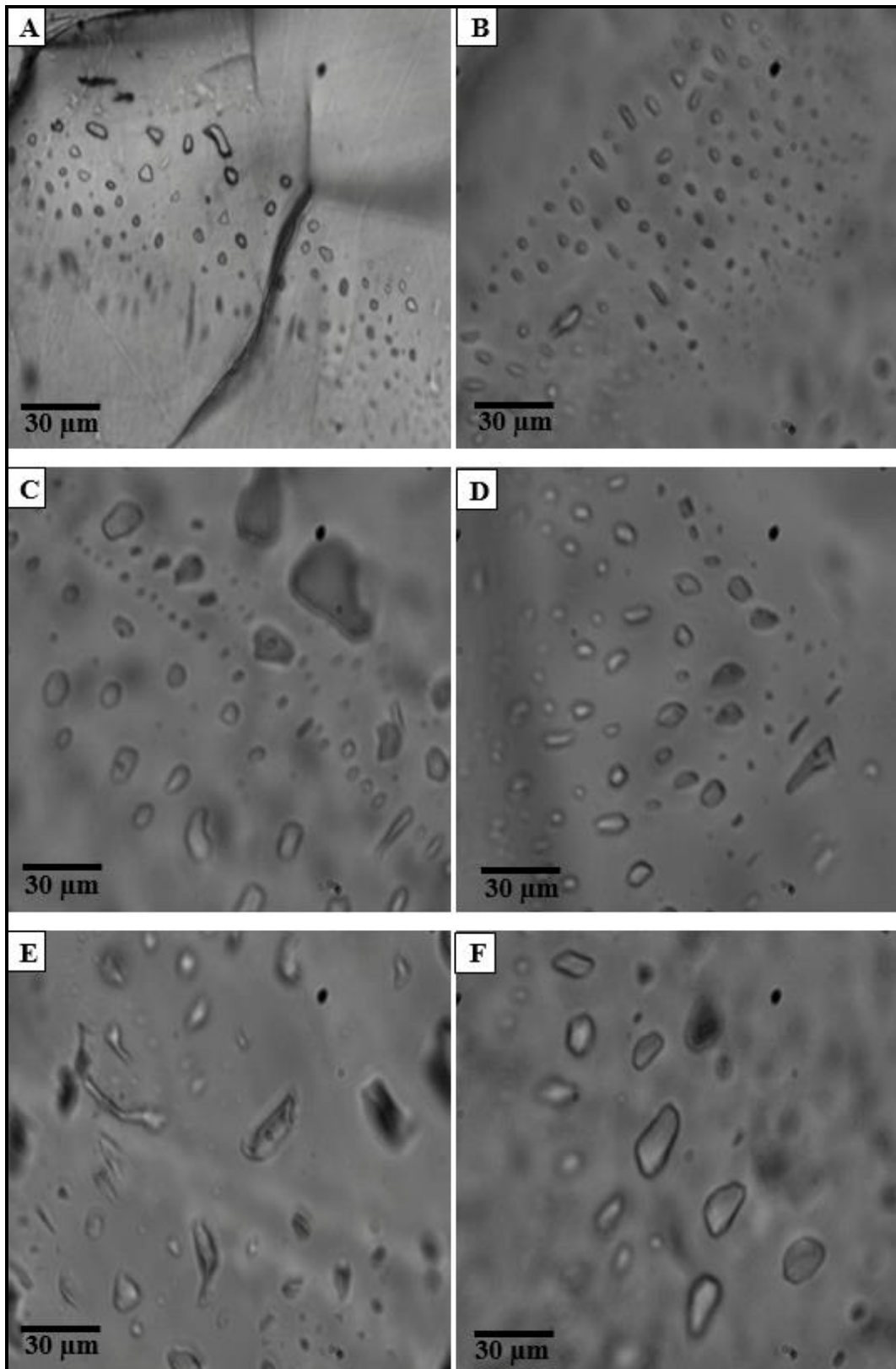


Figure 106 : Primary aqueous inclusions in blocky calcite cement

3.4.2.2.3.2 Raman microspectrometry

Despite the small size of fluid inclusions (mean size ~8 μm), Raman microspectrometry provided huge information of the fluid inclusion composition (Figure 107 to Figure 113). The study of the fluid inclusions by Raman microspectrometry shows the presence of dissolved carbon in water, nitrogen, methane and hydrogen sulphide as a gaseous phase. The solid phase represents the pyrite in the fluid inclusions. Calcite, dolomite, pyrobetumin and quartz were detected during the study of cementation events in the Mishrif Formation.

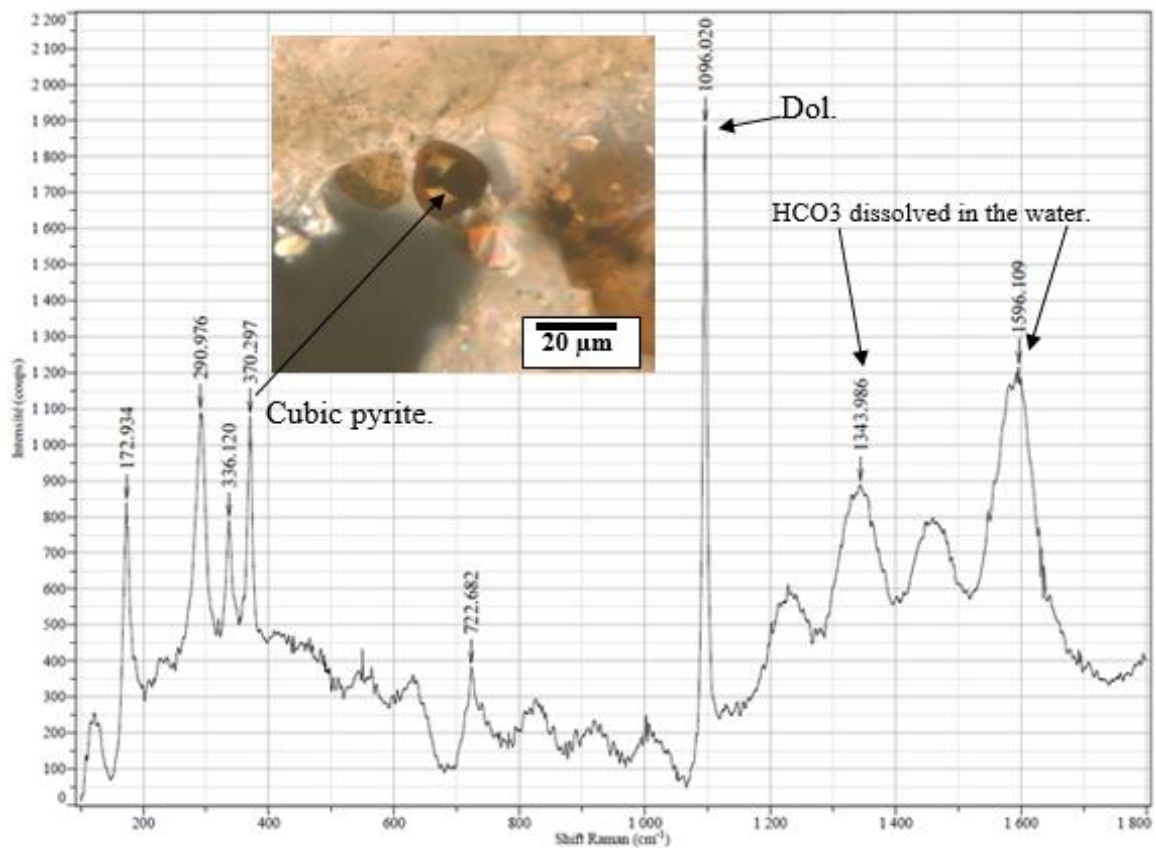


Figure 107 : Raman spectrum shows multiphase inclusion, which is in the calcite cement around moldic porosity in the NS-3 well at depth of 2014.67 m

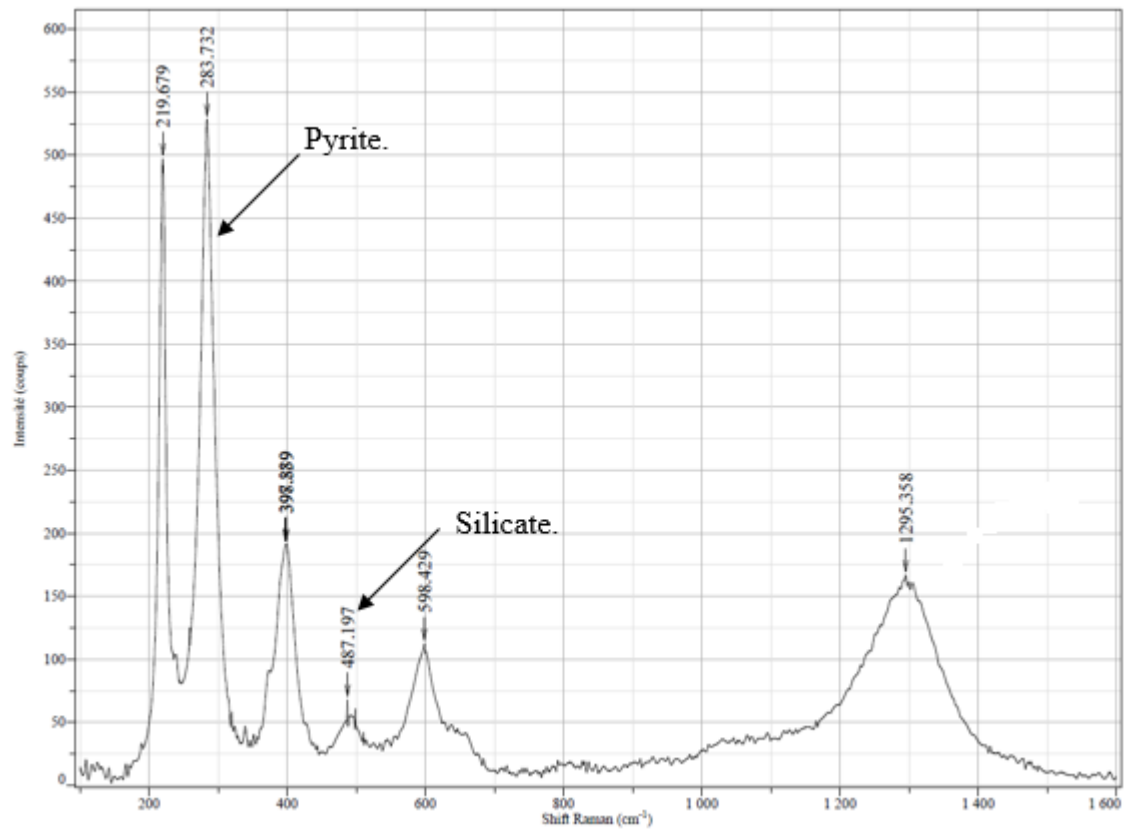


Figure 108 : Raman spectrum of the fluid inclusion shows the pyrite and silicate peaks in the NS-3 well at depth 2014.67 m

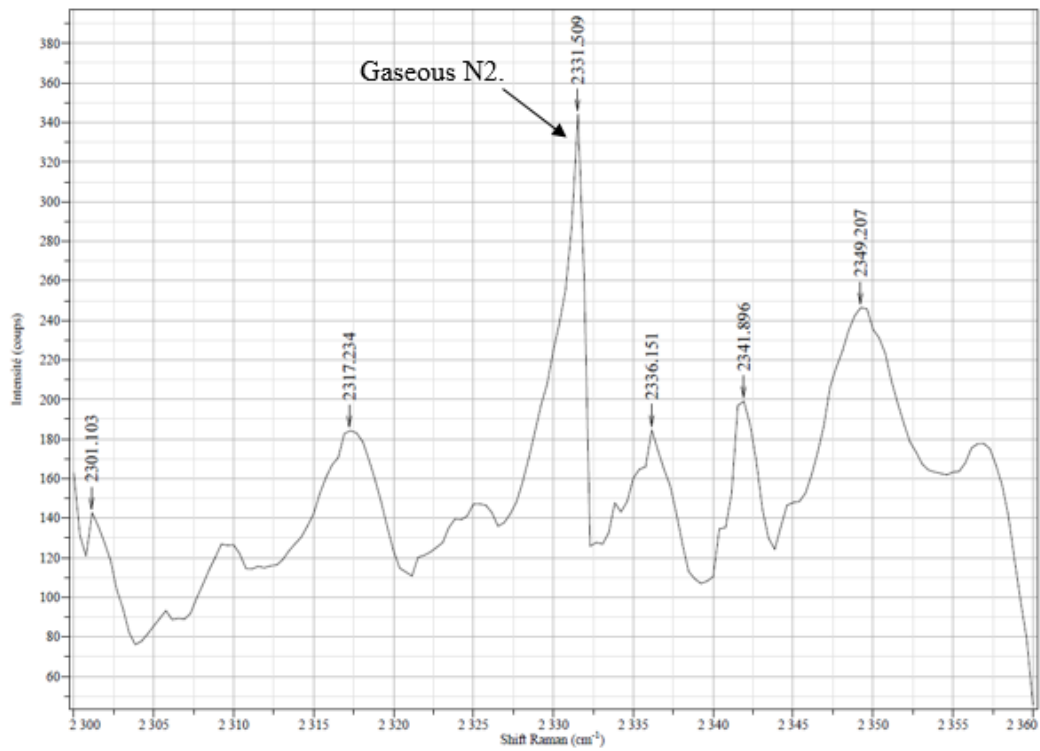


Figure 109 : Raman spectrum shows the peak of N₂ gas in the NS-1 well at depth 2033.80 m

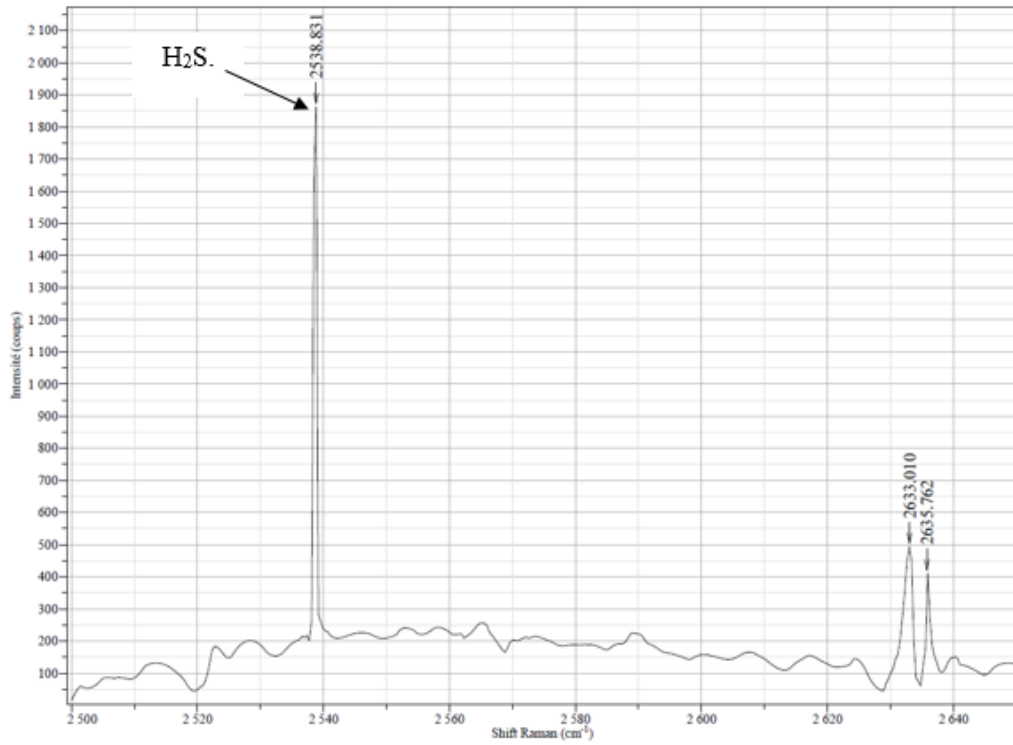


Figure 110 : Raman spectrum of a fluid inclusion indicative of the presence of H₂S gases in well NS-3 at depth 2024.25 m

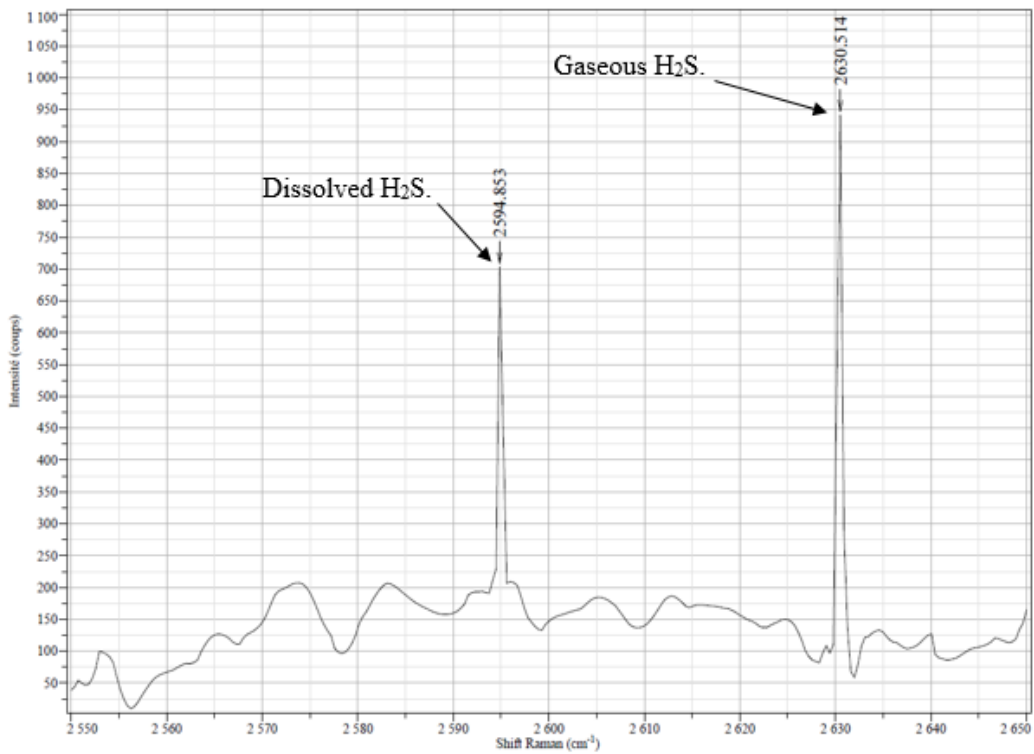


Figure 111 : Raman spectrum shows the range of H₂S peaks in the NS-1 well at depth 2033.80 m

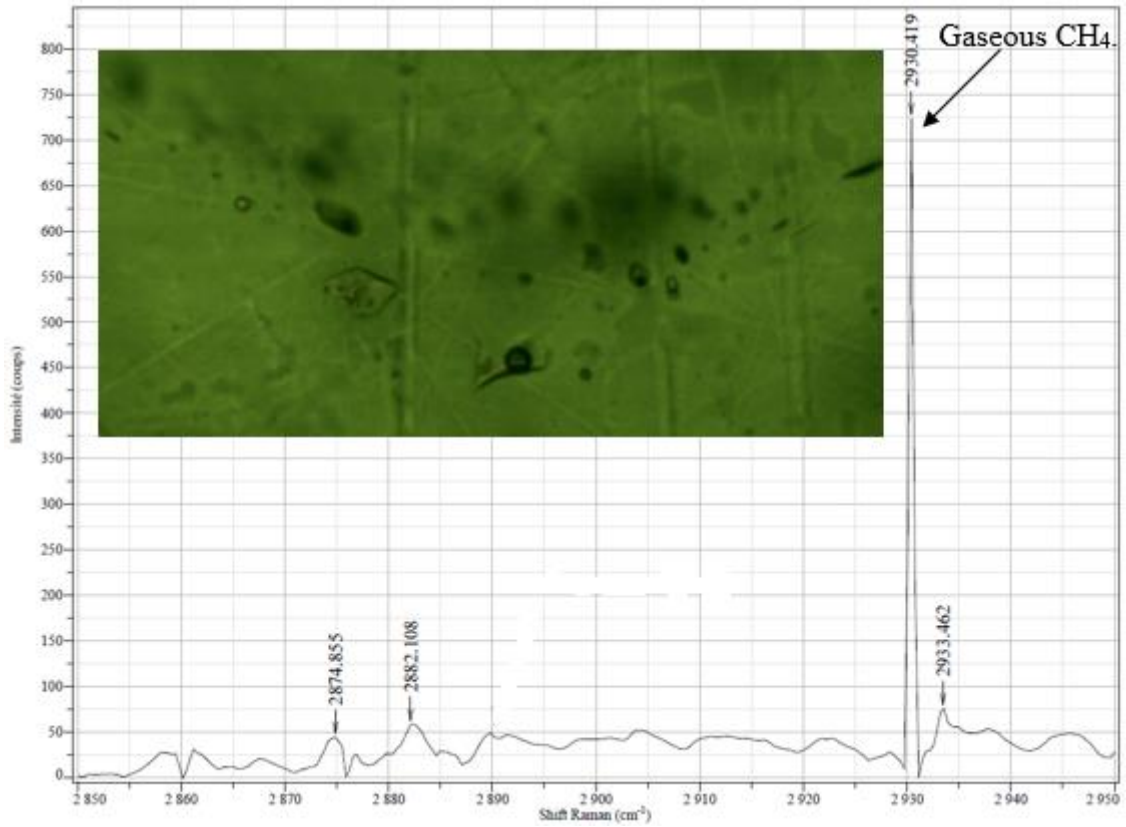


Figure 112 : Fluid inclusions show multi-peaks of methane in the NS-3 well at depth 2024.25 m

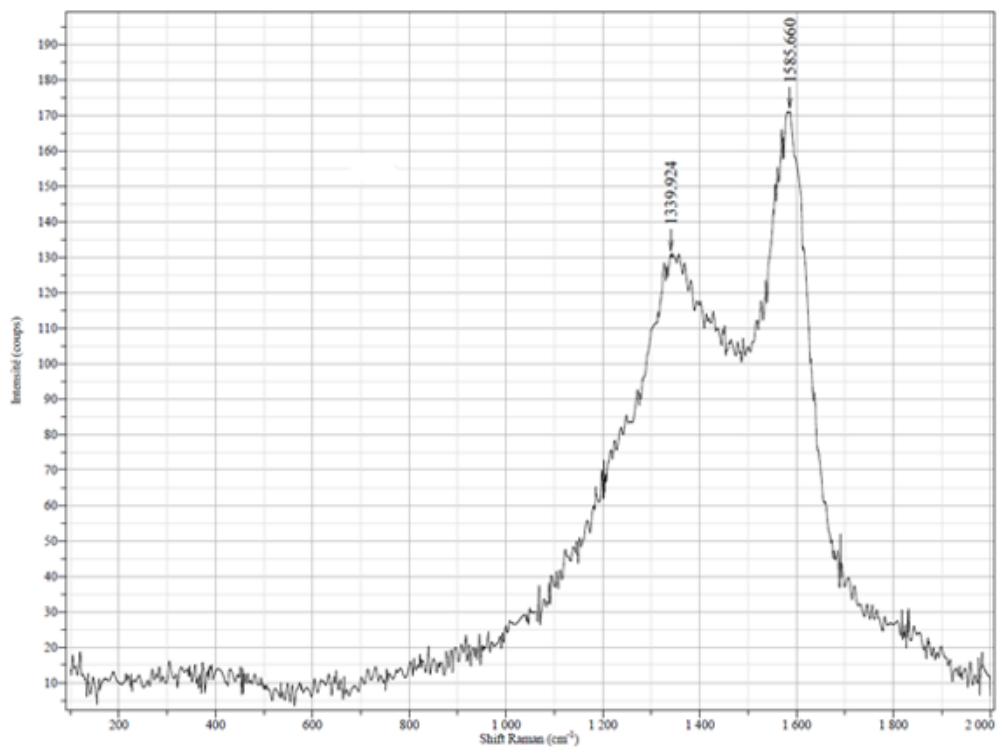


Figure 113 : Raman spectrum shows the peak of dissolved carbon in water

3.4.2.2.4 Conclusions

The fluid inclusions in the Mishrif Formation have textural characteristics, which display poor sealing and necking down features in the aqueous fluid inclusions more than in the petroleum fluid inclusions.

The aqueous fluid inclusions synchronously occurred with the first stage of migration process. Therefore, the huge abundance of aqueous fluid inclusions found in the blocky calcite cement with homogeneous temperatures range from 108°C to 175°C and the most frequency of homogeneous temperatures from 150°C to 175°C (Figure 104).

The aqueous fluid inclusions have mainly composed of H₂O-MgCl₂ system. The salinity rate of the fluid inclusions is shown according to the T_m ice values, which are plotted versus salinity of the MgCl₂ on the double-graph. Salinity ranges from 14.9 to 17.4 wt% of MgCl₂. On one hand, the high salinity of fluid inclusions indicates to the synchronous flow of the brines with trapping of these fluid inclusions. On the other hand, the fluid inclusions represented the origin of salt solutions. However, the aqueous fluid inclusions did not observe in the latter fractures. The homogeneous temperatures of petroleum fluid inclusions in the latter fractures represent the high degrees from 225 °C up to 250°C. The increase of salinity leads to decrease of the final ice melting temperature that means increase of the freezing point.

3.4.2.3 Postdated cementation steps in the stylolite systems

The stylolite systems are considered as information warehouse more than fracture systems, because in the fracture systems the conditions of interaction are different. On one hand, the fluids have velocity more than the fluids in the stylolite systems. On the other hand, stylolite systems have richly occurred in the muddy carbonate rocks comparison with fractures systems existed in the lime packstone microfacies and lime grainstone microfacies. For previous reasons, the distribution and concentration of the organic matter and the major chemical elements have high degrees of existence in the center stylolite and along the both side of stylolite (Figure 114). Muddy vesicles play important role in the support the characteristics of stylolite and enhance the storage capacity of reservoir. Muddy vesicles have clay minerals as an essential constituent with little proportion of the exotic carbonate minerals such as quartz mineral etc.

Through the SEM analyses, clay minerals have a small to large amounts in the stylolite systems (Figure 114). Clay minerals are characterized by wispy fabric with close spaces between their crystals that reflect the ghost texture. The distribution of seams solution exists in the dense zones, which undergo to high degree of compaction (Figure 82). Clay minerals are engulfed the calcite cement on the both side of stylolite that reflect the late occurrence of the clay minerals than other carbonate minerals. For that reason, intercrystalline microporosity has lately created between the crystals of muds inside muddy vesicles that has responsibility of the variable amounts of stylolite porosity.

The data were collected using EDS technique that have treated to become more normalization. Subsequently, the elemental values of these data have re-arranged based on their analytic points with excluding the O₂, C and Ca atoms. First, the oxygen atoms are lighter atoms and maybe the cathode of EDS does not fully recognize on the oxygen atoms.

Second, we use the carbon to cover the thin sections and naturally, their atoms have high ratios, which are not reliable. Third, we exclude Ca values because we work in the limestone and these rich values can be impacted on the final figures (Figure 116 and Figure 117). The difference between the Figure 116 and Figure 117 is the data in (Figure 116) contain the entire elements excepted sulfur element. In the (Figure 117), the data include all the elements with sulfur element.

The study is taking into considered all elements and the V shape in the figures (Figure 116 and Figure 117) refers to the V shape of the stylolite in fact. The presence of sulfur element has approximately 94% of atoms percentage in (Figure 117), of the fifth point of analyses with little amount of the Fe element less than 1% of atoms percentage (Table 10). The sulfur element has a high percentage in the center stylolite, because the sulfur was the later element has transported by stylolite as a pyrite or bitumen. The interaction between sulfates with Ca has early formed the CaSO_4 , which is responsible to expand the dissolution process. Last structures of pores were formed with presence of the anhydrite minerals.

The presence of pyrite in the center of stylolite and vicinity of stylolite lead to confirm the results of elemental analysis of stylolite. Due to the pyrite always lately forms than other minerals in diagenetic environments. Pyrite crystals have framboidal and discrete forms, which are engulfed by the clay minerals (Figure 114). Historical relationship between fractures systems and stylolite systems has shown using the residual materials in the lining of fractures systems and stylolite systems to constitute the paragenetic relationships. The silica element and aluminium element have a high ratio through all values of the stylolite analyses. Except in the fifth point and the ninth point included very low values because the silica and aluminium elements are represented by the primary cement as quartz linings in the primary fracture. For that reason, the primary fracture has lately occurred after the stylolite.

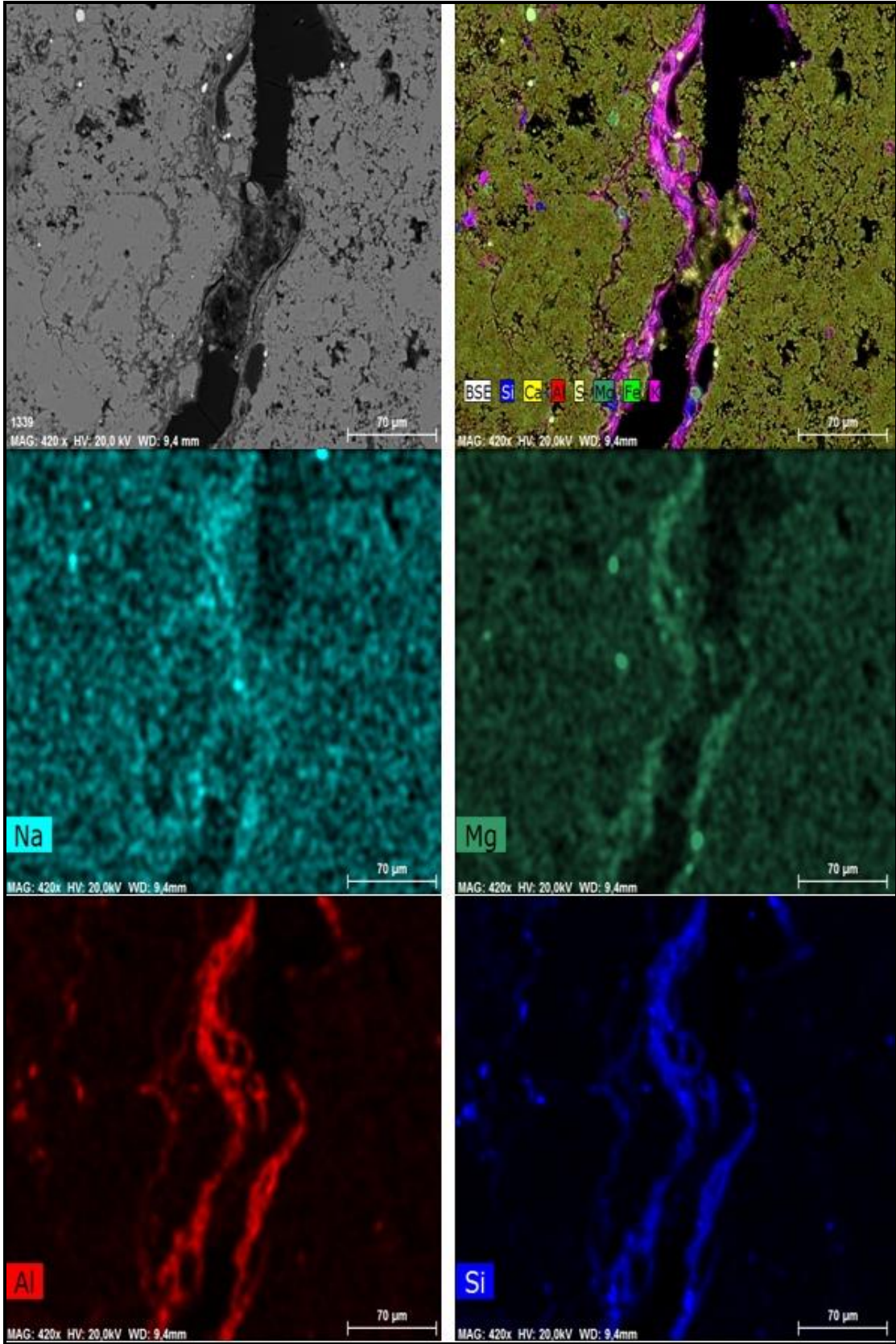
In general, fractures systems (primary and secondary) exist in the lime grainstone microfacies in the NS-5 well. These fractures have occurred as a result of increase the differential compaction, which produces the degassing fractures, included huge cementation in the both sides of fracture. That means, the stylolite systems have early occurred comparison with fractures systems. In the first stage of the differential compaction the stylolite occurs in the soft textures in the lime mudstone microfacies because the stylolite needs low compaction force for forming than fracture.

Carbonate cements occur along the stylolite, included pyrite, dolomite, blocky calcite, anhydrite and clay minerals respectively from recent to later occurrence according to the paragenetic relationship. Magnesium and manganese elements have a high ratio in the ninth point in the (Table 10) that reflect the beginning of formation secondary dolomite crystals. Taking into account, the silica and aluminium elements have little values in the same point of analysis. Euhedral rhombic to subhedral dolomite crystals have early formed than pyrite. In comparison between the ratios of the silica and aluminium elements in the fifth and ninth points lead to find the values of silica and aluminium have reduced with progress of the diagenesis process. These low values of silica and aluminium lead to confirm the dolomite crystals have early formed than pyrite. However, saddle dolomite has low proportion in the secondary fractures.

Finally, the diagenesis process can be concluded according to the values of silica and aluminium elements (Table 10) in three steps. First step is represented by primary cement of the quartz belts along of the both sides of stylolite and this step has high values of silica and aluminium elements. Second step is represented by secondary cement of the euhedral rhombic dolomite crystals in the vicinity of stylolite and this step has little values of silica and aluminium elements in the ninth point. Third step is represented by the post-secondary cement of pyrite and bitumen in the center of stylolite in the fifth point with the low values of the silica and aluminium elements, which reach to less than 1%.

Table 10 : The stylolite data are generated by using EDS technique

N° of test	Na	Mg	Al	Si	K	Mn	Fe	S
1	2,029036	4,212229	35,71465	44,11564	9,371413	0	2,815079	1,741953
2	2,83012	6,96957	30,7863	41,22882	10,43619	0	4,153095	3,595901
3	1,109097	7,757035	29,97736	41,29805	9,429434	0	7,176591	3,252434
4	11,78475	3,531923	26,59462	48,46748	5,98249	0,119356	2,263467	1,255915
5	1,459044	1,453121	0,692165	0,701625	0,661465	0,295629	0,741547	93,9954
6	1,933833	7,645042	26,32195	39,31502	8,826047	0,3166	9,010287	6,631218
7	0,165987	10,77777	28,85028	42,97719	10,13955	0,207414	5,074647	1,807166
8	0,30866	3,894125	25,73741	55,17832	9,701304	0,147303	3,20053	1,832339
9	1,317657	90,92346	1,387854	1,58812	0,339576	0,800996	3,274438	0,367902



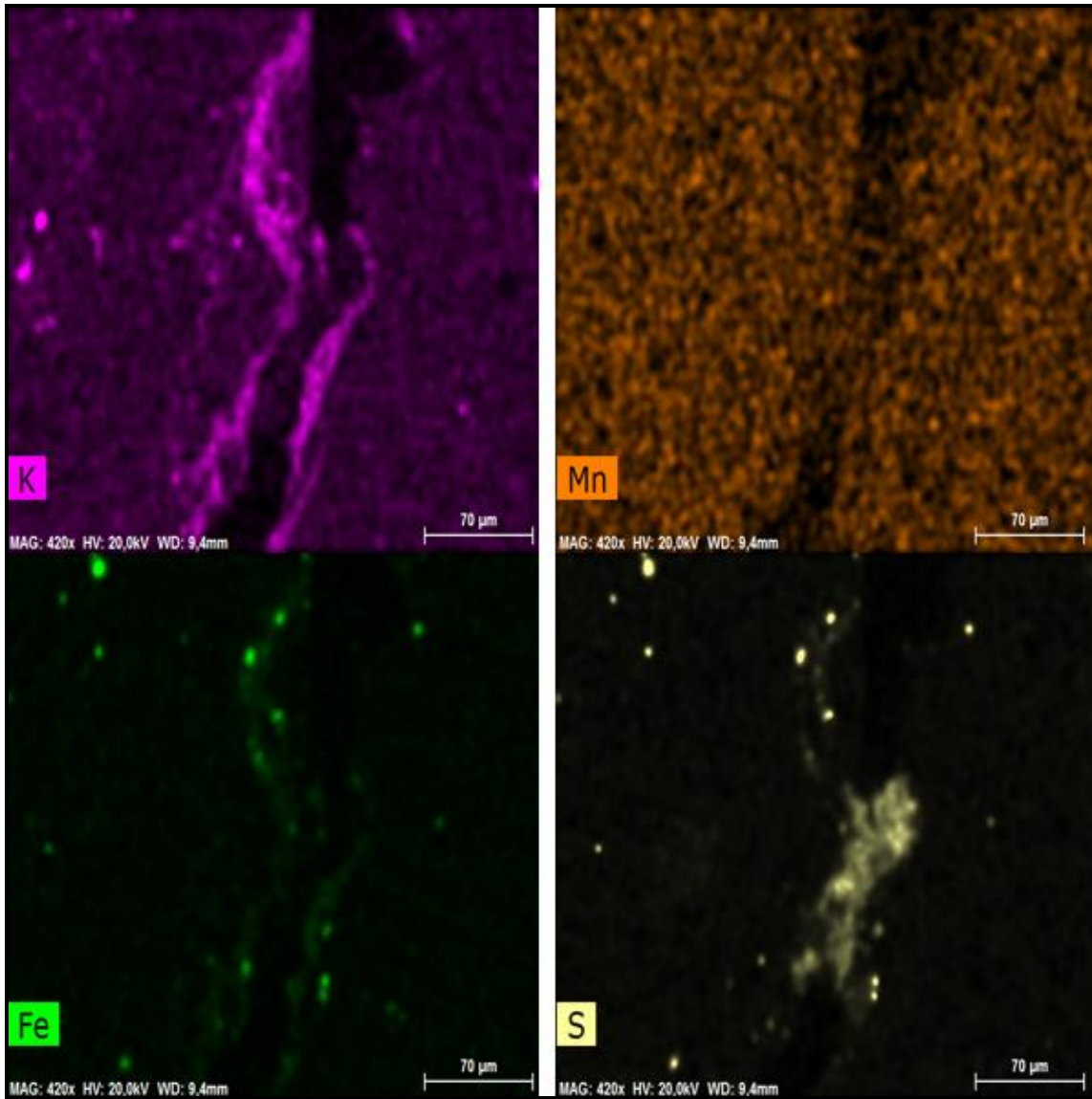


Figure 114 : The images are gained by BSE and EDS elemental map of the stylolite in muddy carbonate rocks

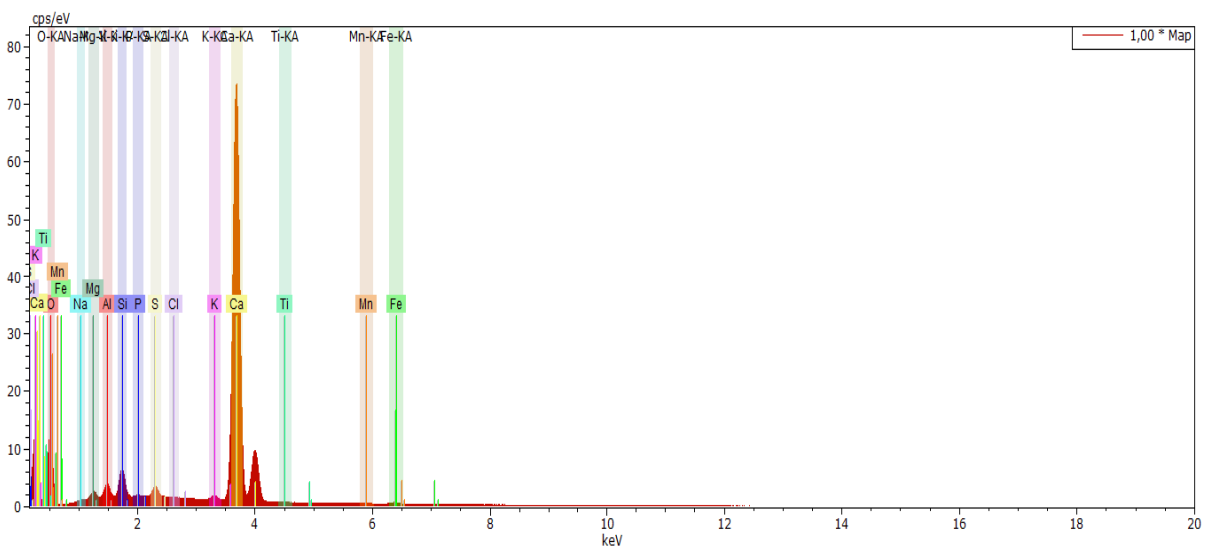


Figure 115 : Spectrum of elemental analysis is acquired by EDS technique, which is accompanied to SEM

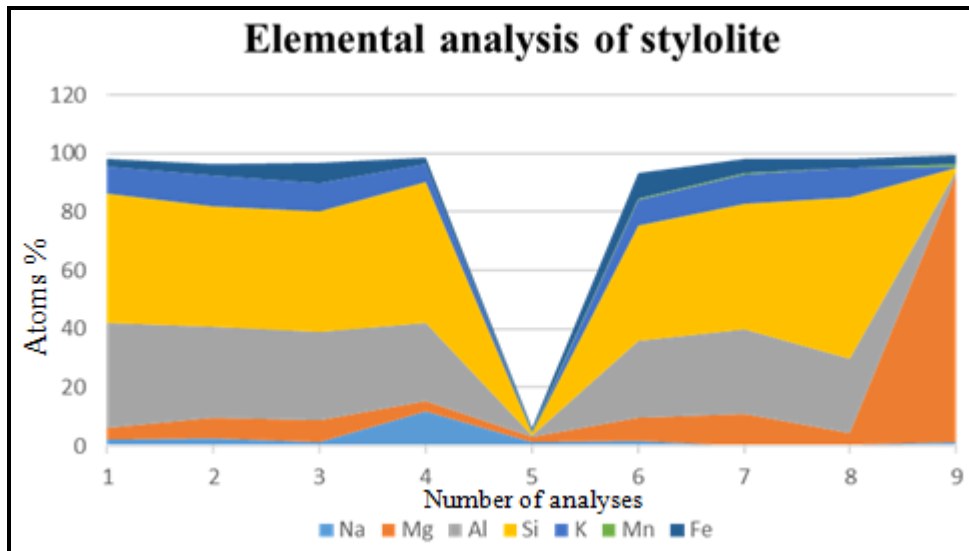


Figure 116 : Scheme of stylolite shows the data are generated by using EDS technique, near the vicinity of stylolite with absence of the sulfur element in the center of stylolite

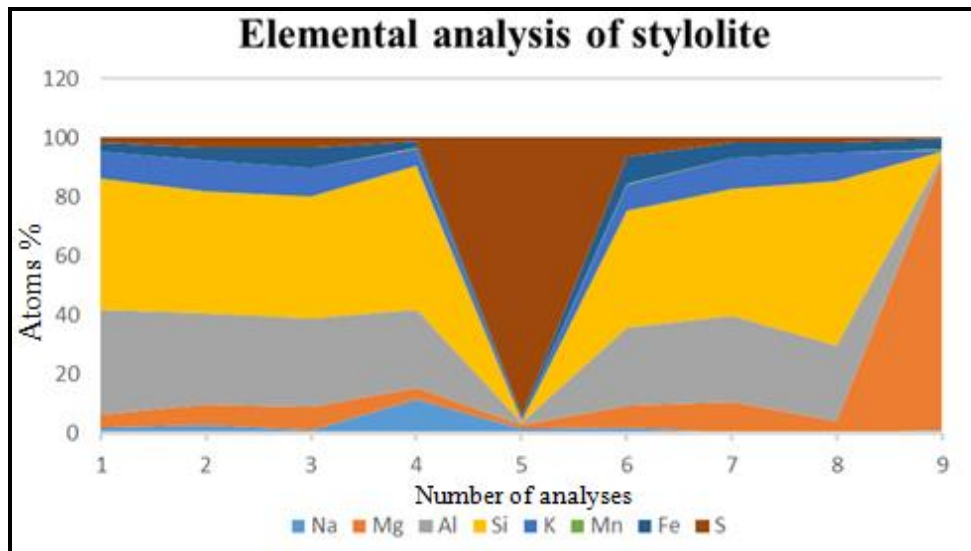


Figure 117: Scheme of stylolite shows the data are generated by using EDS technique, which look alike as a cross section of the stylolite in presence of the sulfur element

3.4.2.3.1 Conclusions

Study of stylolite systems explains the crucial role was played by stylolite in diagenesis of carbonate reservoirs and the important role in the fluid flow during basin evolution. Primary fractures occur before petroleum migration and they underwent to sealing by belts of quartz and calcite as successive belts. Some of stylolite systems were created by chemical compaction (pressure solution) before primary fractures occurrence according to results of the elemental analysis of stylolite (Table 10). Post-stylolites have occurred after primary fractures because they have minerals, which do not exist in the primary fractures. Stylolites have expansion to become post-stylolites with starting dissolution process by cut-off most the up-peak by effect of the organic acids and finally the stylolite systems going to become channels to transfer the hydrocarbon fluids.

Muddy vesicles are located along both sides of stylolite that contain of the elements resources and muddy vesicles can be impacted on the evolution of the stylolite porosity. Increase the chemical compaction process in the some zones, which are classifying as packstone to grainstone microfacies led to create new fractures, which are synchronous to petroleum migration. Secondary fractures synchronously occur with hydrocarbon migration may be named as degassing fractures, which release high amount of carbon dioxide and in the same time, precipitation process produces calcite and dolomite cements as a lining on both sides of fractures.

First type of secondary pores synchronously occurs during starting of dissolution process as vuggy pores. Dissolution regime was covered most sections of study area with beginning of the hydrocarbonic fluids migration, which are responsible on last dissolution processes. It has produced the second stage of vuggy porosity and fracture porosity. Taking into consideration, the role of cementation process works depend on the degree of saturated fluids in salts.

Cementation process took place on the first type of vuggy pores after the oil migration pass through them because there are many petroleum fluid inclusions in sealing of calcite that have yellow colour to blue colour under the florescence microscope. Dolomite mineral also occurs in the center of stylolites and on along both sides of stylolites. The crystals of dolomite have a big size in the saturated oil zone comparing with crystals of dolomite in the saturated water zone. Crystals of dolomite have produced the intercrystalline porosity, which is a secondary porosity.

Dissolution pores again occurs in the different zones of study area by increase production of gases such as a carbon dioxide, hydrogen sulfate and methane. Anhydrate mineral has deposited around nozzles pores. Post- stylolite occurs by increasing the effect of compaction process with impact of acidic fluids. Final mineral who formed was a pyrite, for that pyrite mineral distributes in center post-stylolite and along of both sides of post-stylolites.

Mishrif Formation has several forms of secondary pores, included the most abundance in the first unit of reservoir and in the second unit of reservoir, which contains high-saturated oil. Exception intercrystalline porosity between dolomite crystals is existed in the second unit of reservoir at lower part, which contains of high-saturated water. These pores include the dissolution pores (vuggy), moldic, outgassing, intercrystalline, post-stylolite porosity and fracture porosity. Mostly, these microfacies have muddy sediments with many crystals of dolomite. Exceptionally, the moldic porosity and fracture porosity that belong to coral reef microfacies. Chemical compaction processes maybe reproduced of the new shape of porosity by process of outgassing in the NS-1 well at depth of 2033.80 m (Figure 118).

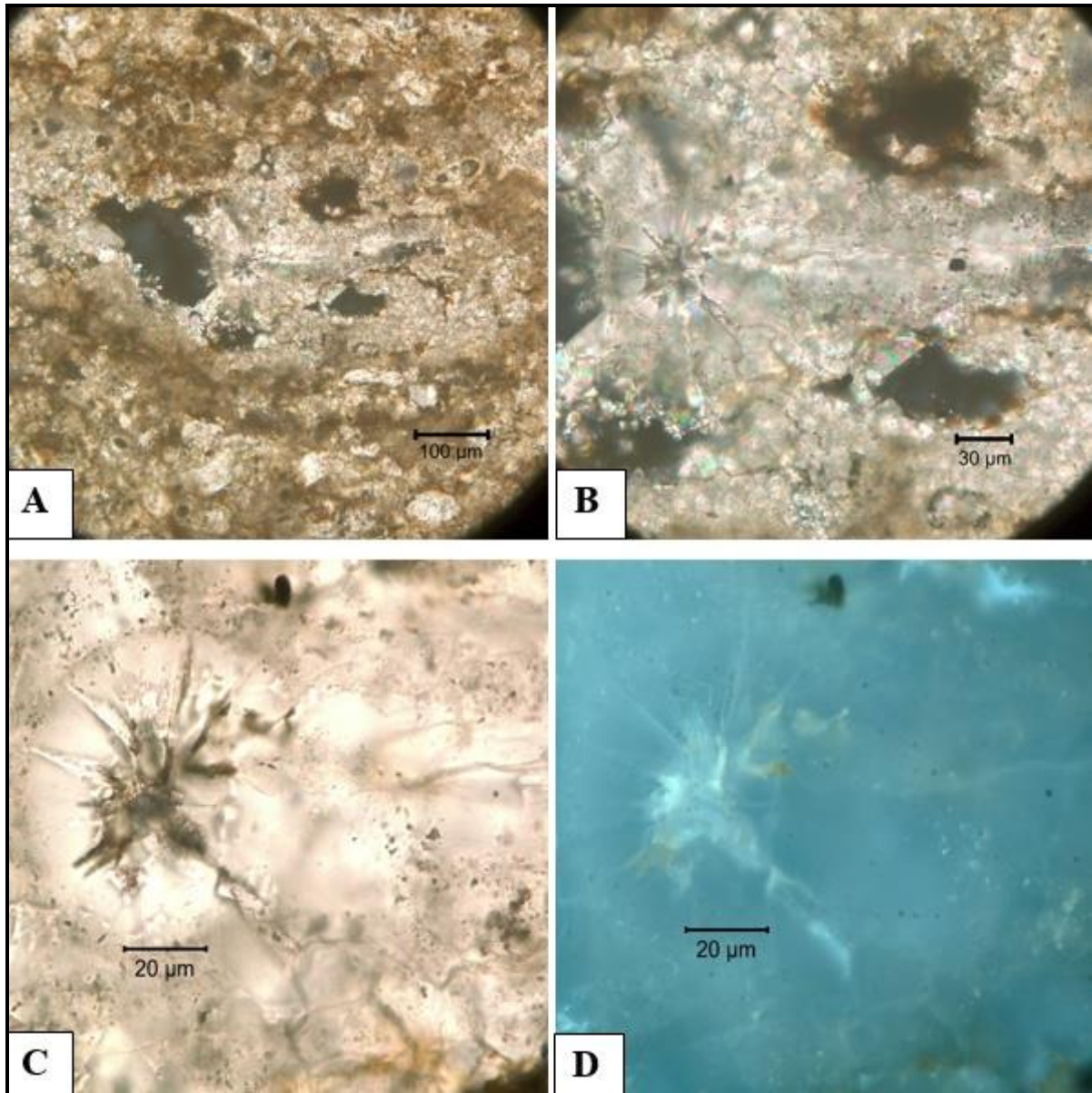


Figure 118 : Fenestral porosity is a pore space, developed by degassing process within the bioturbated wackestone microfacies in the NS-1 well at depth of 2033.80 m. Solution seams are associated by fenestral porosity

Discussion and general conclusion

Discussion and general conclusion

1. Paleogeographic features have involved of the heterogeneous distribution of microfacies in the Mishrif Formation.

Mishrif Formation in the Nasiriyah oil fields belongs to the inner rimmed carbonate shelf due to the Formation has very wide facies belts, which are available in two positions according to the synopsis standard facies belts. The nature of the composition of rudist reefs has characterized by very narrow facies belts. The results of microfacies analysis of Mishrif show the differentiation of composition between the wells in the Nasiriyah oil field. These results of microfacies analysis of the wells NS-1 and NS-2 represent the shallow lagoons environments from the restricted environment to Evaporitic environment in the inner shelf.

In addition, in some units of NS-1 and NS-2 wells, the overlapping layers are existed with other units in NS-3 and NS-5 wells where the last well represents open marine environment. The emergence of Miliolids microfacies, Microbial microfacies, Evaporitic microfacies and the decline of distribution Rudist microfacies comparing with Coral microfacies in the NS-5 well. All these previous criteria are best evidence of the conversion to the euxinic environment.

In general, Mishrif has diverse microfacies, which have represented its paleoenvironments. For explanation, the case of Mishrif Formation particularly the heterogeneous distribution of grains zones (biotic grains and abiotic grains). Mishrif could be characterized by a broad littoral part, which has huge wackestone microfacies. In same time, Mishrif is extended towards to basin part that is represented by open marine environment. Plus, it is extended to sub-continental part, which is represented by the evaporitic environment.

However, the complexity of paleogeography and the renewed impacts of tectonic movements during Upper Cretaceous have been studied. As well as, the role of Tethys Sea is represented by the flood scenario, tidal or fluctuation of sea level during this period. All these reasons above produced the heterogeneous microfacies in the Mishrif Formation. Nevertheless, based on the abundance of grains in the Mishrif Formation, they could be divided into:-

- 1- Benthic Foraminifera represent all depth levels in the Mishrif Formation in the NS-1, NS-3, and NS-5 wells. Except for the NS-2 well includes benthic foraminifera in the depth of 2014.66 m.
- 2- Coral grains represent all depth levels in the NS-5 well only.
- 3- Peloids grains have particularly represented all depth levels in the NS-2 well. Other wells of NS-1, NS-3 and NS-5 have overlapping forms of peloids microfacies.
- 4- Abundance of microbialite grains distributes in the two cycles in the NS-1 well and it exists in the other wells of Nasiriyah oil field due to the nature of paleoenvironment, which represented a shallow water of lagoons environment.
- 5- Other types of grains represent biotic or abiotic grains, which have less abundance than four types above and these other types of grains found as coexisting with the abundant grains.

2. Summary of the paleoenvironments of Mishrif Formation

The paleoenvironments of Mishrif Formation are represented by inner rimmed carbonate shelf environments to the back reef shelf environment because of:

- The abundance of benthic Foraminifera in the all wells at the all depth levels is represented by genus of (Miliolid, Alveolinids, *Discocyclina*, and *Textularia*), which are indicators for semi lagoon environment (feeder branch in the shelf reef).
- The abundance of larger Foraminifera and planktonic Foraminifera are likely interpreted based on the flood scenario or tidal movements.
- The absence of Ammonite fauna belongs to a group of the Mollusca marine environment, dating in the Cenomanian lead us to emphasize that aforementioned Foraminifera belong to back reef or open marine environments.
- The important feature in the shallow water environment is mostly reef-building coral, algae or any shallow water obstacle.
- The abundance of the colonial Corals, Mixed algae zone and Mollusca (Rudist, Gastropods and Bivalves) have classified based on the abundance of their fossils into:-
 - 1- Massive Coral zone indicates to back reef shelf environment, it exists in the NS-5 well at depth from 1999.60 to 2078.32 m.
 - 2- Mixed algae zone contains Chlorophytes and Calcareous green algae. Chlorophytes are best indicator for evaluating paleoclimate, paleolatitudes and paleoenvironmental conditions. Gyrogonites fossils are important indicators for paleosalinity. They are often associated with nonmarine and brackish-water fauna, which exist in the NS-3 well at depth from 2011.66 to 2014.67 m.
 - 3- Mollusca zone contains rudist, gastropods, and bivalves, which indicate to back reef shelf environment, they exist in the NS-3 well at depth from 1992.70 to 2075.90 m.
 - 4- The textural maturity and compositional maturity of the microcoprolite grains, aggregate grains and large skeletal-grains are best indicators of moderate and persistent currents in the shallow subtidal conditions.

3. The microfacies detect the relationship between the end of mass extinction and born new-grains

Microfacies studies show the gregarious distributions of coral species and Miliolid type of Foraminifera. On one hand, Microfacies indicate a drastic decline in abundance of rudists and the drastic decline has occurred in the Cenomanian-Turonian period. On the other hand, microfacies studies suggest that the final mass extinction of the rudist starting before Cenomanian-Early Turonian period.

This study shows the diverse wackestone microfacies comparison with other microfacies such as packstone microfacies and grainstone microfacies. This study explains the emerging new period, which characterizes by the abundance of individual organisms such as large foraminifera, rudist and algae (Chlorophyta). The individual organisms indicate to the beginning of the demise stage. The abundance of peloids grains and anhydrite microfacies are

indicators for lagoon environment too. The anhydrite minerals have typically occurred in the conditions of drought or/and the sediments of evaporite deposit after seawater regression.

Peloids have varied origins and environments. For example, algal and micritization of grains are common in open marine to restricted settings.

Microbial carbonate grains have appeared as a dome shape in NS-1 at depth of 2052.90 m as a first cycle and the second cycle of deposition has existed at depth of 2024.60 m with rounded edges. These rounded edges indicate to the Peritidal environment because of the effect of tidal movement or partially protected lagoons. The microbial microfacies are bearing excellent quality of the chemical carbonate rocks, which started from pellets and peloidal microfacies to the microbialites microfacies passing through the *Favorina* microfacies.

Rounded clastic grains are available in the restricted environment only; they may be able to become the best indicator of the restricted environment. As well as, they can provide much information on the diagenetic evolution of pores, complete migration process of hydrocarbons and abundance of fluid inclusions. Note that, the NS-2 and NS-5 wells do not have any rounded clastic grains. Previous information suggests that Mishrif Formation could become a group of several sub-formations or it should be divided into sub-stratigraphic units because:

- To overcome the complexity of paleogeographic interpretations and the redistribution of the microfacies.
- To avoid the admixture between marked microfacies.
- To determine the overlapping boundaries between Mishrif Formation from side and Kifl, Khasib, and Rumaila formations from another side.

4. Inner platform environments have well developed during Cenomanian-Early Turonian

Regardless of the stratigraphic differences are existed between the abundance of fossils in the Mishrif Formation and the absence these fossils in the Kifl Formation, which interpreted based on the converting from the normal deposition environment to euxinic environment. Euxinic conditions have occurred in the final period of Cenomanian because of drastic decline in seawater and this reason clearly seems in the wells of Nasiriyah oilfield. This observation is very clear in the depth of 2000 m from all wells except the well of NS-5 is going to margins reef.

In our opinion, the evaporitic limestones layers of the stratigraphic units of Kifl Formation in the type section of Nasiriyah oil field at the NS-1, NS-2 and NS-3 wells belong to terminal facies of the Mishrif Formation. Because, the grains maturity in the Mishrif Formation passed through different stages from Peloids grains to Microbialite grains and final stage was Microbial aggregate grains, which are responsible to form Kifl sediments.

In the type section of Kifl, the stratigraphic units are corresponding to upper lithology units of Mishrif Formation. However, the NS-2, NS-1 wells and some parts of NS-3 well respectively represent the evaporitic lagoon environments. While, the well of NS-5 represents freshwater influx (Open marine).

During Cenomanian-Early Turonian, rimmed shelf platform has marked a well-developed in the inner platform environment especial deep lagoon to open marine environments with numerous patches of the coral reefs have been observed in the Mishrif Formation. More likely to say here, it is very difficult to recognize the boundary between Mishrif and Kifl formations because Kifl Formation has gradually grown from Mishrif Formation.

Nevertheless, it is very easy to realize the boundary between Mishrif-Khasib formations from the uppermost boundary of the Mishrif Formation or Mishrif-Rumaila boundary from the lower boundary of the Mishrif Formation by observing the differentiation of mud microfacies. The carbonate muds in the Rumaila and Khasib formations are characterized by gray to blue colour, very fine grains and high concentration of planktonic Foraminifera structures, which have indicated to Marine environment.

Mishrif clearly seems as a sandwich of organic matter with fossiliferous limestone that is surrounding by the zones of carbonate mud from above is a Khasib Formation and from below is a Rumaila Formation. The layers of carbonate mud act as an impermeable cap rock. The role of Kifl Formation is a main way to provide the feedback or reactivation of the reservoir by acidic fluids.

Rumaila sediments have the large interval from the uppermost Albian into the early Turonian. Consequently, Rumaila Formation seems as a collection of facies, which belong to the heterogeneous formations. Rumaila Formation may be seen as the Mishrif Formation in the broader sense because, it is worth to be mentioned the sediments of *Hedbergella* and *Oligostegina* bearing limestone, which does not indicate to the deep basin conditions but rather these sediments indicate to the outer shelf environments.

5. Summary of steps of diagenesis process

- Tectonic fractures have formed as the primary fractures, which have high concentrations of clastic minerals, played an important role to form linings of fractures and in the same time to cover some of the fossil structures.
- Peloids grains form as a part of the secondary cycle of recrystallization process based on the size of peloids grains.
- Moldic pores have occurred as a result of continuous interaction between fluids and fossil structures.
- Reservoir fluids have chemically evolved during the previous periods from siliciclastic fluids to sulfuric liquids.
- Stylolite systems have formed and reflected threshold point of the chemical compaction process.
- Blocky cement has occurred during the second stage of stylolite systems evolution.
- Some of the rounded pores have filled by blocky cement to become post-cementation.
- Expanded stylolite systems have accompanied with formation of the final form of pores (rounded pores).
- Overpressure fracture (zigzag pattern) has formed as a result of balance failure between hydraulic pressure (pressure of pores fluids) and lithostatic pressure (column weight of the buried rocks).

- Reservoir fluids have again chemically evolved during the progress of the transport pathways (stylolite systems and fracture systems) to become hydrocarbonic fluids. This period has reflected the major steps of hydrocarbon migration.
- During evolution process of the reservoir fluids, some of the strong deformations occur on the calcite grains especially, in the endings of calcite grains before they transmute to dolomite crystals and most of the intracrystalline pores in the dolomite crystals belong to these deformations on the crystal faces of calcite grains.
- Change the minerals from calcite grains to dolomite crystals with the change of fluids characteristics, which have a high concentration of Mg cation based on the fluid inclusions analysis.
- Overpressure fractures have dolomite linings because of the huge degassing process of CO₂ comparing with siliciclastic linings in the tectonic fractures.
- Secondary porosity has risen based on the formation of intercrystalline pores between dolomite crystals.
- Some of the saddle dolomite crystals have formed in some places of the overpressure fracture.
- The final stage of diagenesis represents the redistribution of the pyrite and solid pyrobitumen in the center of stylolites and adjacent areas. This process indicates to thermal degradation process of the hydrocarbons, occurred after hydrocarbons placement in the reservoir. As well as, the abundance of the methane gas is indicated by the petroleum fluid inclusion analysis too.

6. Mechanical and chemical compaction process

Microfacies types have often determined the effect degree of the differential compaction. For example, there is not degassing fracture in the mudstone microfacies or in the wackestone microfacies but there is degassing pores in the mudstone microfacies and wackestone microfacies because these microfacies have ductile feature. Degassing fractures have existed only in the grainstone microfacies.

On one hand, the stylolite systems have usually occurred before degassing fractures and they both have occurred because of the effect of differential compaction in the same reservoir but in the different microfacies. On the other hand, the stylolite systems have described the maximum ability of the potential deformation, which has resulted from differential compaction.

For that reason, the stylolite systems have often arisen before degassing fractures, because of the first process after deposition process is a mechanical compaction process, which will produce thin layers, which will allow the water to escape and finally to produce stylolite forms. The microfacies endurance also is an important factor, reflected the anisotropic degrees of the microfacies. For example, the type of grains in these microfacies, soft grains such as the fecal grains, exposed to the deformation very fast. The occurrence of the primary cementation has been supported microfacies. Finally, the failure of the balance case between lithostatic pressure and hydrostatic pressure has firstly shown in the stylolite systems and it has secondly seemed in the fractures systems.

7. Porosity evolution in the Mishrif reservoir

Mishrif Formation shows the high diversity of organisms on the site of corals, which has included the high values of porosity in the NS-5 well. The abundance of organisms reflects the manner in which organisms have affected on the Mishrif characteristics. The abundant organisms will become organic matter with high porosity make them an important potential petroleum reservoir. Pores can be divided into two types based on the environmental conditions and the effect of dissolution process that are:

- The first type exists in the NS-1, NS-2, NS-3 wells and some parts of NS-5 well. It is characterized by secondary pores as round pores, vuggy pores, stylolite pores and channel pores. These pores have reflected the type of microfacies, which is characterized by the huge amounts of muds and these pores are affected by strong dissolution process.
- The second type exists in the NS-5 well with small units of NS-3, NS-1, and NS-2 wells respectively. It represents the moldic pores and it exists in the gregarious grains as well as, in the fossils structures when these grains have primary cementation.

Mishrif Formation has many structures of permeability as fractures, expanded stylolites, channels and connected pores that can be divided into two types:

- The first type occurs by the effect of the tectonic processes in the small-scale as a microfracture intragrain or on a massive scale as a tectonic fracture.
- The second type occurs by the effect of chemical compaction process with relatively wide, as an expanded stylolite, big channel or an overpressure fracture with the zigzag pattern. Perhaps, permeability has a large scale in the NS-5 well more than in the NS-2, NS-1, and NS-3 wells respectively, because of the type and nature of the microfacies in the NS-5 well.

Porosity evolution in the Mishrif reservoir indicates to the three types of effective porosity, which are:

1. Dissolution porosity is the pores that have resulted from the interaction between the fluids and the rocks. It is really an effective porosity and it is secondary porosity because it is still until now opening without cemented cover. Dissolution pores look alike the inner lining of the stomach, which renews every 48 hours that means the interaction is continuous.

2. Moldic porosity is an important type of effective porosity in the first step of fluids migration but now it underwent to partially cementation by the saturated fluids, which have been passed through it at that time. Now, could be say it has not considered as an effective porosity because it is semi-closing. I could say here, petroleum migration has activated after this type of porosity or this type of porosity had not the first place in the petroleum migration because of many reasons, which are:

a) The total of the reserves in the reservoir reach to the **4** billion barrels of oil, according to the Russia's Lukoil Company. Read more: <https://sputniknews.com/business/201504281021473559/> or Total oil in place is estimated to be approximately **16** billion barrels. Read more: <http://www.pcldiraq.com/index.php?p=area>

- b) There are many processes of diagenesis, which have been stopped or in the other words, which had never been to continue along with oil migration (for example the cementation have not happened).
- c) Permeability ranges from 23 to 775 md (Jreou, 2013a).
- d) The huge distribution of the petroleum fluid inclusions in the lithological Mishrif units can be reflected the manner of the reservoir filling and the pathways of oil migrations.

The huge amount of reserves has been found and some of the diagenesis processes have stopped along with oil migration. In addition, high degrees of heterogeneity are in the permeability values. The effective pores were contributing when the reservoir has been filled by the fluids. The third type of the effective porosity is a responsible factor in the formation and filling this reservoir and the path of oil migration that is:

3. Fracture systems have found in the Mishrif reservoir that divided into:

- a) Primary fractures have occurred before oil migration and they are completely out the service right now due to they are blocked by sealing materials.
- b) Secondary fractures are synchronous with oil migration process because these fractures did not close by sealing material and there are many petroleum fluid inclusions, which have been found in them.

The stylolite systems in the two types of fractures above are still right now responsible of the fluid flow and oil migration due to their attitudes or the elastic behavior, which is controlling the characteristics of Formation. In this study, the basin has developed by the critical role of stylolitization process, which is responsible for the fluid flow in the Mishrif reservoir.

Perspective

It is interesting to note that this study is involved to develop the future perspective as a regional scale of the Iraq paleogeography and the northern parts of Arabian Peninsula. On one hand, it highlights the future perspective as a local scale in the Mishrif Formation for the many geological subjects. For example, future outlooks to explore new extensions for the same Formation in the other hydrocarbon fields in the south-west parts of Iraq, related to the reservoir quality, paleodepositional environments, characteristics of fossils, diagenetic process evolution, the maturity of the calcite grains, exotic minerals in the carbonate rocks as a historical record.

1. The important events have determined the paleogeographic boundaries of study area
 - Mishrif Formation in the Nasiriyah oil field represents the end of the effect of Tethys Ocean and the effect of Tethys Ocean has gradually reduced from the NS-1 well towards the NS-5 well respectively.
 - This study opens outlooks to exploration other hydrocarbon fields in the southwest parts of the Iraq.
 - Most of our information on the Iraqi oil fields was resulted by the huge explorations of the hydrocarbons during last century from the 1930s to the 1970s. In the present day with large progress in all branches of technology should be re-study these oilfields to reform the geological and paleogeographic concepts.
2. The nature of paleoenvironment acts as an impact factor of the depositional and diagenetic processes.
 - The paleoenvironment types and the ratio of their fossils show the different values of porosity in the wells of Nasiriyah oil field, which has approximately area 34 km x 14 km. The fossils ratio increases lead to reduce the muds ratio and the vice versa. The best types of the microfacies found in the NS-5 well and this well has high values of porosity among other wells.
 - The characteristics of fossils help us to identify the change of the paleoenvironment types. For example, the transformation from the normal environment to the euxinic environment leads to mass extinction or beginning of new demise stage and at the same time leads to produce new sediments.
3. Study calcite grains in the Mishrif reservoir leads to improve our information about reservoir quality.
 - Maturity of calcite grains includes two ways. Positive way is a conversion of the calcite grains to dolomite crystals. Negative way is a transformation the calcite grains to peloids grains. To interpret this assumption needs many factors. For example, the increasing of the siliciclastic elements (silica and aluminum) will reduce the transformation process of the calcite grains to dolomite crystals. The fluid type in the dissolution-precipitation process can be determined the type of transformation process. The existence of clay minerals (carbonate mud) plays an important role as a resource of Mg elements. The wall type of some fossil structures such as Miliolids, included a

high ratio of Mg elements, helped the high Mg-calcite minerals to transform to dolomite mineral.

- According to our observations of the petrographic study maybe there is a magnetic force, which is responsible of the directing the endings of the calcite crystals (the direction of C-axis) to transform to the dolomite grains. This hypothesis states the Mg cation exists in the endings of calcite crystals, the Mg cation gravitates towards the center of the dolomite grain.

For the same hypothesis, the data is generated by EDS analys that has shown the high concentration of Mg cation in the dark zone at the center of the dolomite grain in the NS-3 well at depth of 2011.66 m (Table 7).

4. The characteristics of exotic minerals in the carbonate rocks give huge information.
 - The analysis of siliciclastic elements gives the important information about incorporated zone of the aluminum and the carbonate elements under high temperature conditions. The information leads to determine the stoichiometry of the calcium aluminates groups. The stoichiometric zone of the calcium silicate mineral can be identified by the incorporated zone of the silica elements in the intracrystalline carbonate minerals under Eh-PH conditions.
 - Fluid inclusions show huge information of the characteristics of paleofluids, which reflect the historical events, occurred by changing the mineral phases (calcite and quartz). The differentiation in the compositions of fluid inclusions reflects the nature of paleofluids evolution, which gives us the support to do this analysis in the other oilfields to identify the affinity, differences and the distribution of paleofluids in the regional scale.
5. The characteristics of Mishrif reservoir are always going to renew.

Usually, the porosity rate gives us the huge information of the reserves volume of the fluids. Permeability gives us information about the filling manner of the reservoir. The continuous interaction between fluids and rocks with increasing the effect of mechanical and chemical compaction leads to generate new properties under different conditions of the tectonic activity and the paleogeographic changes. For that reason, the characteristics of the Mishrif in the time of filling reservoir are different of the characteristics of the Mishrif in present day. By taking into account, the stored volume of the hydrocarbons comparing with porosity and permeability of the reservoir in the present day.

References

References.

- Ahr, W. M., 2011, *Geology of carbonate reservoir: the identification, description and characterization of hydrocarbon reservoirs in carbonate rocks*: John Wiley & Sons.
- AL Naqib, K. M., 1985, *Geology of the Arabian Peninsula southwestern Iraq*: UNITED STATES GOVERNMENT PRINTING OFFICE, U.S. GEOLOGICAL SURVEY, no. Second edition.
- Al-Ameri, T. K., J. Pitman, M. E. Naser, J. Zumberge, and H. A. Al-Haydari, 2011, Programed oil generation of the Zubair Formation, Southern Iraq oil fields : results from Petromod software modeling and geochemical analysis : *Arabian Journal of Geosciences*, v. 4, no. 7–8, p. 1239–1259.
- Al-Dabbas, M., J. Al-Jassim, and S. Al-Jumaily, 2010, Depositional environments and porosity distribution in regressive limestone reservoirs of the Mishrif Formation, Southern Iraq : *Arabian Journal of Geosciences*, v. 3, no. 1, p. 67–78.
- Al-Itbi, N. T. M., 2013, *Reservoir Charact Stratigraphic Relation Formation in Ghar* : University of Baghdad.
- Al-Khafaji, A. J. (2015). The Mishrif, Yamama, and Nahr Umr reservoirs petroleum system analysis, Nasiriya oilfield, Southern Iraq. *Arabian Journal of Geosciences*, 8(2), 781-798.
- AL-Khalidi, Z. A. S., 2004, Determination of effective porosity and petrophysical characterization for Mishrif Formation in Halfayia oil field. M.Sc. Thesis: Baghdad.
- Al-Khersan, H., 1973, *Mishrif Formation—regional study*: INOC library, Baghdad (unpublished report).
- Al-Naqib, K. M., 1967, *Geology of the Arabian Peninsula: South-Western Iraq*, United State Geological Survey, Professional Paper, v. 560, no. First edition.
- Al-Nuaimy, K. A., 1990, *Study of Large Foraminifera in Middle Cretaceous (Albian– Cenomanian) of Iraq*, Unpub : Ph. D. Thesis, University of Baghdad. College of Science.
- Al-Sharhan, A. S., 1995, Facies variations, diagenesis and exploration potential of the Cretaceous rudist-bearing carbonates of the Arabian Gulf: *American Association of Petroleum Geologists*, v. Bulletin 79, p. 531–550.
- Alsharhan, A. S., and C. G. S. C. Kendall, 1986, Precambrian to Jurassic rocks of Arabian Gulf and adjacent areas : their facies, depositional setting, and hydrocarbon habitat : *AAPG Bulletin*, v. 70, no. 8, p. 977–1002.

- Alsharhan, A. S., and A. E. M. Nairn, 1986, A review of the Cretaceous formations in the Arabian Peninsula and Gulf : Part I. Lower Cretaceous (Thamama Group) stratigraphy and paleogeography : *Journal of Petroleum Geology*, v. 9, no. 4, p. 365–391.
- Alsharhan, A. S., and A. E. M. Nairn, 1988, A REVIEW OF THE CRETACEOUS FORMATIONS IN THE ARABIAN PENINSULA AND GULF : PART II. MID-CRETACEOUS (WASIA GROUP) STRATIGRAPHY AND PALEOGEOGRAPHY: *Journal of Petroleum Geology*, v. 11, no. 1, p. 89–112.
- Alsharhan, A. S., and J. L. Sadd, 2000, Stylolites in Lower Cretaceous carbonate reservoirs, UAE.
- Al-Siddiki, A. A., 1978, Subsurface geology of southeastern Iraq, *in* 10th Arab Petroleum Congress, Tripoli, Libya.
- AL-Zaidi, M., 2013, Affinity and distribution of curde oil Nasiriyah oil field, Baghdad.
- Anderson, T. F., and M. A. Arthur, 1983, stable isotope of oxygen and carbon and their application to sedimentologic and paleoenvironmental problems : Tulsa, OK, SEPM Short Course, v. 10, p. 151.
- Aqrawi, A. A. M., J. C. Goff, A. D. Horbury, and F. N. Sadooni, 2010, *The Petroleum Geology of Iraq* : Scientific Press, p. 424 p.
- Aqrawi, A. A. M., G. A. Thehni, G. H. Sherwani, and B. M. A. Kareem, 1998, Mid-Cretaceous rudist-bearing carbonates of the Mishrif Formation: an important reservoir sequence in the Mesopotamian Basin, Iraq: *Journal of Petroleum Geology*, v. 21, no. 1, p. 57–82.
- Banner, J. L., 1995, Application of the trace element and isotope geochemistry of strontium to studies of carbonate diagenesis : *Sedimentology*, v. 42, no. 5, p. 805–824.
- Bathurst, R. G. C., 1975, Carbonate sediment and their diagenesis 2nd Developments in sedimentology: Elsevier Publ. Co., v. 12, p. 658.
- Belaribi, I., 1982, Sedimentary environment and the distribution of facies in Mishrif Formation southern-Iraq : M. Sc Thesis, University of Baghdad.
- Bell, D., and G. ROSSMAN, 1992, Water in earth's mantle- The role of nominally anhydrous minerals: *Science*, v. 255, no. 5050, p. 1391–1397.
- Bellen, R. C. van, H. V. Dunnington, R. Wetzels, and D. Morton, 1959, *Lexique Stratigraphique internal Asie, Irak*.
- Berger, W. H., 1976, Biogenous deep sea sediments: Production, preservation and interpretation, *Treatise on Chemical Oceanography*, 5 JP Riley, R: Chester.

- Berger, B. R., and P. M. Bethke, 1985, *Geology and geochemistry of epithermal systems* : Society of economic geologists.
- Berner, R. A., 1984, Sedimentary pyrite formation: an update: *Geochimica et cosmochimica Acta*, v. 48, no. 4, p. 605–615.
- Bhattacharyya, A., and G. M. Friedman, 1979, Experimental compaction of ooids and lime mud and its implication for lithification during burial: *Journal of Sedimentary Research*, v. 49, no. 4.
- Bhattacharyya, A., and G. M. Friedman, 1984, Experimental compaction of ooids under deep-burial diagenetic temperatures and pressures: *Journal of Sedimentary Research*, v. 54, no. 2.
- Bodnar, R. J., 2003a, Introduction to fluid inclusions: *Fluid inclusions: Analysis and interpretation*, v. 32, p. 1–8.
- Bodnar, R. J., 1990, Petroleum migration in the Miocene Monterey Formation, California, USA: constraints from fluid-inclusion studies: *Mineralogical magazine*, v. 54, no. 375, p. 295–304.
- Bodnar, R. J., 2003b, Reequilibration of fluid inclusions: *Fluid inclusions: Analysis and interpretation*, v. 32, p. 213–230.
- Bodnar, R. J., T. J. Reynolds, and C. A. Kuehn, n.d., Chapter five of *Fluid inclusions systematics in epithermal systems* in the book of *Geology and geochemistry of epithermal systems*: Society of economic geologists, v. 2, p. 73–98.
- Boggs, S., and D. Krinsley, 2006, *Application of cathodoluminescence imaging to the study of sedimentary rocks*: Cambridge University Press.
- Bolli, H. M., J. B. Saunders, and K. Perch-Nielsen, 1985, *Plankton stratigraphy*.: Cambridge (University Press)., p. 1032 p.
- Braithwaite, C. J. R., 1989, Stylolites as open fluid conduits: *Marine and Petroleum Geology*, v. 6, no. 1, p. 93–96.
- Brantley, S. L., 1992, The effect of fluid chemistry on quartz microcrack lifetimes: *Earth and Planetary Science Letters*, v. 113, no. 1–2, p. 145–156.
- Brantley, S. L., B. Evans, S. H. Hickman, and D. A. Crerar, 1990, Healing of microcracks in quartz: Implications for fluid flow: *Geology*, v. 18, no. 2, p. 136–139.
- Briggs, L. I., D. S. McCULLOCH, and F. MOSER, 1962, The hydraulic shape of sand particles: *Jour. Sed. Petrology*, v. 32, p. 645–656.

- Brocks, J. J., G. D. Love, R. E. Summons, A. H. Knoll, G. A. Logan, and S. A. Bowden, 2005, Biomarker evidence for green and purple sulphur bacteria in a stratified Palaeoproterozoic sea: *Nature*, v. 437, no. 7060, p. 866–870.
- Bronnimann, P., 1955, Microfossils incertae sedis from the Upper Jurassic and Lower Cretaceous of Cuba: *Micropaleontology*, p. 28–51.
- Buday, T., 1980a, The regional geology of Iraq: stratigraphy and paleogeography: State Organization.
- Buday, T., 1980b, The regional geology of Iraq: stratigraphy and paleogeography: State Organization.
- Buday, T., and S. Z. Jassim, 1984, Tectonic map of Iraq: DG of geological Survey and mineral investigation, Cartography Department.
- Buday, T., and S. Z. Jassim, 1987, The Regional geology of Iraq, vol. 2: Tectonism, Magmatism and Metamorphism: Publication of GEOSURV, Baghdad, v. 352.
- Budd, D. A., 1997, Cenozoic dolomites of carbonate islands: their attributes and origin: *Earth-Science Reviews*, v. 42, no. 1–2, p. 1–47.
- Budd, D. A., U. Hammes, and W. B. Ward, 2000, Cathodoluminescence in calcite cements: new insights on Pb and Zn sensitizing, Mn activation, and Fe quenching at low trace-element concentrations: *Journal of Sedimentary Research*, v. 70, no. 1, p. 217–226.
- Burne, R. V., and L. S. Moore, 1987, Microbialites: organosedimentary deposits of benthic microbial communities: *Palaios*, p. 241–254.
- Burns, S. J., and P. A. Baker, 1987, A geochemical study of dolomite in the Monterey Formation, California: *Journal of Sedimentary Research*, v. 57, no. 1.
- Burruss, R. C., 1981, Hydrocarbon fluid inclusions in studies of sedimentary diagenesis: Short course in fluid inclusion: Application to petrology. Mineral. Assoc. Canada, v. 6, p. 138–156.
- Burruss, R. C., K. R. Cercone, and P. M. Harris, 1983, Fluid inclusion petrography and tectonic-burial history of the Al Ali No. 2 well: Evidence for the timing of diagenesis and oil migration, northern Oman Foredeep: *Geology*, v. 11, no. 10, p. 567–570.
- Cambridge Carbonates, 2008 cited in Aqrawi, A. A. M., J. C. Goff, A. D. Horbury, and F. N. Sadooni, 2010, *The Petroleum Geology of Iraq*: Scientific Press, p. 424 p.
- Carozzi, A. V., and D. Von Bergen, 1987, Stylolitic porosity in carbonates: a critical factor for deep hydrocarbon production: *Journal of Petroleum Geology*, v. 10, no. 3, p. 267–282.

- Carpenter, A. B., 1978, Origin and chemical evolution of brines in sedimentary basins, *in* SPE Annual Fall Technical Conference and Exhibition: Society of Petroleum Engineers.
- Chatton, M., and E. Hart, 1962, Announcement of a new rock unit: Kifel Formation: Iraq Petroleum Company unpublished report, Oil Exploration Company archive, Baghdad, Iraq.
- Chatton, M., and E. Hart, 1962c, Announcement of a new rock unit, Kifel Formation: Baghdad, Iraq.
- Chatton, M., and E. Hart, 1961, Review of the Cenomanian to Maastrichtian stratigraphy in Iraq, the Cenomanian cycle: Unpublished report, Oil Exploration Company, Baghdad.
- Chatton, M., and E. Hart, 1962b, Review of the Cenomanian to Maastrichtian stratigraphy in Iraq, the Upper Campanian-Maastrichtian cycle: Baghdad, Iraq.
- Choquette, P. W., and N. P. James, 1990, Limestones—the burial diagenetic environment: Diagenesis: Geoscience Canada, Reprint Series, v. 4, p. 75–111.
- Choquette, P. W., and L. C. Pray, 1970, Geologic nomenclature and classification of porosity in sedimentary carbonates: AAPG bulletin, v. 54, no. 2, p. 207–250.
- Collins, A., 1975, Geochemistry of oilfield waters: Elsevier.
- Coogan, A. H., 1970, Measurements of compaction in oolitic grainstone: Journal of Sedimentary Research, v. 40, no. 3.
- Coogan, A. H., and R. W. Manus, 1975, Compaction and diagenesis of carbonate sands: Developments in Sedimentology, v. 18, p. 79–166.
- Couradeau, E., K. Benzerara, D. Moreira, and P. López-García, 2017, Protocols for the Study of Microbe–Mineral Interactions in Modern Microbialites: Hydrocarbon and Lipid Microbiology Protocols: Field Studies, p. 319–341.
- Crawford, M. L., 1981, Phase equilibria in aqueous fluid inclusions: Short course in fluid inclusions: applications to petrology, v. 6, p. 75–100.
- Darmoian, S., 1975, Stratigraphy and micropaleontology of the upper Cretaceous Aruma Supergroup, southwestern Iraq: Journ. Geol. Soc. special issue, p. 89–116.
- Dawson, W. C., 1988, Stylolite porosity in carbonate reservoirs: American Association of Petroleum Geologists, Tulsa, OK.
- Dihny 1998 cited by ,Aqrawi, A. A. M., T. A. Mahdi, G. H. Sherwani, and A. D. Horbury, 2010, Characterisation of the Mid-Cretaceous mishrif reservoir of the southern Mesopotamian Basin, Iraq.: n AAPG GEO Middle East Geoscience Conference, Bahrain, v. 7, p. 10.

- Dickson, J. A. D., and A. H. Saller, 1995, Identification of subaerial exposure surfaces and porosity preservation in Pennsylvanian and Lower Permian shelf limestones, eastern Central Basin platform, Texas.
- Ditmar, V. I., F. A. Begishev, J. T. Afanasiev, M. G. Belousova, B. A. Briousov, E. M. Petcheremnyh, E. I. Shmakova, and N. P. Nazarov, 1972, Geological conditions and hydrocarbon prospects of the republic of Iraq, VII, south Iraq: Int. report, INOC library, Baghdad, Iraq.
- Ditmar, V., and Iraqi-Soviet Team, 1971, Geological conditions and hydrocarbon prospects of the Republic of Iraq (Northern and Central parts): Manuscript report, INOC Library, Baghdad.
- Dominguez, G. C., 1992, Carbonate reservoir characterization: a geologic-engineering analysis: Elsevier.
- Douban, A. F., and F. Medhadi, 1999, Sequence chronostratigraphy and Petroleum Systems of the Cretaceous Megasequences, Kuwait, *in* AAPG international Conference and Exhibition: p. 152–155.
- Dubois, M., 2003, Les grandes étapes du développement de l'étude des inclusions fluides: (COFRHIGEO) Comité Français D'Histoire de la Géologie, v. Troisième série séance du 12 mars 2003, p. 1–22.
- Dunham, R. J., 1962, Classification of carbonate rocks according to depositional textures.
- Dunham, R. J., 1971, Meniscus cement: Carbonate cements, v. 19, p. 297–300.
- Dunham, J. B., and S. Larter, 1981, Association of stylolitic carbonates and organic matter: Implications for temperature control on stylolite formation: AAPG Bulletin, v. 65, no. 5, p. 922–922.
- GeoMika, 2013, http://geomika.com/blog/2013/07/27/carbonate-classification/gloss_dunhams/.
- Dunnington, H. V., 1967a, Aspects of diagenesis and shape change in stylolitic limestone reservoirs, *in* 7th World Petroleum Congress: World Petroleum Congress.
- Dunnington, H. V., 1958, Generation, migration, accumulation, and dissipation of oil in northern Iraq: Middle East.
- Dunnington, H. V., 1967b, Stratigraphical distribution of oilfields in the Iraq-Iran-Arabia Basin: Journal Institute Petroleum, v. 53, p. 129–161.
- Eichenseer, H. T., F. R. Walgenwitz, and P. J. Biondi, 1999, Stratigraphic control on facies and diagenesis of dolomitized oolitic siliciclastic ramp sequences (Pinda Group, Albian, offshore Angola): AAPG bulletin, v. 83, no. 11, p. 1729–1758.

- Elliott, G. F., 1962, More microproblematica from the Middle East: *Micropaleontology*, p. 29–44.
- Enos, P., and L. H. Sawatsky, 1981, Pore networks in Holocene carbonate sediments: *Journal of Sedimentary Research*, v. 51, no. 3.
- Erik, F., 2004, *Microfacies of carbonate rocks: analysis, interpretation and application*: Springer Berlin.
- Ermakov, N. P., 1968, Microinclusions in minerals as a source of scientific information on physico-chemical conditions of deep ore-formation, in *Mineralogical thermometry and barometry*: Moscow, Nauka, Press, v. 1, p. 13–28.
- Ermakov, N. P., 1950, *Research on mineral-forming solutions*: Kharkov Univ. Press, v. 460, p. 1957–58.
- Fjaer, E., R. M. Holt, P. Horsrud, A. M. Raaen, and R. Risnes, 2008, Mechanics of hydraulic fracturing: *Developments in petroleum science*, v. 53, p. 369–390.
- Flügel, E., 1977, Environmental models for Upper Paleozoic benthic calcareous algal communities, in *Fossil algae*: Springer, p. 314–343.
- Flügel, E., 1982, Introduction to Facies Analysis, in *Microfacies Analysis of Limestones*: Springer, p. 1–26.
- Flügel, E., 2010, *New Perspectives in Microfacies: Microfacies of Carbonate Rocks*, p. 1–6.
- Flügel, E., 1981, Paleocology and facies of Upper Triassic reefs in the Northern Calcareous Alps.
- Flügel, E., and Flügel-Kahler, 1997 cited in Flügel, 2010, *New Perspectives in Microfacies*.
- Folk, R. L., 1959, Practical petrographic classification of limestones: *AAPG Bulletin*, v. 43, no. 1, p. 1–38.
- Folk, R. L., 1962, Spectral subdivision of limestone types.
- Folk, R. L., 1974, The natural history of crystalline calcium carbonate: effect of magnesium content and salinity: *Journal of Sedimentary Research*, v. 44, no. 1.
- Folk, R. L., and L. S. Land, 1975, Mg/Ca ratio and salinity: two controls over crystallization of dolomite: *AAPG bulletin*, v. 59, no. 1, p. 60–68.
- Fox 1957 cited in AL-Zaidi, 2013, *ffinity and distribution of curde oil Nasiriyah oil field*.
- Fuloria, R., 1976, *Petroleum prospects analysis of southern Iraq, with particular reference to Yamama Formation*: Iraq National Oil Company unpublished report: Southern Petroleum Organization, Geo—logical Laboratories, Basrah, Iraq.
- Furst, M., 1970, *Stratigraphie und Werdegang der Oestlichen Zagrosketten Iran*, Erlangen.: Geol. Abhandlungen, Erlangen., p. 80.

- Gaddo, J. Z. H., 1971, The Mishrif formation palaeoenvironment in the Rumaila/Tuba/Zubair region of S. Iraq: *Journal of the Geological Society of Iraq*, v. 4, p. 1–12.
- Geological Survey of India, n.d., Standard operating procedure - Fluid inclusion studies.: <http://www.portal.gsi.gov.in/gsiDoc/pub/updated%20sop%20for%20fluid%20inclusion%20lab%202014.pdf>, v. Mission-IV, p. 1–20.
- Gili, E., J.-P. Masse, and P. W. Skelton, 1995, Rudists as gregarious sediment-dwellers, not reef-builders, on Cretaceous carbonate platforms: *Palaeogeography, Palaeoclimatology, Palaeoecology*, v. 118, no. 3–4, p. 245–267.
- Given, R. K., and B. H. Wilkinson, 1985, Kinetic control of morphology, composition, and mineralogy of abiotic sedimentary carbonates: *Journal of Sedimentary Research*, v. 55, no. 1.
- Goldhammer, R. K., 1997, Compaction and decompaction algorithms for sedimentary carbonates: *Journal of Sedimentary Research*, v. 67, no. 1.
- Goldstein, R. H., 2001, Fluid inclusions in sedimentary and diagenetic systems: *Lithos*, v. 55, no. 1, p. 159–193.
- Goldstein, R. H., 2003, Petrographic analysis of fluid inclusions: *Fluid inclusions: Analysis and interpretation*, v. 32, p. 9–53.
- Goldstein, R. H., and T. J. Reynolds, 1994, *Fluid inclusion petrography*.
- Graham, L. E., 1993, *Origin of land plants*: John Wiley & Sons, Inc.
- Guilhaumou, N., N. Szydlowski, and B. Pradier, 1990, Characterization of hydrocarbon fluid inclusions by infra-red and fluorescence microspectrometry: *Mineralogical Magazine*, v. 54, no. 375, p. 311–324.
- Hagemann, H. W., and A. Hollerbach, 1986, The fluorescence behaviour of crude oils with respect to their thermal maturation and degradation: *Organic Geochemistry*, v. 10, no. 1–3, p. 473–480.
- Hallock, P., and E. C. Glenn, 1986, Larger foraminifera: a tool for paleoenvironmental analysis of Cenozoic carbonate depositional facies: *Palaios*, p. 55–64.
- Handel, A. M., 2006, The study of reservoir properties of Mishrif Formation in Nassiriyah field and its relationship with oil production.
- Harris, P. M., S. H. Frost, G. A. Seiglie, and N. Schneidermann, 1984, Regional unconformities and depositional cycles, Cretaceous of the Arabian Peninsula.
- Harrison, W. J., and R. N. Tempel, 1993, Diagenetic pathways in sedimentary basins: *Diagenesis and basin development*, v. 36, p. 69–86.

- Hemming, N. G., W. J. Meyers, and J. C. Grams, 1989, Cathodoluminescence in diagenetic calcites: the roles of Fe and Mn as deduced from electron probe and spectrophotometric measurements: *Journal of sedimentary research*, v. 59, no. 3.
- Henson, R. S., 1951, Observations on the geology and petroleum occurrences in the Middle East, *in* 3rd World Petroleum Congress: World Petroleum Congress.
- Henson, 1940 cited in Buday, T., 1980, The regional geology of Iraq: stratigraphy and paleogeography: State Organization.
- Heydari, E., 1997a, Hydrotectonic models of burial diagenesis in platform carbonates based on formation water geochemistry in North American sedimentary basins.
- Heydari, E., 1997, The role of burial diagenesis in hydrocarbon destruction and H₂S accumulation, Upper Jurassic Smackover Formation, Black Creek Field, Mississippi: *AAPG bulletin*, v. 81, no. 1, p. 26–45.
- Heydari, E., and C. H. Moore, 1989, Burial diagenesis and thermochemical sulfate reduction, Smackover Formation, southeastern Mississippi salt basin: *Geology*, v. 17, no. 12, p. 1080–1084.
- Heydari, E., and C. H. Moore, 1993, Zonation and geochemical patterns of burial calcite cements: Upper Smackover Formation, Clarke County, Mississippi: *Journal of Sedimentary Research*, v. 63, no. 1.
- Homci, 1975 cited in BUDAY, H. A., 1980, Isopach maps of Tithonian to base of Tertiary, INOC Report,.
- Hsu, K. J., 1967, Chemistry of dolomite formation: *Developments in Sedimentology*, v. 9, p. 169–191.
- Hughes, G. W., 2012, Late Permian to Late Jurassic micropaleontological assignments and roles in the palaeoenvironmental reconstructions: *GeoArabia*, v. 18, p. 57–92.
- Hughes, G., 2013, Micropaleontologists of Saudi Arabia and other Gulf countries.
- Irish, J. P. R., and R. H. Kempthorne, 1987, The Study of Natural Fractures in a Reef Complex Norman Wells Oil Field Canada.
- Jacobson, R. L., and H. E. Usdowski, 1976, Partitioning of strontium between calcite, dolomite and liquids: An experimental study under higher temperature diagenetic conditions, and a model for the prediction of mineral pairs for geothermometry: *Contributions to Mineralogy and Petrology*, v. 59, no. 2, p. 171–185.
- James, G. A., and J. G. Wynd, 1965, Stratigraphic nomenclature of Iranian oil consortium agreement area: *AAPG Bulletin*, v. 49, no. 12, p. 2182–2245.

- Jassim, S. Z., and J. C. Goff, 2006, *Geology of Iraq: DOLIN*, sro, distributed by Geological Society of London.
- Jiang, S., 2012, Clay minerals from the perspective of oil and gas exploration, *in* *Clay Minerals in Nature-Their Characterization, Modification and Application: InTech*.
- Jreou, G., N. S., 2013, A Preliminary Study to evaluate Mishrif Carbonate reservoir of Nasiriya oil filed.: *International Journal of Engineering & Technology IJET-IJENS*, v. Vol:13 No:05, no. 5.
- Kauffman, E. G., and C. C. Johnson, 1988, The morphological and ecological evolution of Middle and Upper Cretaceous reef-building rudistids: *Palaios*, p. 194–216.
- Khorasani, G. K., 1987, Novel development in fluorescence microscopy of complex organic mixtures: application in petroleum geochemistry: *Organic Geochemistry*, v. 11, no. 3, p. 157–168.
- King Jr, D. T., and E. G. Hargrove, 1991, Sequence stratigraphy of the Smackover Formation in the northern half of the Manila Embayment, southwestern Alabama.
- Kinsman, D. J., 1969, Interpretation of Sr⁺ 2 concentrations in carbonate minerals and rocks: *Journal of Sedimentary Research*, v. 39, no. 2.
- Koepnick, R. B., 1984, Distribution and vertical permeability of stylolites within a Lower Cretaceous carbonate reservoir, Abu Dhabi, United Arab Emirates: Stylolites and Associated Phenomena: Relevance to Hydrocarbon Reservoirs. Abu Dhabi National Reservoir Foundation, Spec. Publ, p. 261–278.
- Kretz, R., 1982, Transfer and exchange equilibria in a portion of the pyroxene quadrilateral as deduced from natural and experimental data: *Geochimica et Cosmochimica Acta*, v. 46, no. 3, p. 411–421.
- Kreutzberger, M. E., and D. R. Peacor, 1988, Behavior of illite and chlorite during pressure solution of shaly limestone of the Kalkberg Formation, Catskill, New York: *Journal of structural geology*, v. 10, no. 8, p. 803–811.
- Lahann, R. W., 1978, A chemical model for calcite crystal growth and morphology control: *Journal of Sedimentary Research*, v. 48, no. 1, p. 337–347.
- Land, L. S., and D. R. Prezbindowski, 1981, The origin and evolution of saline formation water, Lower Cretaceous carbonates, south-central Texas, USA: *Journal of Hydrology*, v. 54, no. 1–3, p. 51–74.
- Longman, M. W., 1980, Carbonate diagenetic textures from nearsurface diagenetic environments: *AAPG bulletin*, v. 64, no. 4, p. 461–487.

- Longman, M. W., 1985, Fracture porosity in reef talus of a Miocene pinnacle-reef reservoir, Nido B Field, the Philippines, *in* Carbonate petroleum reservoirs: Springer, p. 547–560.
- Lumsden, D. N., and J. S. Chimahusky, 1980, Relationship between dolomite nonstoichiometry and carbonate facies parameters.
- Lyons, T. W., and R. A. Berner, 1992, Carbon-sulfur-iron systematics of the uppermost deep-water sediments of the Black Sea: *Chemical Geology*, v. 99, no. 1–3, p. 1–27.
- Machel, H.-G., 1985, Cathodoluminescence in calcite and dolomite and its chemical interpretation: *Geoscience Canada*, v. 12, no. 4.
- Machel, H.-G., 1987, Saddle dolomite as a by-product of chemical compaction and thermochemical sulfate reduction: *Geology*, v. 15, no. 10, p. 936–940.
- Mazeel, M. A., 2011, Hydrocarbon reservoir potential estimated for Iraq bid round blocks: *Oil & Gas Journal*, no. 3, p. 42–46.
- McHargue, T. R., and R. C. Price, 1982, Dolomite from clay in argillaceous or shale-associated marine carbonates: *Journal of Sedimentary Research*, v. 52, no. 3.
- McIntire, W. L., 1963, Trace element partition coefficients—a review of theory and applications to geology: *Geochimica et Cosmochimica Acta*, v. 27, no. 12, p. 1209–1264.
- McKee, E. D., and R. C. Gutschick, 1969, History of the Redwall Limestone of northern Arizona: *Geological Society of America Memoirs*, v. 114, p. 1–700.
- McLimans, R. K., 1987, The application of fluid inclusions to migration of oil and diagenesis in petroleum reservoirs: *Applied Geochemistry*, v. 2, no. 5–6, p. 585–603.
- McNaughton, D. A., and F. A. Garb, 1975, Finding and Evaluating Petroleum Accumulations in Fractured Reservoir Rock; *Exploration and Economics of the Petroleum Industry*, v. 13: New York, NY.
- McQuillan, H., 1985, Fracture-controlled production from the Oligo-Miocene Asmari Formation in Gachsaran and Bibi Hakimeh fields, southwest Iran, *in* Carbonate Petroleum Reservoirs: Springer, p. 511–523.
- Metz, S., J. H. Trefry, and T. A. Nelsen, 1988, History and geochemistry of a metalliferous sediment core from the Mid-Atlantic Ridge at 26 N: *Geochimica et Cosmochimica Acta*, v. 52, no. 10, p. 2369–2378.
- Miracle, 2002, <http://www.ucl.ac.uk/GeolSci/micropal/foram.html>.
- Moore, C. H., 1989, Carbonate diagenesis and porosity: Elsevier.

- Moore, C. H., 2001, Carbonate reservoirs porosity evolution and diagenesis in sequence stratigraphic framework: Elsevier, v. 55, p. 61–64 pp.
- Moore, C. H., 1985, Upper Jurassic subsurface cements: a case history.
- Moore, C. H., and F. C. Brock Jr, 1982, Porosity Preservation in the Upper Smackover (Jurassic) Carbonate Grainstone, Walker Creek Field, Arkansas: Response of Paleophreatic Lenses to Burial Processes: DISCUSSION: Journal of Sedimentary Research, v. 52, no. 1.
- Moore, C. H., and Y. Druckman, 1981, Burial diagenesis and porosity evolution, upper Jurassic Smackover, Arkansas and Louisiana: Aapg Bulletin, v. 65, no. 4, p. 597–628.
- Morrow, D. W., 1990, Synsedimentary dolospar cementation: a possible Devonian example in the Camsell Formation, Northwest Territories, Canada: Sedimentology, v. 37, no. 4, p. 763–773.
- Morse, J. W., and F. T. Mackenzie, 1990, Geochemistry of sedimentary carbonates: Elsevier.
- Morse, J. W., Q. Wang, and M. Y. Tsio, 1997, Influences of temperature and Mg: Ca ratio on CaCO₃ precipitates from seawater: Geology, v. 25, no. 1, p. 85–87.
- Mucci, A., and J. W. Morse, 1983, The incorporation of Mg²⁺ and Sr²⁺ into calcite overgrowths: influences of growth rate and solution composition: Geochimica et Cosmochimica Acta, v. 47, no. 2, p. 217–233.
- Munz, I. A., 2001, Petroleum inclusions in sedimentary basins: systematics, analytical methods and applications: Lithos, v. 55, no. 1, p. 195–212.
- Nadoll, P., J. L. Mauk, T. S. Hayes, A. E. Koenig, and S. E. Box, 2012, Geochemistry of magnetite from hydrothermal ore deposits and host rocks of the Mesoproterozoic Belt Supergroup, United States: Economic Geology, v. 107, no. 6, p. 1275–1292.
- Nairn, A. E. M., and A. S. Alsharhan, 1997, Sedimentary basins and petroleum geology of the Middle East: Elsevier.
- Narteau, C., 2007, Formation and evolution of a population of strike-slip faults in a multiscale cellular automaton model: Geophysical Journal International, v. 168, no. 2, p. 723–744.
- Nasiriya Integrated Project., n.d., Nasiriya Field, <http://www.pcldiraq.com/index.php?p=area>.
- Nelson, R., 2001, Geologic analysis of naturally fractured reservoirs: Gulf Professional Publishing.
- Nelson, R. A., 1981, Significance of fracture sets associated with stylolite zones: geologic notes: AAPG Bulletin, v. 65, no. 11, p. 2417–2425.

- Nurmi, R., and E. Standen, 1997, Carbonates: the inside story: Middle East Well Evaluation Review, v. 18, p. 28–41.
- Owen, R. M. S., and S. N. Nasr, 1958, Stratigraphy of the Kuwait-Basra area: Habitat of oil: AAPG, p. 1252–1278.
- Oxtoby, N. H., A. W. Mitchell, and J. G. Gluyas, 1995, The filling and emptying of the Ula Oilfield: fluid inclusion constraints: Geological Society, London, Special Publications, v. 86, no. 1, p. 141–157.
- Peryt, T. M., 1983, Classification of coated grains, *in* Coated Grains: Springer, p. 3–6.
- Pettijohn, F. J., 1957, Sedimentary rocks.
- Peybernes, 1979 cited in Flügel, 2010, New Perspectives in Microfacies.
- Plaziat, J.-C., and W. R. Younis, 2005, The modern environments of Molluscs in southern Mesopotamia, Iraq: A guide to paleogeographical reconstructions of Quaternary fluvial, palustrine and marine deposits: Carnets de Géologie/Notebooks on Geology, Brest, Article, v. 1.
- Powers, R. W., L. F. Ramirez, C. D. Redmond, and E. L. Elberg, 1966, Geology of the Arabian peninsula: Geological survey professional paper, v. 560, p. 1–147.
- Purser, B. H., 1984, Stratiform stylolites and the distribution of porosity: Examples from the Middle Jurassic limestones of the Paris basin: Stylolites and associated phenomena: Relevance to hydrocarbon reservoirs: Abu Dhabi National Reservoir Research Foundation Special Publication, p. 203–217.
- Purser et al, 1982 cited in Plaziat, J.-C., and W. Younis, 2005, The modern environments of Molluscs in southern Mesopotamia, Iraq: A guide to paleogeographical reconstructions of Quaternary fluvial, palustrine and marine deposits. Carnets Géologie Notebooks Geol Brest Artic.
- Qing, H., and E. W. Mountjoy, 1994, Origin of dissolution vugs, caverns, and breccias in the Middle Devonian Presqu'île barrier, host of Pine Point mississippi valley-type deposits: Economic Geology, v. 89, no. 4, p. 858–876.
- Rabanit, P. M. V., 1952, Rock units of Basrah area: Unpublished, Basra Petroleum Company (BPC). Iraq National Oil Company Archives, Baghdad, No. BGR, v. 8.
- Racki, G., 1982, Ecology of the primitive charophyte algae; a critical review: Neues Jahrbuch für Geologie und Paläontologie, Abhandlungen, v. 162, p. 388–399.
- Radoicic, R., 1987, On some Western Iraqi Desert subsurface formations, Block 7: Bulletin de l'Académie Serbe des Sciences et des Arts, Classe des Sciences Mathématiques et Naturelles, v. 27, p. 49–56.

- Railsback, L. B., 1993, Contrasting styles of chemical compaction in the Upper Pennsylvanian Dennis Limestone in the Mid-Continent region, USA: *Journal of Sedimentary Research*, v. 63, no. 1.
- Raiswell, R., and R. A. Berner, 1985, Pyrite formation in euxinic and semi-euxinic sediments: *American Journal of Science*, v. 285, no. 8, p. 710–724.
- Ramsden, R. M., 1952, Stylolites and oil migration: *AAPG Bulletin*, v. 36, no. 11, p. 2185–2186.
- Reid, R. P., I. G. Macintyre, and N. P. James, 1990, Internal precipitation of microcrystalline carbonate: a fundamental problem for sedimentologists: *Sedimentary Geology*, v. 68, no. 3, p. 163–170.
- Rittenhouse, G., 1971, Mechanical compaction of sands containing different percentages of ductile grains: a theoretical approach: *AAPG Bulletin*, v. 55, no. 1, p. 92–96.
- Roedder, E., 1972, Composition of fluid inclusions.
- Roedder, E., 2002, *Encyclopedia of Physical Sciences and Technology*: New York: Academic Press.
- Roedder, E., 2003, Significance of melt inclusions: Elsevier.
- Roedder, E., 1984, Volume 12: Fluid inclusions: Mineralogical.
- Roehl, P. O., and R. M. Weinbrandt, 1985, Geology and Production Characteristics of Fractured Reservoirs in the Miocene Monterey Formation, West Cat Canyon Oilfield, Santa Maria Valley, California, *in Carbonate Petroleum Reservoirs*: Springer, p. 525–545.
- Ross, D. J., and P. W. Skelton, 1993, Rudist formations of the Cretaceous: a palaeoecological, sedimentological and stratigraphical review: *Sedimentology Review*/1, p. 73–91.
- Saint Marc, P., 1979, Stratigraphic distribution of large benthic foraminifera from the Aptian, Albian, the Cenomanian and Turonian in the Mediterranean regions.: *Journal Espanola of Micropaleontology*, no. 9, p. 317–326 p.
- Sassen, R., and C. H. Moore, 1988, Framework of hydrocarbon generation and destruction in eastern Smackover trend: *AAPG Bulletin*, v. 72, no. 6, p. 649–663.
- Schiffries, C. M., 1990, Liquid-absent aqueous fluid inclusions and phase equilibria in the system $\text{CaCl}_2\text{-NaCl-H}_2\text{O}$: *Geochimica et Cosmochimica Acta*, v. 54, no. 3, p. 611–619.
- Schlager, W., and N. P. James, 1978, Low-magnesian calcite limestones forming at the deep-sea floor, Tongue of the Ocean, Bahamas: *Sedimentology*, v. 25, no. 5, p. 675–702.

- Schofield, K., 1984, Are pressure solution, neomorphism and dolomitization genetically related: Stylolites and associated phenomena: Relevance to hydrocarbon reservoirs: Abu Dhabi National Reservoir Research Foundation Special Publication, p. 183–202.
- Scholle, P. A., and D. S. Ulmer-Scholle, 2003, A Color Guide to the Petrography of Carbonate Rocks: Grains, Textures, Porosity, Diagenesis, AAPG Memoir 77: AAPG.
- Schrauder, M., and O. Navon, 1993, Solid carbon dioxide in a natural diamond: *Nature*, v. 365, no. 6441, p. 42–44.
- Schweigert, G., D. B. Seegis, A. Fels, and R. R. Leinfelder, 1997, New internally structured decapod microcoprolites from Germany (late Triassic/early Miocene), southern Spain (early/middle Jurassic) and Portugal (late Jurassic): Taxonomy, palaeoecology and evolutionary implications: *Paläontologische Zeitschrift*, v. 71, no. 1, p. 51–69.
- Seilacher, A., 2007, Trace fossil analysis: Springer Science & Business Media.
- Shafiq, T., 2009, Iraq's Oil Reserves Revisited and Implications: www.IraqOilForum.com.
- Shannon, R. T., and C. T. Prewitt, 1969, Effective ionic radii in oxides and fluorides: *Acta Crystallographica Section B: Structural Crystallography and Crystal Chemistry*, v. 25, no. 5, p. 925–946.
- Shepherd, T. J., A. H. Rankin, and D. H. Alderton, 1985, A practical guide to fluid inclusion studies: Blackie.
- Shinn, E. A., and D. M. Robbin, 1983, Mechanical and chemical compaction in fine-grained shallow-water limestones: *Journal of Sedimentary Research*, v. 53, no. 2.
- Sibley, D. F., 1982, The origin of common dolomite fabrics: clues from the Pliocene: *Journal of Sedimentary Research*, v. 52, no. 4.
- Sibley, D. F., and J. M. Gregg, 1987, Classification of dolomite rock textures: *Journal of Sedimentary Research*, v. 57, no. 6.
- Simo, J. T., R. W. Scott, and J.-P. Masse, 1993, Cretaceous Carbonate Platforms: An Overview: Chapter 1.
- Słowakiewicz, M., and Z. Mikołajewski, 2011, Upper Permian Main Dolomite microbial carbonates as potential source rocks for hydrocarbons (W Poland): *Marine and Petroleum Geology*, v. 28, no. 8, p. 1572–1591.
- Smith, J. V., 2000, Three-dimensional morphology and connectivity of stylolites hyperactivated during veining: *Journal of Structural Geology*, v. 22, no. 1, p. 59–64.
- Smosna, R., 1987, Compositional maturity of limestones-a review: *Sedimentary geology*, v. 51, no. 3–4, p. 137–146.

- Smout, A. H., 1956, Three new Cretaceous genera of foraminifera related to the Ceratobuliminidae: *Micropaleontology*, p. 335–348.
- Sorby, H. C., 1858a, On the microscopical, structure of crystals, indicating the origin of minerals and rocks: *Quarterly Journal of the Geological Society*, v. 14, no. 1–2, p. 453–500.
- Steinhauff, D. M., 1989, Marine cements: The fabric of cements in Paleozoic limestones (Ed. KR Walker). University of Tennessee. *Studies in Geology*, v. 20, p. 37–53.
- Sternbach, C. A., and G. M. Friedman, 1984, Ferroan carbonates formed at depth require porosity well-log correction: Hunton Group, deep Anadarko Basin (Upper Ordovician to lower Devonian) of Oklahoma and Texas: *Transaction of Southwest section: Am. Assoc. Petrol. Geology*, p. 167–17.
- Sterner, S. M., and R. J. Bodnar, 1984, Synthetic fluid inclusions in natural quartz I. Compositional types synthesized and applications to experimental geochemistry: *Geochimica et Cosmochimica Acta*, v. 48, no. 12, p. 2659–2668.
- Steuber, T., 1998, Biogeographie und phylogenese von Ober-kreide-Rudisten (Mollusca: Hippuritacea)-Chemostrati-graphie, Morphometrie und pa Wontologische Oatenbanken.: *Terra Nostra* 98 (3), p. V353–V354.
- Steuber, T., 2002, Plate tectonic control on the evolution of Cretaceous platform-carbonate production: *Geology*, v. 30, no. 3, p. 259–262.
- Steuber, T., and H. Löser, 2000, Species richness and abundance patterns of Tethyan Cretaceous rudist bivalves (Mollusca: Hippuritacea) in the central-eastern Mediterranean and Middle East, analysed from a palaeontological database: *Palaeogeography, Palaeoclimatology, Palaeoecology*, v. 162, no. 1, p. 75–104.
- Stockdale, P. B., 1926, The stratigraphic significance of solution in rocks: *The Journal of Geology*, v. 34, no. 5, p. 399–414.
- Strauss, H., and N. J. Beukes, 1996, Carbon and sulfur isotopic compositions of organic carbon and pyrite in sediments from the Transvaal Supergroup, South Africa: *Precambrian Research*, v. 79, no. 1–2, p. 57–71.
- Taylor, S. R., and S. M. McLennan, 1985, *Its Composition and Evolution: An Examination of the Geochemical Record Preserved in Sedimentary Rocks*: Blackwell Scientific.
- Thomas, J. B., R. J. Bodnar, N. Shimizu, and A. K. Sinha, 2002, Determination of zircon/melt trace element partition coefficients from SIMS analysis of melt inclusions in zircon: *Geochimica et Cosmochimica Acta*, v. 66, no. 16, p. 2887–2901.
- Tucker, M. E., 2001, *Sedimentary Petrology*.-272 pp: Blackwell Publishing.

- Tucker, M. E., and V. P. Wright, 1990, Carbonate mineralogy and chemistry: Carbonate Sedimentology, p. 284–313.
- Tucker, M. E., and V. P. Wright, 2009, Carbonate sedimentology: John Wiley & Sons.
- Tyszka, J. (2006). Taxonomy of Albian Gavelinellidae (Foraminifera) from the Lower Saxony Basin, Germany. *Palaeontology*, 49(6), 1303-1334.
- Veizer, J., 1983a, Chemical diagenesis of carbonates: theory and application of trace element technique.
- Veizer, J., 1983b, Trace elements and isotopes in sedimentary carbonates: Reviews in Mineralogy and Geochemistry, v. 11, no. 1, p. 265–299.
- Veron, J. E., 2008, Mass extinctions and ocean acidification: biological constraints on geological dilemmas: Coral Reefs, v. 27, no. 3, p. 459–472.
- Voigt, D. E., and S. L. Brantley, 1991, Inclusions in synthetic quartz: *Journal of crystal growth*, v. 113, no. 3–4, p. 527–539.
- Volery, C., E. Suvorova, P. Buffat, E. Davaud, and B. Caline, 2011, TEM study of Mg distribution in micrite crystals from the Mishrif reservoir Formation (Middle East, Cenomanian to Early Turonian): *Facies*, v. 57, no. 4, p. 605–612.
- Wanless, H. R., E. A. Burton, and J. Dravis, 1981, Hydrodynamics of carbonate fecal pellets: *Journal of Sedimentary Research*, v. 51, no. 1.
- Warren, J., 2000, Dolomite: occurrence, evolution and economically important associations: *Earth-Science Reviews*, v. 52, no. 1, p. 1–81.
- Watanabe, K., 1987, Inclusions in flux-grown crystals of corundum: *Crystal Research and Technology*, v. 22, no. 3, p. 345–355.
- White, A. F., 1978, Sodium coprecipitation in calcite and dolomite: *Chemical Geology*, v. 23, no. 1–4, p. 65–72.
- Whitford, D. J., M. J. Korsch, P. M. Porritt, and S. J. Craven, 1988, Rare-earth element mobility around the volcanogenic polymetallic massive sulfide deposit at Que River, Tasmania, Australia: *Chemical Geology*, v. 68, no. 1–2, p. 105–119.
- Wildeman, T. R., 1970, the distribution of Mn²⁺ in some carbonates by electron paramagnetic resonance: *Chemical Geology*, v. 5, no. 3, p. 167–177.
- Willis, D. G., and M. K. Hubbert, 1955, 3. Important Fractured Reservoirs in the United States (USA), *in* 4th World Petroleum Congress: World Petroleum Congress.
- Wilson, J. L., 1975, Carbonate facies in geological history. 471 pp: Google Scholar.
- Wolf, K. H., 1979, Mikrofazielle Untersuchungsmethoden von Kalken: *Earth-Science Reviews*, v. 14, no. 4, p. 368–370.

- Woronick, R. E., and L. S. Land, 1985, Late burial diagenesis, lower Cretaceous Pearsall and lower Glen Rose formations, south Texas.
- Zemann, J., 1969, Crystal chemistry: Handbook of geochemistry, v. 50, p. 12–36.
- Zhang, J. W., and G. H. Nancollas, 1990, Mechanisms of growth and dissolution of sparingly soluble salts: Reviews in Mineralogy and Geochemistry, v. 23, no. 1, p. 365–396.
- Zhao, L., H. Liu, R. Guo, M. Feng, Z. Zhang, Y. Zhang, and J. Wang, 2012, Integrated Formation Evaluation for Cretaceous Carbonate Khasib II of AD Oilfield, Iraq, *in* SPE Asia Pacific Oil and Gas Conference and Exhibition: Society of Petroleum Engineers.
- Zhong, S., and A. Mucci, 1989, Calcite and aragonite precipitation from seawater solutions of various salinities: Precipitation rates and overgrowth compositions: Chemical Geology, v. 78, no. 3–4, p. 283–299.

Appendix 1: Fluid inclusions analysis.

Table 11 : Petrography of the fluid inclusions and microthermometry data

Fluid Inclusion Petrography and Microthermometry Data.								
Chip number	Samples number of Fls.	Description of phase of Fls.	Relative volume of Fls.	Real size of Fls.	Relative age	T _h aqueous (°C)	T _m ice (°C)	Eutectic T (°C) as First granulation.
NS-1 2033.80	1	3 phases	30%	13 µm	Primary	205,7	-20,9	-36,8
Zone n°1	2	3 phases	30%	18 µm	Primary	209,3	-22	-35,8
	3	2 phases	20%	18 µm	Primary	158,2	-22,2	-35,8
	4	2 phases	30%	18 µm	Primary	127,6	-21,1	-35,2
	5	2 phases	30%	15 µm	Primary	130,2	-20,9	-34
	8	2 phases	10%	8 µm	Primary	132,7	-21,1	-34,2
	9	2 phases	10%	10 µm	Primary	179	-22,1	-36,3
	10	2 phases	10%	8 µm	Primary	108	-22,2	-40,1
Zone n°2	1	2 phases	10%	6 µm	Primary	194,6	-22,7	-36,2
	2	2 phases	20%	6 µm	Primary	195,7	-21,3	-36
	3	3 phases	30%	5 µm	Primary	218	-22,8	-34,6
	4	3 phases	40%	6 µm	Primary	241	-21,9	-36,2
	5	3 phases	40%	5 µm	Primary	243,5	-18,3	-34
	1	2 phases	20%	6 µm	Primary	128,8	-22,8	-39,2
	2	2 phases	30%	9 µm	Primary	121,4	-16,4	-36
Zone n°3	1	2 phases	20%	9 µm	Primary	162,2	-22,1	-33
	2	2 phases	40%	10 µm	Primary	171,4	-21,7	-33,6
	3	2 phases	40%	18 µm	Primary	179,1	-22,1	-35,3
	4	2 phases	40%	7 µm	Primary	170	-21,2	-31,6
	5	2 phases	30%	17 µm	Primary	172,4	-21,8	-33,6
	6	2 phases	10%	11 µm	Primary	161,3	-21,9	-35,1
	7	2 phases	20%	8 µm	Primary	130,3	-21,8	-37,1
	8	2 phases	30%	7 µm	Primary	148,3	-21,1	-37,5
	9	3 phases	20%	16 µm	Primary	243,2	-21,8	-36,1
	10	2 phases	40%	5 µm	Primary	173,9	-22,2	-36,1
	11	2 phases	20%	6 µm	Primary	157,8	-21,2	-35,1
	12	2 phases	10%	6 µm	Primary	162,9	-21,9	-35,5
	13	2 phases	30%	4 µm	Primary	143,3	-19,2	-34,5
	14	2 phases	20%	7 µm	Primary	170,7	-18,8	-34,6
	15	2 phases	20%	5 µm	Primary	146,6	-21,6	-36,2
	16	2 phases	20%	5 µm	Primary	133,8	-22	-34
	17	2 phases	30%	4 µm	Primary	168,2	-22,6	-36,1
NS-3 2024.25	4	2 phases	40%	5 µm	Primary	247,8	-22,2	-35,6
	6	2 phases	20%	4 µm	Primary	146,6	-21,6	-36,1
	7	2 phases	10%	4 µm	Primary	157,2	-22,1	-36,9
	8	2 phases	10%	6 µm	Primary	120	-22,3	-35,8
	9	2 phases	20%	5 µm	Primary	150,5	-22,5	-35,8
	10	2 phases	40%	4 µm	Primary	210,6	-21,5	-36,1
	1	2 phases	10%	6 µm	Primary	171,1	-22,6	-36,7
	1	2 phases	30%	4 µm	Primary	173,2	-22,9	-34,1
	2	2 phases	30%	5 µm	Primary	245,3	-21,7	-36,2
NS-5 2014.10	1	3 phases	40%	9 µm	Primary	227,2	-21,8	-36,8
	2	3 phases	20%	18 µm	Primary	245,3	-21,3	-35,8
	3	3 phases	20%	8 µm	Primary	240,4	-22,6	-37,1
	Total : 44						Mean : -21,6	Mean : -35,6

TITLE OF THE THESIS :
PALEOENVIRONMENTAL CONDITIONS AND DIAGENETIC EVOLUTION OF
THE MISHRIF FORMATION (NASIRIYAH OIL FIELD, IRAQ)

ABSTRACT :

The aim of the present study is related to understand the paleofluid-rock interactions in carbonate rocks and its relation with oil potential during upper Cretaceous. Paleogeography studies, geological descriptions and geochemistry analyses of the reservoir rocks were conducted on the Mishrif Formation of the Nasiriyah oil field (southeast of Iraq).

The data of drill cores from 5 drillholes (NS-1 to NS-5), exploration reports and production data of the Nasiriyah oil field have been used. The microfacies analyses show that Mishrif includes foraminifera, coral, rudist, algae, microbialite, Favosites microcoprolite, pellets, peloids, aggregate grains and rounded clastic grains. Therefore, shallow-water environments represent Mishrif paleoenvironments, included evaporitic zone to the back-reef zone of the interior carbonate platform shelf.

Transport system in the Mishrif contains stylolite networks, fractures and porosity systems. The scanning electron microscope (SEM) shows the balanced distribution of the transport systems regardless of the microfacies type. The aqueous fluid inclusions are mainly composed of H₂O-MgCl₂ system. Homogenization temperatures of the aqueous fluid inclusions range from 150 to 175°C. Homogenization temperatures of the petroleum fluid inclusions in the latter fractures represent high degrees from 225 up to 250°C.

Cementation process exhibits four phases of the cementation events. The first phase took place before the hydrocarbon migration. The second occurred during the hydrocarbon migration. Third phase happened after process of the hydrocarbon migration and the last phase represented the thermochemical sulfate reduction by the distribution of bitumen.

TITRE DE LA THESE :
LES CONDITIONS PALÉO-ENVIRONNEMENTALES ET L'ÉVOLUTION
DIAGÉNÉTIQUE DE LA FORMATION DE MISHRIF (LE CHAMP PÉTROLIFÈRE
DE NASSIRIYA, IRAK)

RESUME :

Le but de cette étude est de comprendre les relations entre les roches carbonatées et les paléofluides qui les traversent. Les études paléogéographiques et les descriptions géologiques ainsi que les analyses géochimiques des roches réservoirs ont été réalisées sur la Formation de Mishrif dans le champ pétrolier de Nasiriya (sud-est de l'Iraq).

Les données de 5 forages carotés (NS-1 à NS-5), les rapports de prospections et les données de production du champ de Nassiriya, ont été utilisés. Les analyses des microfaciès montrent que la Formation de Mishrif contient une grande variété d'organismes tels que des foraminifères, des coraux, des rudites ainsi que des algues, microbialites, des pellets, des peloides, des grains aggrégés et des grains arrondis. Par conséquent, la formation de Mishrif serait représentative d'un environnement d'eau de subsurface de la zone évaporitique jusqu'à la zone de récif arrière.

Le système de transport des fluides dans la Formation de Mishrif se fait au travers des réseaux de stylolite, des fractures ainsi que du réseau poral. Les inclusions des fluides aqueuses sont composées du système H₂O-MgCl₂. Les températures d'homogénéisation des inclusions des fluides aqueuses varient entre 150 et 175 °C. Les températures d'homogénéisation des inclusions des fluides pétrolières représentent les degrés élevés de 225 à 250 °C.

Les processus de cimentation indiquent quatre phases d'évènements. La première phase a eu lieu avant la migration d'hydrocarbure. La seconde phase s'est produite pendant la migration de ces hydrocarbures. La troisième phase arrive après le processus de migration. Enfin, la quatrième phase est représentée par la distribution du bitume.